technical steel research

Properties and in-service performance

Development of design rules for steel structures subjected to natural fires in closed car parks

Report

STEEL RESEARCH

EUROPEAN COMMISSION

Edith CRESSON, Member of the Commission
responsible for research, innovation, education, training and youth

DG XII/C.I — Competitive and sustainable growth I — Materials

Contact: ECSC Steel publications
Address: European Commission, rue de la Loi/Wetstraat 200 (MO 75 1/16),
B-1049 Brussels — Fax (32-2) 29-65987; e-mail: ECSC-steel@dg12.cec.be

TABLE OF CONTENTS

1. *INTRODUCTION*

The following financially independent partners participate in the research :

- ProfilARBED, Luxemburg, leader of the research
- University of Liège, Belgium
- CTICM, France
- TNO, The Netherlands
- LABEIN and ENSIDESA, Spain.

The technical coordination is handled by ProfilARBED Department "Recherches et Promotion Technique Structure (RPS)".

A first meeting was held in Esch/Alzette the 8th of September 1993; the second one in Paris the 20th of January 1994; the third one in Esch/Alzette the 5th and 6th of July 1994; **the fourth one in Maizières-les-Metz** the 19th and 20th of January 1995; the fifth one in Delft the 4th and 5th of May 1995; the sixth one in Maizières-les-Metz the 21st and 22nd of September 1995; **the seventh one in Esch/Alzette** the 16th and 17th of November 1995; the eight one in Bilbao the 28th and 29th of February 1996; **the nineth one in Delft** the 20th and 21st of June 1996; **the tenth one in Paris** the 14th and 15th of November 96 and **the last meeting in Esch/Alzette the 27th and 28th of February 1997**.

Only one ECSC report including the work description of all partners has been written by ProfilARBED. Contributions were provided by Mr Franssen of the University of Liège, Mr. Twilt and Van Oerle of TNO, Mr Kruppa and Mr Joyeux of CTICM and Mr Aurtenetxe of LABEIN.

Amongst these meetings, four meetings (written in Bold hereabove) have involved the Advisory Committee which was composed of

BELGIUM:	**Major HERREMAN**
	Service d'Incendie de l'Agglomération de Bruxelles
	Mr. P. HOURLAY
	Ministère de l'Intérieur
FRANCE:	**Mr. H. TEPHANY**
	Ministère de l'Intérieur
THE NETHERLANDS:	**Mr. G. BIJLSMA**
	Brandweer Amsterdam
	Mr. H.C. DE BEER
	Brandweer Utrecht
	Mr. A. VAN SCHAGEN
	Brandweer Amersfoort
SPAIN:	**Mr. José POSADA ESCOBAR**
	Dir. Gral. Arquitectura y Vivienda
	M.O.P.T.

Thanks to these meetings, the experts were able to give their comments and to guide the research in a satisfactory way for their point of view.

2. *GENERAL GUIDELINES OF THE RESEARCH*

They can be deduced from the General Guidelines established for the Large Compartments [1] (see final report of the ECSC research 7210-SA-210/317/517/619/932). For large compartments, the calculation is divided into four main steps :

1. Define the fire.
2. Check whether the fire is localised or not (if localised, the procedure can continue, otherwise not).
3. Calculation of the air temperature field.
4. Thermo-mechanical calculation of the structure.

These four steps can be simplified in case of a closed car park (see figure 2.1).

1. Definition of the fire : the fire is one burning car or a wave of several burning cars for which a Rate of Heat Release curve can be defined (see chapter 3.4).

   - In case of sprinkler, only ONE burning car will be assumed.
   - Otherwise, the fire spreads to another car every other 12 minutes (see chapter 3.4).

(Optional) 2. Design of the ventilation so that

   - the occupants can easily and safely leave the car park,
   - the firemen can easily and safely gain access to the fire.

   The ventilation design can be carried out easily by hand using the Belgian Standard NBN S21-208 [2] about smoke and heat evacuation and its annex for Closed Car Park [3] or by using more sophisticated programs (Two-Zone Model or CFD).

   Note: For instance by applying [2] and [3], the needed forced ventilation to guarantee a free zone of 1.8m is equal to about 60000 m^3/h (RHR = 4 MW and Fire Perimeter W_{fi} = 12m). For instance, for a car park of 50m x 31m (=80 cars), this implies to multiply by 5 the ventilation necessary to evacuate the CO produced by running cars (see chapter 4 : 80 cars x 150 m^3/h parking bay x 5 = 60000 m^3/h). It should be underlined that this factor becomes 1,25 if the French requirement for Heavy traffic is considered (see chapter 4 : 600 m^3/h parking bay). However the ventilation used to evacuate CO is not obviously adapted for smoke evacuation (critical temperature for the fans, extraction points in the upper zone, inlet of fresh air in the bottom part,...).

3. The simplified air temperature calculation formulae like or Hasemi's method [4] combined with a calculation of the mean temperature of the hot gases (see [1]) can be applied or CFD calculation programs like FLUENT or VESTA can be used.

4. Thermo-mechanical calculation of the structure.

Closed Car Park

Design Fire ①
- RHR curve
- Fire perimeter
- Number of burning cars
- Fire Spread

Active Fire Fighting
Measures Influence
(Sprinkler, smoke
detection)

Objective
Smoke evacuation
in case of fire

Present situation

②

Ventilation
Design
- Free Zone layer Height
  Y ≥ 1,8 m during the first 15'
    (Safety for occupants)
  Y ≥ 1,5 m (Safety for firemen)
- Mean Temperature of the
  Hot Zone < 500 °C

Usual
Ventilation
- Aim : to evacuate
  CO produced by the
  running cars
- see chapter 4
  150 m³/h (parking bay)

③
Air temperature field
calculation
Hasemi's method
combined with the mean
temperature of the hot gases

④
Temperature field in
the structure
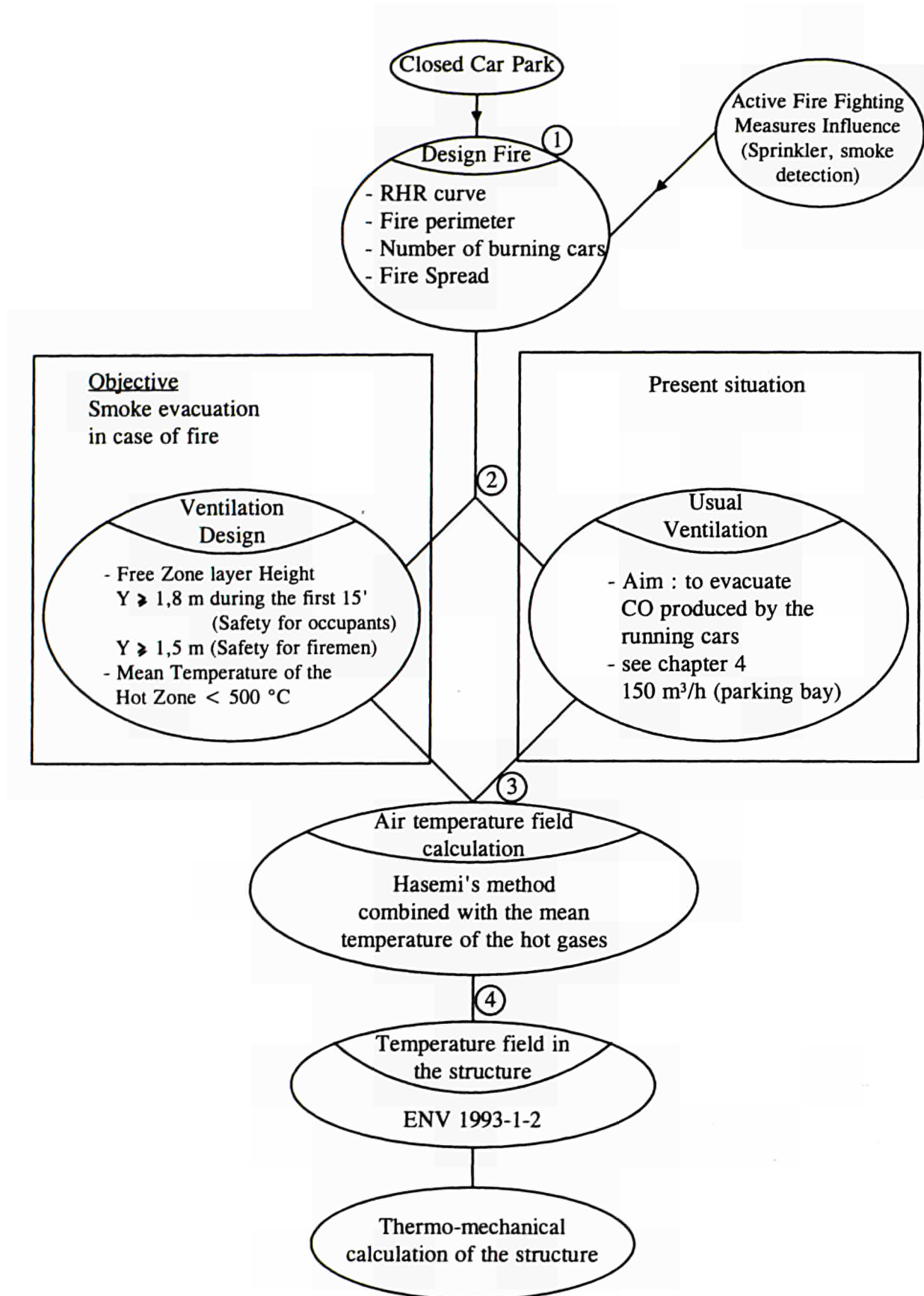ENV 1993-1-2

Thermo-mechanical
calculation of the structure

Figure 2.1 : General guidelines of the research

3. *DESIGN FIRE*

3.1. *Statistical study in Closed Car Park*

Introduction

For this project, a number of large scale experiments have been carried out, including some experiments in which two adjoining cars will be tested. For these experiments an estimation is necessary of the (mean) distance between cars in practice situations.

To obtain this data, the partners of the project have carried out a survey in 18 different carparks in 4 countries. A total of 1624 measurements of parking distances were taken.

The scope of the survey was limited to the actual parking distances; this was done to limit the amount of work needed for the survey and the analysis of the measured data.

Due to this limited scope no information is available on:

- The distribution of cars in the carpark (Eg. most cars near the exit)
- The relation between the number of free parking spaces and the parking distance
- Maximum car density in the carparks.

Results

All data has been compiled in the table and a number of figures below.

| Name	Town	Country	Parking bay [m]	Parking angle [ ]	Number of measurements	Mean parkdistance [cm]	Standard deviance	Structure beams	Structure ceiling	Distance floor-ceiling [m]	Distance floor-beam [m]	Fire doors (y/n)	Sprinklers (y/n)	Forced ventilation (y/n)	Carpark type
Zoetermeer b	Zoetermeer	Netherlands	2,2	0'	38	91	13,6	Concrete	Concrete	3,6	2,6	No	No	No	Closed
Zoetermeer a	Zoetermeer	Netherlands	2,2	0'	61	85	15,4	= =	Concrete	2,5	= =	No	No	No	Closed
Groothandel	Zoetermeer	Netherlands	2,3	0'	45	79	23,5	Concrete	Concrete	3,5	2,5	No	No	No	Closed
Supermark Eroski	Leioa	Spain	2,4	0'	28	77	32,3	Concrete	Concrete	4,0	3,4	No	Yes	Yes	Closed
Dr Areilzapark	Bilbao	Spain	2,4	0'	40	78	21,4	= =	Concrete	2,25	= =	No	No	Yes	Closed
Dr Areilzapark 1st	Bilbao	Spain	2,4	0'	7	79	13,3	Steel	?	2,52	2,22	No	No	Yes	Closed
Santa Casilda	Bilbao	Spain	2,5	0'	67	85	20,1	= =	Concrete	2,31	= =	No	No	Yes	Closed
Baracaldo MaxC	Baracaldo	Spain	2,45	0'	82	72	23,4	= =	Concrete	2,95	= =	No	Yes	Yes	Closed
Aeroport Paris	Paris	France	2,3	0'	23	74	16,0	Concrete	Concrete	2,92	2,43	Yes	No	No	Closed
Gare Rambouillet	Rambouillet	France	2,4	0'	76	75	19,0	Concrete	Concrete	3,1	2,4	Yes	No	Yes	Closed
Immeuble	Montrouge	France	2,3-2,5	0'	23	85	19,1	Concrete	Concrete	2,5	2,1	Yes	No	Yes	Closed
Cathedrale	Liège	Belgium	2.3-2,5	0'	88	80	25,5	R.C.	R.C.	2,4	2	No	No	No	Open
Max SNCB	Liège	Belgium	2,5	0'	80	101	25,9	R.C.	R.C.	3,61	2,6	No	No	No	Open
Airport	Zaventem	Belgium	2,5	45'	58	83	22,9	Steel	Compos.	2,52	2,15	No	No?	No	Open
Rosegäertchen	Luxembourg	Luxembourg	2,3	0'	206	67	18,1	Concrete	Concrete	3.33/2.66	2.1/2.12	No	No	Y/N	Closed
Knuedler	Luxembourg	Luxembourg	2,3	0'	360	61	20,2	Concrete	Concrete	2.86/2.76	2.45/2.1	No	No	Y/N	Closed
Aldringen	Luxembourg	Luxembourg	2,3	0'	146	71	21,0	Concrete	Concrete	2,45	= =	No	Yes	Yes	Closed
Theatre Capucins	Luxembourg	Luxembourg	2,3	0'	220	62	21,3	Concrete	Concrete	2,6	2,1	No	Yes	Yes	Closed
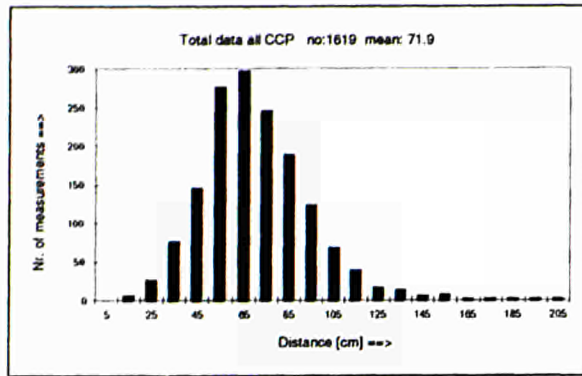
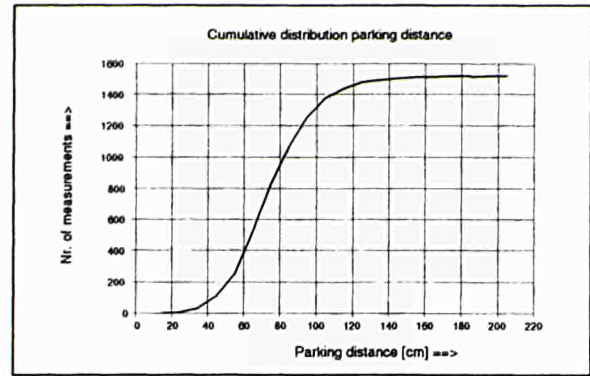Figure 3.1 : Distribution of the parking distance
for all measurements

Figure 3.2 : Cumulative distribution of the parking
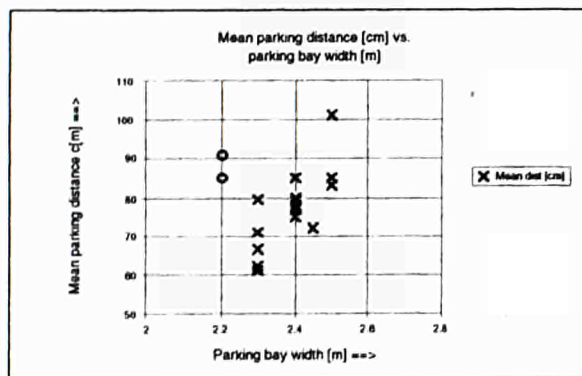distance for all measurements

Figure 3.3 : Mean distance per carpark versus
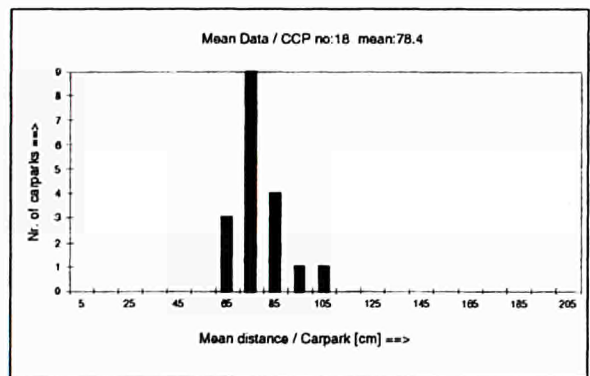the width of the parking bays

Figure 3.4 :Distribution of the mean parking distance
per carpark for the 15 carparks

Conclusion

From the data the following conclusions can be drawn:

a. The mean parking distance of all measurements is **71,9 cm**.
b. The mean value of "the mean parking distance per carpark" for 15 carparks is 78,4 cm
c. The correlation between parking distance in a carpark and the width of the parking bays is weak. There is a tendency to larger distances for larger parking bays. On the basis of simple considerations the correlation is expected to be much stronger. But the weak correlation is due only to the 2 points with a parking bay of 2.2 meters (see **O** on figure 3.34). If these 2 points are deleted from the graph, then the best fitted linear curve given by EXCEL is exactly $b=1.6+d$ with b being the parking bay width and d the mean distance between the cars. In this equation, 1.6 meters corresponds to the average width of a car. This means that this equation is exactly what we would expect to find. The 2 points which create the trouble are Zoetermeer b and Zoetermeer a from the Netherlands. In these 2 car parks, the marks were so little clear indicated that the people have parked their car like as no parking bay limitation exist.

3.2. Fire tests

3.2.1. Review around the world

Introduction

A number of tests results carried out on open car parks was carried out and these results were collected together and can be found in a document entitled "Fire Safety in Open Car Parks"-Modern Fire Engineering [5]. This chapter attempts to do the same but in this case with closed car parks. The document includes various tests carried out by organisations whose references can be found in the bibliography.

Australian car park fire tests

A total of nine tests involving 20 cars was carried out at the BHP Melbourne Research laboratories in 1988 [6]. The procedure for all of the tests was similar. The fire was started in the car designated as the test car. Continuous or repeated readings of the data commenced. While visibility allowed, the progress of the fire was observed directly, but once smoke made this impossible the fire was observed using an infra-red television camera and monitor. During tests in which the operation of the sprinkler system was not automatic the temperature of the steelwork were checked and the sprinkler system turned on if any of the steel temperatures exceeded 500°C. Otherwise, the fire was allowed to determine its own course and burn itself out.

In all of the tests except test 8 the fire was started in the car designated as the test car by placing approximately one kilogram of rags soaked in about one litre of petrol under the front seat and ignited through the open driver or passenger side window. In test 8 the fire was started by igniting four litres of petrol in an open dish placed directly under the petrol tank of the test car.

a) Test Building

The building represents a segment of a large car park, although the relatively small volume would make the build up of heat more severe than in a larger building. The building in test condition was entirely enclosed with the only intentional openings being three small peepholes (100mm x 200mm), a ventilation inlet (1200mm x 800mm) and a ventilation system outlet duct (650mm square).

The lower half of the walls were precast concrete panels. The upper half of the walls were sandwich panels constructed of steel sheeting on each side of 50mm of mineral fibre insulation. The building structure comprised of steel column and beam sections supporting reinforced concrete floors which utilise steel decking as form work and as reinforcement.

b) Car Layout

Configuration 1 was used for nearly all the tests except for test number 4 where configuration 2 was used and test number 8 where configuration 3 was used.
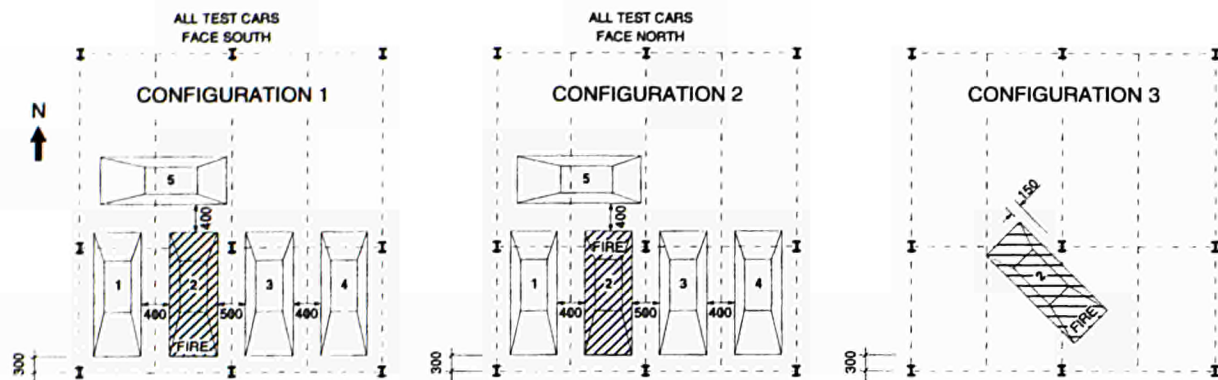
Figure 3.5 : Test configuration

c) Differing Test Procedures

Test	Important Aspects			
Number	Ventilation	Petrol Tank	Sprinkler	Basic Description of the Ignition Car
1	Operating (1m³/s)	Plastic	Automatic	Plastic bumper bars, plastic grille, some small plastic body panels, plastic external rear vision mouldings.
2	Operating (1m³/s)	Steel	Automatic	Steel bumper bars, plastic grille etc.
3	Not Operating	Steel	Automatic	Steel bumper bars, plastic strips along sides, plastic grille.
4	Not Operating	Plastic	Automatic	Plastic bumper bars, plastic grille, some small plastic body panels, plastic external rear vision mouldings.
5	Operating (1m³/s)	Steel	Manual	Steel bumper bars, plastic grille etc.
6	Operating (1m³/s)	Plastic	Manual	Plastic bumper bars, plastic grille, some small plastic body panels, plastic external rear vision mouldings.
7	Not Operating	Steel	Manual	Steel bumper bars, plastic grille etc.
8	Not Operating	Plastic	Manual	Plastic bumper bars, plastic grille, some small plastic body panels, plastic external rear vision mouldings.
9	Not Operating	Plastic	Manual	Plastic bumper bars, plastic grille, some small plastic body panels, plastic external rear vision mouldings.

d) Results

In the tests in which the operation of the **sprinkler** system was **automatic** there was little damage to the paint or body work of the test car, and in all cases there was no sign of damage to the adjacent cars. In all cases the fire did not progress out of the cabin of the car and there appears to have been no likelihood of spread of fire from car to car.

When the **sprinkler** system was operated **manually** the fire burnt out of the cabin of the car, in most cases involving the petrol tank, and with the more recent cars the considerable amount of plastic on the outside of the car at the front and/or rear. Spread of fire to cars other than the test car occurred only in tests 6 and 9 in which the more recent test cars were used. The fire had been burning for about 30 minutes in tests 6 and 9 before it was decided to turn on the sprinklers. In tests 5 and 7 there was no spread of fire from the test car and the temperatures reached in the steelwork were not high enough to warrant turning on the sprinklers.

e) Conclusions

The sprinkler system was shown by this research program to be the main factor influencing the development of fire in the closed car park.

A second factor which appeared to have some influence on the development of the fires was the model of the test car. The more recent model test cars appeared to increase the likelihood of fire spreading from car to car, probably due to the plastic petrol tank and increased use of plastics on the exterior of the cars. The ventilation system (3600 m^3/h) had no noticeable impact on the severity of the fire and the resulting temperatures in the steelwork. It was not effective in removing smoke from the building.

It is concluded that in a closed car park with a functioning sprinkler system there is no need for fire protection of the steelwork.

Further Australian car park fire tests

A further set of tests concerning fires in closed parking areas was carried out in the BHP Melbourne Research Laboratories in 1990. These results are laid down in a document entitled Fire Safety in Car parks [5] in which can be found more information on tests carried out in car parks which will also be summarised in this document later.

These tests were entitled fire tests in partially closed car parks. This may lead us to believe that this information is irrelevant for this report as we are studying closed car parks, but it can be viewed that, because of the limited volume of the test compartment and the heat build up in this relatively small test volume, rather elevated temperatures were measured.

There were numerous tests carried out in this test cell but only tests C1 to C3 will concern us as these are the only ones featuring real cars. The rest were attempted to be simulated by burning trays of petrol. Thus a total of three tests were carried out. In test C1 the fire was started in the car designated as the test car by placing approximately one kilogram of rags soaked in about one litre of petrol under the front seat and ignited through the open passenger side window. In this test there were a total of 5 cars in the car park arranged as shown below. In tests C2 and C3 the fire was started by igniting four litres of petrol in an open tray placed directly under the petrol tank of the test car. In these tests only the test car was in the car park.
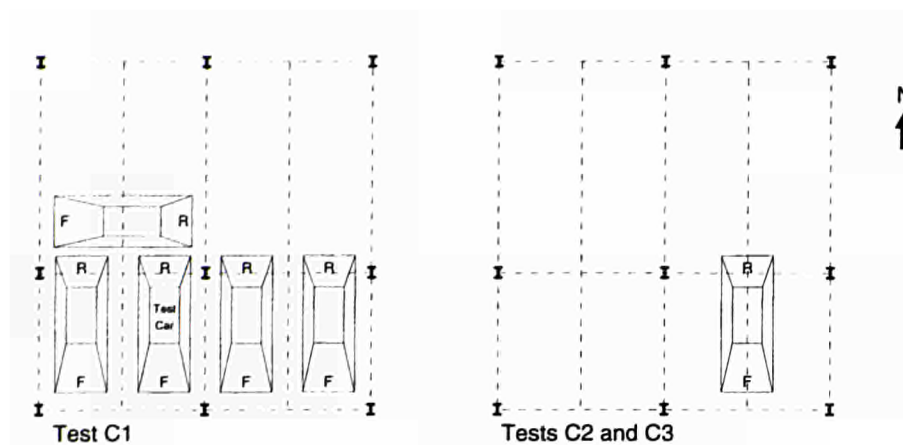
Figure 3.6 : Layout of cars for tests C1, C2 and C3

a) Test Building

The test building constructed at MRL was designed to represent a segment of a large building consisting of an office floor over a car park. The building structure was comprised of steel column and beam sections supporting reinforced concrete floors which utilise steel decking as form work and as reinforcement. During all of the fire tests, the lower 50% of the car park walls were enclosed with precast concrete panels and the upper half of the east and west walls were enclosed with sheet steel panels insulated with mineral fibre blankets. For tests C1 and C2 the upper half of the western side of the north and south walls were also enclosed with sheet steel panels insulated with mineral fibre blankets. Thus for these tests the only openings in the walls were a quarter of the wall area of the north and south walls. In test C3 the whole of the upper half of the north and south walls were open.

b) Results and test observations

Test C1

The fire was initiated in the cabin and had developed rapidly inside the car within 30 seconds. By 13 minutes the rear of the car was fully involved in fire. After 15 minutes, the petrol tank of the test car appeared to rupture and petrol spread over the floor to the adjacent cars which then began to burn also. The sprinklers were activated after 22 minutes.

There was significant damage to all of the cars in the car park. Some minor local buckling of the bottom flange of the beam directly above the test car occurred.

Test C2

In this test the sprinklers were initiated only 100 seconds after ignition and thus very little damage was done.

Test C3

In this test the car was allowed to burn out which took approximately 45 minutes. In this test there was a more severe exposure condition for the structural members within the car park. Although some spalling of the concrete wall slab occurred, no damage to the steelwork was apparent when it was inspected.

Temperatures of the steelwork

Maximum steel temperature [°C]			Column
test C1	test C2	test C3	or Beam
590	50	270	200 UC46
480	40	100	310 UC198
700	/	610	150 UC23
860	170	430	Beams

c) Conclusions

The temperatures reached in both air and the steelwork in the tests in which the sprinkler system was permitted to react automatically were low enough to be of no concern whatsoever, and **it is concluded that in a partially closed car park with a functioning sprinkler system there is no need for fire protection of the structural steelwork.**

Generally, the conditions measured in the partially closed car park in this series of tests were found to be similar to those previously encountered in the closed car park tests and substantially more severe than those measured in the open deck tests. Consequently it is recommended that in general a car park which does not clearly comply with the requirements for an open deck car park should be treated as a closed car park for the purpose of determining the required fire protection measures.

Japanese tests

In 1970 the Nippon Steel Company conducted five tests with varying ventilation. The resulting maximum temperatures in the unprotected steel members did not exceed 245°C [8].

Swiss tests

Fire tests in car parks were conducted in Switzerland in 1969 and 1970 [9,10]. The first series of tests were carried out in an underground car park and included measurement of the temperatures produced by the fire and the production of smoke. The temperatures measured in these tests were not high and the conclusion reached was that the **main danger lies in the spread of dense smoke.**

The second series of tests were in an enclosed car park and were aimed at studying the fire development, the probability of spread of fire, the production of smoke and the effectiveness of automatic alarm and extinguishing systems. The findings of these tests

largely related to the low probability of fire spread and the effect of the operation of the sprinkler system on the smoke spread and obscuration.

The Channel Tunnel Tests

This report presents the results of full scale fires in two private motor vehicles conducted under instrumented calorimeter hoods for the Channel Tunnel Safety Unit [11]. Although this is not a closed car park the test is carried out within a enclosed volume with the test items being cars. Thus this research does bear some relevance to this document.

The aim of the study was to measure the worst case fire behaviour parameters of burning motor cars, under controlled conditions and with an unlimited supply of air for the fire. Two tests were carried out, one involving a fire within a passenger compartment (i.e. seating) the other under the chassis/engine (fuel spill). Both were initiated by a fairly severe fire source.

a) Test Building

The test compartment was a reproduction of the conditions that would be encountered in the Channel Tunnel (figure 3.7). It was decided to use two calorimeters due to the amounts of smoke that would be produced and the way in which these were set up can be seen overleaf.

A canopy was constructed to join the two calorimeters. Sheet steel cladding, insulated on the outside with ceramic fibre blanket, enclosed both sides of the canopy over the full height. The steel clad rig provided a surface that would closely resemble the interior of a shuttle wagon and the ventilation conditions thus imposed would be typical of the loading or unloading phases of a shuttle wagon journey.
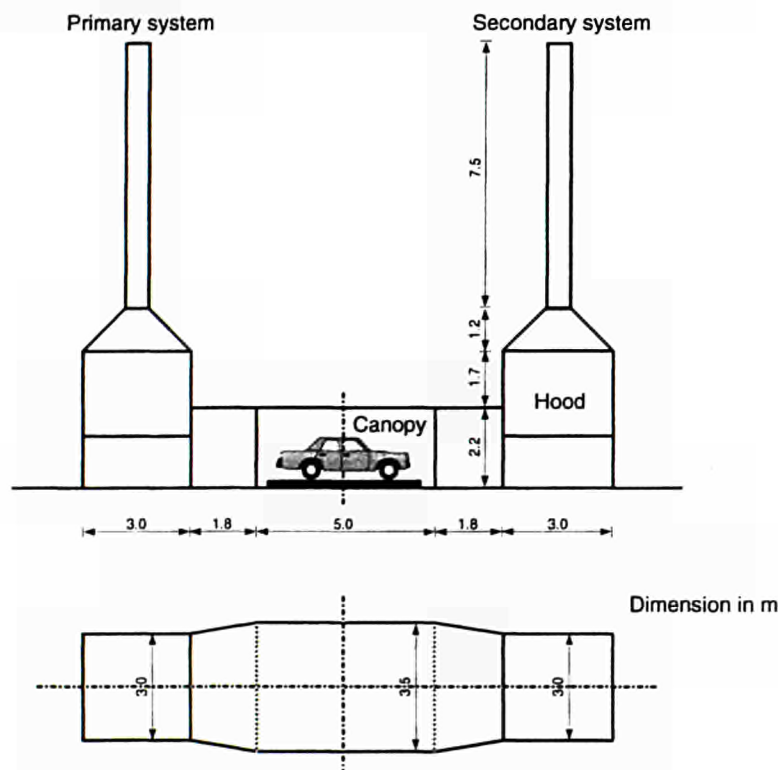
Figure 3.7 : Test compartment reproduction

b) Selection of cars

Findings of a project carried out on this subject indicated that there was likely to be an increased use of plastics in car body panel construction and while such materials may not be particularly flammable it might be expected that their fire resistance would be significantly different from steel and that a fire might not spread easily. Following this review it was agreed that the two cars would be a 1982 model Austin Maestro and a 1986 model Citroen BX. The Maestro was used for the seat ignition test. The Citroen used for the engine ignition test. The cars were in a condition representative to those used in the tunnel; they had at least three quarter filled fuel tanks, some luggage in the boot, papers on the seats and dashboard and had their front windows open and doors closed. The suspension system, and other pressurised components, which have been known to explode in fires, were left intact. Batteries were left connected.

c) Observations and results

The fires were well ventilated and allowed to develop fully before fire fighting intervention. Of the two tests the first burned for 17 minutes with the gas temperature in the rig reaching 1250°C and with a peak total heat output of at least 7.5 MW before being extinguished. The other burned for 57 minutes with gas temperatures reaching 1125°C and a peak heat output of 4.5 MW. These finding appear very high compared to other measurements. The ventilation conditions and the heat feedback of the walls could explain the differences noticed in the Channel tunnel tests. The RHR curves of these tests are given in figure 3.27(FRS) of chapter 3.2.2.

3.2.2. CTICM car fire tests

Introduction

Car fires have been studied since numerous years. But the study of the rate of heat release of cars has begun only with car tests of VTT in Finland (1991) [12,13] and more recently by the Fire Research Station and the CERCHAR in France [14]. Other tests have been performed by the VTT, but the cars of these tests had burnt in a simulated open car park.

The aim of the new tests is the same (knowledge of the rate of heat release), but the configuration is different. The local is a simulated closed car park. The differences are the air income, the confinement, the smoke evacuation, the radiative and convective feedback on cars ...

Configuration of the car tests

9 tests have already been performed : 2 in January 1995, 3 in July 1995 and 1 in September 1995, 1 in June 1996, 1 in July 1996 and 1 in October 1996.

a) The simulated closed car park

A part of a closed car park has been simulated and is shown in figure 3.8. The floor surface was 5m x 5m corresponding to 2 parking baies. The photo 3.1 shows the simulated closed car park under the calorimetric hood.

Parts of steel profiles were used to determine the heating of the steel structures in a real car park.

For the 6 first tests, these profiles were above the car roofs, an IPE 240 (1m length) with a massiveness ratio of 235 and an HEB 300 (1m length) with a massiveness ratio of 116, and behind the car an IPE 600 relative to a real closed car park.

During the tests n°7 to n°9, two HEB 240 steel columns were placed between parking baies at the front and rear position. Even, two IPE 500 steel beams were also put under the ceiling between cars during the test n°9.

The height of the volume was for the two first tests 2.30m and increased for the following tests up to a more usual value, 2.60m.

The tests were performed in a corner configuration for the 5 first tests and a closed volume with a window of 1.90 m x 0.55 m for the test n°6. In the cases of the three last tests, the volume had only one wall. These data are summed up in the table 3.1.

The tests are described in details in the CTICM reports ([14] ; [21]).
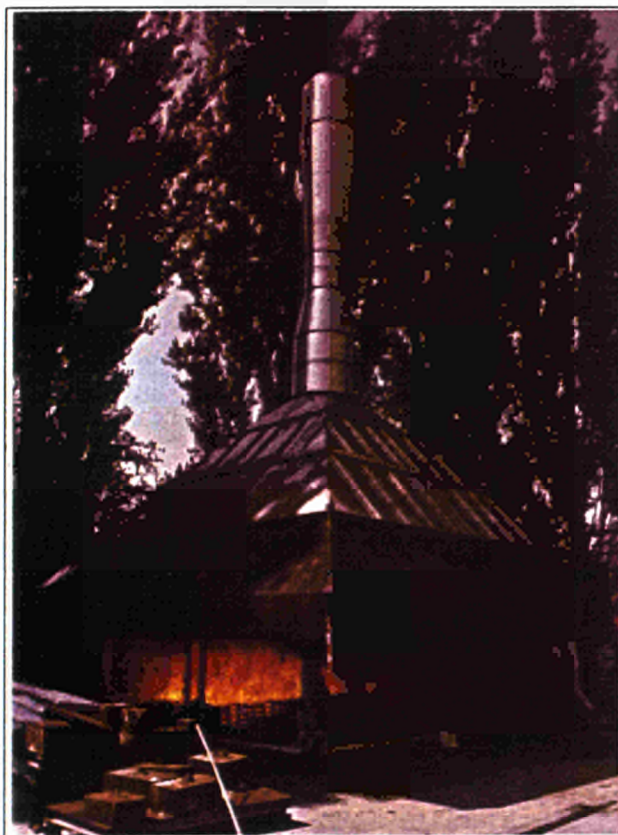
Photo 3.1 : Experimental device

b) The test car

In all tests, the cars were equipped as in practice with oil, 4 tyres and a spare tyre, and the fuel tank was 2/3 full. The cars are described in the table 3.1 for the nine tests.

In the test n°9, the tank of the large car was empty and the tank of the small car was only ¼ fulfilled. This condition was necessary to perform the test under the hood limited to about 10 MW.

The cars made in 1996 may be divided in 5 categories. These categories are described in the table 3.2. The category 5 is defined by the monospace of the different trade-marks. The small car used in the tests n°8 and n°9 belongs to the category 1, and the large car of tests n°7 and n°9 comes from the category 3. The different categories are also described by their characteristics of mass, possible mass loss and the total released energy during a fire. These values are obtained by a 'theoretical approach' by taking to piece of cars. The global results are described in [24]. A mean value by category is given in the table 3.3. The 'theoretical released energy' corresponds to a complete combustion and considers a fully filled tank.

c) The ignition

In the 7 first tests, the car was ignited with 1.5 l of the petrol in an open tray under the left front seat. The left front window was completely open, and the right front window was half open. All doors were closed. In the case of study with two cars, the doors and windows of the second one were closed.

In the test n°8 and n°9, the cars were ignited under the car at the gear box level with 1 liter of petrol, as a procedure sometimes used by car manufactures.

test	cars number	car n°1	car n°2	mass car n°1	mass car n°2	volume height (m)	system	date
n°1	2	Mazda 323	Talbot Solara	820	not measured	2.30	corner	12/01/95
n°2	1	Renault 18		951		2.30	corner	20/01/95
n°3	1	Renault 5		757		2.60	corner	24/07/95
n°4	1	Renault 18		955		2.60	corner	26/07/95
n°5	2	BMW	Renault 5	1150	736	2.60	corner	28/07/95
n°6	2	Citroën BX	Peugeot 305	870	1073	2.60	closed	22/09/95
n°7	1	large car		1303		2.60	opened	19/06/96
n°8	1	small car		830		2.60	opened	05/07/96
n°9	2	small car	large car	789	1306	2.60	opened	03/10/96

Table 3.1 : Configuration of tests

trade-marks	category 1	category 2	category 3	category 4	category 5
Peugeot	106	306	406	605	806
Renault	Twingo-Clio	Mégane	Laguna	Safrane	Espace
Citroën	Saxo	ZX	Xantia	XM	Evasion
Ford	Fiesta	Escort	Mondeo	Scorpio	Galaxy
Opel	Corsa	Astra	Vectra	Omega	Frontera
Fiat	Punto	Bravo	Tempra	Croma	Ulysse
Wolkswagen	Polo	Golf	Passat	//	Sharan

Table 3.2 : Definition of car categories

category	car mass (kg)	mass loss (kg)	released energy (MJ)
1	850	200	6000
2	1000	250	7500
3	1250	320	9500
4	1400	400	12000
5	1400	400	12000

Table 3.3 : Mean car mass, mass loss and energy available to be released versus category

Instrumentation

A hood was built above the volume to collect all smokes, combustion products and pollutants emitted during the fire. In this exhaust duct, a Venturi was placed and different measurements have been done :

- temperature in the Venturi,
- differential pressure between the contraction section and before the contraction section,
- gas analysis O_2, CO_2 and CO concentration by chromatography.

So the temperature and the differential pressure allow to calculate the mass flow rate in the exhaust duct. Moreover, if all smokes and combustion products are collected, then the rate of heat release can be calculated. Formulas and calculation assumptions are indicated in the annex 1.

During the tests n°2 all smokes and combustion products had not been collected, so the rate of heat release measured is not the effective heat release rate. During tests n°5, the severity of the fire had limited our experimental device, the rate of heat release had been measured during only the first 20 minutes.

In the volume, measurements were also made :

- temperatures : gas temperature above the car, and temperature inside the car were measured with K thermocouples. About 90 thermocouples were placed in the volume. Temperatures of steel structure elements were also recorded with H56 thermocouples of 8mm length.

- heat flux : heat flux was measured by radiometers. A radiometer was placed either in front of the right front door at 70 cm (mean distance between two cars) or/and behind the cars at 50 cm of height.

- mass loss : the cars were placed on a weighing platform recording the mass of the car during the test.

Moreover these active measurements, cameras recorded visually the scenario.

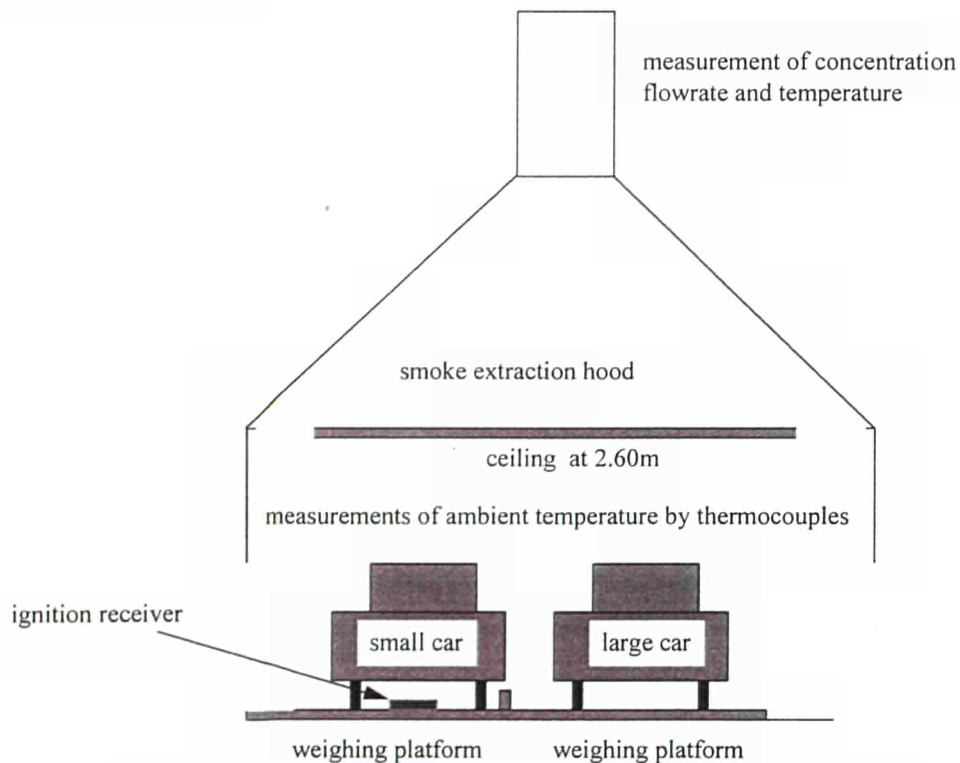The experimental device is summed up in the figure 3.8. The photo 3.2 shows the car fire test n°5 where 2 cars burnt.

measurement of concentration flowrate and temperature

smoke extraction hood

ceiling at 2.60m

measurements of ambient temperature by thermocouples

ignition receiver

small car

large car

weighing platform   weighing platform

Figure 3.8 : Configuration of the experimental device for the test n°9

Photo 3.2 : Test n°5

Results

a) Energy, time, and mass

The tables 3.4 and 3.5 sum up the main results : fire duration, propagation time for tests with two cars, time corresponding to the beginning of real contribution of the car fire, the mass loss, maximum rate of heat release (RHR), energy release (E).

The times t_1, t_2, t_3 and t_4 correspond respectively to propagation time to the second car, real contribution to the rate of heat release for the first car, real contribution to the heat release rate for the second car, and duration of fire (with a criteria of about 0.25 MW, or end of mass loss, or video approximation). These four times are described in figure 3.9.
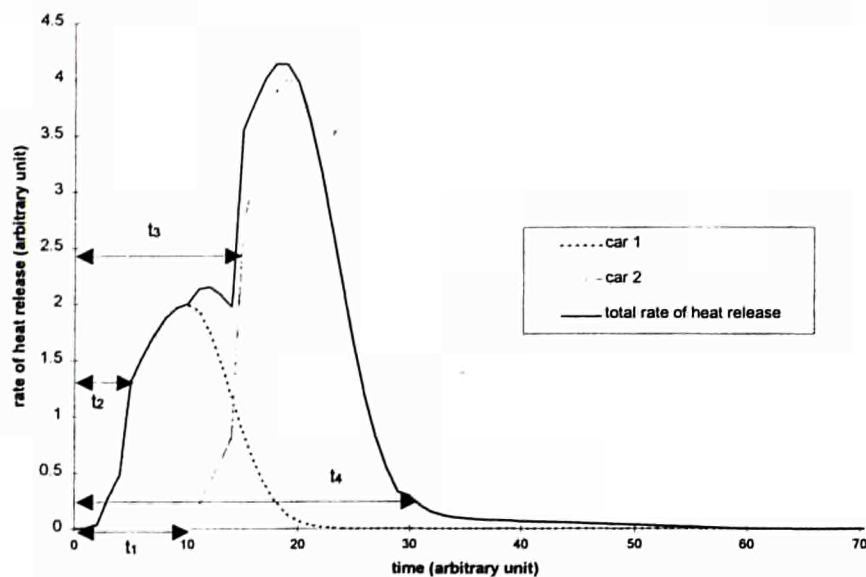
Figure 3.9 : Definition of the times t_1, t_2, t_3 and t_4

The duration of the fire given in table 3.5 shows that all fires last between 50 and 60 minutes independently of the car. Only the fire of the small car of the test n°3 was quicker.

When it exits a ventilation control (test n°6), there is not self-extinction of the fire due to oxygen lack, but the fire duration is longer. A ventilation such as the test n°6 implies a fire duration of 2 hours.

The height of the volume (2.30m for tests n°1 and n°2 , 2.60m for others) has no strong effects on the rate of heat release. The results of tests n°2 and n°4 with the same car are similar. But this last point about temperature are discussed in the next section.

In the tests n°1, n°5, n°6 and n°9, two cars has been used to assess the probability of fire propagation. During these four tests, the second car was at 70 cm from the first one and the fire has been propagated to the second car at about 10 minutes. In all cases, the fire has been propagated by the ignition of rubber.

In the test n°4, a tyre was placed on the floor at 70 cm from the car. The tyre ignited after 29 minutes.

In the test n°8, four tyres were placed at 4 different distances from the car (0.50m, 0.75m, 1.00m and 1.25m), but all tyres ignited at about 20 minutes after ignition of the car fire.

In the test n°9, four tyres were placed at 4 different distances from the second car (0.50m, 0.75m, 1.00m and 1.25m) in order to evaluate the fire propagation to an eventual third car, all tyres ignited at about 20 minutes after ignition of the first car fire.

For some of cars, theoretical values of combustible mass and energy potential are known. These values have been deduced from car dismounting. The energy potential is evaluated considering a complete combustion. A combustion efficiency factor (often defined as the 'm factor') is calculated and shown in the table 3.6. A mean m factor is about 0.57 for old car, but about 0.8 for recent ones.

The mass loss measured during the tests varies from 15 % to 19 % of the initial mass of the car. These values are very closed to theoretical values of 80ths cars (16%). The mass loss and the heat release allow to deduce a combustion heat of the combustible mass of the cars. This combustion heat varies during tests from 16.6 MJ/kg (test n°3) to 29 MJ/kg (test n°9).

In most of the tests a good correlation exists between rate of heat release and mass loss, deducing a relatively constant combustion heat in time. This can be seen in figures 3.10 and 3.11 relating the heat release and the mass loss by time unit for the test n°3 and test n°9. One can remark a decay between heat release curve and mass loss curve of about 1 minute.

test	E (GJ)	RHR (MW)	mass loss car n°1 (kg)	mass loss car n°2 (kg)
n°1	4.98	3.5	136	138 (estimation)
n°2	not measured	not measured	185	//
n°3	2.1	3.5	138	//
n°4	3.08	2.15	145	//
n°5	not measured	10	198	not measured
n°6	8.51	1.7	250	not measured
n°7	6.67	8.3	275	//
n°8	4.09	4.07	184	//
n°9	8.89	7.5	124	172

Table 3.4 : Energy released and mass loss of cars

test	t_1 (min)	t_2 (min)	t_3 (min)	t_4(min)
n°1	12	4	25	60
n°2	//	8	//	50
n°3	//	4	//	32
n°4	//	6	//	55
n°5	9	15	16	60
n°6	12	6	20	140
n°7	//	4	//	60
n°8	//	14	//	55
n°9	8	16	16	50

Table 3.5 : Time description of the fire

test	experimental			theoretical		m factor
	heat release (GJ)	mass loss (kg)	heat combustion (MJ/kg)	heat potential (GJ)	combustible mass (kg)	
n°2		185		5.27	174	
n°3	2.1	138	16.6	3.73	122	0.56
n°4	3.08	145	23.6	5.27	174	0.58
n°7	6.67	275	23	8.20	288	0.81
n°8	4.09	184	24	4.90	177	0.83
n°9	7.92	296	29	10.7	465	

Table 3.6 : Deduction of the 'm factor' from tests
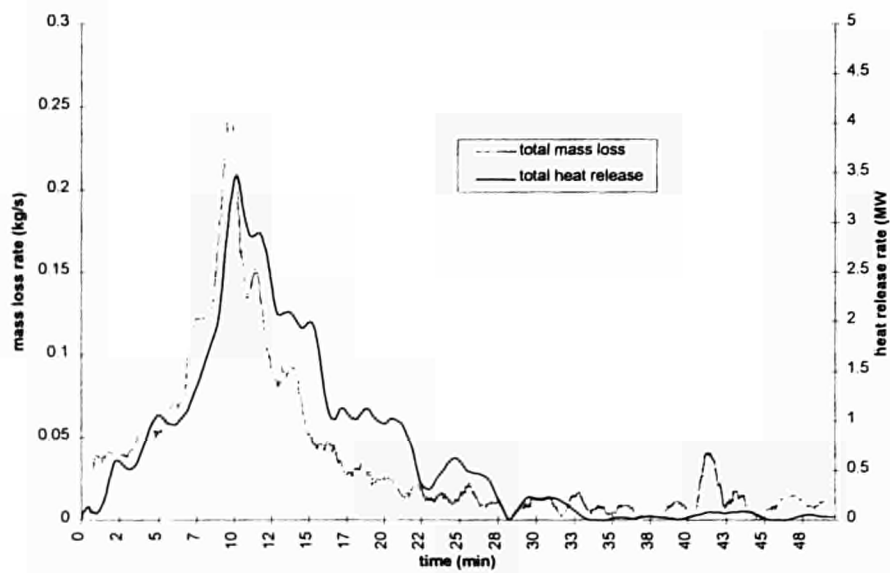
Figure 3.10 : Heat release and mass loss by time unit during the test n°3

23
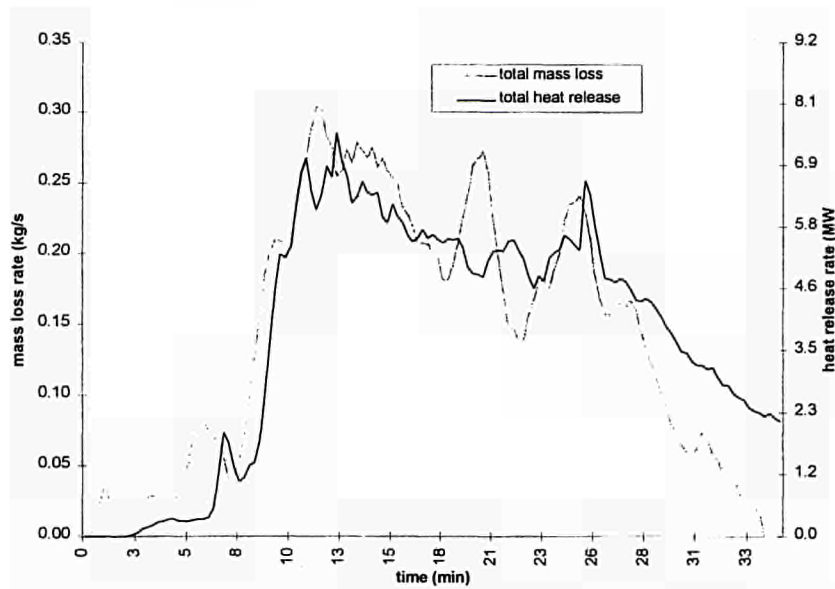
Figure 3.11 : Heat release and mass loss by time unit during the test n°9

b) Air temperature

About 40 thermocouples measured the ambient temperature in the compartment. These thermocouples were dispatched on 10 vertical lines and 4 or 5 horizontal planes.

The maximum temperature obtained in the compartment and the maximum temperature obtained just under the ceiling (10 cm) are shown in the table 3.7. One can remark that the maximum of the ambient temperature in the compartment and under the ceiling are equals or rather similar. The highest values are obtained, firstly in the test n°5 where the heat release rate had reached about 10MW in a very fast fire, secondly when the ceiling height was the lowest and the position value is obtained during the test n°7 in which the heat release rate reached 8.3MW.

The figure 3.12 shows the mean temperature of the ambient air just under the ceiling in function of time for each test. This temperature can represent a mean temperature of the smoke zone under the ceiling. The same remarks can be about the maximum of the mean temperature under the ceiling : firstly the test n°5 with highest heat release rate, secondly the tests n°1 and n°2 with a ceiling height of 2.30m and at the third position the test n°7 with the highest rate of heat release (8.3MW).

According to these remarks, it can be concluded the height of the ceiling has a very strong effect on temperature because of the heat repartition and heat loss. This conclusion will also be done with the steel temperature results in the next section.

24

test	max air temperature in the compartment (°C)	max air temperature under the ceiling (°C)
n°1	1220	1220
n°2	1330	1298
n°3	1100	1100
n°4	1062	1062
n°5	1348	1346
n°6	1214	1175
n°7	1280	1269
n°8	1080	1077
n°9	1210	1194

Table 3.7 : Maximum ambient temperatures measured during tests
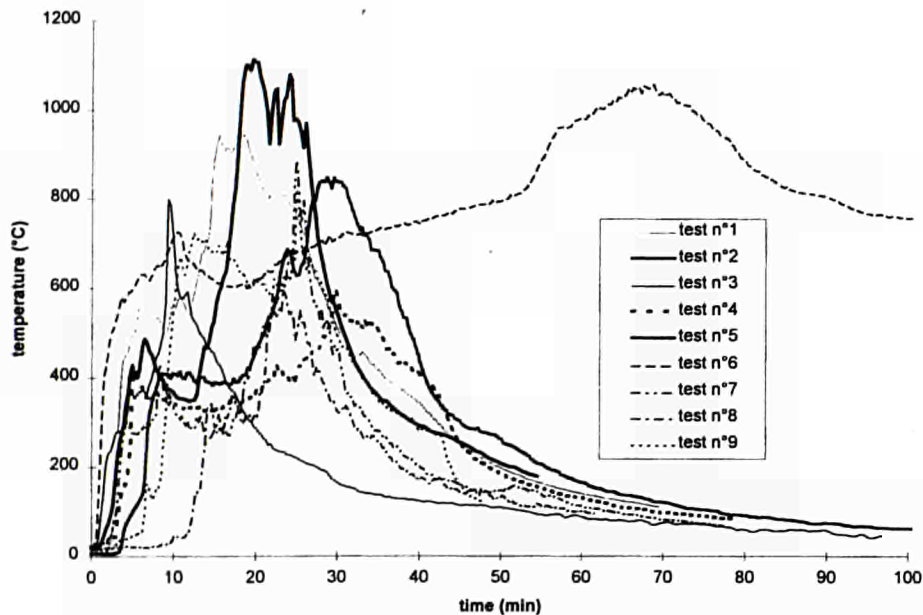
Figure 3.12 : Mean ambient temperature under the ceiling

c) Steel element temperatures

Different steel elements were put in the box in order to estimate the impact of the fire to the steel structure of a car park.

These elements, not present at all tests, were the following :

- HEB 300 beams on the car roof,
- PE 240 beams on the car roof,
- HEB 240 columns between cars,
- IPE 500 beams between cars,
- IPE 600 beam behind car.

The localisation of the elements is shown in figure 3.13, where the numbers in brackets indicates the presence of these steel elements during the different tests.

small car   **large car**
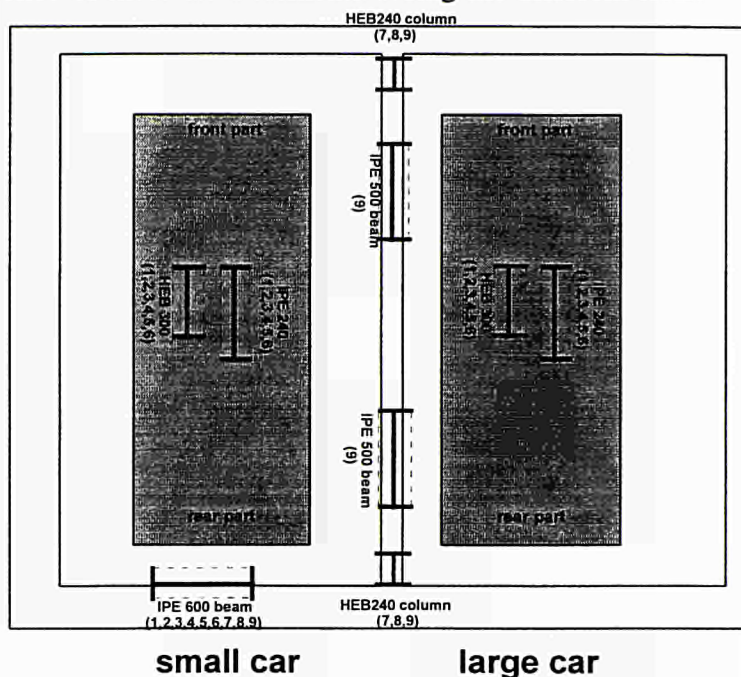
Figure 3.13 : Localisation of steel elements during the test

The temperature of flanges and web surfaces were measured during tests. The maximum of temperatures measured were summed up in the tables 3.8 to 3.16.

In some of these tables, a comparison with temperatures obtained during two tests in which 380 kg of wood (on a parking bay of 2.5m x 5m, so about 500 MJ/m^2) was used instead of a car. The test 'wood 1' was performed with a ceiling height of 2.30m and the test 'wood 2' with a ceiling height of 2.60m.

The bold number shows the value and the number of the test in which the temperature is the higher. One can remark the highest values are determined in tests 5 and 9 where two cars have been burned very fastly.

However, the temperature is higher in the test n°5 than in the test n°9. This can be explained by two factors : there was no petrol in tanks during the test n°9, and the system was opened in test n°9 instead of a corner system in the test n°5 creating a more confined volume.

tests	n°1	n°2	n°3	n°4	**n°5**	n°6	n°7	n°8	n°9	wood 1	wood 2
lower flange	610	660	330	570	**940**	820	460	350	380	600	670
web	610	710	370	570	920	710	600	430	400	600	670
upper flange	530	460	220	480	800	840	440	280	340	500	570

Table 3.8 : Temperature IPE 600 beam behind the car

tests	n°1	n°2	n°3	n°4	n°5	n°6	n°7	n°8	**n°9**
lower flange									**660**
web									660
upper flange									590

Table 3.9 : Temperature front IPE 500 beam between cars

tests	n°1	n°2	n°3	n°4	n°5	n°6	n°7	n°8	**n°9**
lower flange									**600**
web									630
upper flange									490

Table 3.10 : Temperature rear IPE 500 beam between cars

tests	n°1	n°2	n°3	n°4	**n°5**	n°6	n°7	n°8	n°9	wood 1	wood 2
lower flange	750	860	440	470	**1100**	970				860	820
web	770	840	440	450	1100	970				840	800
upper flange	590	710	320	390	880	900				720	640

Table 3.11 : Temperature HEB 300 beam above the first car

tests	n°1	n°2	n°3	n°4	**n°5**	n°6	n°7	n°8	n°9	wood 1	wood 2
lower flange	790	510	350	330	**1120**	1000				540	550
web	790	510	350	380	1120	1000				580	580
upper flange	650	390	240	310	790	980				400	460

Table 3.12 : Temperature HEB 300 beam above the second car or unoccupied place

tests	n°1	n°2	n°3	n°4	**n°5**	n°6	n°7	n°8	n°9	wood 1	wood 2
lower flange	840	1010	560	520	**1290**	1000				1040	840
web	840	1020	590	520	1290	1000				1040	880
upper flange	740	860	460	510	1240	960				1040	880

Table 3.13 : Temperature IPE 240 beam above the first car

tests	n°1	n°2	n°3	n°4	**n°5**	n°6	n°7	n°8	n°9	wood 1	wood 2
lower flange	1000	710	360	400	**1180**	1040				710	580
web	1000	710	380	420	1180	1040				710	600
upper flange	840	660	290	350	1060	1000				640	510

Table 3.14 : Temperature IPE 240 beam above the second car or unoccupied place

tests	n°1	n°2	n°3	n°4	n°5	n°6	n°7	n°8	n°9
flange in side							400	290	**700**
web							440	320	640
flange outside							380	260	640

Table 3.15 : Temperature front HEB 300 column between cars

tests	n°1	n°2	n°3	n°4	n°5	n°6	n°7	n°8	n°9
flange in side							490	340	**520**
web							500	340	500
flange outside							400	250	480

Table 3.16 : Temperature rear HEB 300 column between cars

In order to verify the co-ordination between ambient temperature and steel temperature, to know if local ambient temperature can be used to determine the steel temperatures, a simulation of the thermal transfer in the steel structures from the measured ambient temperature closed the steel elements has been done by numerical simulations.

For example, the figures 3.14 and 3.15 shows the comparison of measured and calculated steel element temperatures, during the test n°9. The steel elements are the front HEB240 column and the rear IPE 500 beam between cars. One can remark a rather good correlation for flanges and web in the both cases.
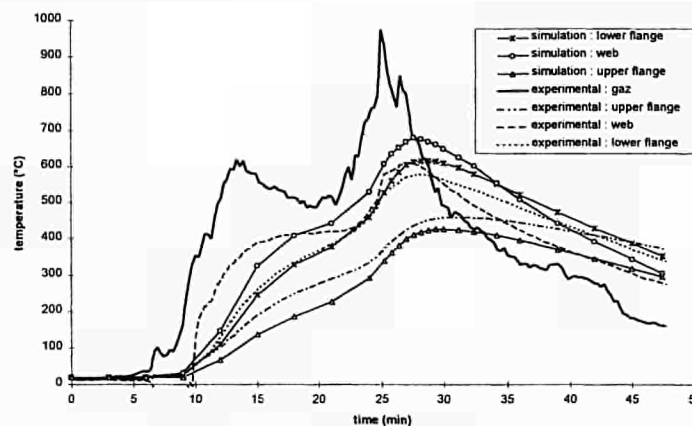
Figure 3.14 :   Correlation between gaz and steel temperatures around the rear IPE 500 beam (test n°9)
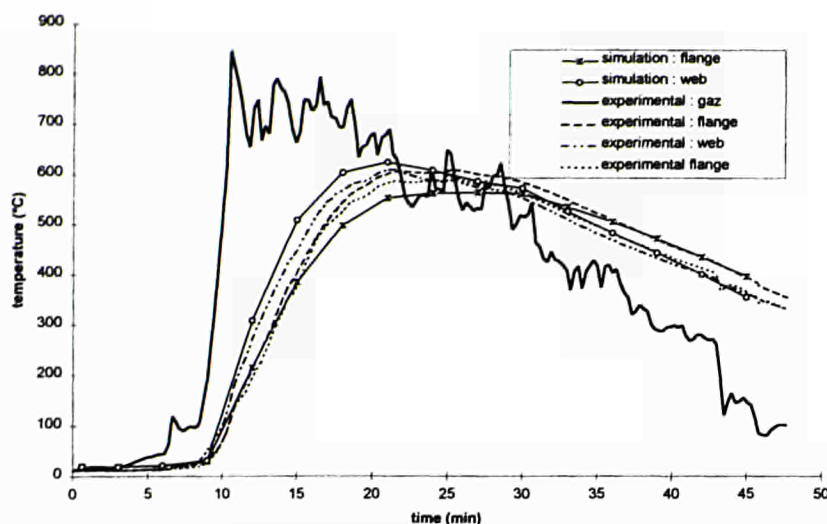
Figure 3.15 :   Correlation between gaz and steel temperatures around the front HEB 240 column (test n°9)

Conclusion

In the first 6 tests, the cars came from 80ths. A CTICM study has shown an increase of cars calorific potential versus years [24] . Even, the first five tests were performed considering a corner configuration that is representative to a very severe scenario.

The test n°6 was performed considering an important ventilation control and a confined volume limiting the fire to a theoretical heat release rate of 2 MW that is near the measured value 1.7 MW. Simulation of a real car park calculated by TNO (VESTA) and LABEIN (FLUENT) shows the air entrainment existing at the fire source (cars) is very strong and does not allow the ventilation control. This interesting car fire test n°6 was not representative of the car fire in a large closed car park, but representative of an individual garage.

So it was decided to perform other tests which are more representative of a car fire in a closed car park :

* cars from 90ths,
* configuration with only one wall simulating one of the four walls of the closed car parks.

The tests n°7 and n°8 in such configuration have been performed with new cars, made in 1995. Tyres placed near the cars show the fire propagation from one car to another. Even, the tests have shown that energy released by car made in 1995 are twice than the energy released by cars of 80ths, but in a same fire duration.

So the rate of heat release measured during the test n°7 with a large new car can be the reference heat release rate-time curve of the one car fire. This can be seen in the figures 3.16 and 3.17 showing the rate of heat release curves of car fire involving only one car measured during CTICM car fire tests and obtained in the literature respectively.

These last curves come from Finland, UK and Germany. The Finland curve is an average curve deduced from tests in VTT, the UK curves are deduced from tests performed in France by the Fire Research Station and the German curve comes from a private communication with Professor Schneider.
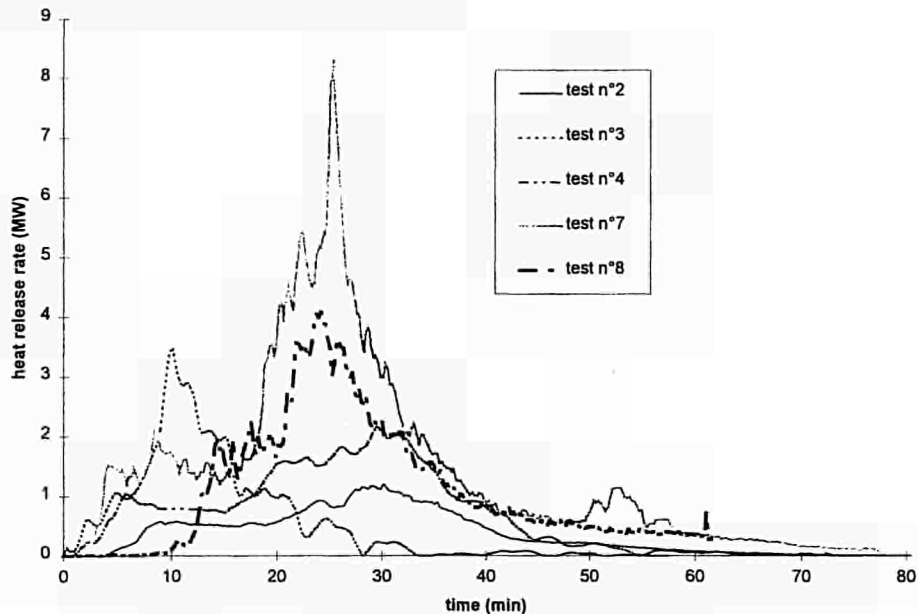
Figure 3.16 :   *Rate of heat release of car fire involving only one car measured in CTICM car fire tests*
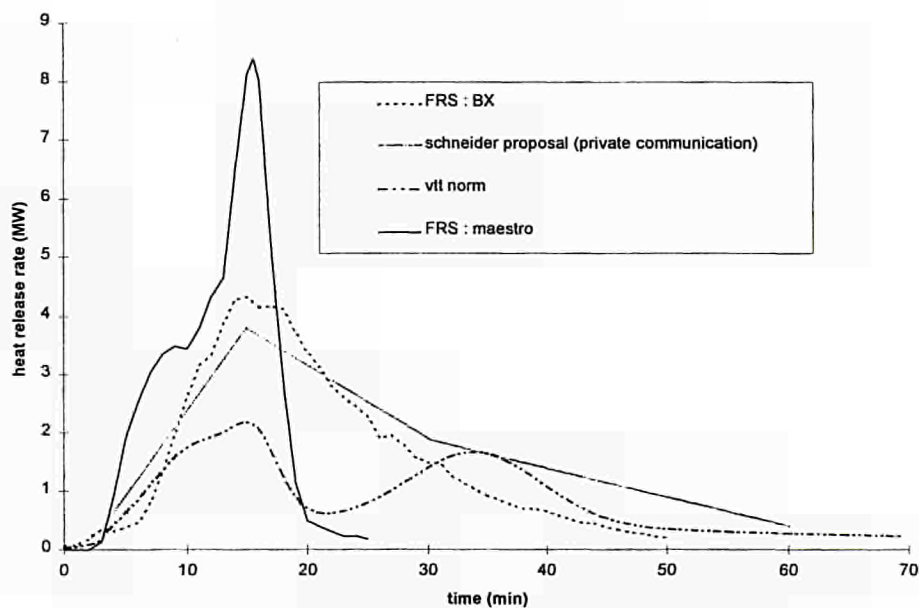
Figure 3.17 :   *Rate of heat release of car fire involving only one car available in the literature*

A fire propagation from one car to another has a probability of occurrence that may not be neglected. Nevertheless, the rate of heat released by the fire of one car burning alone is not the rate of heat released by the car fire coming from a fire propagation.

In order to estimate this difference, another test has been performed, the test n°9, involving two cars similar to the cars of tests n°7 and n°8.

The figure 3.18 shows the rate of heat release measured during the tests n°7, n°8 and n°9.

The figure 3.19 compares the heat released during the test n°9 but considering a contribution of the petrol normally contained in the tank and the simple addition of the rate of heat release measured during test n°7 with the heat release of the test n°8 in which a delay of 8 minutes is added in order to take into account the fire propagation time.
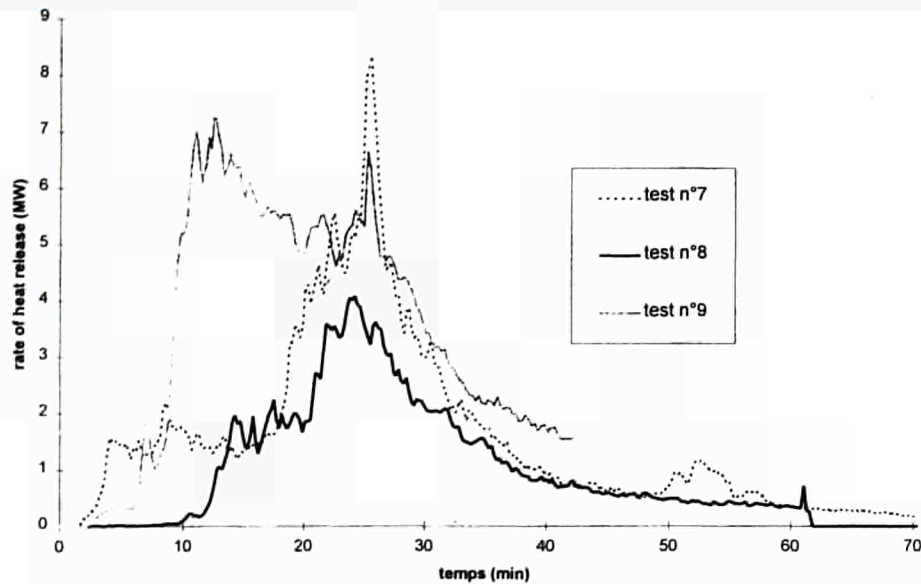
Figure 3.18 : Rate of heat release measured during tests n°7, n°8 and n°9
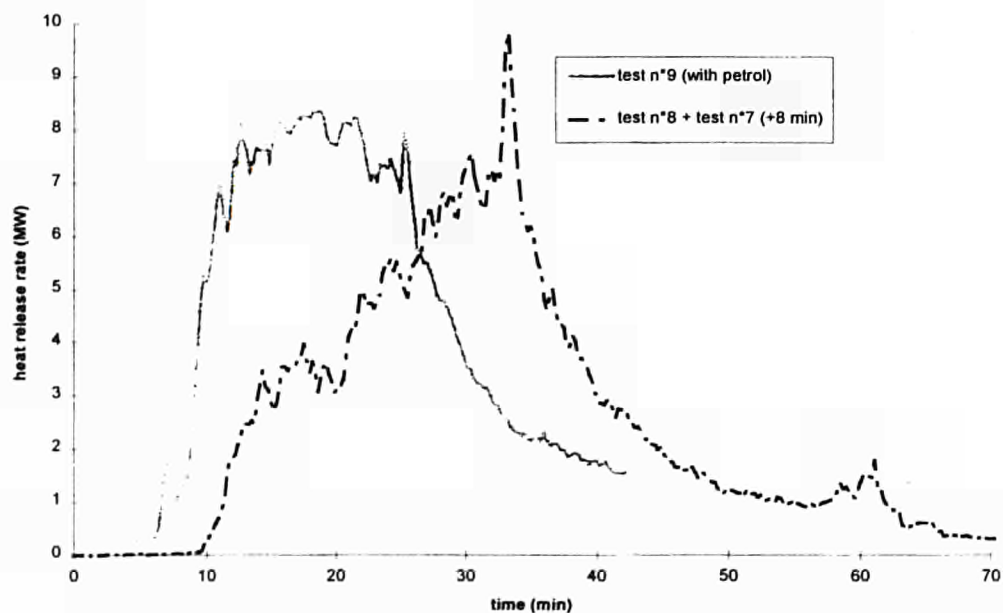
Figure 3.19 :   Comparison between rate of heat release of test n°9 and addition of heat release rates from test n°8 and from test n°8 (taking into account of 8 minutes of delay for propagation time)

31

In order to understand the different combustion process occurring during the test n°9 comparing to the test n°7 and n°8, the mass loss rate of the cars is compared in figure 3.20 and figure 3.21 for the large car and the small car respectively. This can be done thanks to the independent weighing platforms used in test n°9 for the two cars.

The figure 3.20 shows the large car fire has the same duration in the test n°7 than in the test n°9. This can be explain by the pre-heat of the car during the test n°9 which allows an acceleration of the combustion process.

The figure 3.21 shows the small car fire seems to be the same in both tests, but just a quicker ignition occurs during the test n°7. This fast ignition is not explainable, but the development of the fire is the same after this ignition. So it exists only a decay of 7 minutes during the both fire development.
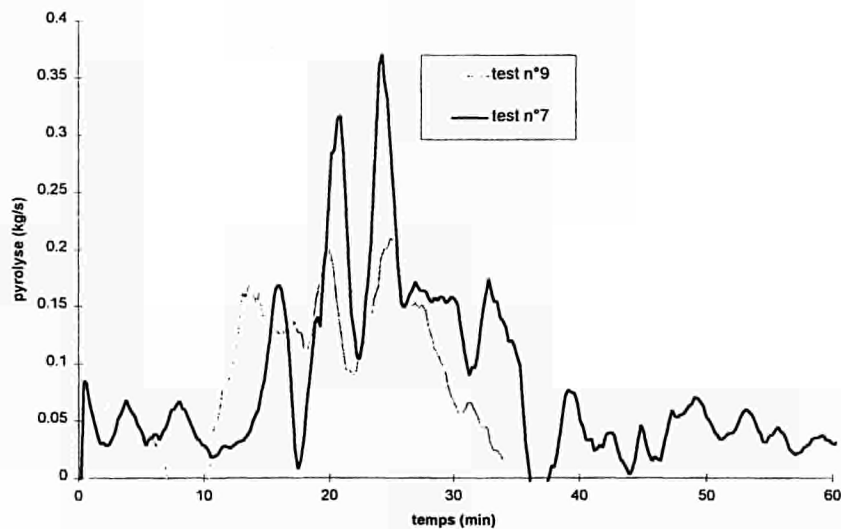
Figure 3.20 : Comparison of mass loss rate of the large car during test n°7 and test n°9
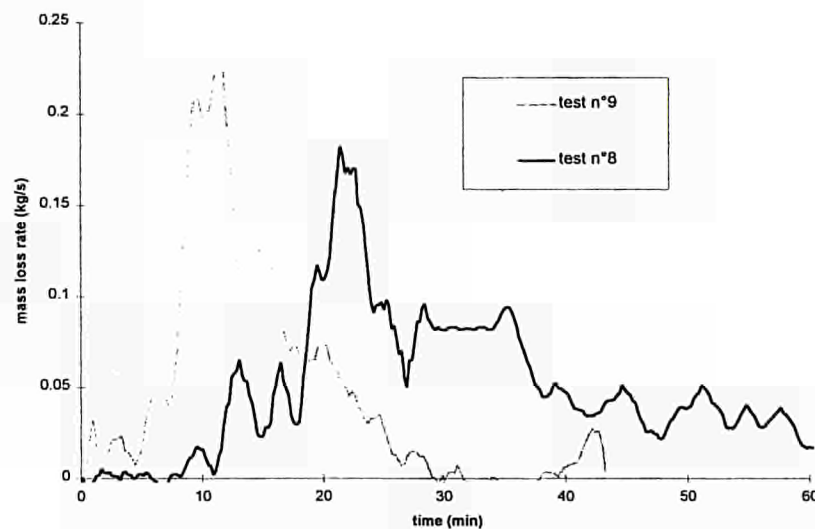
Figure 3.21 : Comparison of mass loss rate of the small car during test n°8 and test n°9

32

According to the mass loss rate comparisons, a comparison between heat release rate of tests n°7 and n°8 with test n°9 can be made with some correction of the heat release rate of tests n°7 and n°8.

In fact, the decay of 7 minutes is done on the heat release rate curve of small car fire of test n°8. This decay is shown on figure 3.22. The pre-heat of the large car during the test n°9, can be evaluated in the test n°7 with addition of the heat released during the first 8 minutes with the heat released the period of 8 minutes to 16 minutes. This new curve can be seen in figure 3.23.

The addition of the both new curves deduced from tests n°7 and n°8 can be compared with the heat release rate measured during test n°9 (with the petrol contribution). This comparison is made in figure 3.24.
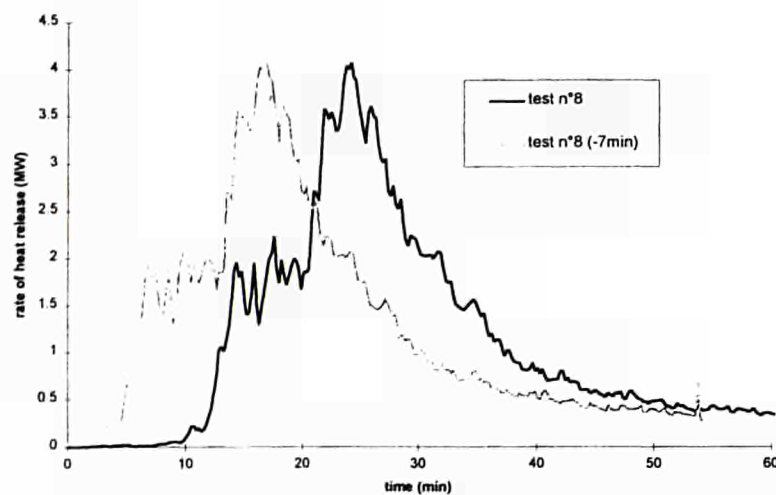
Figure 3.22 : Heat release rate during test n°8 : decay of 7 minutes
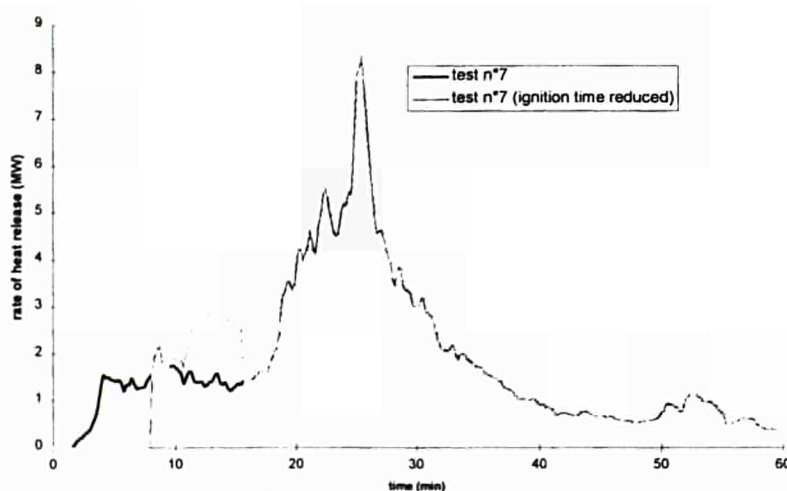
Figure 3.23 :   Heat release rate during test n°7 : pre-heat process inducing an ignition time reduction
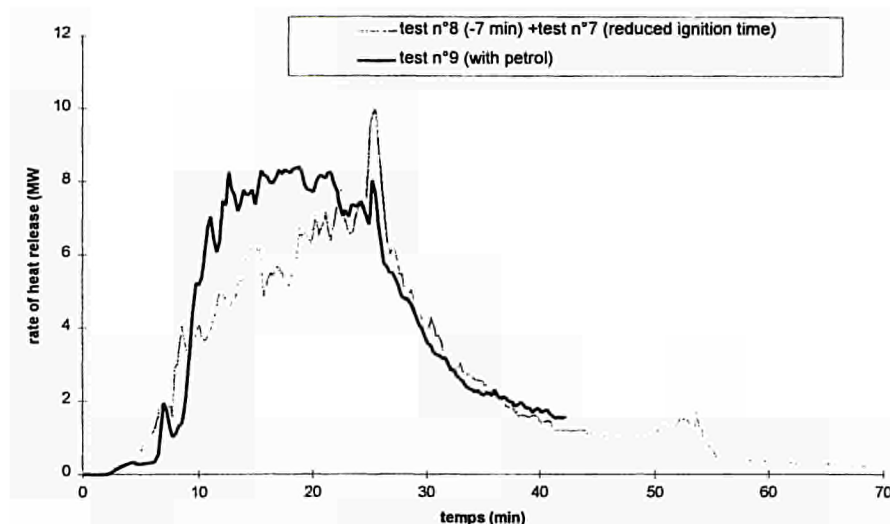
*Figure 3.24 :   Comparison of the heat release rate from test n°9
and from modification of tests n°7 and n°8*

Reference curves for fire safety engineering

The conclusion hereinbelow allows to deduce a reference curve of heat release rate representing a car fire in a closed car park.

In the case of only one car is involved in the fire, a reference curve is deduced from the test n°7. This reference curve is defined by the couples (time, heat release rate) given in the table 3.17 and is shown figure 3.25. The global energy released is 6.8 GJ.

According to all the rate of heat release measured by tests coming from CTICM or published in literature, this reference curve gives the highest values. This can be seen in the figures 3.26 and 3.27 in which all the results are shown (a decay of the curves has been done to compare the results).

time (min)	heat release rate (MW)
0	0
4	1.4
16	1.4
24	5.5
25	8.3
27	4.5
38	1
70	0

Table 3.17 : Reference curve of heat release rate of one car fire

34
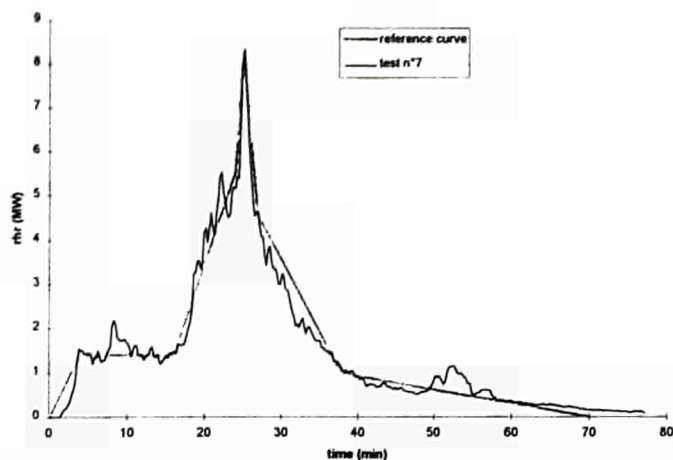
Figure 3.25 : Reference curve of heat release rate of one car fire and test n°7 curve
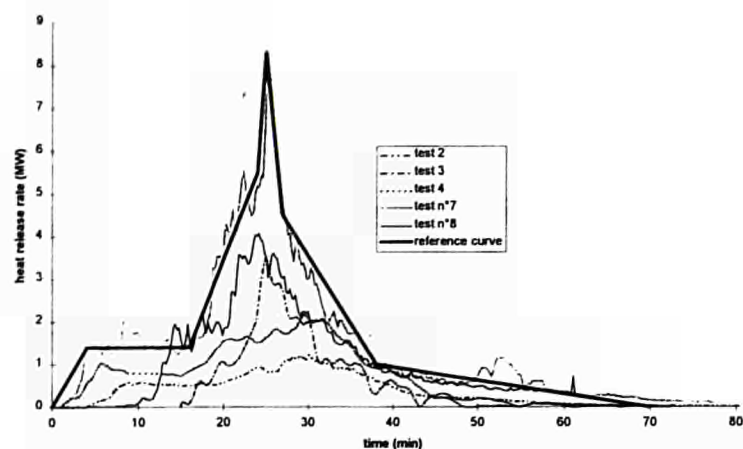
Figure 3.26 : *Comparisons of the reference curve with the heat release rate of one car fire measured during CTICM car fire tests*
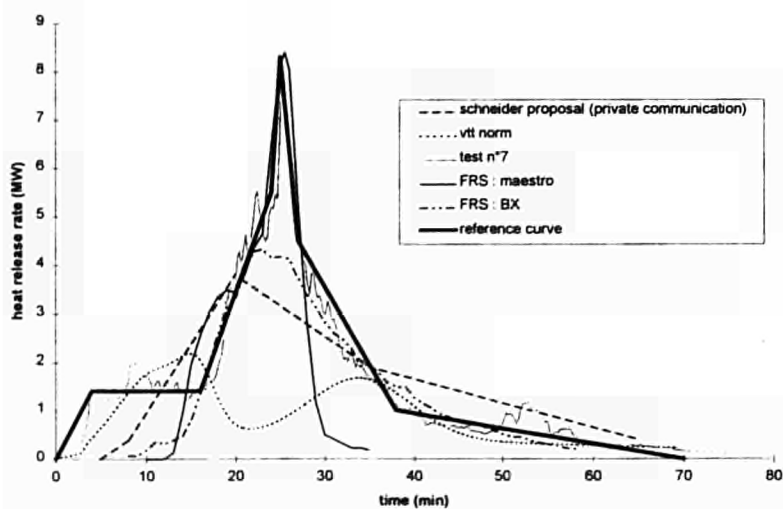
Figure 3.27 : *Comparisons of the reference curve with all heat release rate of one car fire of the literature*

35

In the case of a car fire propagation, the heat release rate of the car submitted to the fire propagation is deduced from the modified heat release curve of the test n°7 shown figure 3.23. This reference curve is defined by the couples (time, heat release rate) given in the table 3.18 and shown in figure 3.28.

time (min)	heat release rate (MW)
0	0
8	0
9	2.4
18	2.4
24	5.5
25	8.3
27	4.5
38	1
70	0

Table 3.18 : Reference curve of heat release rate from fire propagation
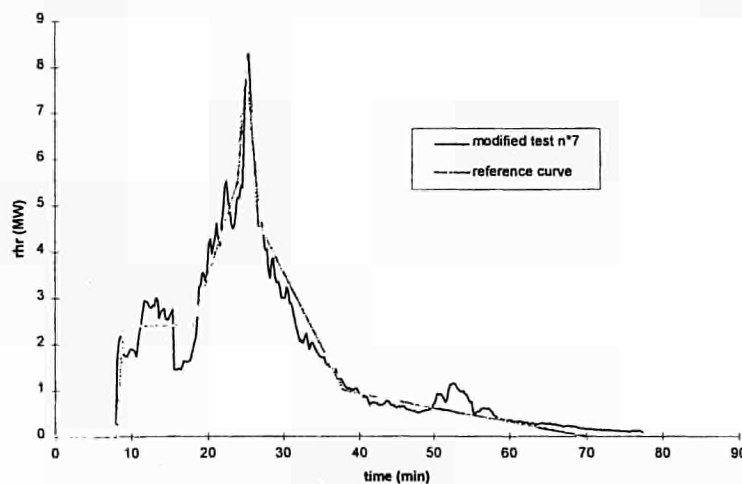
Figure 3.28 :   *Reference curve of heat release rate from fire propagation and the modified test n°7 curve*

3.2.3. TNO full scale test

A. Introduction

A large number of carparks in Amsterdam will be destroyed to make way for the building of new residential buildings. This was a good opportunity to have a real scale car fire test in a (semi-) closed carpark.

The test has been performed on the 22 of May 1996, in the carpark « FEERDE » in the South-East part of Amsterdam.

The carpark was designed as an open carpark, but for reasons of comfort the carpark was converted into a (semi-) closed carpark by installing glazing.

36

The dimensions of one level of the carpark are roughly 55m x 85m with a height of 3.0m; the carpark is made of concrete floors and beams (prestressed elements). The floor of the carpark is not horizontal; the slope of the floor is about 1.25, along the length of the carpark.

B. Test set-up

Global description

The test was done with three 'used cars' standing next to each other in adjacent parking bays, see figure 3.29. The cars were arranged for by the local governement, and were of considerable age (over 10 years old).

> Car n°1:   DATSUN STANZA
> Car n°2:   FORD FIESTA
> Car n°3:   OPEL RECORD

Car n°1 was the middle car and was ignited (see figure 3.29 A and B).

The parking distance between the cars was 0.5m and 0.7m (resp. 75 and 35 percentile : see figure 3.30). This figure is obtained from the statistical survey carried out for this CCP project on parking distances in carparks (see chapter 3.1). The fuel tank of the car number 1 was on the same side than the car number 2.

The cars were placed in one segment next to a wall of 7.5m width (see figure 3.29). The beams under the ceiling in the carpark from a kind of smoke reservoir of 17.5 x 7.5 wide and a depth of 0.8m under the ceiling.

To make the test as close to reality as possible, the car have not been prepared. The fuel tank of the center car was filled to about 50% (approx. 30 liter). In the other two cars the fuel tanks were filled with about 10 liters of fuel.

Ignition of the fire

In the tests a small steel tray filled with approximately 0.5 liter of fuel was positioned just beneath the driver seat and was ignited to start the fire. The amount of fuel is choosen to ensure good ignition, with as little fuel as possible. This amount of fuel can be neglected relative to the total amount of combustibles in the car.

For the development of the fire in the car where the fire is started, the ventilation conditions (windows opened/closed) are important. The ventilation conditions in the car to be ignited was varied until a satisfactory fire in this car was obtained in the 2nd test (i.e. flash-over is reached).

TEST 1 = In the first test the windows of all cars were closed. The aim of this test was to verify the often used assumption that a fire that starts in the passenger

compartment will not reach flash-over if the windows are closed; the reason for this being the lack of oxygen.

TEST 2 = This test was done because the fire in test 1 died. Since very little damage was done to the ignited car in test 1, the same car was used for test 2. In this test the two side windows of the middle car will be half-opened. In these conditions enough oxygen was available for the fire to reach a fully involved stage.

Measurements

Temperatures:
A number of 'thermocouples trees' was placed under the ceiling to measure temperatures under the ceiling oh the carpark at three levels (approx. 0.05; 0.5 and 1.0m beneath the ceiling). Three extra thermocouple tree was used to measure the temperature inside car n°1 and 3.

Heat flux:
Car n°2, closest to the middle car (0.5m distance) is fitted with three water cooled radiant fluxmeters to measure the heatflux. Two radiometers were directed to the fire; they were positioned flush with the car-body, just below the sidewindow (signal str2) and just above the rear tyre (signal str3). With these two meters the radiation of the fire was measured. The third meter (signal str1) was placed in the roof of car n°2 -flush with the roof- directed to the ceiling, to measure the radiation from the hot gases and ceiling.

Mass loss:
The middle car that was set on fire, was put on a weighing platform to enable measurement of the rate of mass loss during the test, giving an estimate of the actual rate of heat release. The mass of the other cars was not be measured. The measurement of the mass of car n°1 did not give consistent results during the test, presumably due to a failure in the connection to pressure measuring devices. No realistic value of the rate of mass loss (ks/s) during the test can be obtained.

Video/photo:
With a video cameras the test was recorded. Photos were taken during the test.

C. Results of the experiments

Test 1:
The test with all windows of car n°1 closed, showed the exact effect as expected. The fire died down within 3 minutes after ignition due to a lack of oxygen in the car. In the car n°1 the temperature was measured at two positions, just below the ceiling right above the fire (signal car7), and on the passenger seat (signal car9).

In figure 3.31 the measured temperatures are given. The temperature reached a maximum of 500°C. This temperature is high enough to result in sustained flaming, so the lack of oxygen makes the fire die. After this test 1 inspection of the car n°1 showed that no

significant damage was done to the interior of this car. Because of this the same car was used for test 2.

Test 2:
For this test a window on both sides of car n°1 were opened for about 50% to ensure sufficient oxygen to sustain the fire.

The graphs of the temperature measurements are given in the annexe.
Figure 3.31 :   Temperature in car n°1. Test I
Figure 3.32 :   Temperature in car n°1. Test II
Figure 3.33 :   Temperature above car n°1. Test II
Figure 3.34 :   Temperature just beneath the ceiling at various positions. Test II
Figure 3.35 :   Heat flux measured at three positions on car n°2. Test II

Time [min]	Observation
0	Ignition of test II
4.5	Left rear window of car n°1 collapses
5.5	Explosion heard in car n°1, presumably the fuel tank
7.5	Rear window of car n°1 collapses; car n°1 fully involved in fire
8	Car n°2 ignites; side window rubber and tyres are burning
12	Car n°2 side window collapses; flaming from window
14.5	Flames from car n°1 reach the body side of car n°3; three cars surrounded flames; no clear view available due to smokelogging
16	Start of extinguishing by the fire brigade : END OF TEST

Table 3.19 : Observations during the test II

During the time at which only car n°1 is significantly on fire (the first 9 minutes after ignition) the heat flux to the side of car n°2 is farely constant at about 20 - 30 kW/m^2. The radiation from the smoke layer in this period is less than 5 kW/m^2, and will have little effect on the spread of fire (see figure 3.35).

The temperature in the car n°1 (ignited) range from 800 to 1000°C in the first 9 minutes after ignition. Only after the three cars become surrounded by flames, the maximum temperature in the car n°1 rises to 1200°C (see figure 3.34).

D. Discussion and conclusion

At the start of this project a survey was done on available international statistics on carfires in carparks. The survey showed that the fire does seldom spread to other cars; in most fires only one car was on fire.

Recent information has come available about real fires in carparks, in which more than one car were involved in the fire. Also the results of recent experiments ('95/'96) with cars carried out at CTICM in a calorimeter set-up, show that a spread of fire to adjacent cars can occur. The test in Amsterdam in a real carpark (reported here) is intended to check if the fire will spread in case of a carfire in a real carpark. If the fire does spread, the test should give information about the speed at which the fire spread from one car to another.
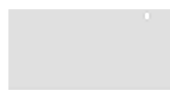
The test results show that in a semi-closed carpark with large dimensions (85x55x3m) made of non-insulated concrete walls and ceiling, a fire can spread from one car to another. If the fire starts in the passenger compartment with all windows closed the fire will die, due to a lack of oxygen. If the fire starts in the passenger compartment with a window opened, the fire will reach flash-over in the car, and can spread to an adjacent car. During the test the spread of fire occured to the car that was closest (0.5m) to the ignited car. Because of the 'open' structure of the motor compartment, a car fire starting in this compartment is not expected to die due to lack of oxygen; such fires could be compared to the situation of a fire that starts in the passenger compartment with the side-windows opened.

The fire test reported here (test 2) shows that within 8 minutes after ignition of the first car the outside (window rubber and the tyre) of the second car starts to burn. Within 12 minutes after ignition the interior of the second car becomes involved in the fire. About 15.5 minutes after the ignition of the fire, the flames from car n°1 reach the bodywork of car n°3; all cars are involved in the fire. At this moment the visibility was very poor due to smoke logging. About 17.5 minutes after ignition the fire brigade started extinguishing the fire.

Conclusion

The assumption that in case of fire in large carpark in most cases the fire will be restricted to only one car can no longer be used.

The assumption that the spread of fire to the second car occurs only after the first car is largely burnt-out should be used with care; spread of fire can occur earlier, possibility depending on the actual parking distance. This can lead to progressive spread of fire to a number of cars, that can be only contained by active measures (i.e. detection, sprinkler, fire brigade).

Figure 3.29A :   Front view of the cars in the car park, with the numbering of the cars; car n°1 was ignited
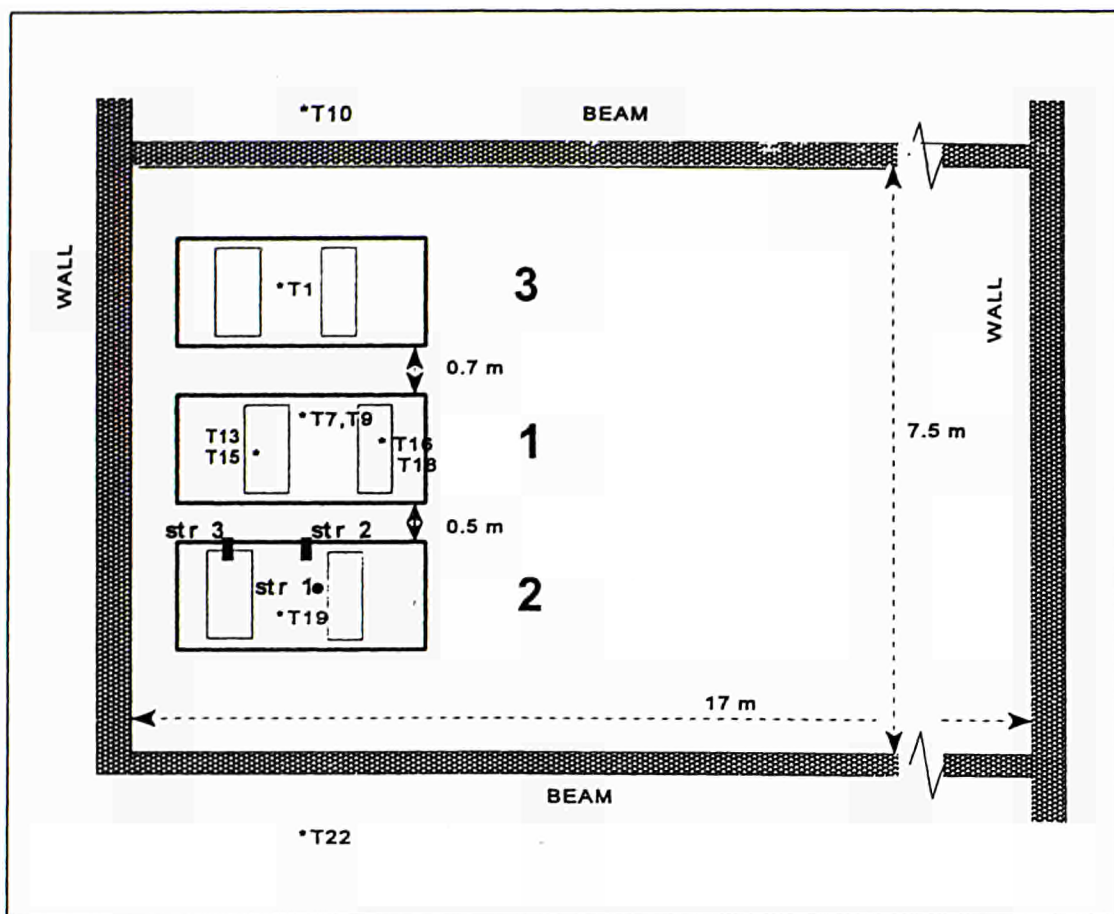
Figure 3.29B :   *Top view of test section of the car park, with the location of the thermocouples and radiometers (not on scale)*
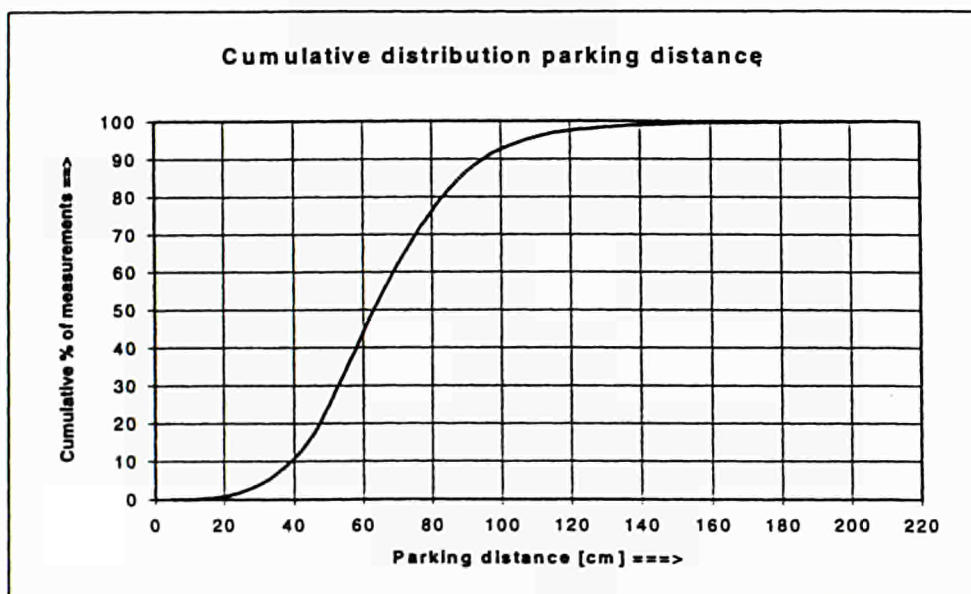
Figure 3.30 :   *Distribution of parking distance in car parks. Cumulative percentage of all measurements*

41
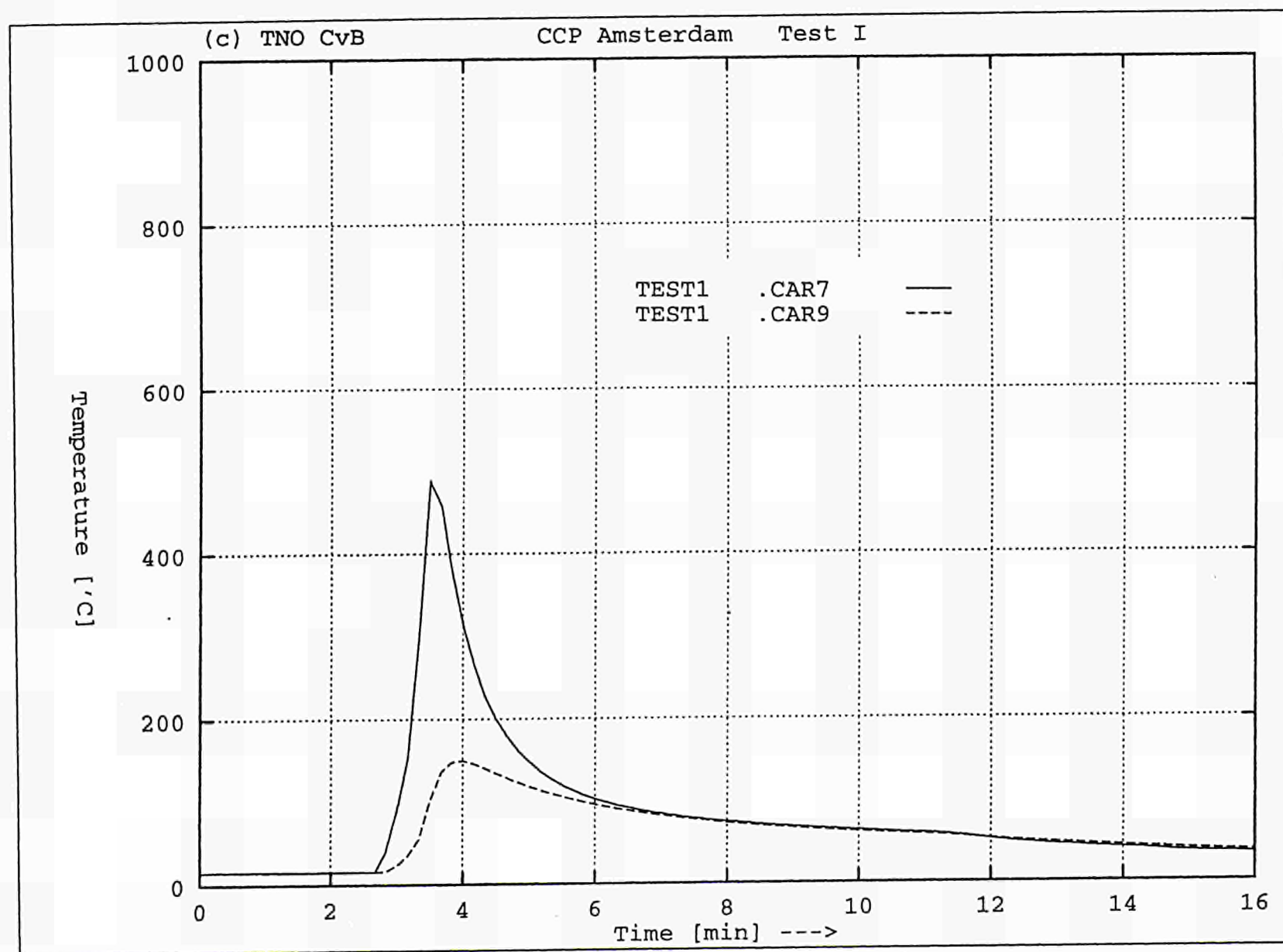
Figure 3.31 : Temperatures in car n° 1
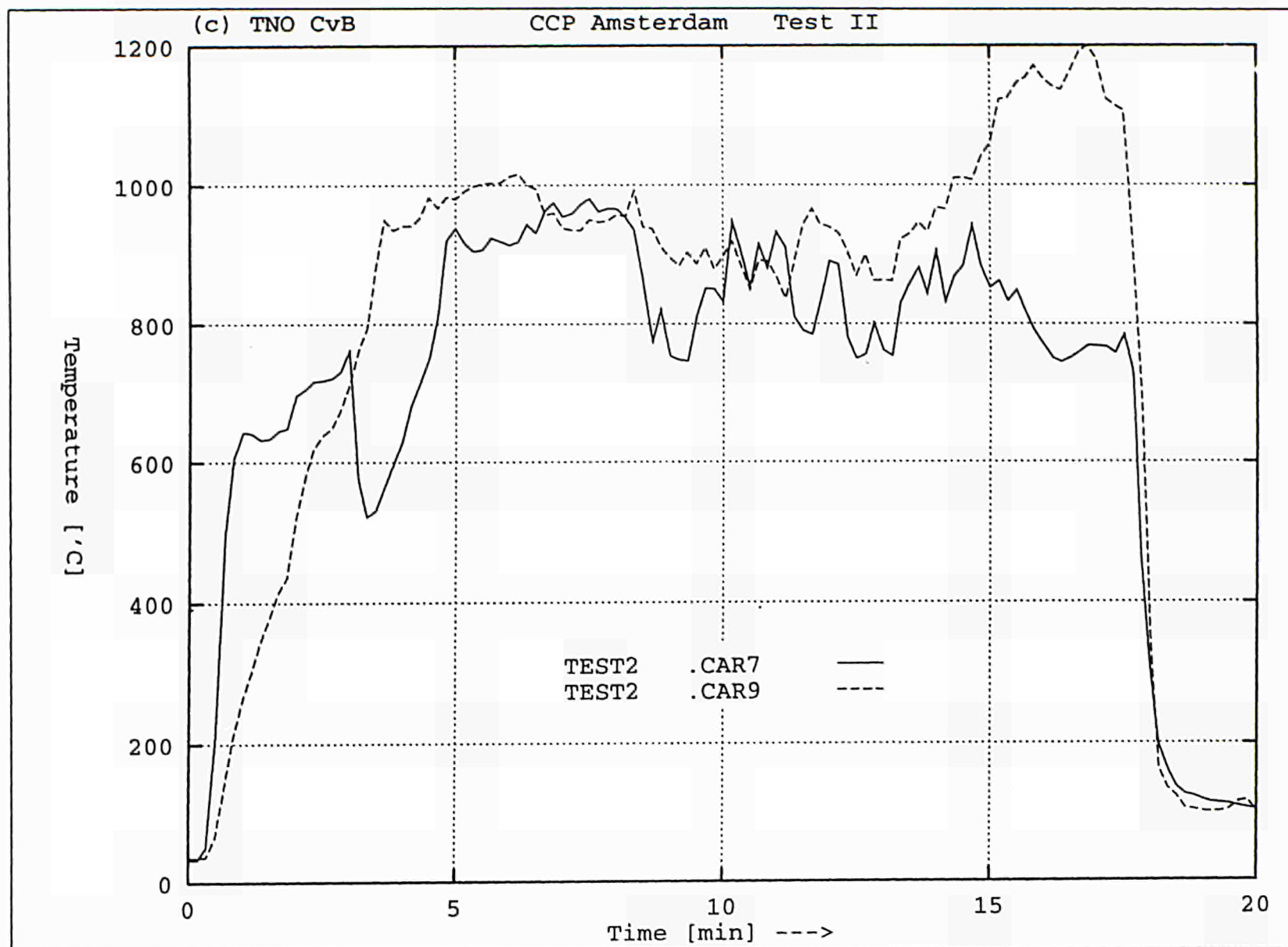
Figure 3.32 : Temperatures in car n°1

43
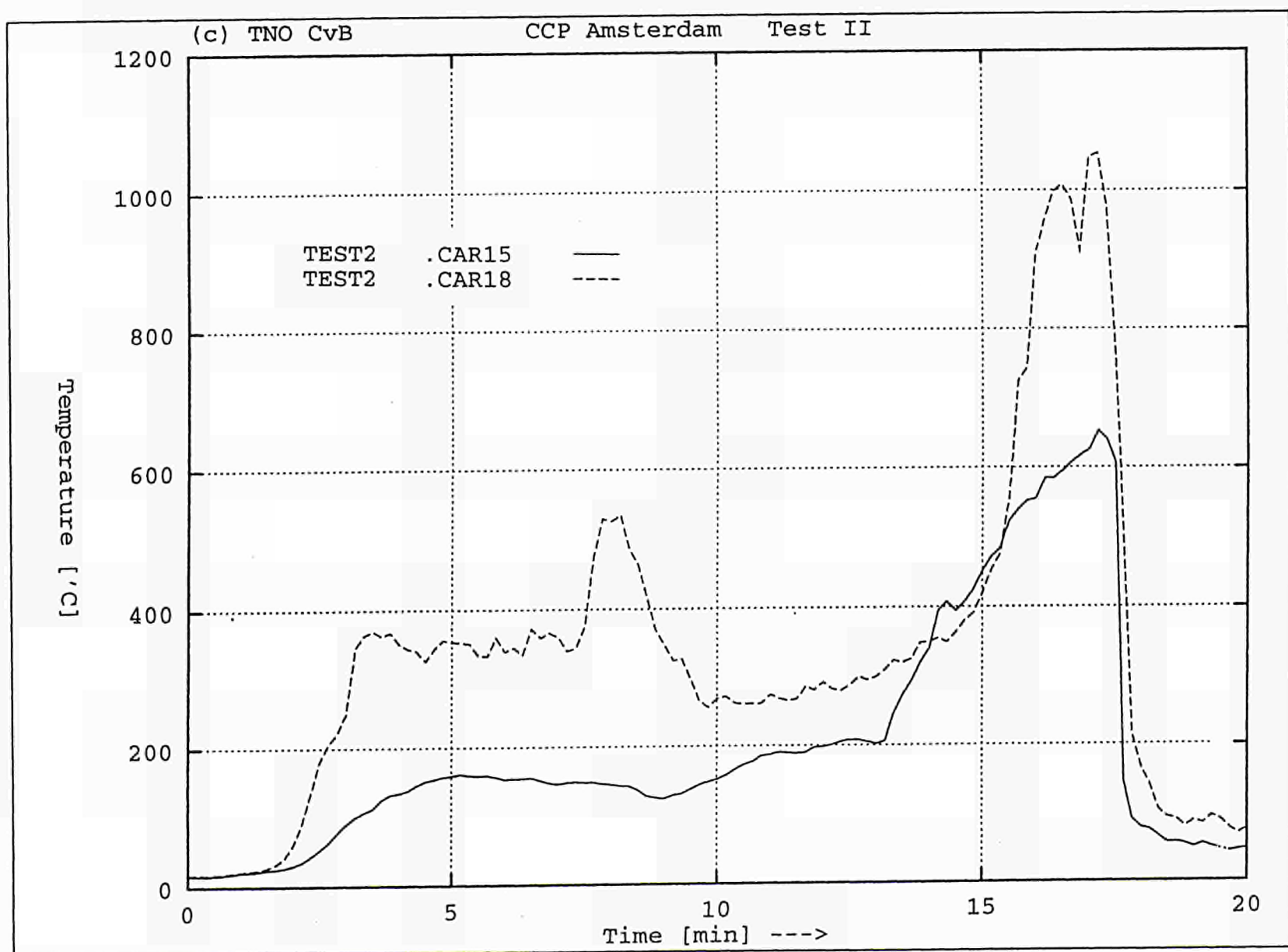
Figure 3.33 : Temperatures above car n°1 - Position just above front (15) and rear (18) window

44
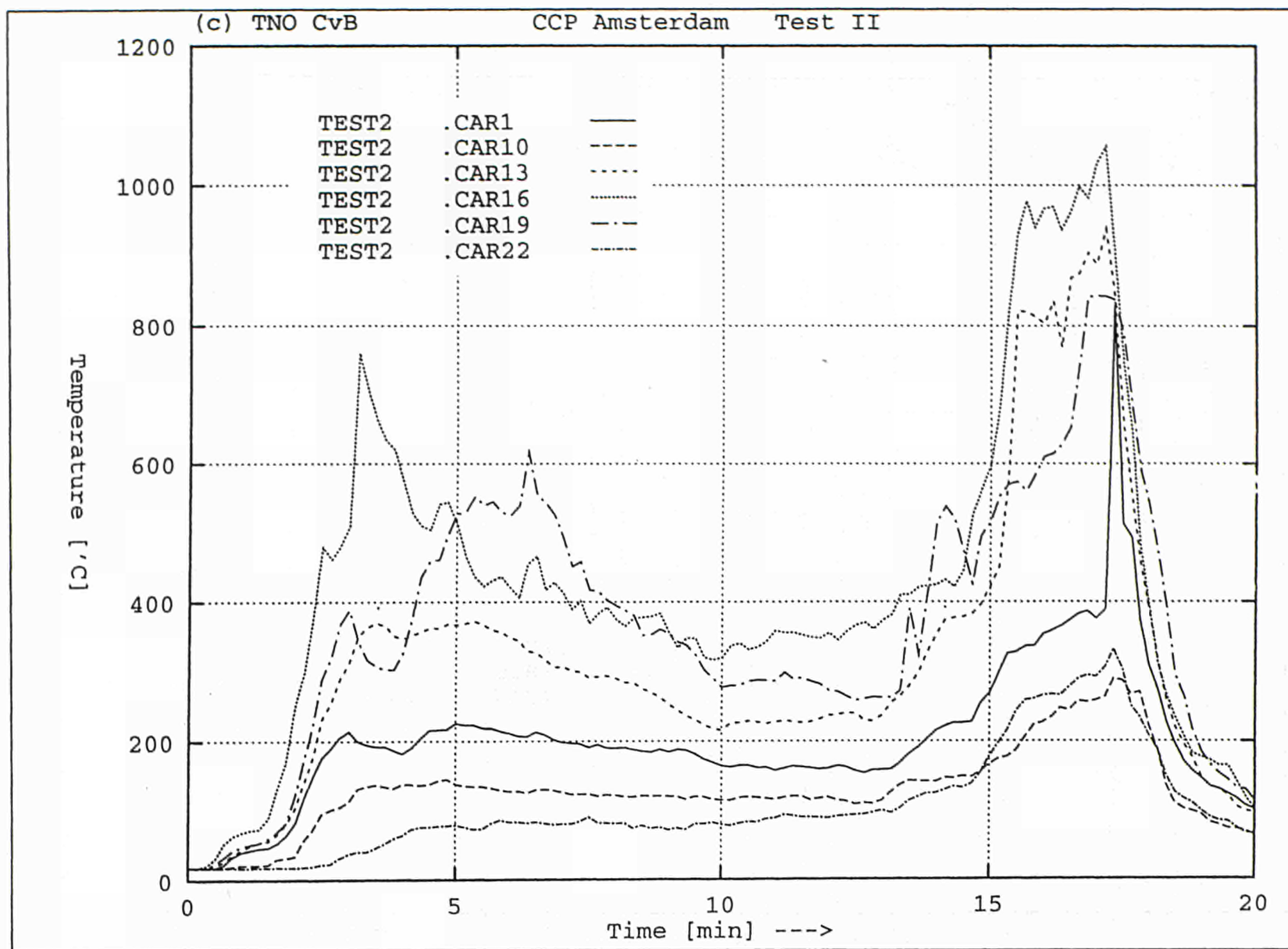
Figure 3.34 : Temperatures just beneath the ceiling
Various positions

(c) TNO CvB   CCP Amsterdam   Test II

Heatflux [kW/m2]

TEST2   .STR1   ⎯⎯⎯
TEST2   .STR2   ⎯ ⎯ ⎯
TEST2   .STR3   ⋯⋯⋯

Time [min] --->
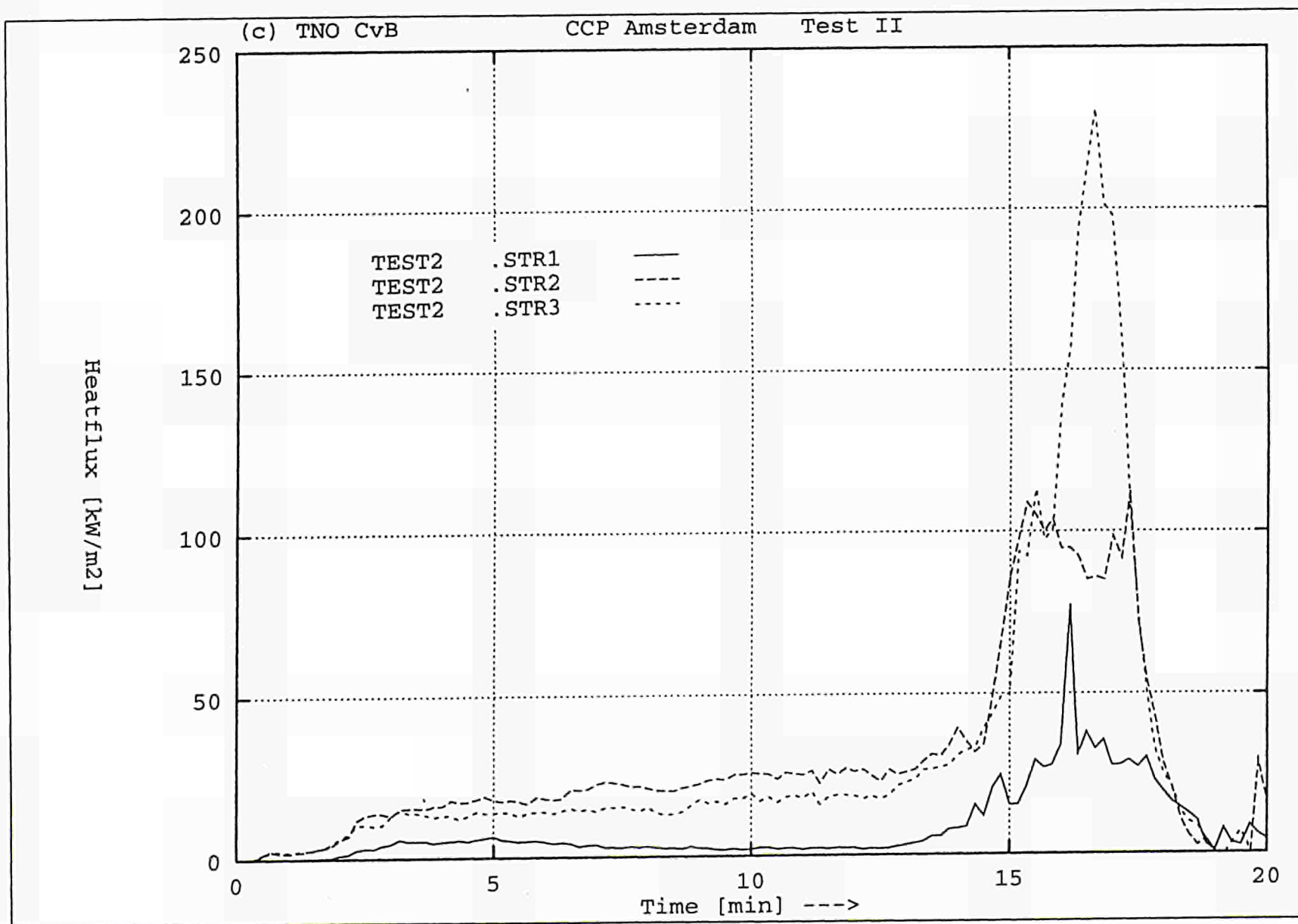
Figure 3.35 :   Heat fluxes on car n°2
Str1 = roof ; Str2 and Str3 sidebody of car

46

3.3. Fire spread time

Statistical data

Over 1.4 million fires are estimated to occur in the United States each year. Of these approximately 450 are parking garage fires. There has been a study carried out in which 404 car park fires have been studied over the period of time 1986-1988. This report is entitled- Parking garage fires (A Statistical Analysis of Parking Garage Fires in the United States: 1986-1988)[25].

These 404 charted fires in this study occurred in over 100 cities in 30 states. The types of these garages were different in most of the cases (even if the difference is minimal) and the level at which the fire occurred varied from the fourth level below ground level to the ninth level above.

For the spread of the fire, fire did not spread from the vehicle in 93% of the incidents. Of all 28 vehicle spread fires it can be seen from results that when some degree of spread does occur it is limited 93% (see Table 3.20 : (18+8)/28 = 93%) of the time to affecting one or two adjacent vehicles. In only two incidents the fire spread to more than two vehicles (the maximum come across is 4 cars in addition to the first ignited car). There are no cases of spread to another level of the garage, or to adjacent buildings. The table 3.20 below shows for the 28 vehicle spread fires, the number of exposure vehicles in spread fires.

Number of vehicles involved by the fire	1	2	3	4	5	Total
Number of incidents	376	18	8	1	1	404
Total %	93	4.5	2	0.25	0.25	100

Table 3.20 : Number of vehicles in spread fires

It can be seen from·this information that the occurrence of spread of fire in car park structures is very rare indeed. This statement is also backed up by many other sources :

The American Iron and Steel Institute has published two surveys of the fire experience in car parks [27,28] The conclusions of these reports were:

- Car parks had an excellent fire safety with no recorded loss of life or injury.
- The building damage reported was minimal with $2000 millions worth of real estate having damage of only $0.13 millions reported.
- No beam, column or floor was replaced as a consequence of fire damage.
- The loss of and damage to cars was minor [In the first report 368 out of 395 fires damaged only one car (93.2%) in the second report 98 out of 105 fires damaged only one car (93.3%)]
- No use of sprinkler systems was reported in the control of any fires.

A more recent study in [28,29] looked at the loss experience in car parks using the National Fire Association analysis of fire losses for the period 1982 to 1986. The car parks considered include underground, enclosed and open deck car parks. The losses are stated to be extremely low. Fires in non-combustible construction had minimal losses, and vehicle fires produced no injuries and very small losses.

A statistical investigation about fire in car parks has been made for the canton of BERN in Switzerland and covers the period July 1986 to December 1992 [5]. Of 36 fires in closed car parks only 6 cases was there reported damage of over 100000 Frs. The total damage value is extremely low compared to the total assured capital. This can be explained by the choice of the building materials (non-combustible), by the fact that very important public car parks are monitored by detectors and of course that the fire is normally limited to one or two cars.

While all the statistical information show that the occurrence of spread of fire in car park is very rare, the results of the recent tests (the Amsterdam test of the 22nd of May 1996 and the CTICM tests described in chapters 3.2.2 and 3.2.3) and some real fires ([29], one in the Netherlands at the end of 96) have pointed out that a multiple car fire scenario may not be excluded and should be accounted for.

In order to take into account the multiple car fire, a "wave" hypothesis has been adopted. This "wave" assumption consists of considering a fire composed of cars which started to burn one after the other with a delay of 12 minutes; this value come from the table 3.5 of chapter 3.2.2 and the chapter 3.2.3. It has to be pointed out that this spread time value is rather conservative as, in the Amsterdam test, the distance between car was only 50 cm, which covers 75% of the cases (see figure 3.30).

As after about 60 minutes the RHR of a burning car is at the end of the cooling phase (RHR < 0.5 MW), the fire spread in a closed car park can be considered as a "wave" of about five burning cars moving in the compartment.

48
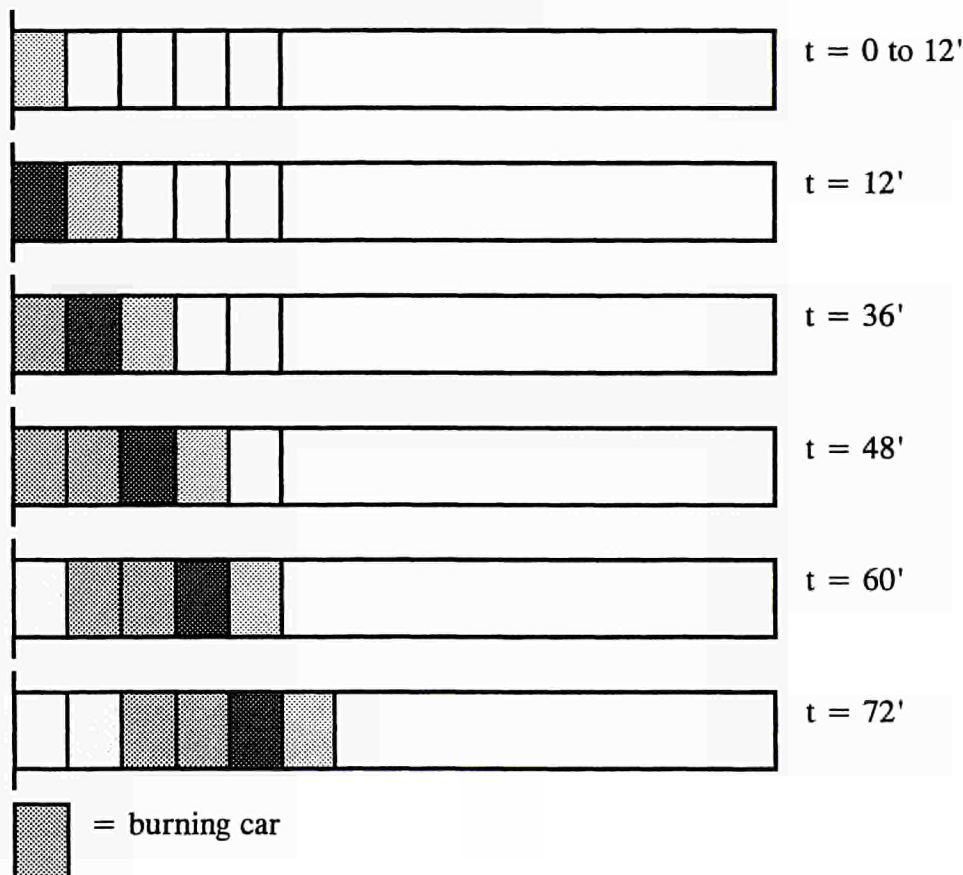
3.4. Rate of heat release : reference curves

3.4.1. Reference curve for one burning car (see chapter 3.2.2)
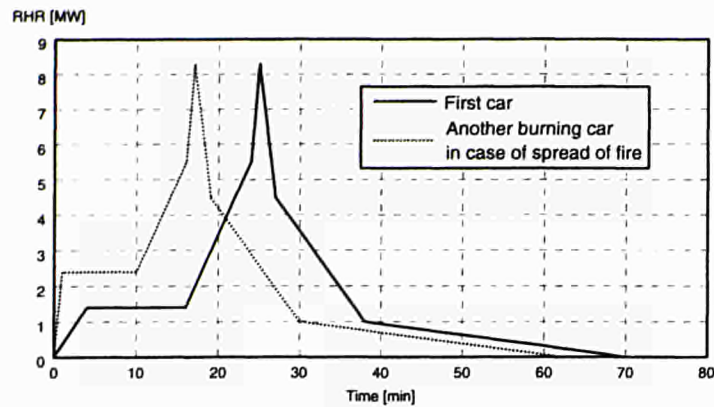
Figure 3.36 : Reference RHR curves for one burning car

Time [min]	First car [MW]	Time [min]	Another car [MW]
0	0	0	0
4	1.4	1	2.4
16	1.4	10	2.4
24	5.5	16	5.5
25	8.3	17	8.3
27	4.5	19	4.5
38	1	30	1
70	0	62	0

Total fire load = 6.8 GJ

Table 3.21 : Reference RHR values for one burning car

3.4.2. Reference curve for one burning car used in the CFD calculation

As the sharp peak of the RHR curve produced some convergence problems for the CFD programs, the following equivalent curve is proposed for CFD users.
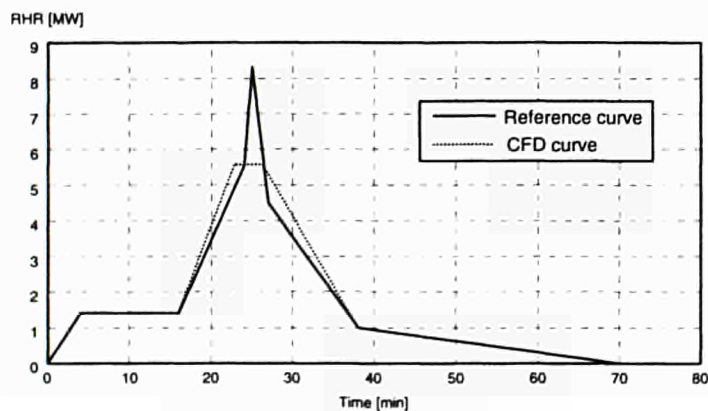
Figure 3.37 : CFD curve

49

Time [min]	CFD curve [MW]
0	0
4	1.4
16	1.4
23	5.53
26	5.53
38	1
70	0

Fire source:
Height = 0.55m
Width = 1.71m
Length = 3m

Total fire load = 6.9 GJ

Table 3.22 : Reference RHR values for one burning car

3.4.3. Reference curve for the wave of burning cars
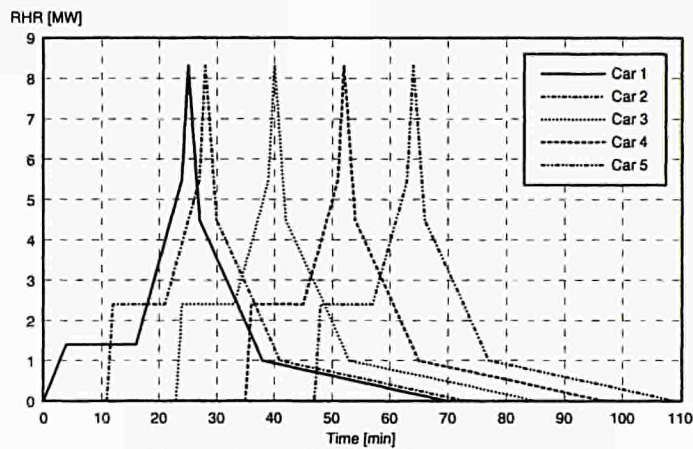
Figure 3.38 : Wave of 5 burning cars

3.4.4. Reference curve for calculation by a two-zone model taking into account the wave of burning cars
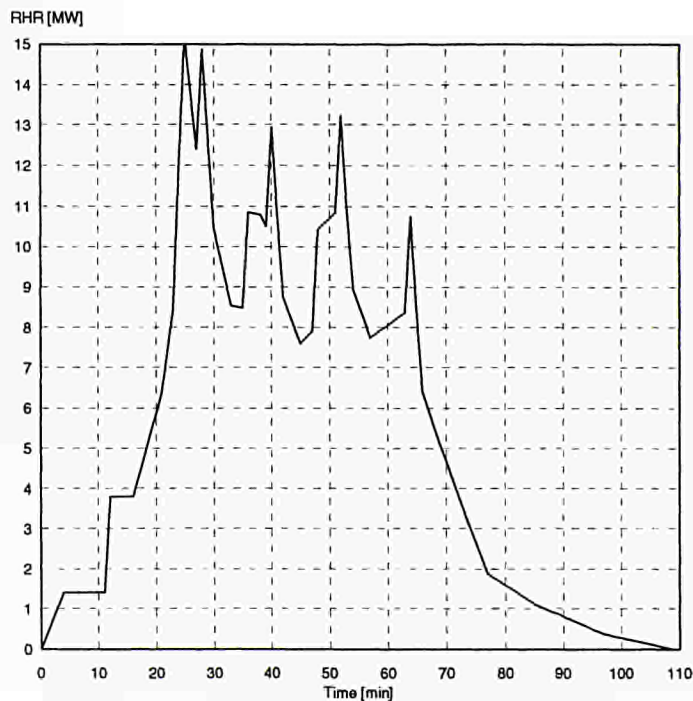
Figure 3.39 : Total RHR curve given by 5 burning cars

50

3.5. Numerical simulations of the tests

3.5.1. Introduction

In the final report of the research 'Natural Fires in Large Compartment' [1], it is described the method to calculate the steel temperature of a beam subjected to a given RHR. This method is a combination of the Hasemi´s model and of a two zone calculation. It has been applied to the CTICM test n°4 in [1] (see chapter 4.5 of [1]). The same procedure has been used to calculate the test n°3 involving one burning car and the test n°9 involving two burning cars. From the total heat flux q'' the net heat flux entering the profile q''_{net} has been deduced

$$q''_{net} = q'' - 25(T_s - 293) - 0,5\sigma(T_s^4 - 293^4)$$

with T_s = steel temperature in [K]
    σ = Stefan-Boltzmann constant.

Then the ENV 1993-1-2 [34] enables to deduce the increase of temperature $\Delta\theta_{a,t}$

$$\Delta\theta_{a,t} = \frac{A_m / V}{C_a \rho_a} q''_{net} \Delta t$$

where A_m/V is the section factor for unprotected steel members [m^{-1}];
    C_a is the specific heat of steel [J/kgK];
    q''_{net} is the net heat flux per unit area [W/m^2];
    Δt is the time interval [s];
    ρ_a is the unit mass of steel [kg/m^3].

3.5.2. One burning car (test n°4)

The data for this calculation are as follows :
- vertical position of the fire source H_s = 0,6 m
- characteristic length of the fire source D = 3,91 m
- height of the compartment H_f = 2,6 m
- beam profile : HEB 300
- section factor used to calculate the steel temperature : A_m/V = 96 m^{-1}
- steel temperature calculated just above the fire (r=0)
- measured Rate of Heat Release given by the O_2 depletion technique
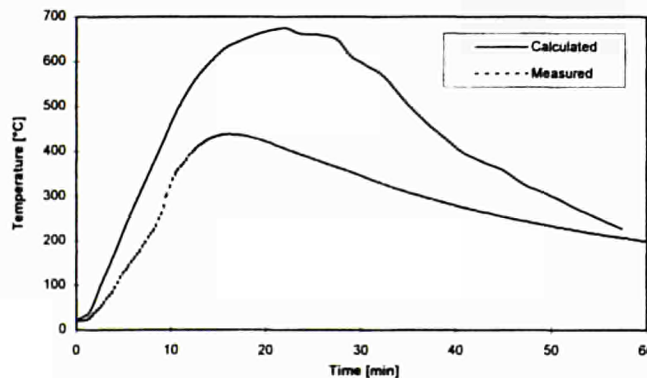
Figure 3.40 : Steel temperature just above the fire as a function of the time

51

3.5.3. Two burning cars (test n°9)

For the test number 9 the steel elements have been put between the two cars (see figure 3.13). The figures 3.41 and 3.42 show the steel temperature as a function of the time and of the radial distance from the fire. In order to obtain these results, the Hasemi's model has been used with the following data for each car :

- vertical position of the fire source H_s = 0,6 m
- characteristic length of the fire source D = 3,91 m
- height of the compartment H_f = 2,6 m
- beam profile : IPE 500
- section factor used to calculate the steel temperature : A_m/V = 132 m^{-1}
- temperature calculated in a beam between the two cars
- measured Rate of Heat Release deduced from the mass losses measurement and a combustion heat of 26,3 MJ/kg

and has provided the heat fluxes q_1'' and q_2'' [kW/m^2] received by the steel elements between the cars and produced by the car 1 and the car 2. These heat flux have been added to obtain a total heat flux q''.
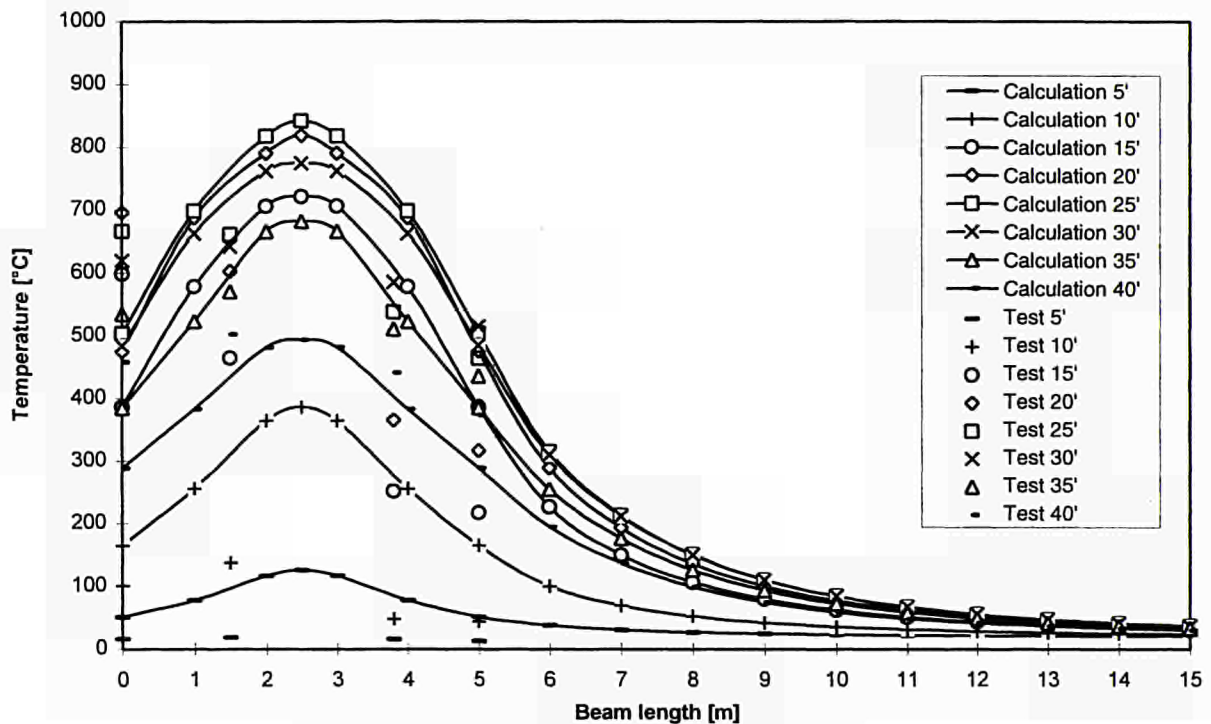
Figure 3.41 : Steel temperature along the beam

52
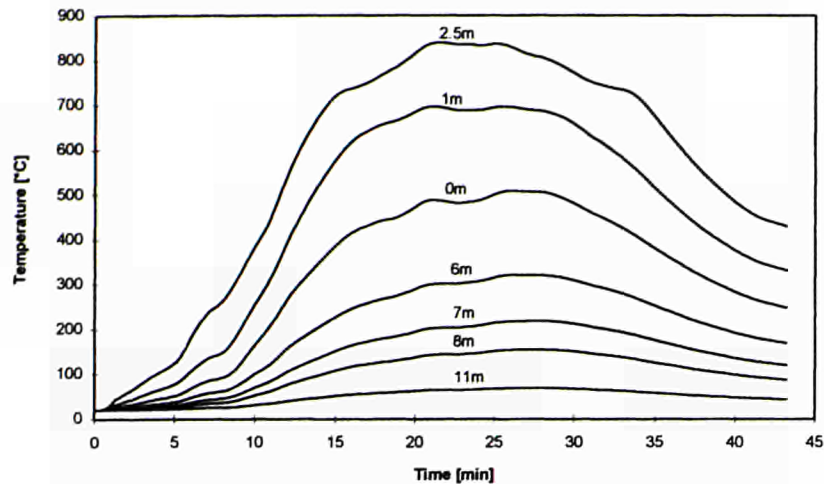
Figure 3.42 : Temperatures at different points along the beam

On the figure 3.41 the calculated temperatures are compared to the measured values which correspond to the maximum temperatures in the two HEB 240 and IPE 500 (see figure 3.13). It has to be noticed that both profiles has the same section factor A_m/V.

The figure 3.42 points out that the calculations are on the safe side compared to the measurements at 1,5m, 3,7m and 5m from the wall but are unconservative for the thermocouples in the HEB240 nearby the wall. That´s why the temperature distribution on the side of the wall has been modified. At a distance of 2,5m from the wall, the temperature curve reaches the maximum θ_{max}. At the wall, it is proposed to adopt a reduction of 10%, this means $\theta_{max} * 0,9$. Between the two positions the temperatures are linearly interpolated as shown by the figure 3.43. In that way, the thermal calculations enables to take into account the influence of the Rate of Heat Release, the height of the ceiling, the height of the beam, the distance from the beam to the fire, the presence of a wall.
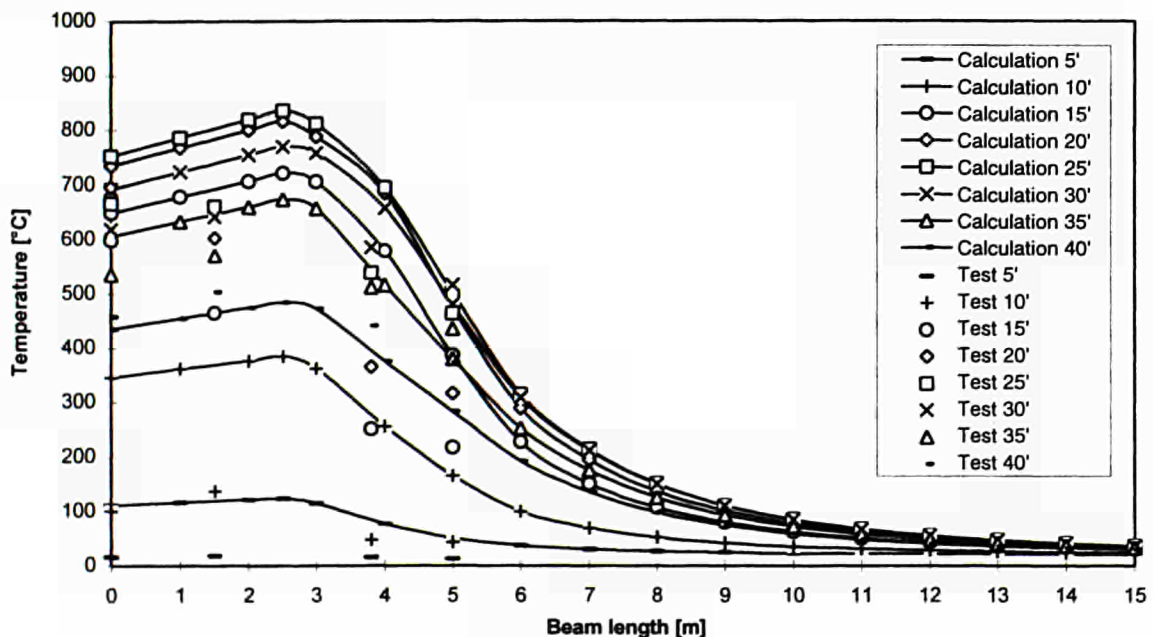
Figure 3.43 : Adjusted steel temperature along the beam

53

3.5.4. Heating of column

The figure 3.43 shows that the maximum temperature of the steel column can be conservatively foreseen. Concerning the evolution along the height of the column, the measurements can be seen on the figure 3.44. The assumption to adopt the calculated top temperature for the whole column is a conservative hypothesis as attested by the figure 3.44.
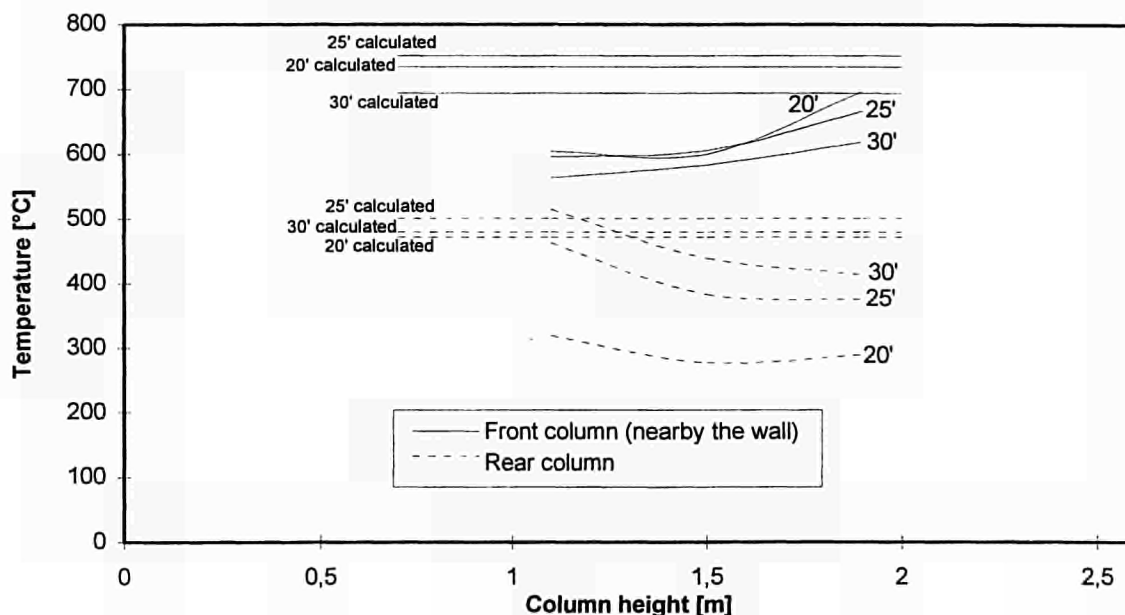
Figure 3.44 : Measured and calculated temperature along the columns for 20, 25 and 30 minutes

3.6. Fire scenarii

In order to define some fire scenarii, a typical car park structure was chosen (see figures 3.45 and 3.46). It corresponds to the car park structure designed according to standards [30] and often met in practice. The usual types of car park structures are described in the ECCS - AC1 document 'Multi-storey car parks' [31].

3.6.1. Dimensions of the structure

The chosen structure (see figures 3.45, 3.46, 3.47 and 3.48) is composed of several rows of three columns joined by two beams of 15.5m span. The cross section of the columns is a HEA 280 section. An IPE 600 connected to a 15cm thick concrete slab forms the composite beams. The distance between beams is 5.0m and the effective width considered in the calculations is 2.4m. The structure was designed according to Eurocodes and optimized in order to be just sufficient to bear the loads with the safety required by the Eurocodes. The details of the calculations which underline that the structure is really not overdesigned is given in [30]. The arrangement of the parking bays is defined by figures 3.45 to 3.48; the parking bays are 5.0m long and 2.5m wide.

3.6.2. Fire scenario 1 (figures 3.45 and 3.46)

The first fire scenario implies only **one car burning at mid-span under the beam**. It corresponds to the maximum bending moment position and so the most critical situation for the beams.

Only one burning car has been supposed because it is not realistic to have simultaneously two cars which are improperly parked, burning, just beneath the steel beam and at mid-span. The RHR curve has been given in chapter 3.4.1.

3.6.3. Fire scenario 2 (figures 3.47 and 3.48)

A wave of burning car has been considered. The time between ignition of the first car and the second car is 12 minutes. Five burning cars have been considered and the RHR curves have been given in chapter 3.4.3.

In case of sprinkler system or a reliable detection automatically connected to the fire brigade combined with sufficient fire fighting devices, the assumption of only one burning car could be adopted. If only one car is burning, the scenario 1 is relevant.

3.6.4. Ventilation conditions

The ventilation can be natural (only for upper groung car park) or forced. The ventilation can be designed to evacuate the CO produced by the running cars (room temperature design) or to evacuate the smoke in case of fire (smoke evacuation design). Concerning the smoke evacuation, the objective could be to guarantee a clear layer of 1.8m during the first 15' for the safety of the occupants and of 1.5m during the whole duration of the fire for the safety of the firemen. We have used the software ARGOS [32] to calculate the mean temperature of the gas and the free zone height for two ventilation cases.

ARGOS results for the Closed Car Park of figures 3.45, 3.46, 3.47 and 3.48		
Fire scenario	Room temperature design	Smoke evacuation design
	12000 m³/h	60000 m³/h
1 (one burning car)	$\Theta_{mean}^{max} = 136°C$ $y^{min} = 0$ m	$\Theta_{mean}^{max} = 134°C$ $y^{min} = 2.3$ m
2 (five burning cars)	$\Theta_{mean}^{max} = 200°C$ $y^{min} = 0$ m	$\Theta_{mean}^{max} = 189°C$ $y^{min} = 0$ m

where y is the height of the free zone

IPE 600

HE 280 A

15.5 m   15.5 m

50 m

5 m   2.5 m   2.5 m

B

A

B

A

Automatic Fire Doors

Ramp

Natural ventilation :
Openings for one level = 2 x 4 x (0.4m x 1.5m)
= 4.8 m² = 0.06 m²/parking bay * 80
or Forced ventilation:
150 m³/h/parking bay = 12000 m³/h
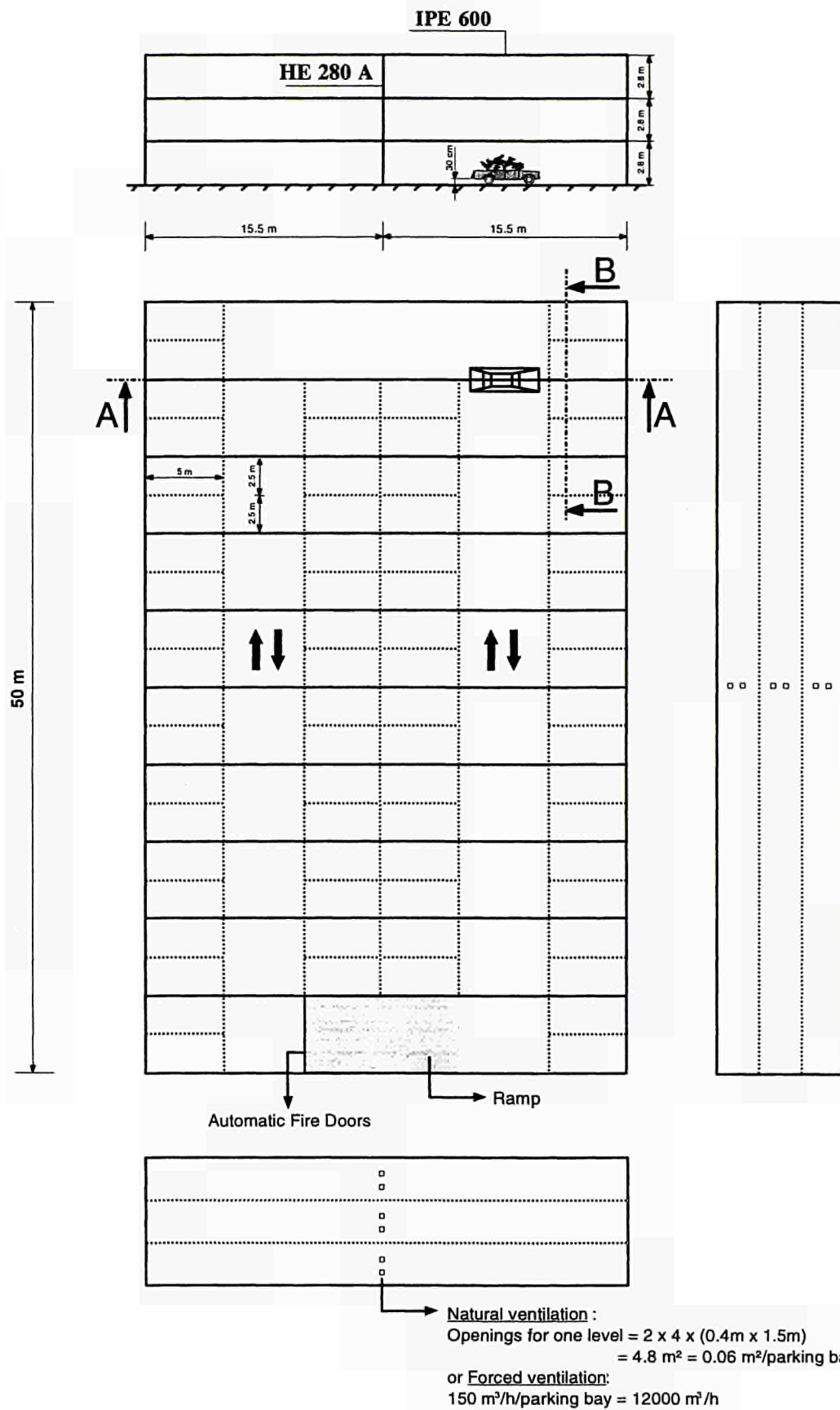
Figure 3.45 : Fire scenario 1

56

top view

5000

5000

2500

A

B

B

A

15500

15500

31000

section A-A

150

slab

IPE 600

2050

15500

150

section B-B

600

2050

5000

5000
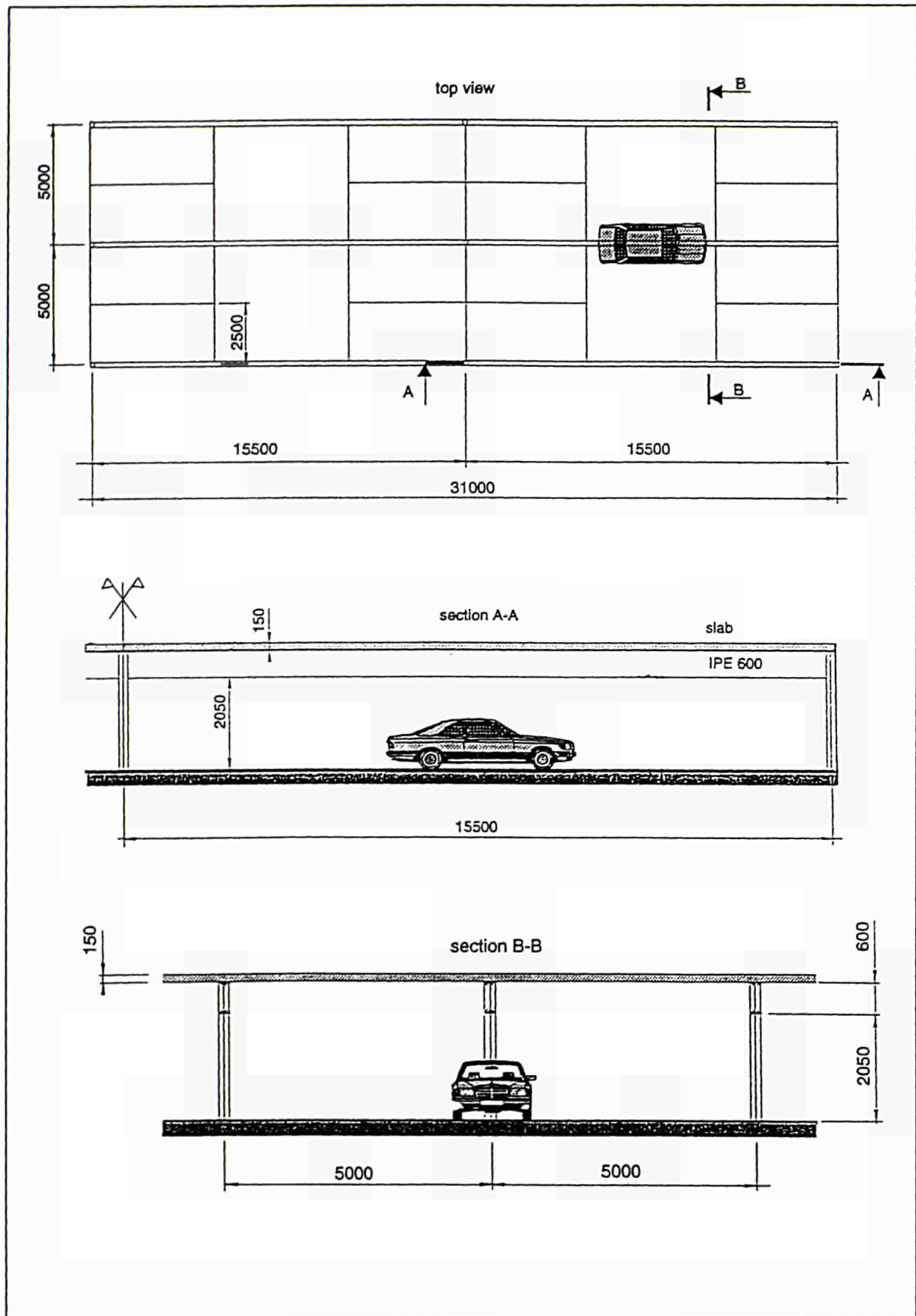
Figure 3.46 : Fire scenario 1

57

IPE 600

HE 280 A

28 m

28 m

30 cm

28 m

15.5 m   15.5 m

B

5 m   2.5 m   2.5 m

A   A

B

50 m

Ramp

Automatic Fire Doors

Ventilation :
5 x the ventilation of scenario 1 = 60000m³/h
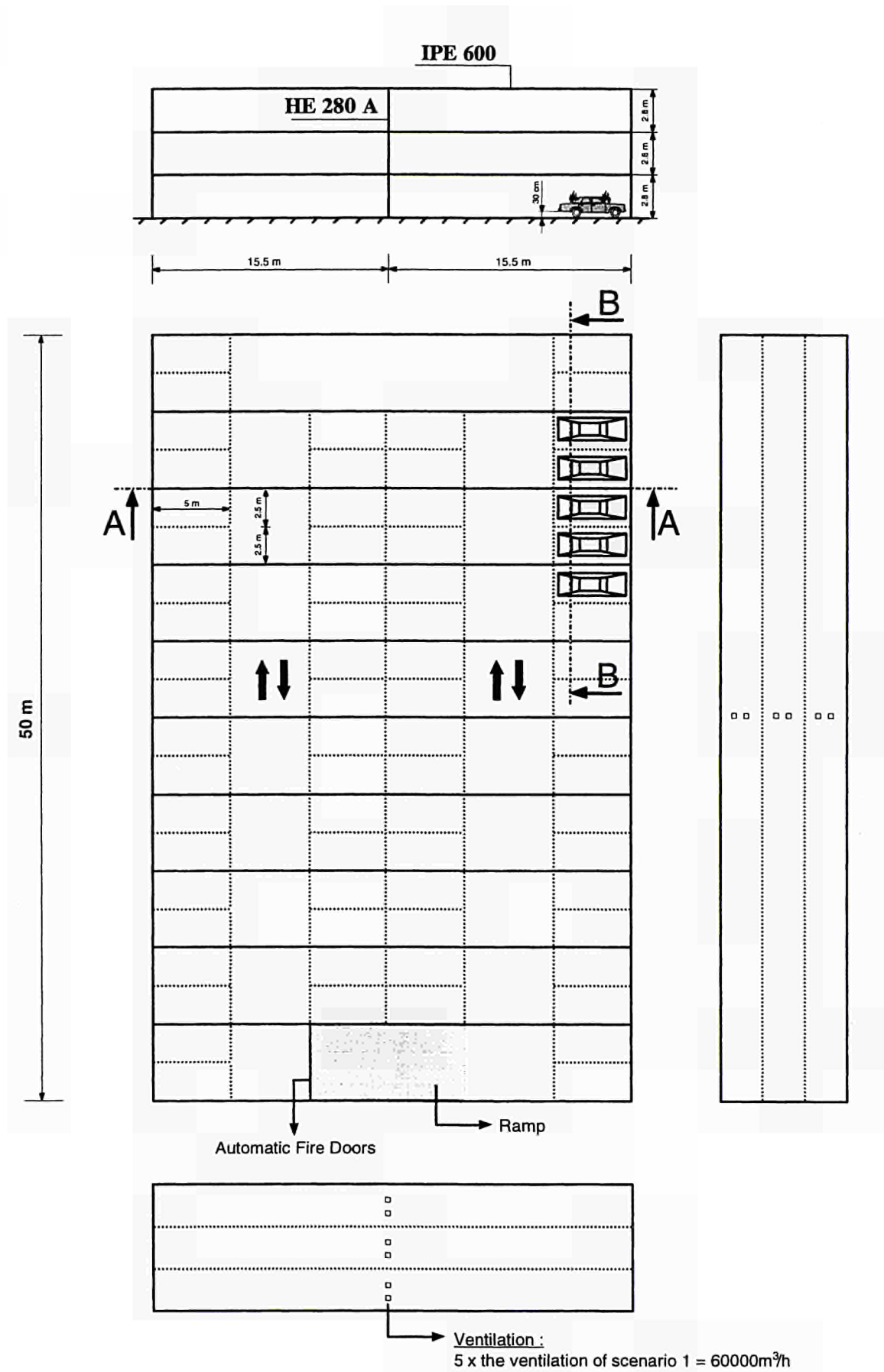
Figure 3.47 : Fire scenario 2

58

top view

5000

5000

2500

15500

15500

31000

section A-A

150

slab

IPE 600

2050

15500

section B-B

150

600

2050

5000

5000
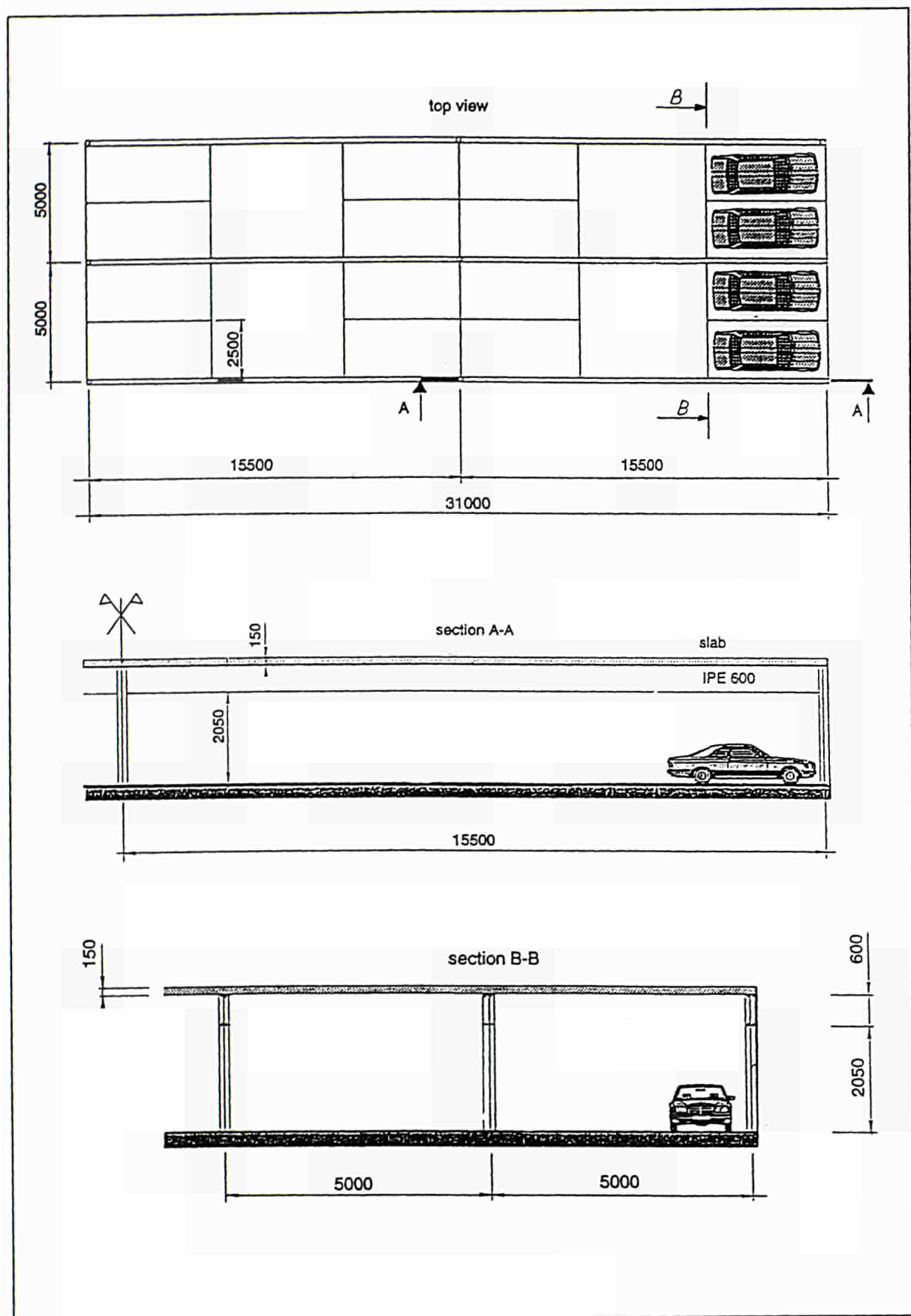
Figure 3.48 : Fire scenario 2

4. REQUIREMENT IN CLOSED CAR PARK

4.1. Ventilation required to evacuate the CO produced by running cars

The following tables provides the different values found for the countries involved in the research.

<table>
<tr><td colspan="5" align="center">STUDY OF THE VENTILATION CONDITIONS IN
CLOSED CAR PARKS AT ROOM TEMPERATURE</td></tr>
<tr><td></td><td align="center">Natural
Ventilation</td><td align="center">Reference</td><td align="center">Forced Ventilation</td><td align="center">Reference</td></tr>
<tr><td>Netherlands</td><td>0,06m²/place</td><td>Code of Practice
NPR-2443
§ 7.1.6</td><td>$q = \dfrac{T \cdot P_{CO} \cdot 10^{-3}}{M - Ca}$
72 Cars
time = 130 seconds
M-Ca = 0,095 . 10⁻³ cm³/m³
230 m³/h/place</td><td>Code of Practice
NPR-2443
§ 7.1.11.1</td></tr>
<tr><td>Belgium</td><td>0,06m²/place</td><td>RECKNAGEL
§ 53</td><td>12 m³/h.m²
150 m³/h/place</td><td>RECKNAGEL</td></tr>
<tr><td>France</td><td>0,06m²/place</td><td>Traité Pratique de
Sécurité Incendie
(CNPP 1983-86)</td><td>Normal : 300 m³/h/place
Heavy traffic : 600 m³/h/place</td><td>Traité Pratique de
Sécurité Incendie
(CNPP 1983-86)</td></tr>
<tr><td>Germany</td><td>0,06m²/place</td><td>Merkblatt 211
Parkbauten
2.Auflage 1972
§2.5 14 Lüftung
(6)</td><td>12m³/h.m²
150 m³/h/place

$V_{A-CO} = \dfrac{q_{CO}}{CO - CO_A}$
230 m³/h/place</td><td>Merkblatt 211

VDI 2053 Blatt 1
Example § 2.2.3.2
pages 7 and 8</td></tr>
<tr><td>Spain</td><td>0,5m²/ 200m² of
useful floor area
(0,03 m²/place)</td><td>Fax from
LABEIN
19th of July 1994</td><td>6 changes an hour
360 m³/h/place</td><td>Fax from
LABEIN
19th of July 1994</td></tr>
</table>

<table>
<tr><td colspan="4" align="center">MAXIMUM OF CO AUTHORIZATED IN A CLOSED CAR PARK</td></tr>
<tr><td></td><td align="center">Time period</td><td align="center">maximum of CO</td><td align="center">Reference</td></tr>
<tr><td>Netherlands</td><td>< 30 min
30 min
8 hours</td><td>200 ppm (*)
100 ppm
50 ppm</td><td>Code of Practice
NPR-2443
§ 7.1.2 and § 7.1.3</td></tr>
<tr><td>Belgium</td><td>at each instant
20 min
8 hours</td><td>200 ppm
100 ppm
50 ppm</td><td>RECKNAGEL
§ 51</td></tr>
<tr><td>France</td><td>at each instant
20 min
8 hours</td><td>200 ppm
100 ppm
50 ppm</td><td>Traité Pratique de Sécurité
Incendie
(CNPP 1983-86)</td></tr>
<tr><td>Germany</td><td>10 min
30 min
60 min</td><td>250 ppm
100 ppm
50 ppm</td><td>VDI 2053 Blatt 1
Example § 2.2.1
page 4</td></tr>
<tr><td>Spain</td><td>/</td><td>/</td><td>/</td></tr>
</table>

(*) 1 ppm = 100 cm³/ m³ of air

4.2. Fire safety requirements

The fire safety requirements for France, Belgium, Switzerland, Spain and the Netherlands are listed in the following table.

Fire Requirements (Active and Passive Measures) for Closed Car Parks

	FRANCE		BELGIQUE
	[36] Parking Area $A_f < 6000$	[37] 6000 < Parking Area $A_f < 20000$	[38]
SPRINKLER	Sprinkler for the 6 th basement and below (discharge : 3.5 l / m² / min)		
DETECTOR	If 3, 4 or 5 basements, detection from the third basement and below If 6 basements or more, detection for all the basements If 5 levels upperground of more, detection from the fifth level and above	Automatic detector when mechanical ventilation	
EXIT	maximum distance : - no stair case further than 40 m - 25 m to walk in a blind alley - stair width ≥ 0.8 m	maximum distance : - no stair case further than 40 m - 25 m to walk in a blind alley - stair width ≥ 0.9 m	A least 2 stair cases in a compartment - no stair case further than 40 m - stair width : ≥ 0.8 m - for floor area < 500 m² ⇒ 1 stair case is enough - complementary marking on the ground
VENTILATION	ventilator : 200°C during 60 min	ventilator : 200°C during 60 min	

COMPARTIMENTATION	for upperground levels
	A_f < 6000 m²
	for basement
	Af < 3000 m²
	wall compartimentation: R_f 1h
	walls and floors:
	R240 for high level habitations
	R180 for public building
	R120 in the other cases
	doors: R_f 1/2 h
		for upperground levels
		A_f < 6000 m²
		for basement
		Af < 3000 m²
		wall compartimentation: R_f 1h
		walls and floors:
		R240 for high level habitations
		R180 for public building
		R120 in the other cases
		doors: R_f 1/2 h
			walls : Rf 60 min : for Low Buildings
			                          : for Medium High Buildings
			            Rf 120 min : for High Buildings (+/- 8 floors)
			doors : Rf 30min : for Low Buildings
			                          : for Medium High Buildings
			            Rf 150 min : for High Buildings (+/- 8 floors)

SAFETY LIGHT	at max 0.50 m from ground level	at max 0.50 m from ground level min 15W (self governing)	
EXTINGUISHER	1 / 15 cars 1 box of sand of 100 litres with a shovel	1 / 15 cars 1 box of sand of 100 litres with a shovel	
STRUCTURAL FIRE RESISTANCE	bearing elements: R120 H ≥ 28m R90 H ≤ 28 m with more 2 levels R60 max 2 levels R30 max 1 level	bearing elements: R120 H ≥ 28m R90 H ≤ 28 m with more 2 levels R60 max 2 levels R30 max 1 level	

61

Fire Requirements (Active and Passive Measures) for Closed Car Parks			
	SUISSE	**SPAIN**	**NETHERLANDS**
	[39]	[40]	
SPRINKLER	basement levels: sprinkler if completely closed compartments > 4000 m² sprinkler if adjoining closed compartments contain connections > 2000 m² above ground levels: sprinkler if completely closed compartments > 4000 m² sprinkler if partially opened compartments > 8000 m²	Sprinkler if $10000 \leq A_f \leq 20000$ m²	
DETECTOR		If A_f > 500 m² or if mechanical ventilation	If mech. ventilation
EXIT		one exit : ways $\leq$ 35 m various exits : ways $\leq$ 50m alternative ways to different exits at $\leq$ 25 m from any point.	various exit : ways $\leq$ 50m minimum 2 exits
VENTILATION		Extraction point at $\leq$ 25 m from any point	
COMPARTIMENTATION	basement levels: if completely closed compartments Af < 4000 m² if adjoining closed compartments contain connections Af < 2000 m² above ground levels: sprinkler if completely closed compartments Af < 4000 m² if partially opened compartments Af < 8000 m² doors: R_f 1/2 h	for commercial or public premises : Af $\leq$ 10000 m² Af $\leq$ 20000 m² if sprinkler Not required if ways to exits are $\leq$ 35 m and the ventilation area (natural or mechanical) is twice not required.	Af $\leq$ 5000 m²
SAFETY LIGHT		In any case	Always
EXTINGUISHER		$\leq$ 15 m from any point Dry column if more than 3 storeys Hose reels if more than 30 car places	1 extinguisher every 25 places
STRUCTURAL FIRE RESISTANCE	for L-1 only : Rf 30 min for L-1, L-2, ... : Rf 60 min for L 0, L+1 : Rf 30 min for L0 for L 0, L+1, L+2... : Rf 60 min for L0	R120 if car park below occupancies R90 if not	R60 R30 if the number of storeys is less or equal to 2

5. *TEMPERATURE FIELD IN THE AIR*

5.1. One burning car

5.1.1. CFD calculation - Simulation 4 ≡ Scenario 1 (Normal ventilation)

5.1.1.1. Natural ventilation

A. VESTA

In this chapter the CFD-calculations made by TNO for simulation 4 are given. The CFD computergram is called VESTA (Computational Fluid Dynamics), and was developed by TNO.

Description: Closed carpark with a burning car in one corner, located just beneath a steel beam. Calculations to be carried out on the conditions in the carpark (temperature, smoke density etc) and the resulting temperature in the steel beam.

Carpark: Type Closed,
             Ventilation naturally ventilated: 8 openings of 0.4m x 1.5m
             Dimensions 50m x 31m x 2.65m
             ConstructionConcrete, with unprotected steel beams IPE600.

Burning car: The RHR curve is the 'Camel back' curve deduced from the VTT test of 1990 (see figure 5.3 and 3.27).
             The curve had been choosen because, when the CFD simulation started, the reference RHR curve (see chapter 3.4) was not yet available.

Description of the modelling

In figure 5.1 the actual modelling of the carpark for the CFD-calculation is given. The two beams closest to the fire are modelled. The columns and the beams further away from the fire in the carpark are not modelled. The openings are modelled at the exact location. Figure 5.1 is not true-scale: the height is enlarged to be able to show any detail.
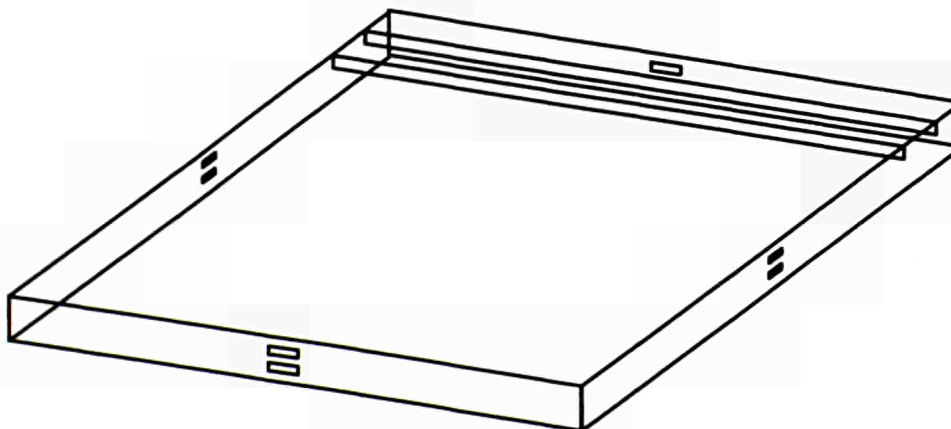
Figure 5.1

The following aspects of the modelling are described below:

a. Geometry
b. Radiation/Emissivity smoke/gases
c. Heat transfer to walls
d. Heat transfer to the beams
e. Flow in the openings
f. Combustion model

a) Geometry

Number of calculation cells: 53 x 41 x 19 = 41.000 cells. (L x W x H). The mean real-volume of the calculation cells is Vmean $\cong 0.1$ m^3.

The mesh is finer at the locations where the largest velocity/pressure/temperature values and gradients can be expected: i.e. near the fire, the beams and the openings, leading to much lower cell-volumes where needed.

b) Radiation

The system of "inverse ray tracing" is used with 64 directions for the rays. The emissivity of the smoke/gases is calculated with the "Fusegi" model, based on the sum of grey-gases assumption.

c) Heat transfer to walls

Outside walls fixed convection coefficient $\alpha = 10$ W/m^{2}K.
Inside walls: radiation and convection are calculated with the following model.
Modelling for a flow in x direction, y perpendicular to wall.

2-dimensional boundary layer flow:
$$\frac{\partial}{\partial y}[\mu + \mu_t]\frac{\partial U}{\partial y} = 0$$

integrate from 0 to y:
$$[\mu + \mu_t]\frac{\partial U}{\partial y} = \tau_w$$

with
$$u^+ = \left(\frac{\tau_w}{\rho}\right)^{\frac{1}{2}}$$

$$u^+ = \frac{u}{u^*}$$

$$y^+ = \rho u^* y / \mu$$

The enthalpy equation in the boundary layer is as follows:
$$\frac{\partial}{\partial y}\left(\frac{\mu}{\sigma} + \frac{\mu_t}{\sigma_t}\right)\frac{\partial H}{\partial y} = 0$$

N.B.
$$\frac{\mu}{\sigma} = \frac{\lambda}{C_p}$$

integration leads to

$$\left(\frac{\mu}{\sigma} + \frac{\mu_t}{\sigma_t}\right)\frac{\partial H}{\partial y} = -q_w$$

d) Heat transfer to the beams

Geometry of the beams

The beams are modelled on IPE 600 beams, but with the following assumptions:

Height   : 600 mm
Width   : 220 mm
Web thickness   : 20 mm
Flange thickness : 20 mm

For the purpose of the VESTA calculations, this geometry has been modified to a three-sided hollow rectangular element with the same mass of steel as the real beam. The thickness is therefore 14mm (see figure 5.2).
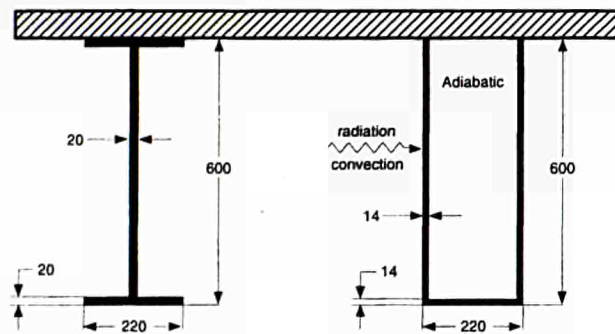
Figure 5.2 : Modelling of the steel beam in CCP simulation 4

Heat transfer to the beam

The inside surface of the beam is considered adiabatic (no heat flux to other sides). The outside surface of the beam is subjected to convective and radiative heating. The radiative heat flux is determined by the radiation sub-model within VESTA, which is the so-called Discrete Transfer Model described earlier. The convective heat flux is determined by VESTA as well, using a wall function which leads to a different heat transfer coefficient at every cell adjoining the steel wall.

Heat transfer within the beam

A one-dimensional numerical heat conduction model is applied to calculate the temperature distribution normal to each cell. 10 (ten) numerical cells are used, which has been checked to give an accurate description. The thermal properties of steel have been set as follows:

heat conductivity   : $\lambda = 40$ W/mK
heat capacity   : $\rho\,C_p = 1.14*10^7$ J/m^{3}K

This model therefore neglects any heat conduction in the axial direction of the beams. Local temperature peaks observed in the calculations will therefore be exaggerated (conservative assumption)

e) Flow in openings

For the flow in the small openings a "Bernoulli-like" approach is taken. This approach can be used adequately since the size of the openings are small relative to the dimensions of the walls

$$V = 0{,}8 \cdot A \cdot (dP)^{0.5}$$

with:

V = Flow through the opening, in m^3/s
A = Surface of the opening, in m^2
dP = Pressure difference over the opening, in Pa

f) Combustion model

In the CFD code VESTA two combustion models are available to estimate the rate of heat release, dependent upon the amount of combustible gases and O_2 available in the compartment.

1. The "eddy-break-up" model, in which the rate of combustion is determined by the turbulent mixing process, and
2. the "flame sheet" model; in this more simple model the rate of combustion is infinitely fast, if O_2 and combustible gases are present in a specific volume.

For the simulation 4 calculations **no** combustion modelling is used. The rate of heat release is deduced from the results of car fire experiments with a calorimeter. The RHR used for the experiments is divided amongst two sources at different locations simulating the fire/plume rising from the front-window and the rear window of the burning car, as found in the experiments [5].

In figure 5.3 this RHR is illustrated as a function of time.
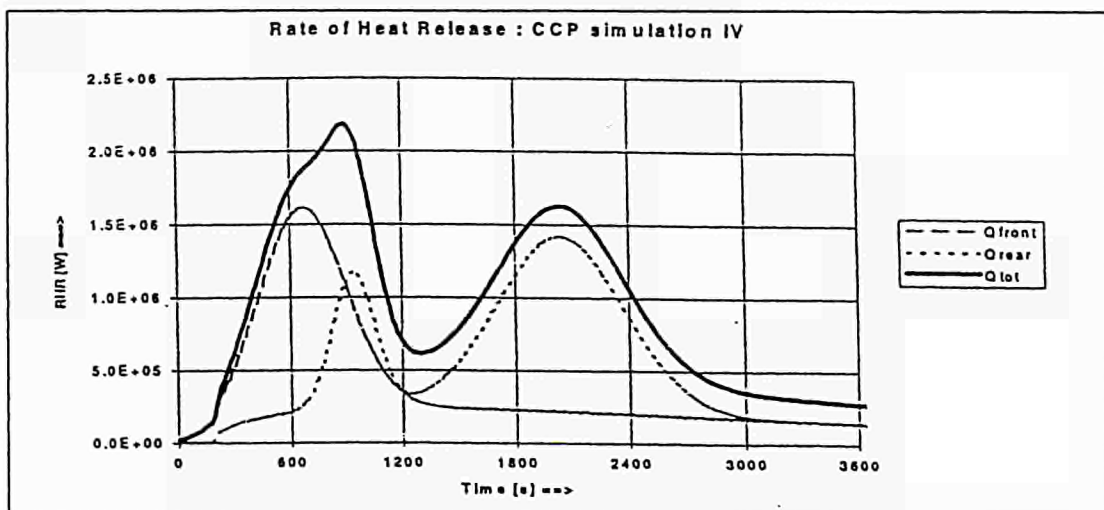
Figure 5.3 : Rate of heat release of the car-fire, based on experiments

66

The CFD simulations considering the RHR curve of chapter 3.4 are given in annex 3.

Results

With the Computational Fluid Dynamic calculations the conditions in the carpark at any moment in time and at any location are available. For example the temperature and density of the smoke, the temperature and the heat-loss to the structure and the temperature of the unprotected steel beams can be calculated.

a) 3-D: Temperature distribution

In figure 5.5 the temperature in the carpark is given at $t = 2040$ s, just after the second peak in the RHR, leading to the peak-values for air temperature. The colour setup was chosen to show as much detail as possible; the red colour indicates temperatures of 120°C or higher.
From figure 5.5 the following qualitative conclusions can be drawn:

a. **The car fire can be described as a localized fire; the high temperatures (T > 120°C) only occur in the vicinity of the fire.**
b. The beams function as channeling screens for the smoke/gases. The spread of smoke perpendicular to the beams is much smaller than the spread parallel to the beams.
c. **The heat-loss to the walls and ceiling is considerable.**

b) 3-D: Smoke density distribution

Figure 5.6 gives, from the same 3-D point of view at the same time, the result of the scaled smoke mass fraction SMF.

The visibility through the smoke in m can be calculated from this SMF as follows:

$$L_{Vis} = \frac{0,25}{SMF}$$

with L_{Vis} = Visibility through smoke for well lit objects, in m
  SMF = Scaled mass fraction of smoke (given in the figure 5.6)

The conclusion can be drawn that the visibility for well lit objects is well below 10 to 15m in the largest part of the carpark. Only close to the lower openings where the fresh air enters through these lower openings is the visibility better. The amount of natural ventilation through the eight openings is not enough to establish a "smoke-free" zone in the carpark.

c) Ventilation factor

In figure 5.4 the actual ventilation-factor that is calculated in the simulation is plotted vs. time.

During most of the simulated period (3600 s) the smoke flows out through all four upper openings, while fresh outside air flows in through the four lower openings.

The flow pattern and the resulting flow through the openings is not the same for all upper openings. This is to be expected because the temperature distribution and the flow-pattern in the carpark are not uniform/symmetrical.

The ventilation-factor is calculated by dividing the total flow into the carpark by the volume of the carpark.

$$V_{total} = \sum_{1}^{4} \left(V_{lower;i} \right)$$

$$X_{Vent} = \frac{V_{total}}{Vol_{CCP}}$$

where V_{total} = Total flow into the CCP (through the lower openings), in m^3/h
        Vol_{CCP} = Total volume of the Carpark, in m^3
        X_{vent} = Ventilation factor, in times per hour.

For a quantitative analysis of the air/smoke temperature and steel temperature 2-dimensional graphs are more suited.
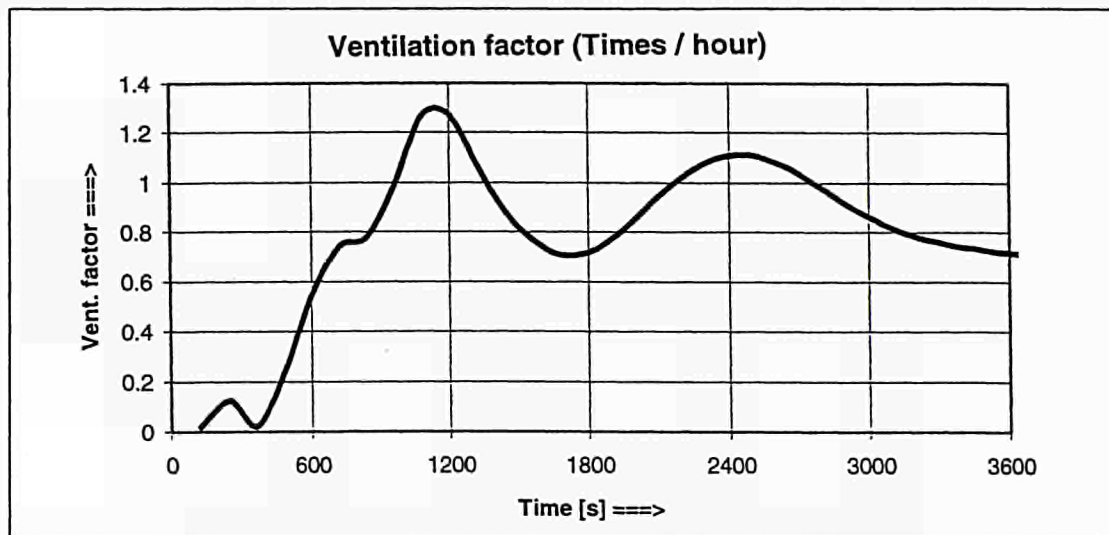
Figure 5.4 : Ventilation factor of the CCPvs time, in times per hour

d) 2-D: Maximum air temperatures

In figure 5.7 the maximum air/smoke temperatures in the vicinity of the most heated beam (-located just above the carfire-) at different times are given as a function of the horizontal distance along the beam.

In this figure it can be seen that the areas with high air/smoke temperatures are rather localized; the position of these areas coincides approximately with the position of the two fireplumes (front and rear window of the car). Further away from the fire, the air temperatures drop steeply. The location of the maximum air temperatures is next to the beam (on the side closest to the wall opening) just beneath the ceiling. This result of the exact location has little meaning, since the profile of the I-beam has been modelled as a hollow rectangular element, with an equivalent amount of steel.(see part B of this report for a description).
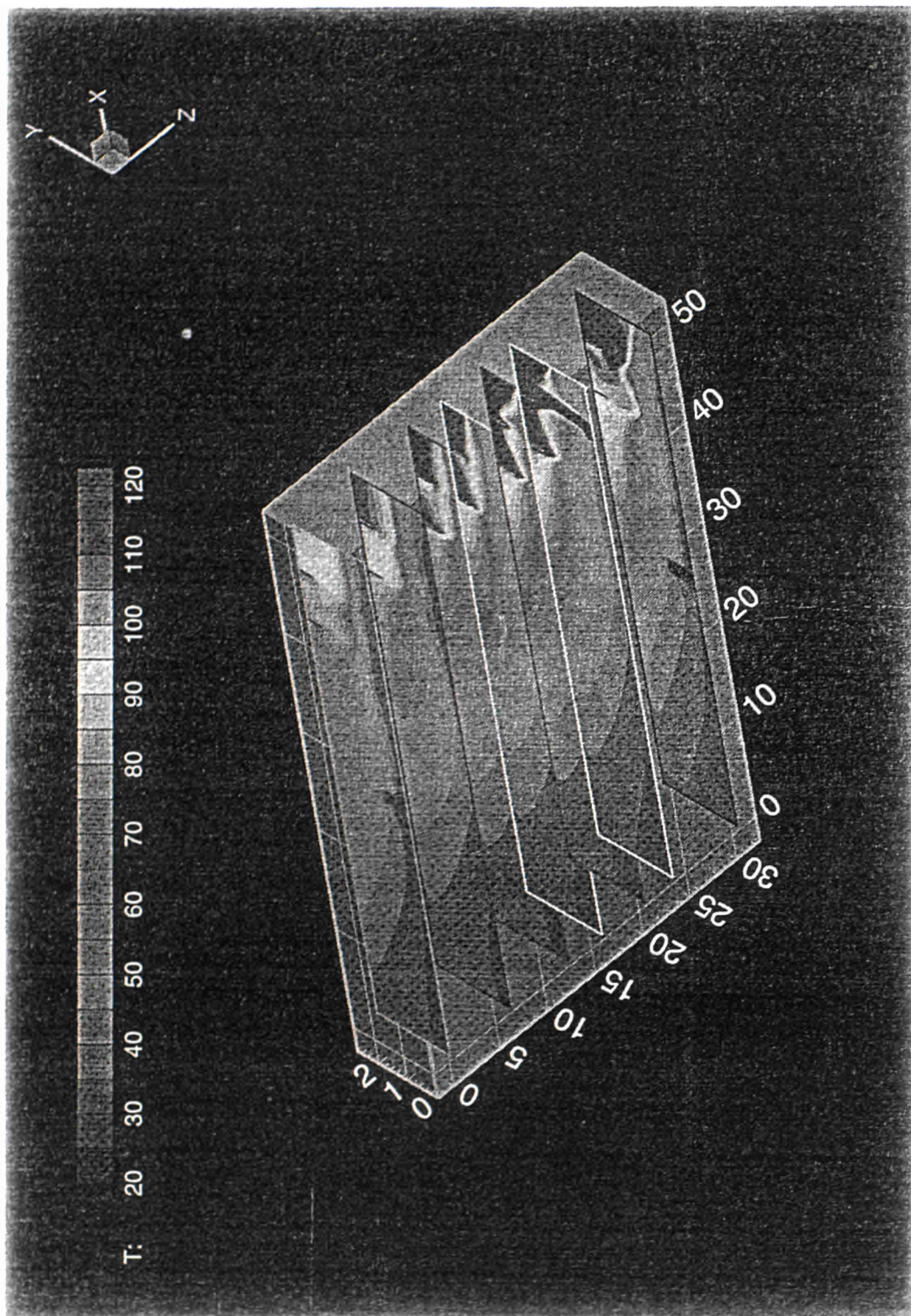
Figure 5.5 : Temperature distribution at t=2040s in the car park
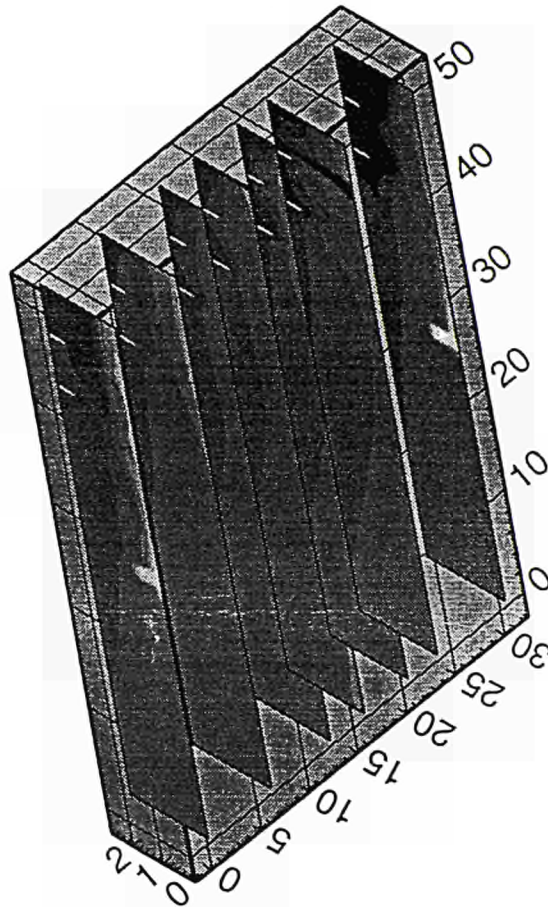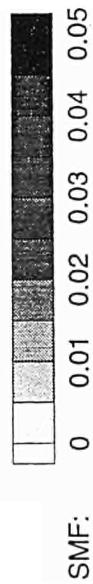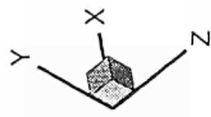
Figure 5.6 : *The scaled mass fraction of the smoke in the CCP at t=2040s. The visibility can be calculated from this value. Visibility is well below 10m in the largest part of the car park.*
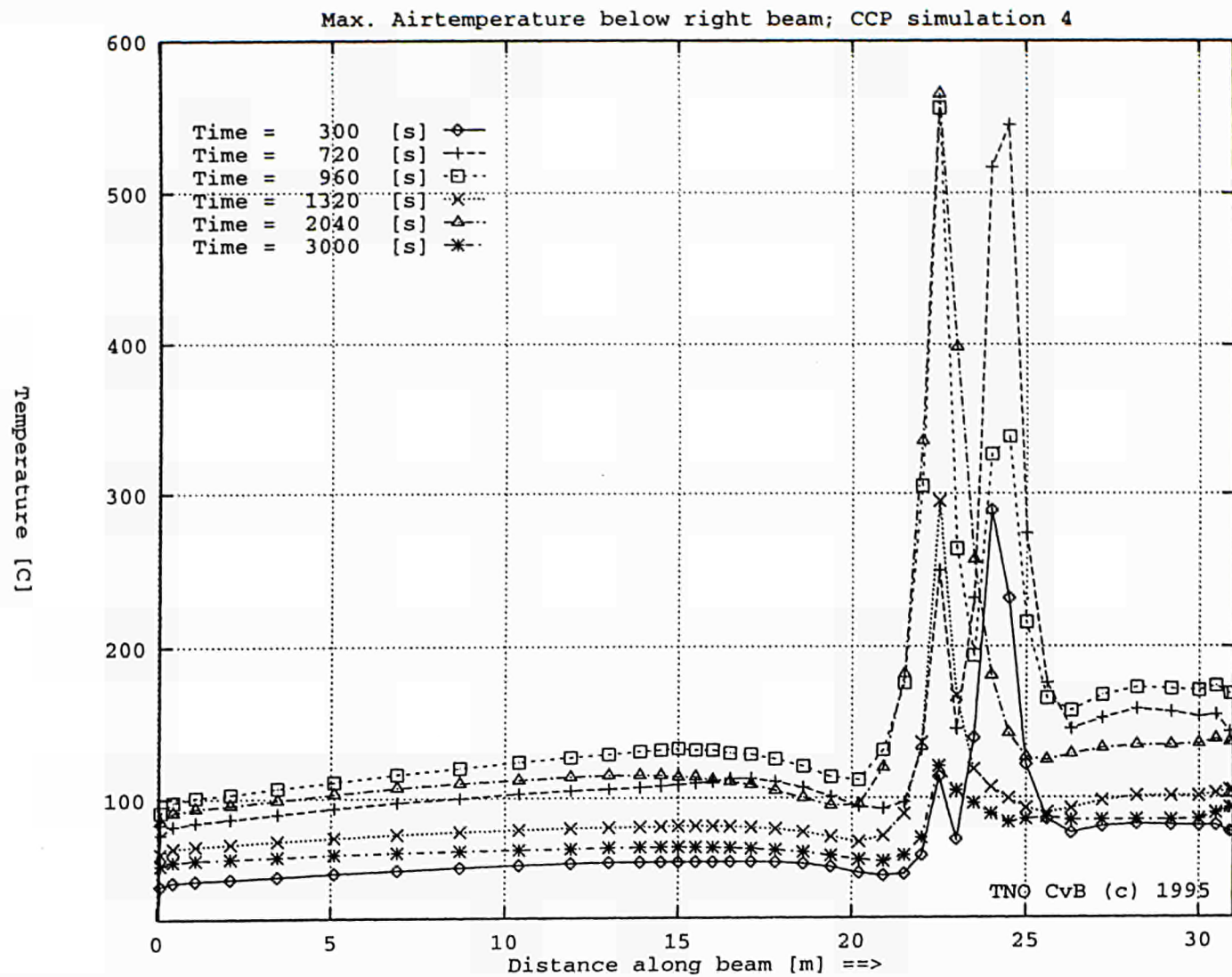
Figure 5.7 : Air temperature distribution along the most-heated beam (above the fire). The localized effect is easy recognized; also the relatively low temperatures can be noticed.

B. FLUENT

The air temperature field in fire scenario 1 has been calculated up to 60 minutes. The modelization was setup using 18088 cells (38*17*28).

The geometry of the garage is shown in fig 5.8 and 5.10, both cases, Simulation 4 and Forced Ventilation, have the same geometry, although they have different boundary conditions at the openings. The boundary conditions are (see figure 5.9):

- Concrete: Conductivity = 1.6 W/mK
                Cp = 1000 J/kgK
                ρ = 2500 kg/ m^3
                Emissivity = 0.94

- Steel: Conductivity = 45 W/mK
                Cp = 520 J/kgK
                ρ = 785 kg/m^3
                Emissivity = 0.6

- The pressure at windows is plenum pressure and a temperature of 293 K is defined where the fluid goes into the garage.

- The external wall has defined a convection coefficient of 10 W/m^{2}K.

Turbulence K-ε model has been used with taking into account the effect of buoyancy on turbulence. This buoyancy effect on turbulence can be taken into account by introducing some sources in the turbulence kinetic energy and turbulence dissipation transport equations :

$$\frac{\partial(\rho.K)}{\partial t} + \frac{\partial(\rho.u_i.k)}{\partial X_i} = \frac{\partial}{\partial X_i} \cdot \frac{\mu}{\sigma_k} \cdot \frac{\partial k}{\partial X_i} + G_k + G_b - \rho\varepsilon$$

$$\frac{\partial(\rho\varepsilon)}{\partial t} + \frac{\partial(\rho.u_i.\varepsilon)}{\partial X_i} = \frac{\partial}{\partial X_i} \cdot \frac{\mu}{\sigma_\varepsilon} \cdot \frac{\partial \varepsilon}{\partial X_i} + C_1 \frac{\varepsilon}{k} \cdot (G_k + G_b) \cdot (1 + C_3 \cdot R_f) - C_2 \cdot \rho \cdot \frac{\varepsilon^2}{k}$$

where

$$G_k = \mu_t \cdot \left(\frac{\partial u_j}{\partial X_i} + \frac{\partial u_i}{\partial X_j} \right) \cdot \frac{\partial u_j}{\partial X_i}$$

is the turbulent kinetic energy shear production source,

$$G_b = -g_i \cdot \frac{\mu_t}{\rho.\sigma_t} \cdot \frac{\partial \rho}{\partial X_i}$$

is the turbulent kinetic energy source due to buoyancy and,

$$R_f = -\frac{G_b}{G_k + G_b}$$

is the Richardson number.

When buoyant effect on turbulence (BEOT) is considered the two layers considered by the two zones model can be observed, whilst without BEOT the layers do not appear. The definition of the two layers can be explained by the turbulence kinetic energy reduction due to buoyancy effect, which produces a reduction of the mixing rate into the garage. The final effect is the definition of two layers, the hot layer at the top end the cold layer at the bottom, with a very low heat exchange between them.

The temperature distribution along the frame above the car, figure 5.11, shows three maximums. The higher one is reached at point 5 above the front source 11 minutes, while the other two maximums are placed in the same beam section above the rear source for 16 minutes and 34 minutes and present similar temperatures. Although there are two maximums in the same section of the beam they are spaced out over time, and with a big drop of temperature in between, so the negative effect of these two peaks should not worry us too much.

Figure 5.12 shows, in detail, the temperature profile in the worst section, which is situated above the rear source, see figure 5.11. The figure shows that there are three points with high temperatures 5b, 5c, 5d. Point 5c has the highest temperature and the peak is almost as thick as the peak of point 5d, so point 5d is less unfavourable than point 5c. Point 5b and 5d present a similar maximum temperature, as profile 5b presents a narrower peak than point 5d, it becomes clear that 5b is less unfavourable than 5d. So the most unfavourable point of the beam above the car, and so in the garage, is the point 5c.

The outlet velocities at windows near the burning car are shown in figure 5.13.

Figure 5.8: Garage geometry - The car is under beam 1

External heat transfer wall,
Convection coefficient=10 J/sm²K.
External Temperature= 20°C.

Conducting wall, concrete

Initial conditions
P=Patm
T=20°C

External heat transfer wall,
Convection coefficient=10 J/sm²K.
External Temperature= 20°C.

Figure 5.9

75
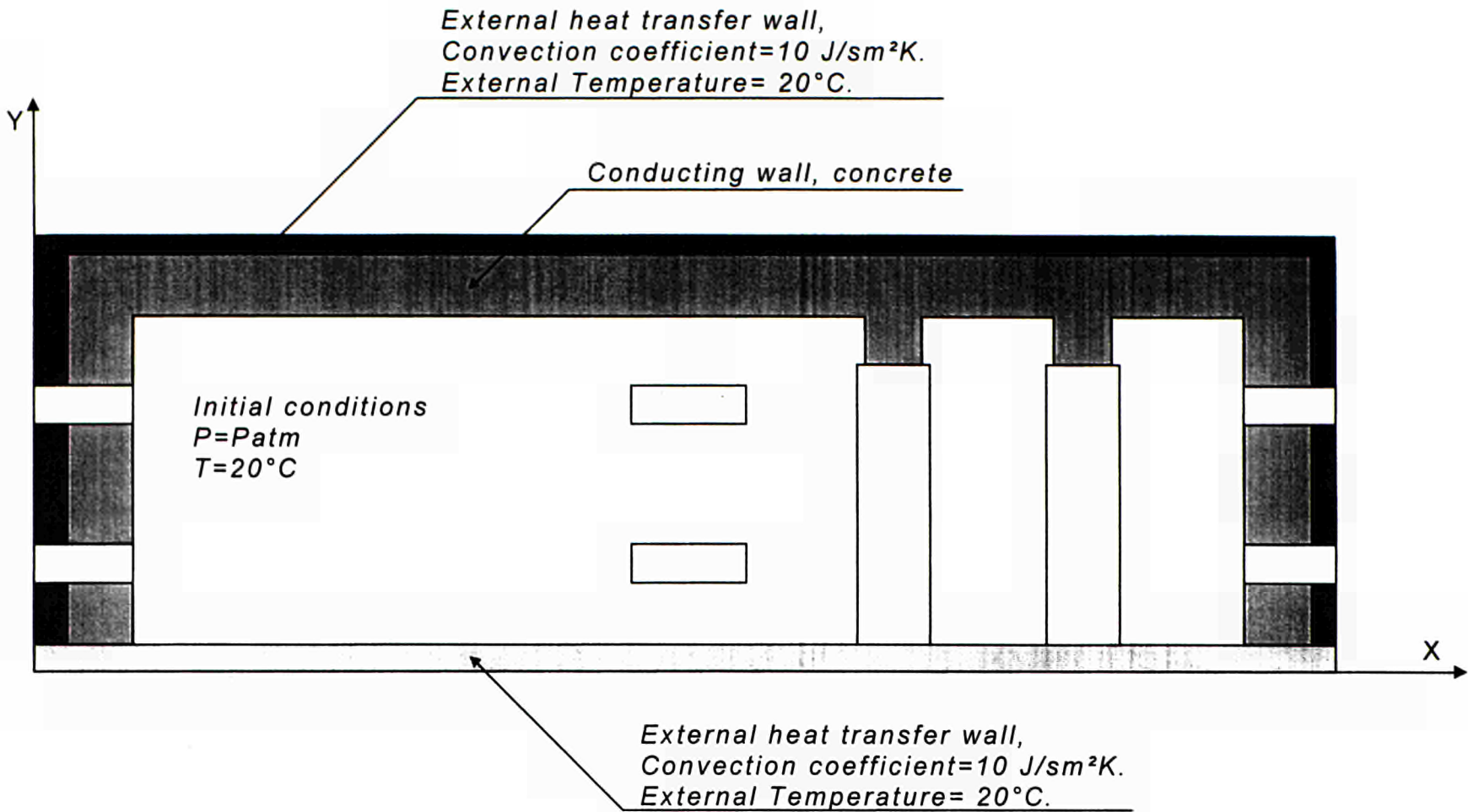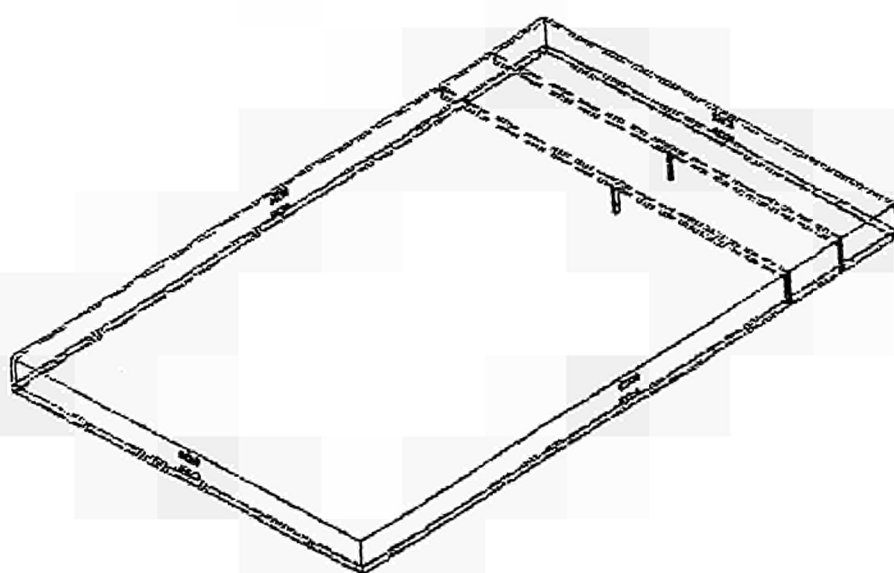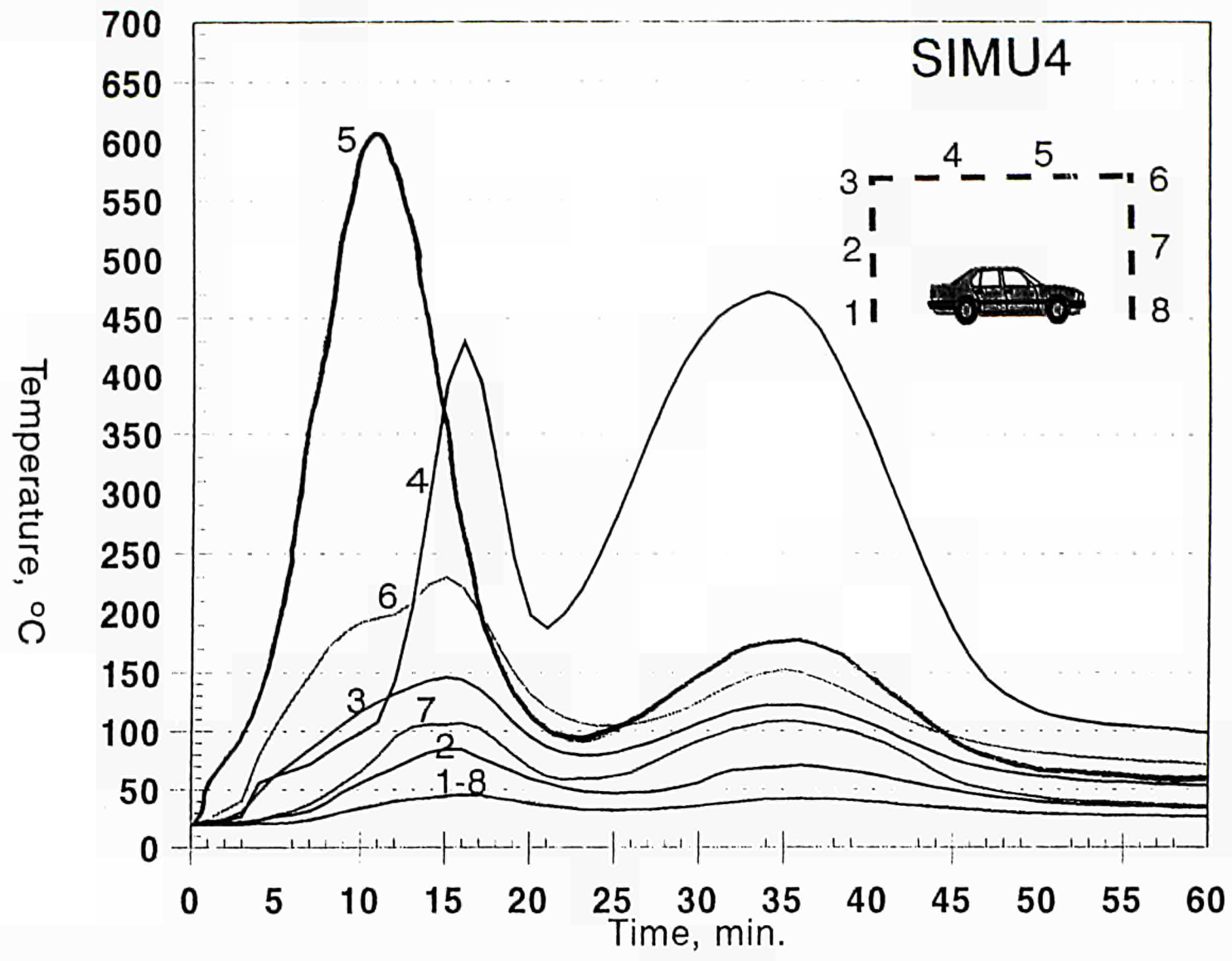
Figure 5.10

Figure 5.11 : Temperature of the air around beam 1 and its columns for different points
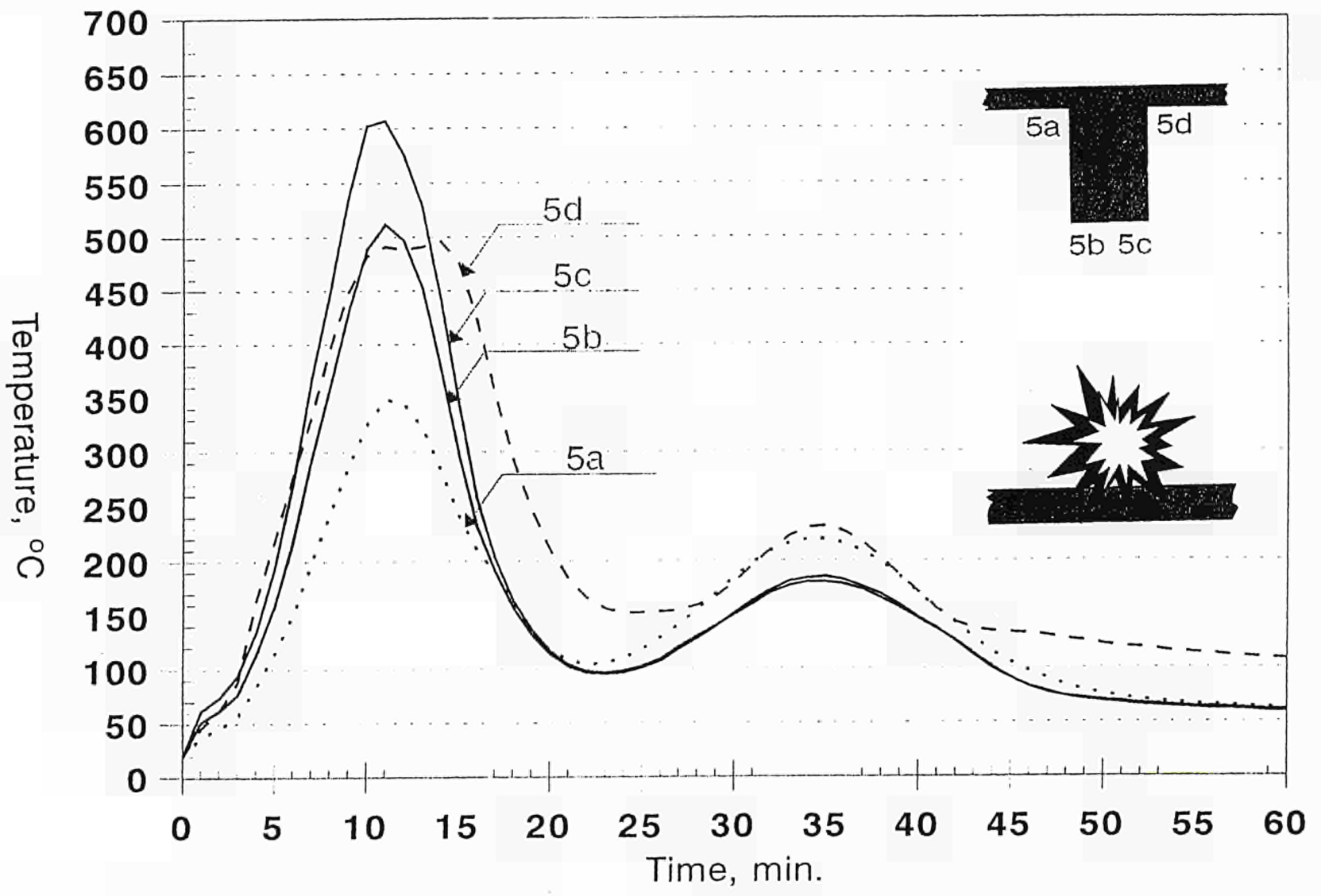
Figure 5.12 : Temperature of the air around worst section of beam 1 for different points

Figure 5.13 : Outlet velocities of the fluid for four windows

C. Comparison VESTA-FLUENT
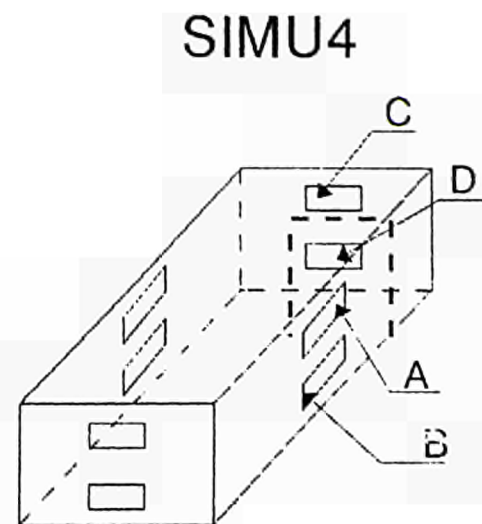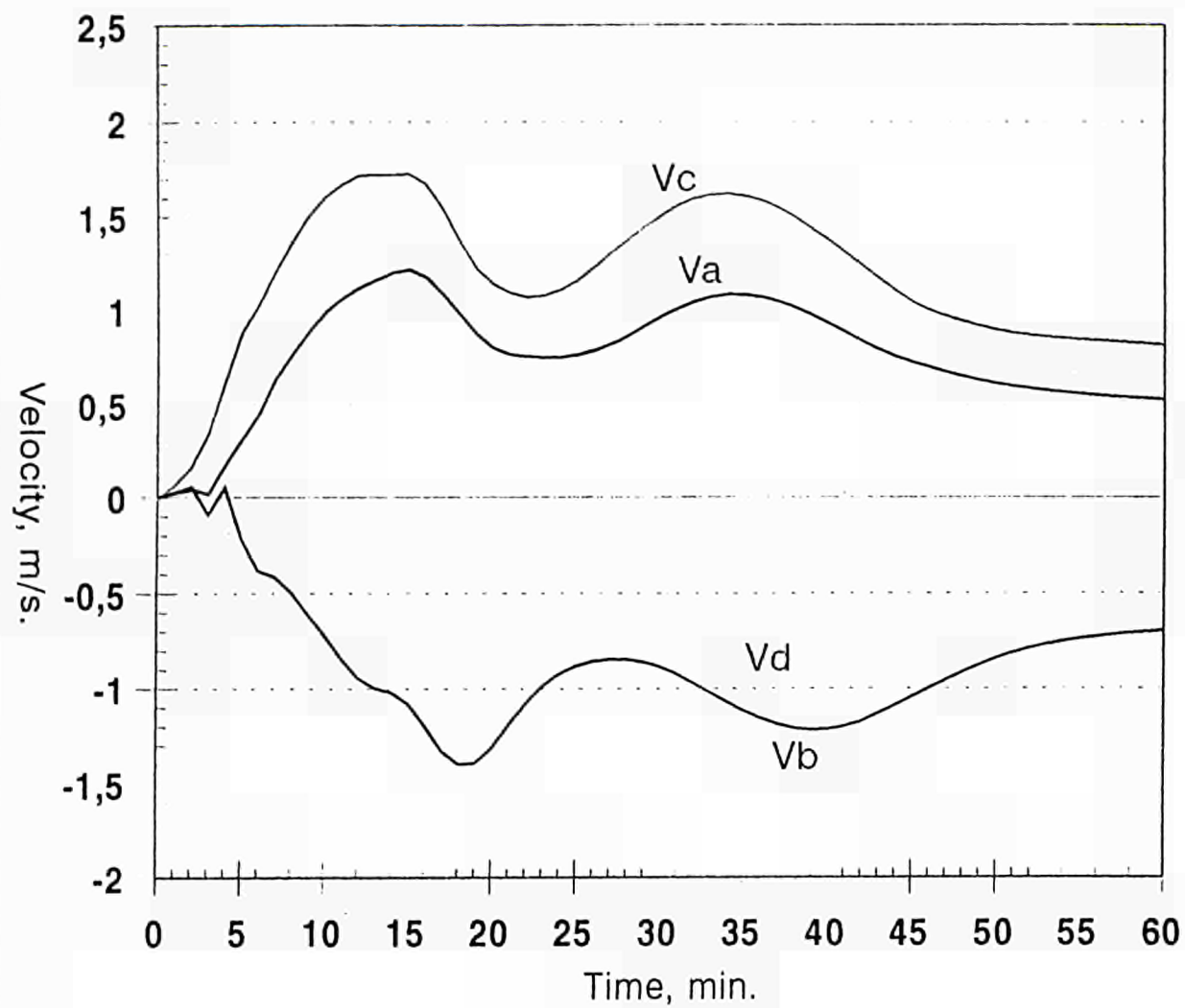
The eight following figures show the results of TNO and LABEIN for the different points 1 to 8 of the frame situated above the car. It can be noticed that the agreement between both calculations is quite satisfactory.

Simulation 4
RESULTS
POSITION OF THE CONSIDERED POINTS

80 cars * 0,06 m²
= 4,8 m² of opening

Temperatures in Point 1 : SIMULATION 4

Temperatures in Point 2 : SIMULATION 4
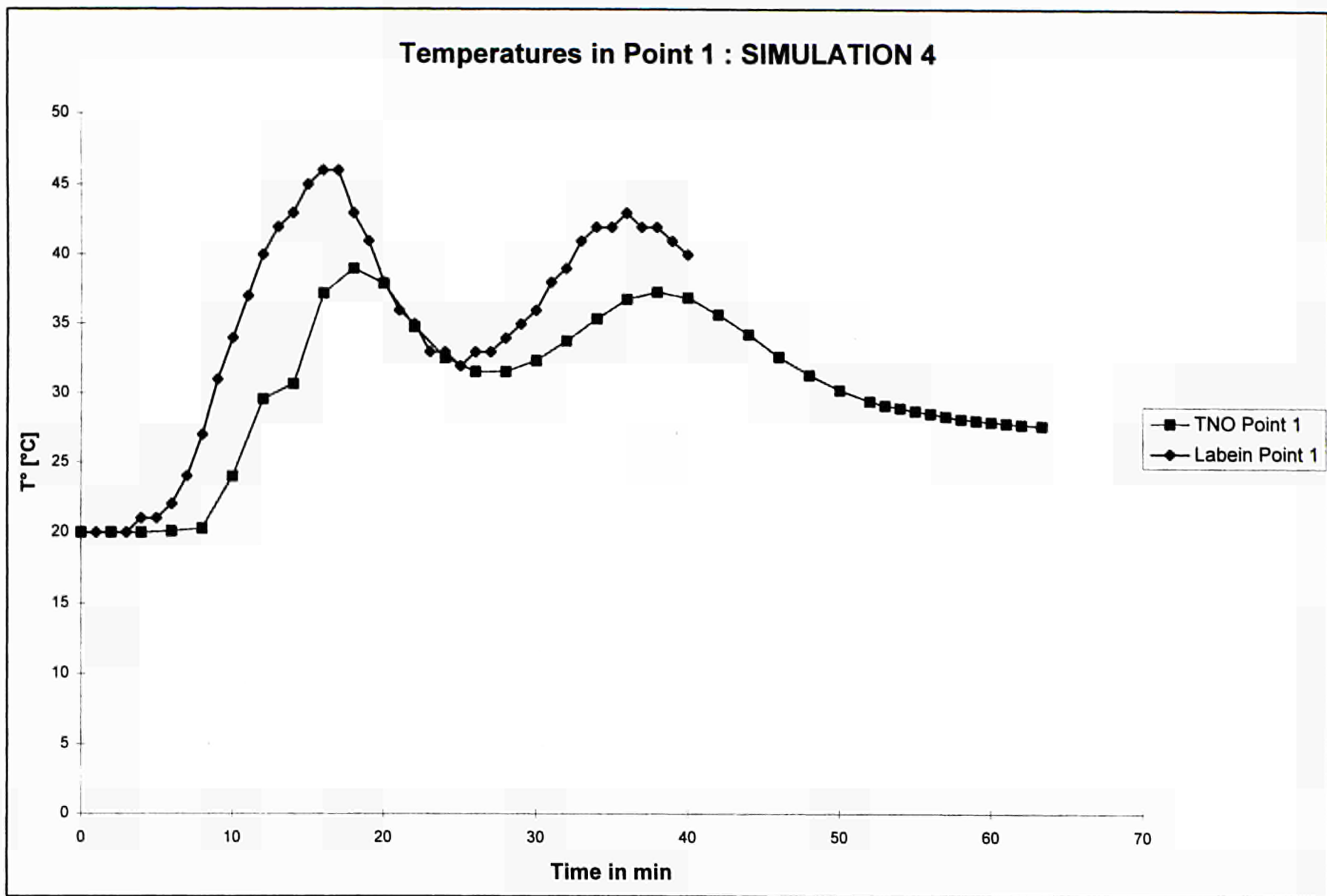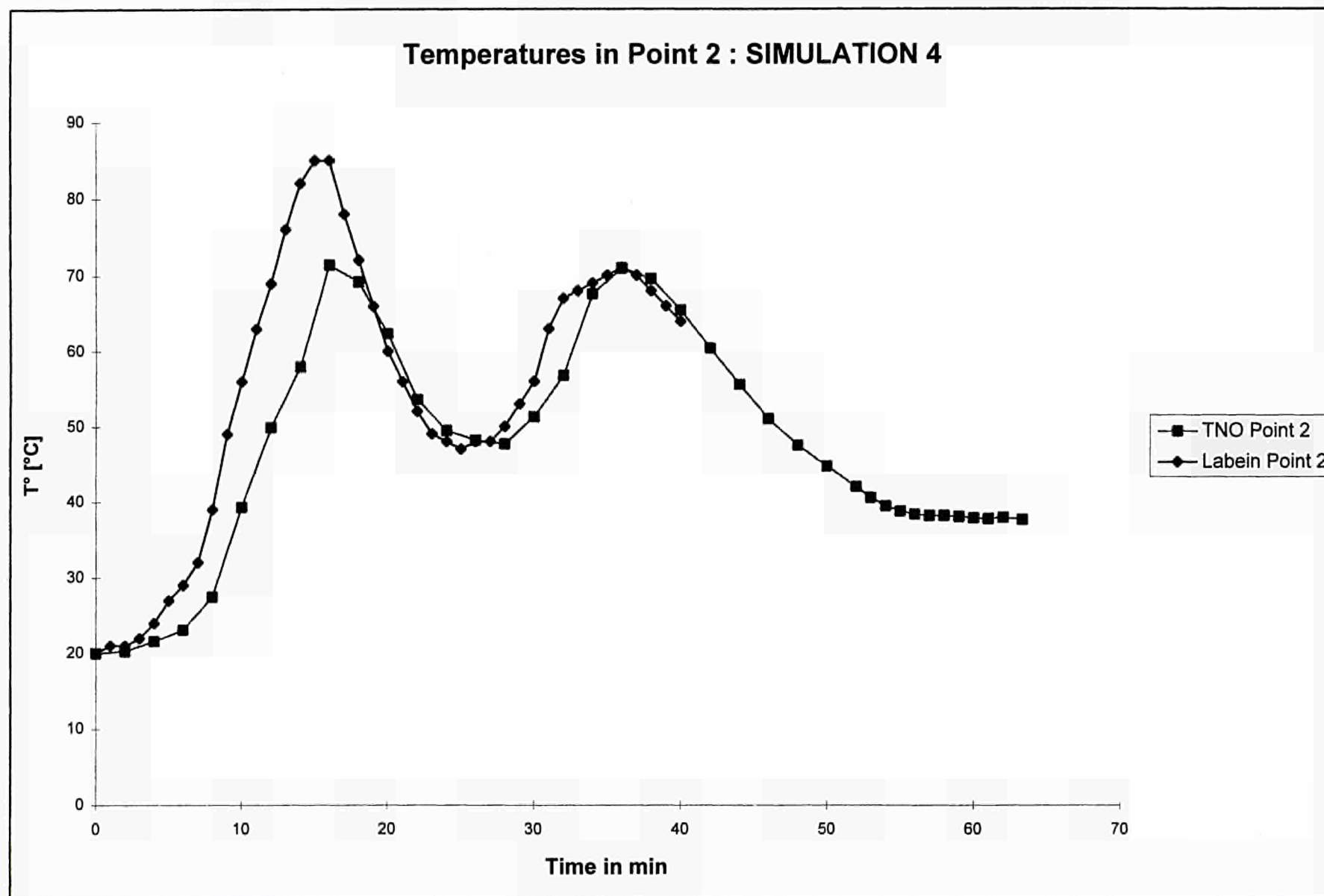
Temperatures in Point 3 : SIMULATION 4

Temperatures in Point 4 : SIMULATION 4

Temperatures in Point 5 : SIMULATION 4

85

Temperatures in Point 6 : SIMULATION 4

Temperatures in Point 7 : SIMULATION 4

Temperatures in Point 8 : SIMULATION 4
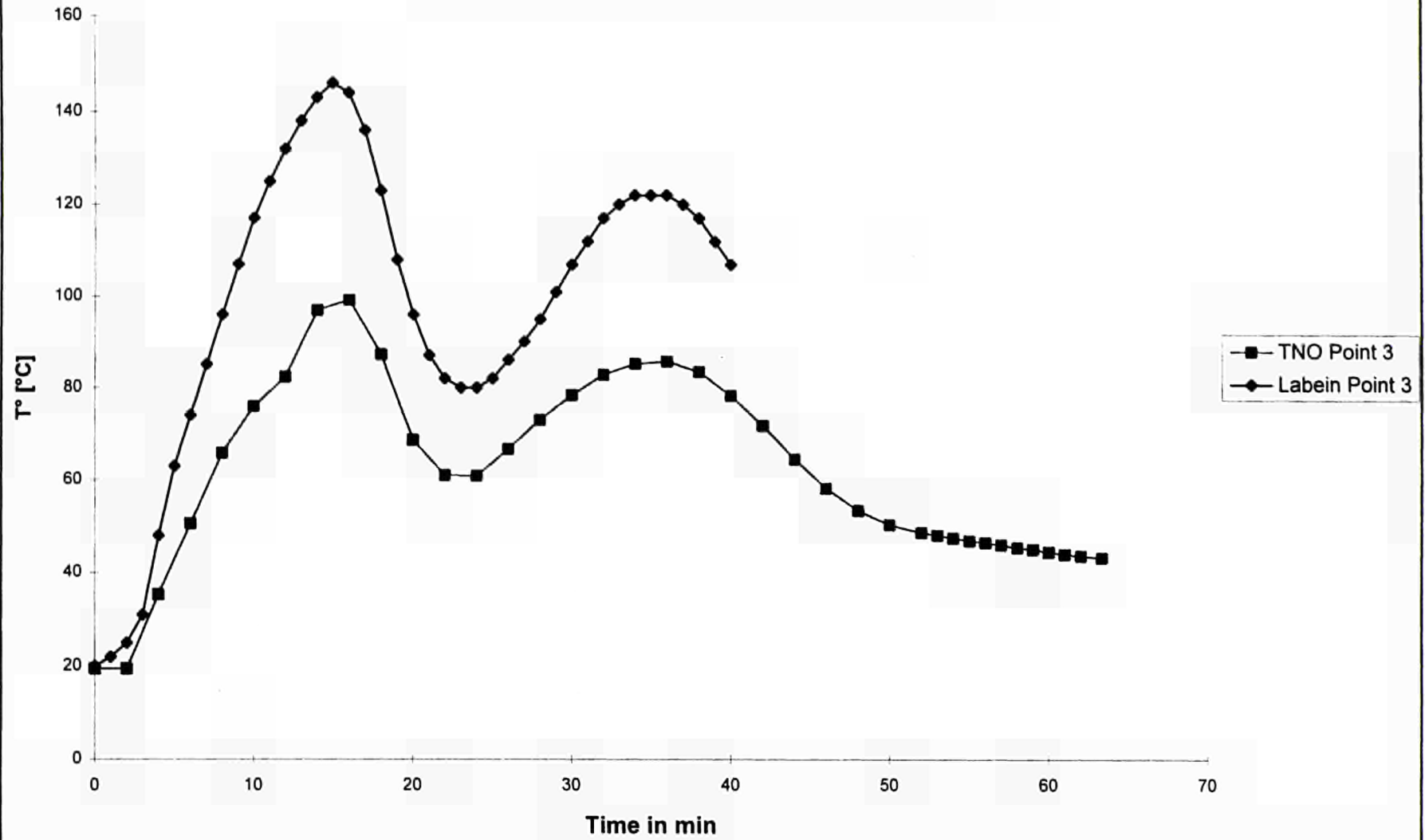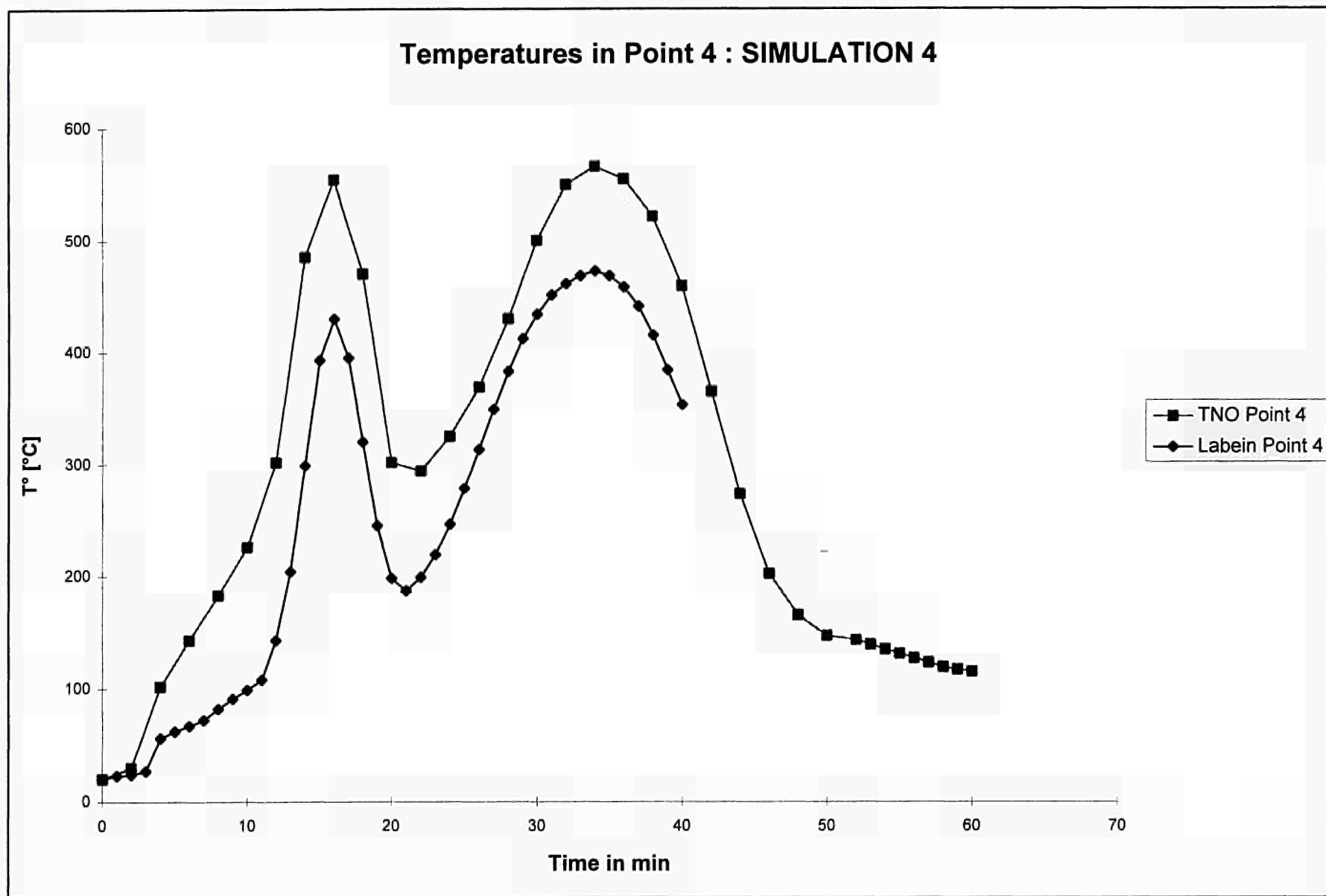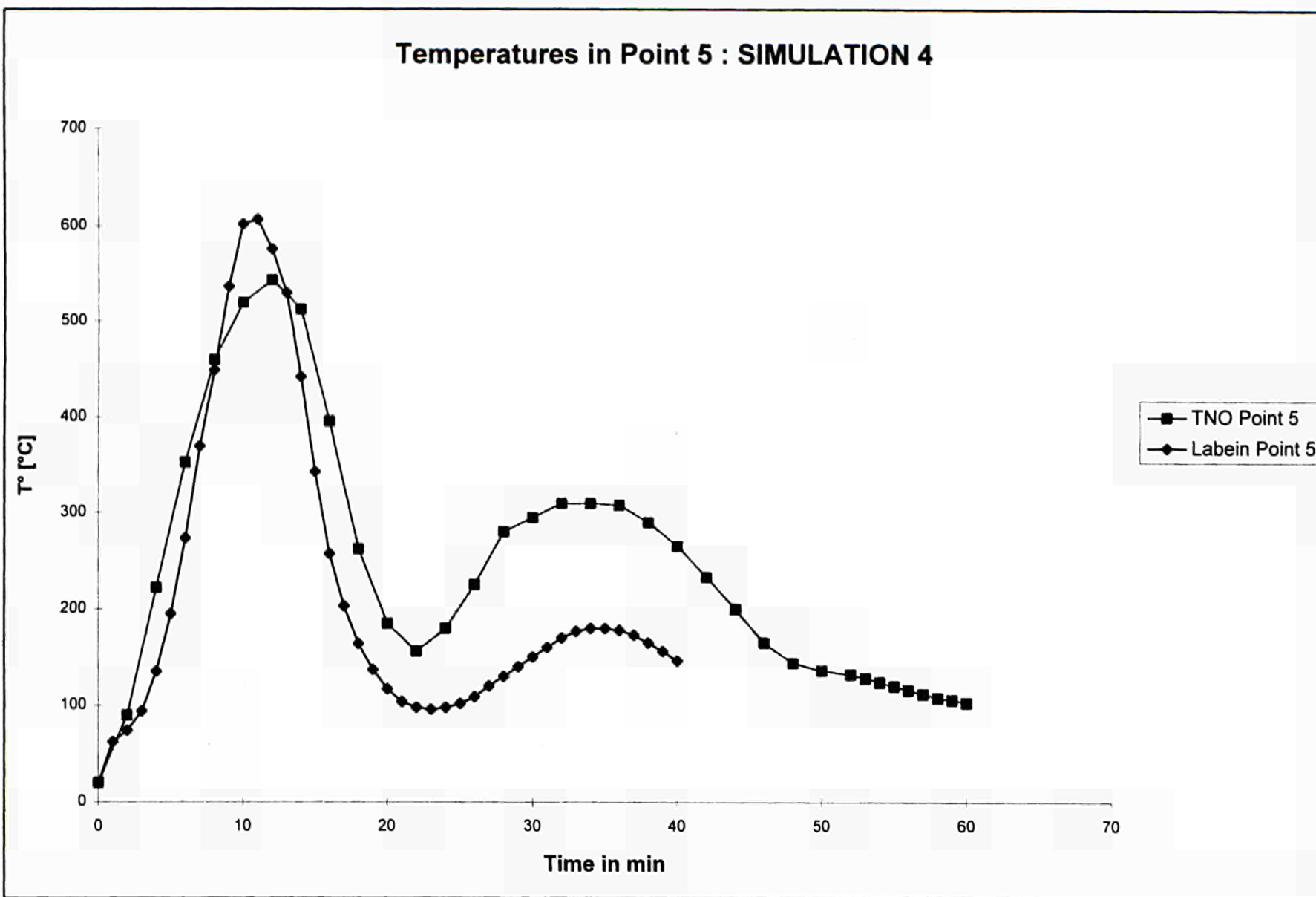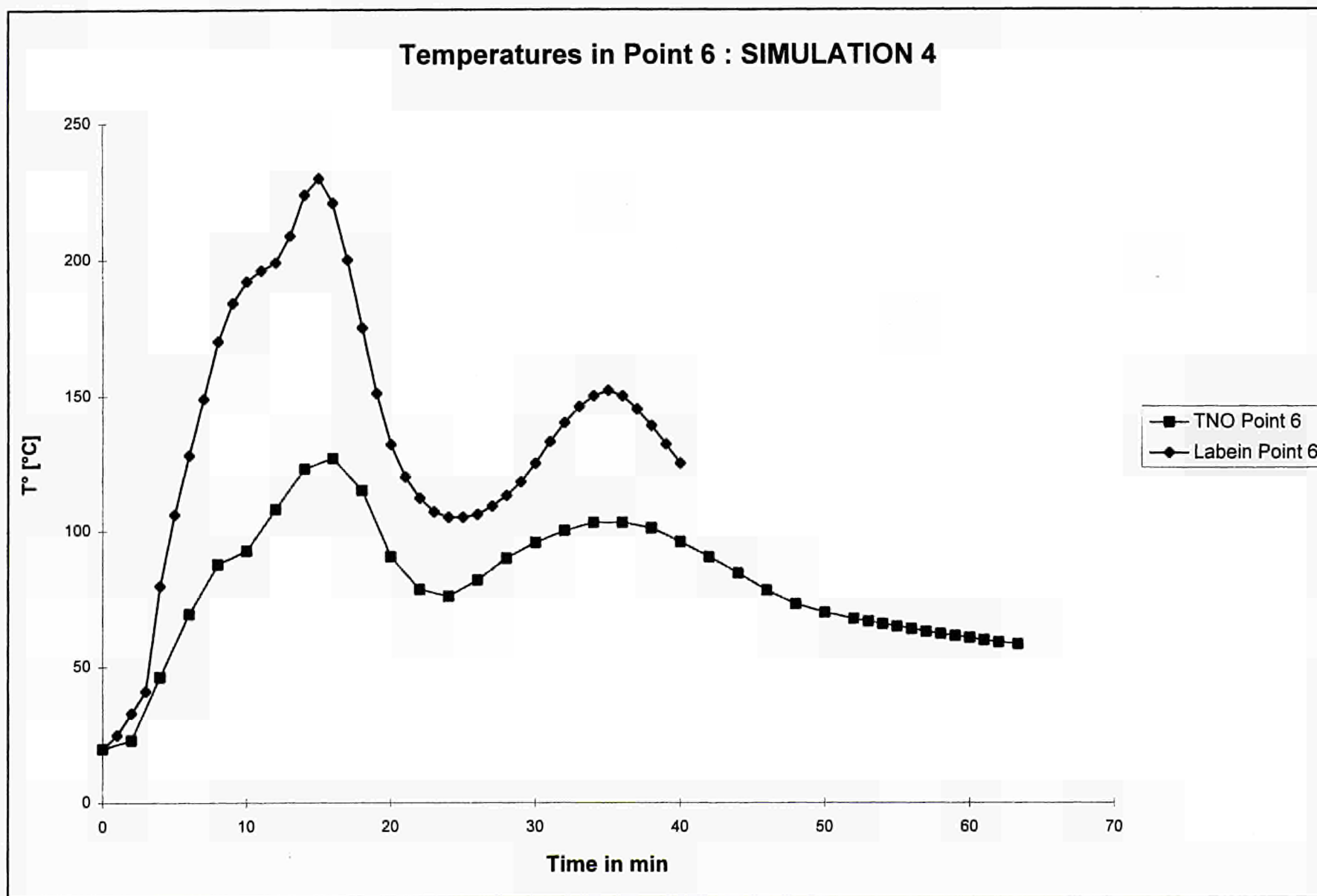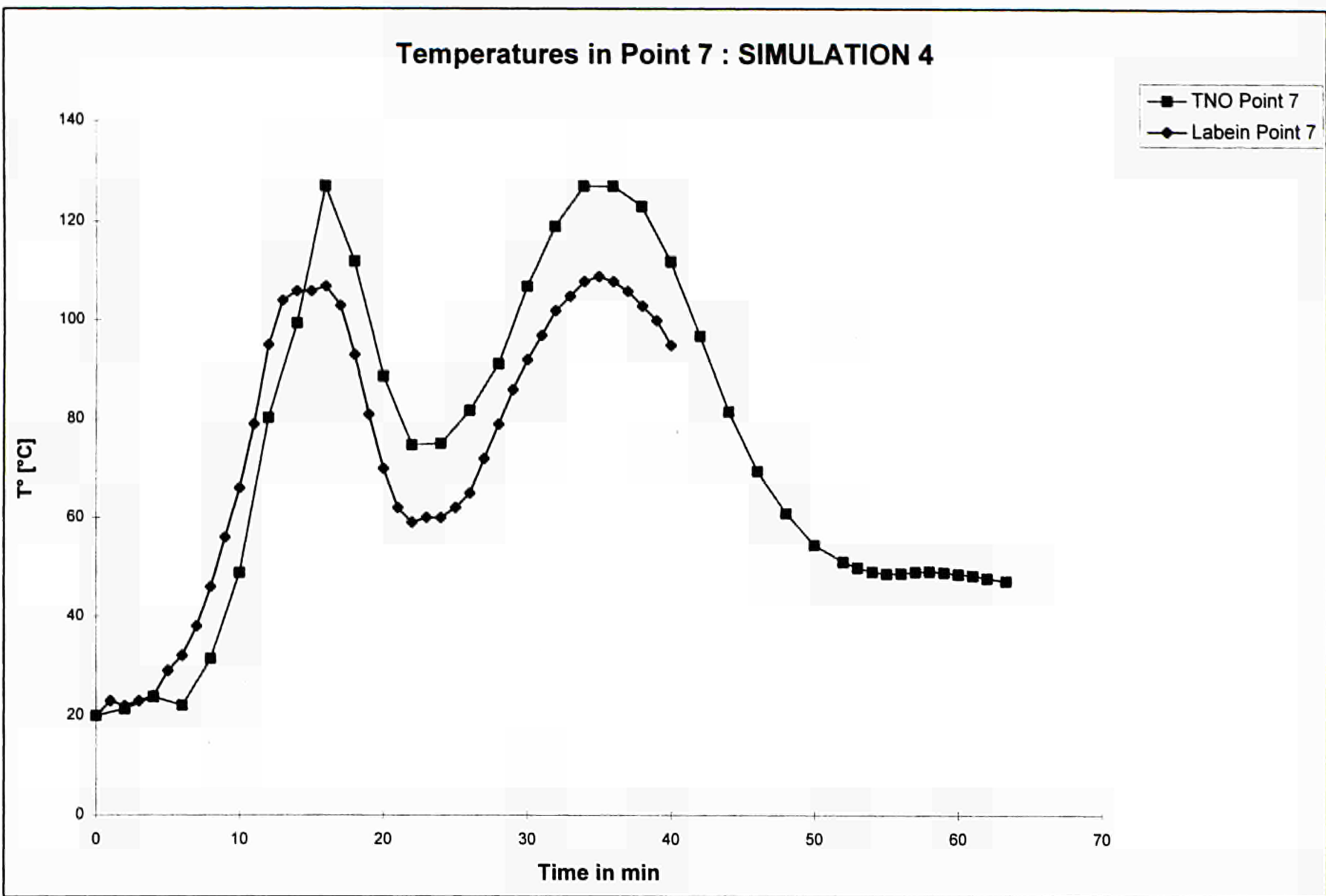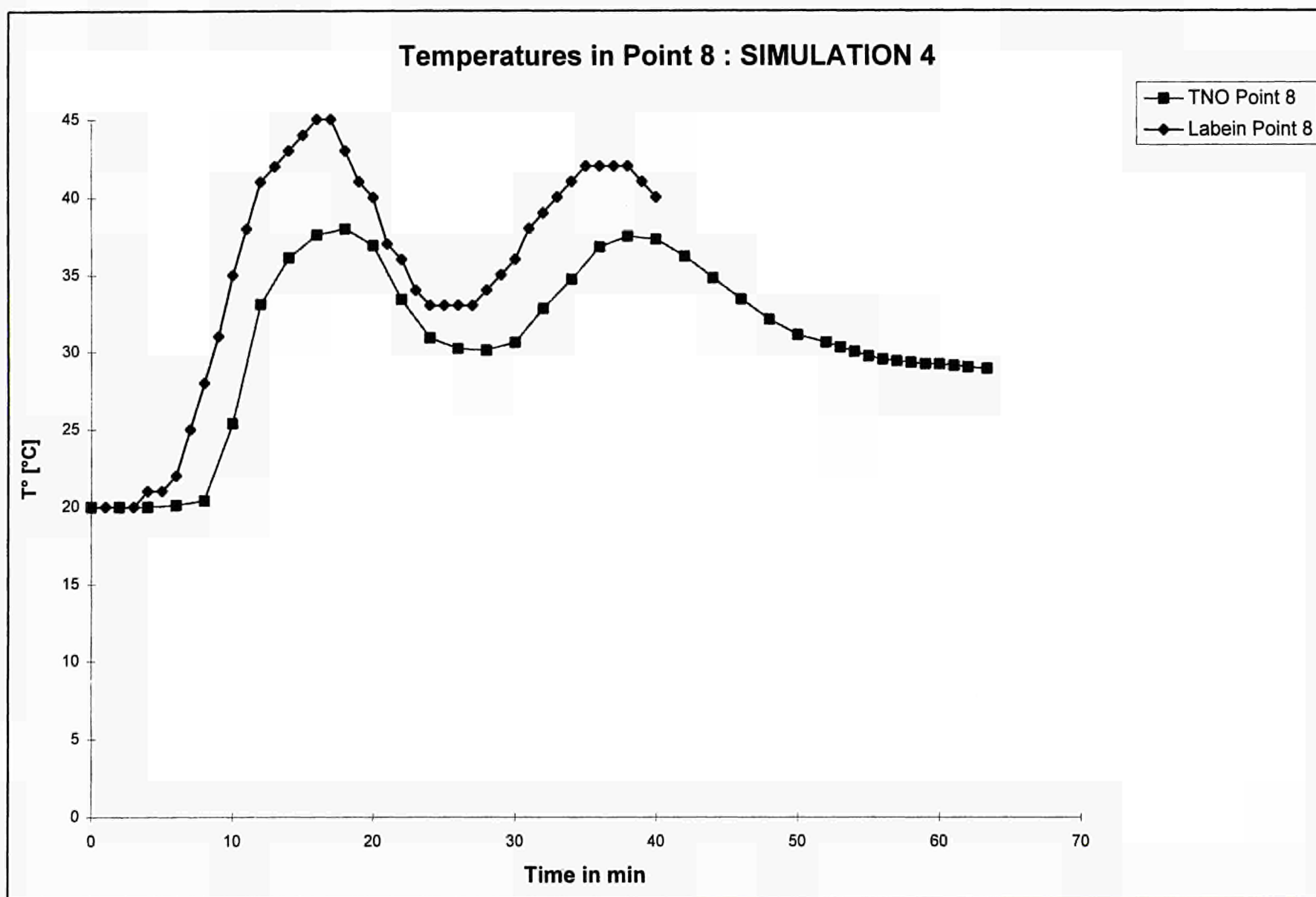
5.1.1.2. Forced ventilation

Model

Simulation 4 with forced ventilation consists of the same geometry calculated for simulation 4, with some minor changes. In order to achieve a more precise temperature level in the steel beams avoiding the need of representing their geometry precisely, what would cause a extremely big number of cells, these have been modeled as a 220mm x 600mm box composed of a surrounding steel sheet 11mm thick and a core of concrete. A boundary condition of zero heat flux at the interface between steel and concrete completes this improvement.

The scenario is forced ventilated through the four top windows. The outlet velocity of 1.39m/s fixed at these locations generates a rate of 12000 m^3/h (= 150m^3/h * 80 parking bays) which is the amount of air extraction rate requested by several standards in order to extract CO.

The other general boundary conditions remain as they were in the simulation 4. That means:

- Buoyant effect on turbulence (BEOT).
- Windows at the bottom of the garage have a fixed plenum pressure and a temperature of 293 K.
- The external wall has a defined convection coefficient of 10 W/m^2K.
- The physical properties used for the concrete and steel are :

        Concrete : Conductivity = 1.6 W/mK
                            Cp = 1000 J/kgK
                            ρ = 2500 kg/m^3
                            Emissivity = 0.94

        Steel :   Conductivity = 45 W/mK
                            Cp = 520 J/kgK
                            ρ = 7850 kg/m^3
                            Emissivity = 0.6

The resulting model after the modifications has a grid of 43 * 19 * 27 = 22059 cells, what implies a bigger computational effort.

Results

As expected, the resulting temperature distribution presents three maximums located along the beam over the burning car, see figure 5.14. As it happened in simulation 4, the first maximum, and the highest one, is reached above the front source after 11minutes. The other two maximums are reached after 16 and 34 minutes respectively and both of them are located above the rear source. Again, these two peaks reach similar values of temperature ($\approx$ 450°C) at the same section. Nevertheless, the time spacing them out and the enough drop of temperature between them allow not to consider this coincidence as a big problem.
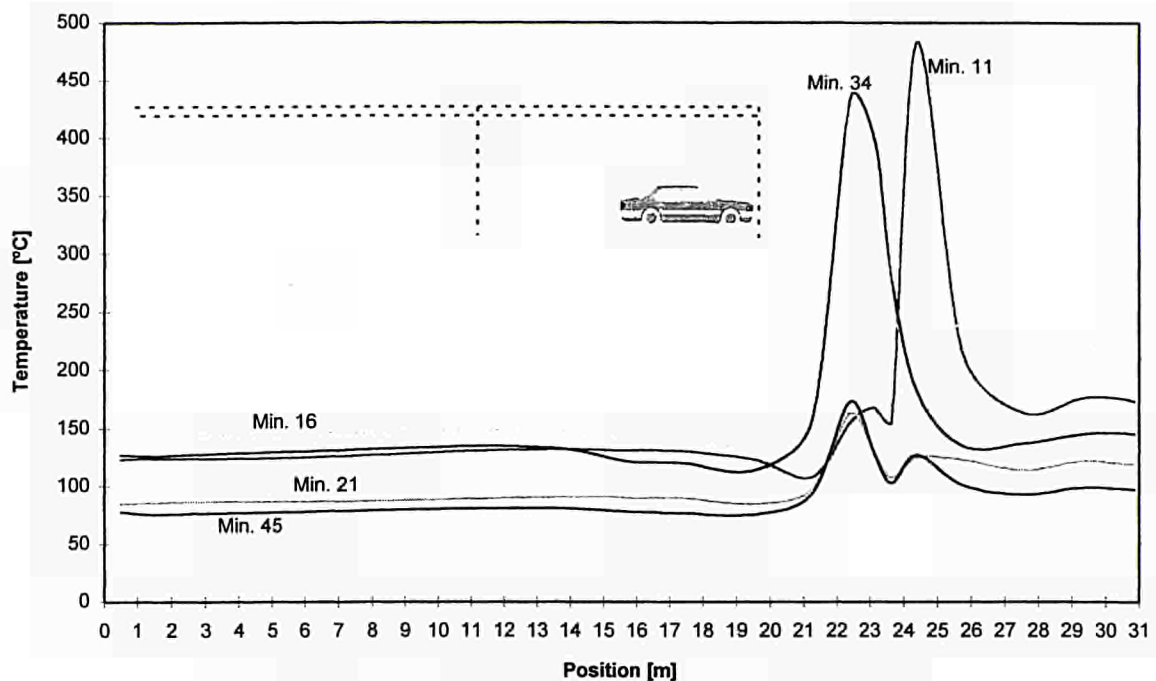
Figure 5.14 : Forced Ventilation - Temperatures above the beam

Assuming that the point C is the worst location in the section of the beam (see justification in figure 5.12) the figure 5.15 shows the local temperatures at this point over the front and the rear source allowing to compare the results of simulation 4 and the new conditions (forced ventilation) results. As expected, the maximum temperature value has decreased (from 630 to 500 °C, approx.) while the peaks over the rear source has a smaller diminution.
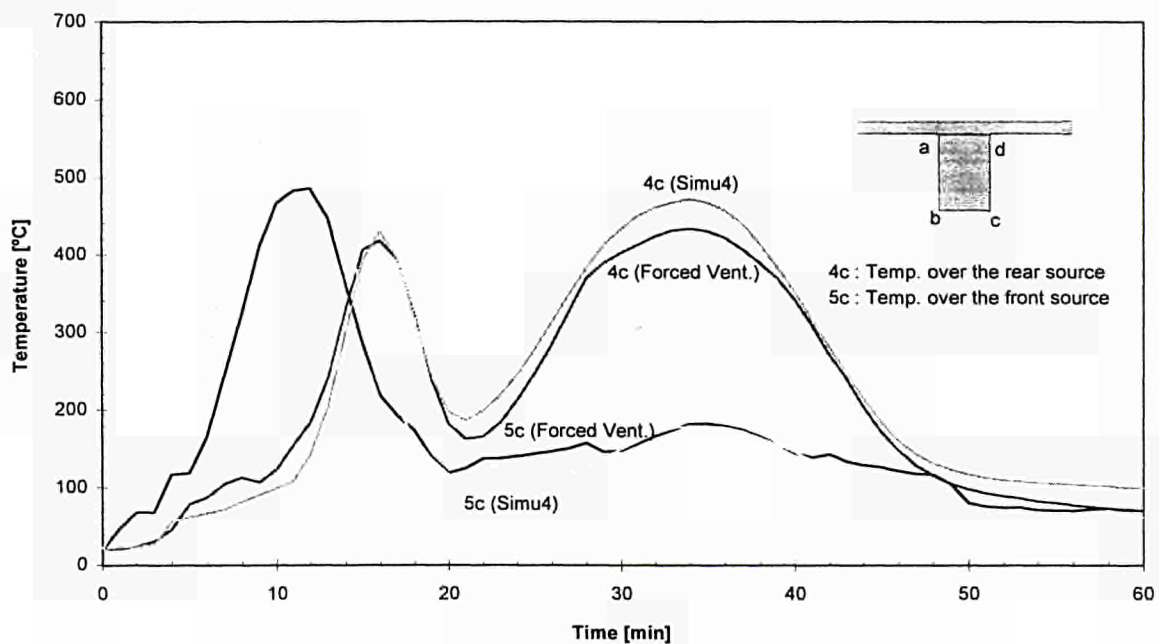
Figure 5.15 :   SIMU 4 and Forced ventilation comparison.
Temperatures over the heat sources.

90

Comparing the temperature profile along the height of the garage we can confirm that the forced ventilation conditions carries out a general decrease of the temperatures. See figure 5.16.
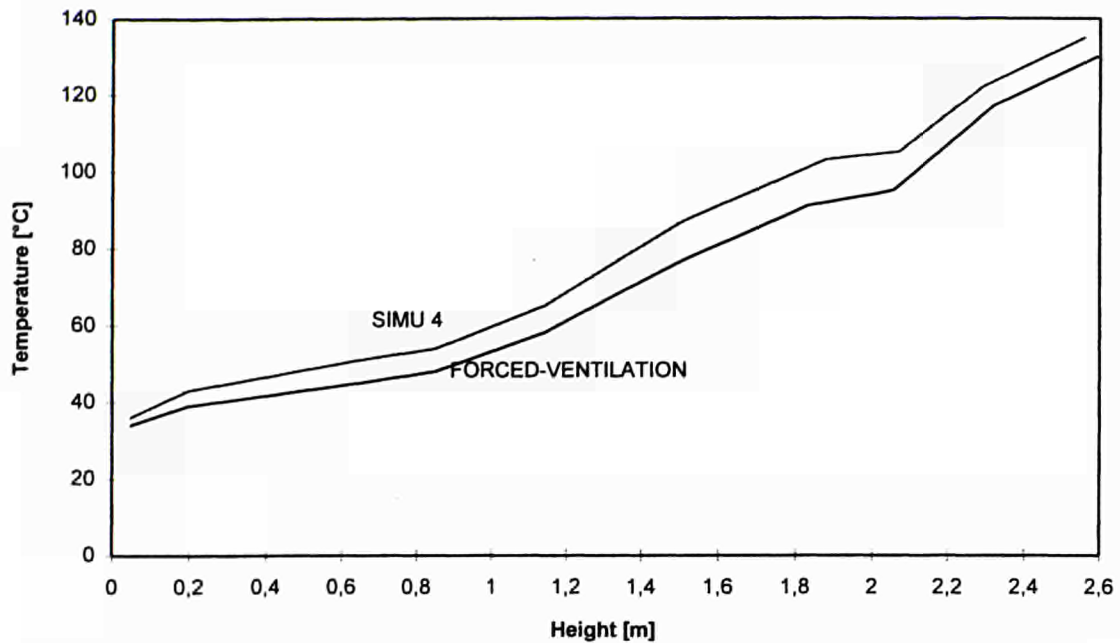
Figure 5.16 : SIMU 4 and Forced Ventilation temperature comparison - Point 4 - Minute 22

Figure 5.17 shows the comparison between the outlet velocities at the windows near the burning car (see figure 5.18) for the forced ventilation pattern and the previous one (simulation 4) showing that forced ventilation conditions are not very far from natural ventilation conditions.
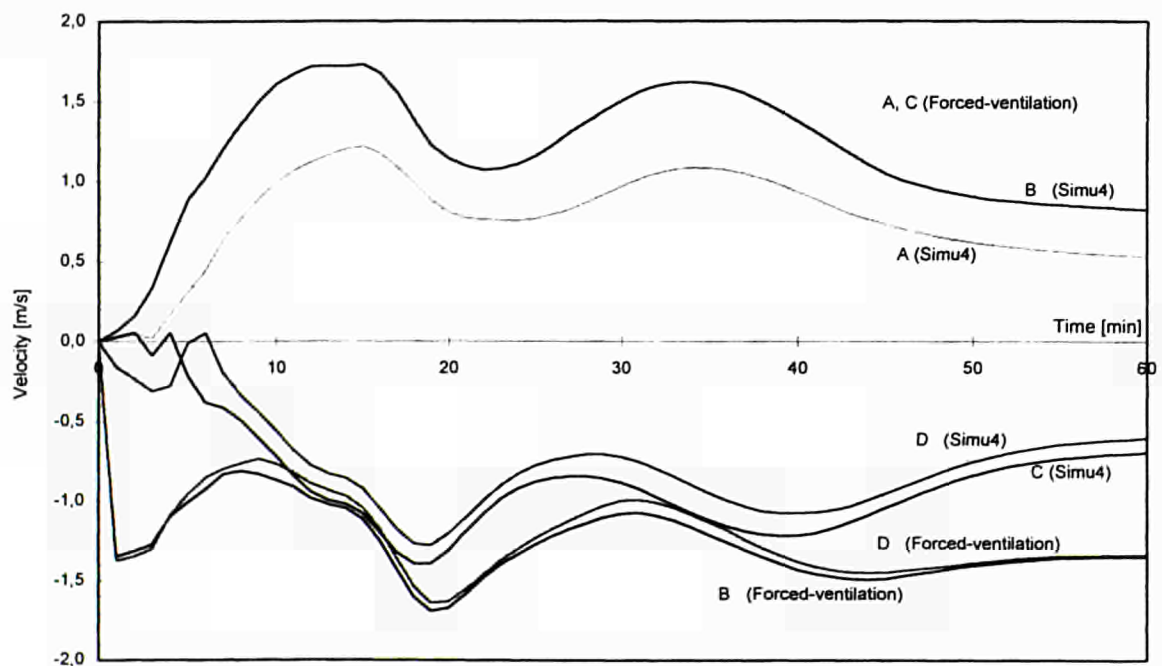
Figure 5.17 : Outlet velocities of the fluid for four windows - Comparison
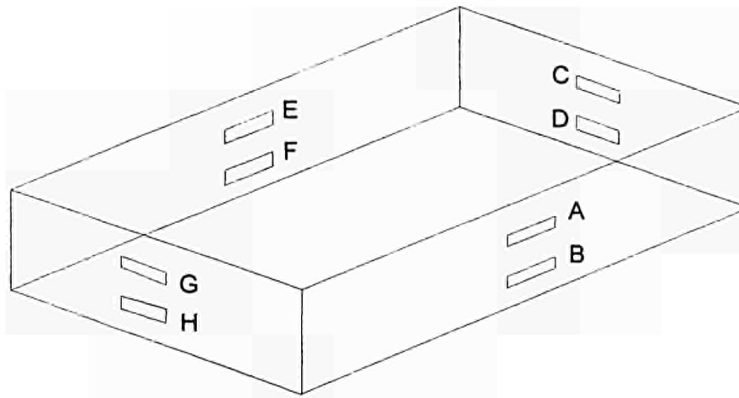
Figure 5.18 : Outlet velocities of the fluid for four windows - Geometry

Figures 5.19 and 5.20 depict the heat lost by the radiation and conduction-convection at each time. The former, in their absolute values and the latter in relative value (%).
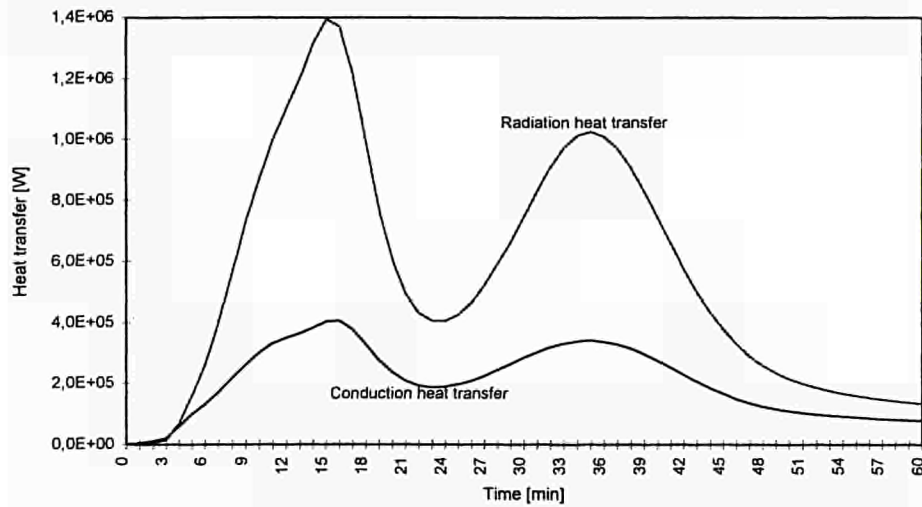
Figure 5.19 : Forced Ventilation - Conduction and radiation heat transfer
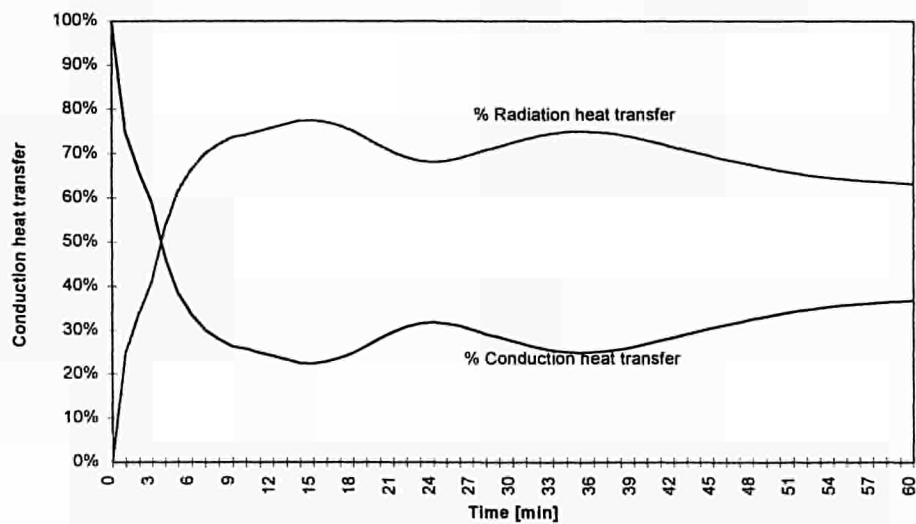
Figure 5.20 : Forced Ventilation - % of conduction and radiation heat transfer

A detailed analysis of incoming radiation flux and convection flux at each cell of the beam above the car has been carried out, providing data to analyse the temperature field in the beam.

Comparison with Alpert's formula

In order to estimate the accuracy of the expression proposed by Alpert [5] for the temperature distribution beneath a ceiling submitted to a fire source for this case, different comparisons have been made between the results obtained from the simulation and the Alpert's formula. Figure 5.21 shows an example of this comparison. This way it has been verified that for all contrasted cases, the Alpert's formula brings to over-estimate the temperatures reached beneath the beam. As already explained in chapter 3.5 and in [1], the simplified method over-estimates the maximum temperature but has to be combined to a two-zone model because the low temperature far away from the fire are too small with the simple model (Alpert in this case).
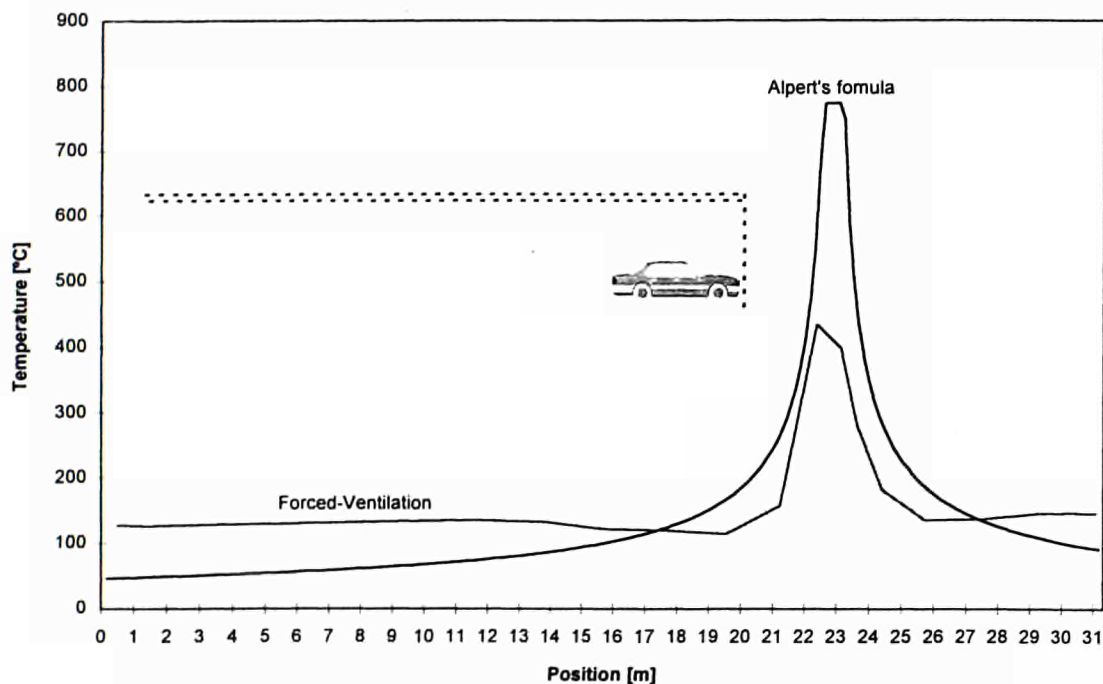
Figure 5.21 : Forced Ventilation - Comparison with Alpert´s formula - Minute 34

5.1.2. Simplified Method

5.1.2.1. With the RHR curve corresponding to the VTT test

In order to compare with the CFD calculation of the previous chapter, the RHR curve of figure 5.3 has been considered when using the simplified approach. The simplified method has been already explained and used in chapter 3.5. The two following figures (figures 5.22 and 5.23) show the heat flux q'' received by the IPE 600 beam.
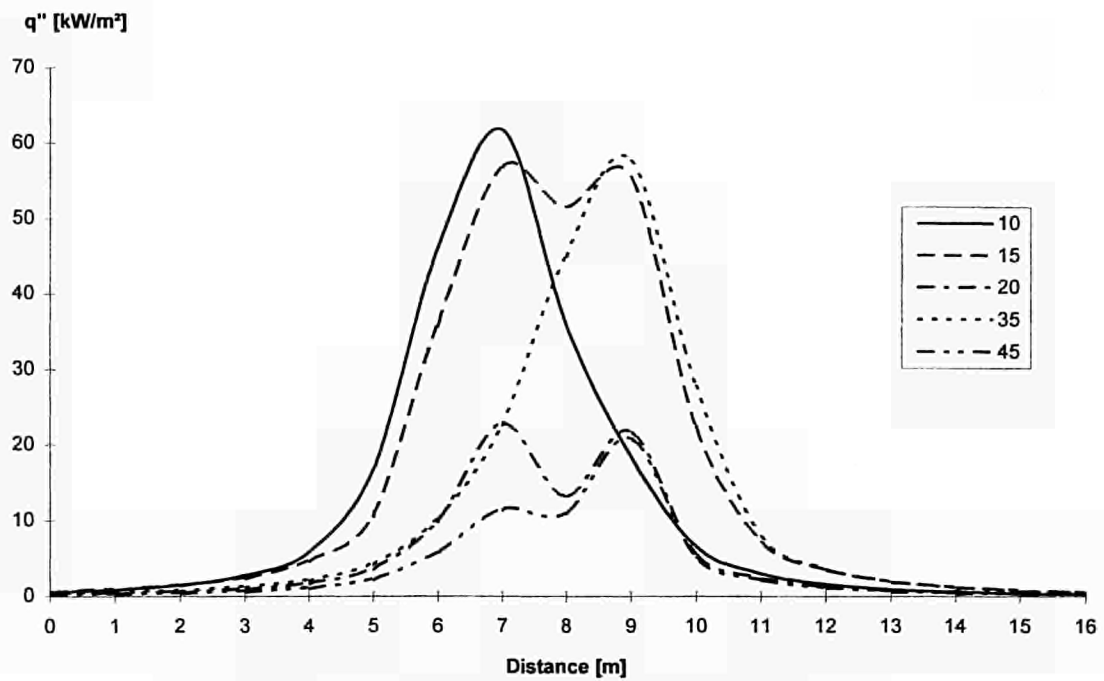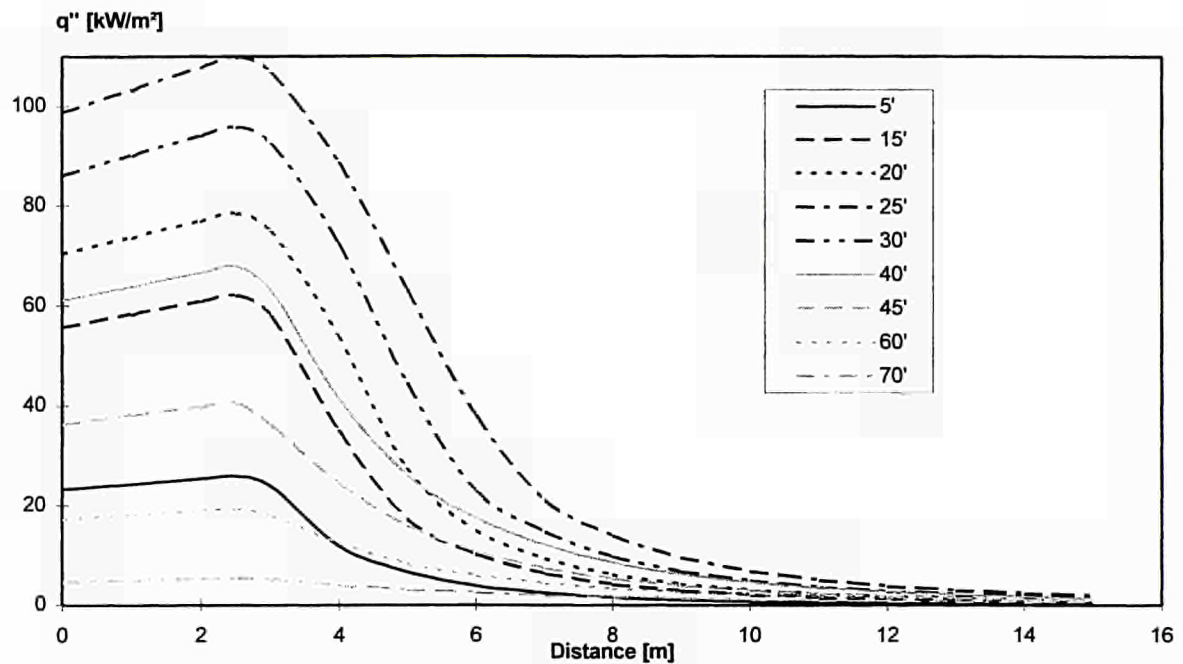
Figure 5.22 : q'' in function of the distance for different times
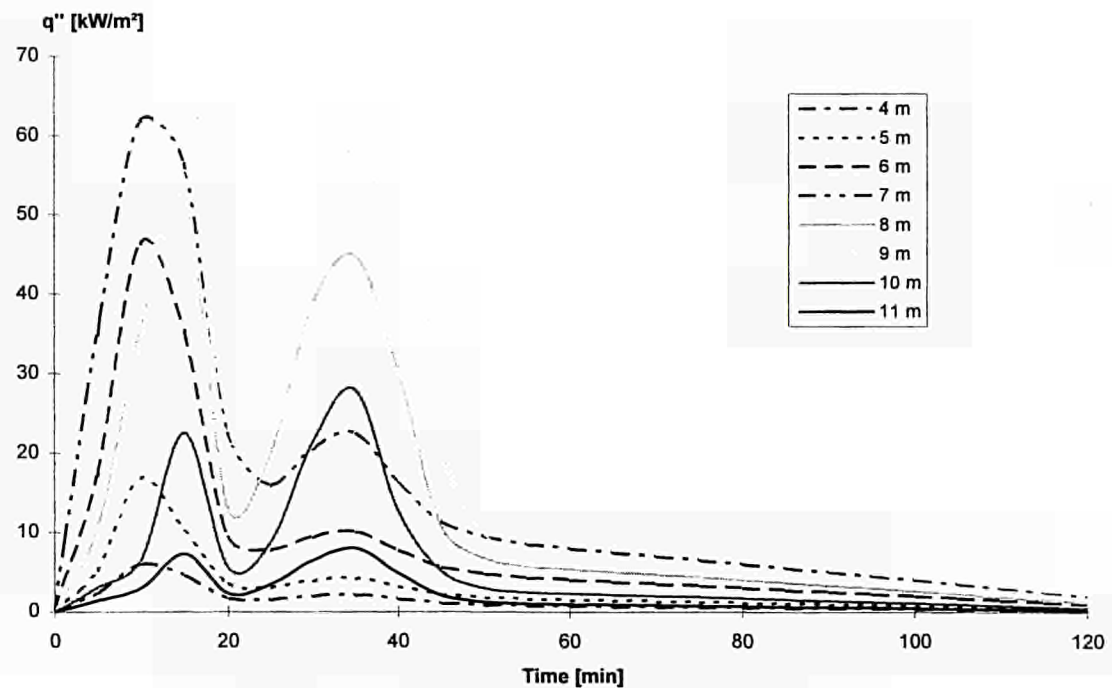
*Figure 5.23 : q'' in function of the time for different distances*

5.1.2.2. With the reference RHR curve of chapter 3.4

The similar figures are given below (figures 5.24 and 5.25) but the reference curve deduced from the CTICM tests has been used (see chapter 3.4).
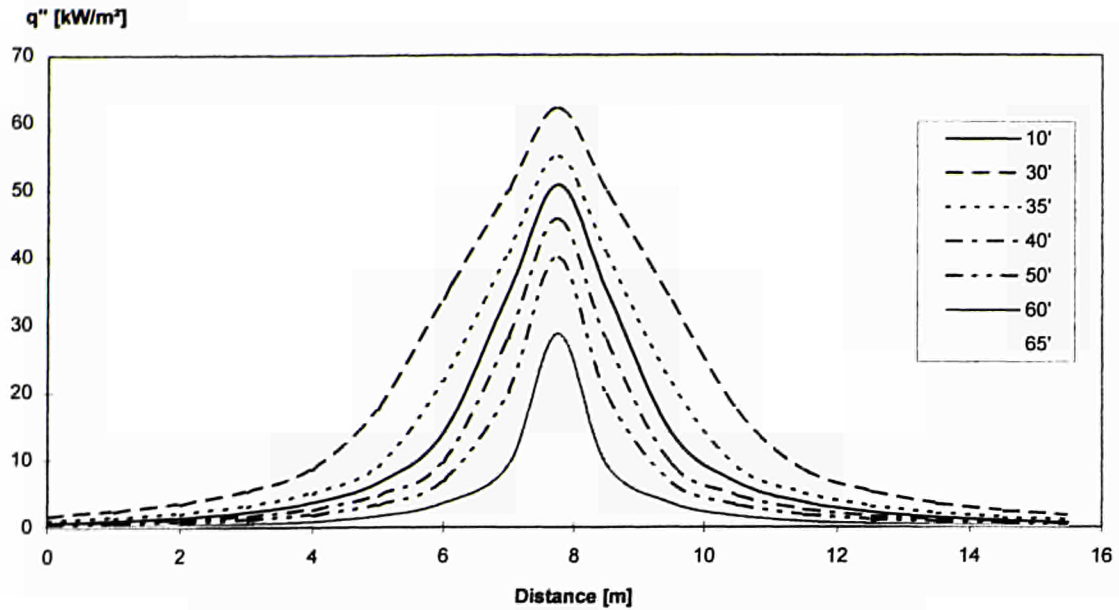
Figure 5.24 : q'' in function of the distance for different times
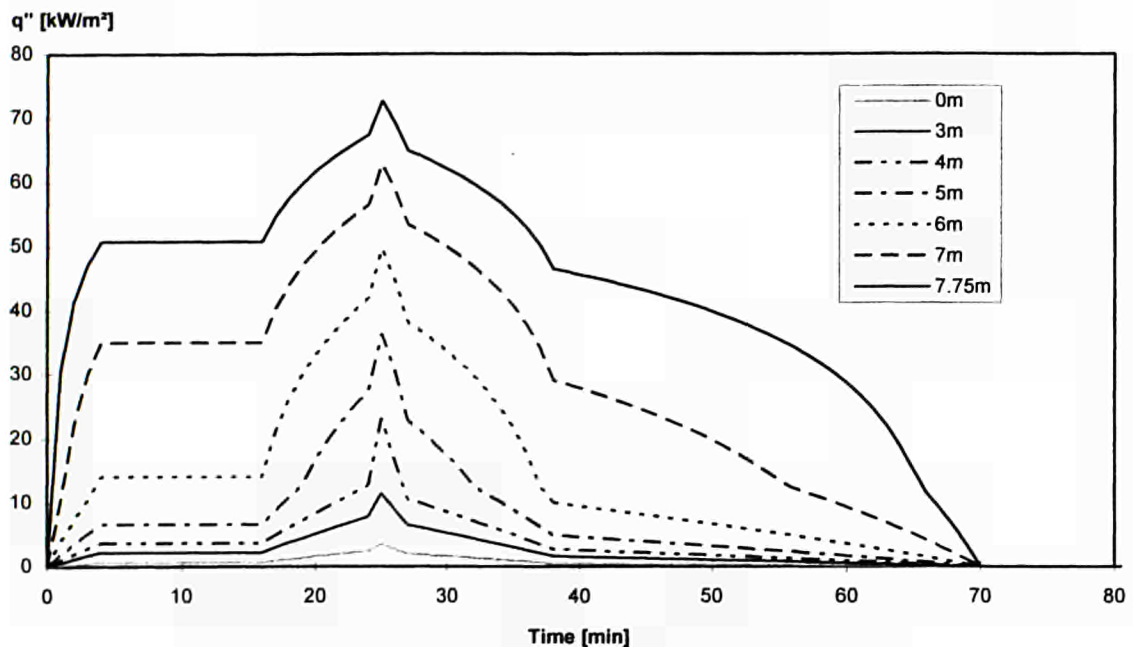
Figure 5.25 : q'' in function of the time for different distances

5.2. Scenario 2 : wave of several burning cars

Five cars have been considered. The time between ignition of the different car is 12'. The RHR curve of cars during the spread is given in chapter 3.4.1. The different RHR curves for the five cars are shown in chapter 3.4.3.

The heat flux q'' reaching the beam situated between car 1 and car 2 (see figure 5.26) taking into account the influence of the five cars is represented on the figures 5.27 and 5.28. This corresponds to the most severe position of the cars; it has been shown that a

beam situated between car 2 and car 3 would be subjected to a less severe heat flux and steel temperature field. The Hasemi´s model adapted to consider the walls (see figure 3.43) has been used.

Figure 5.27 : q'' in function of the distance for different times
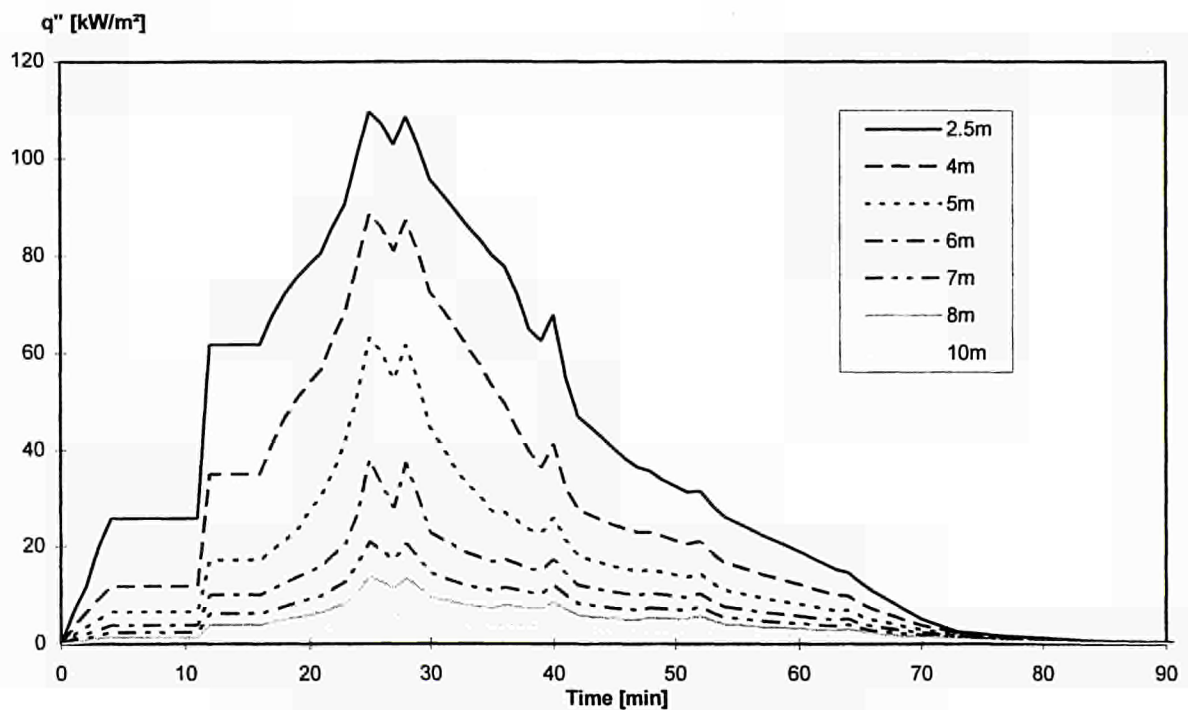
Figure 5.28 : q'' in function of the time for different distances

96
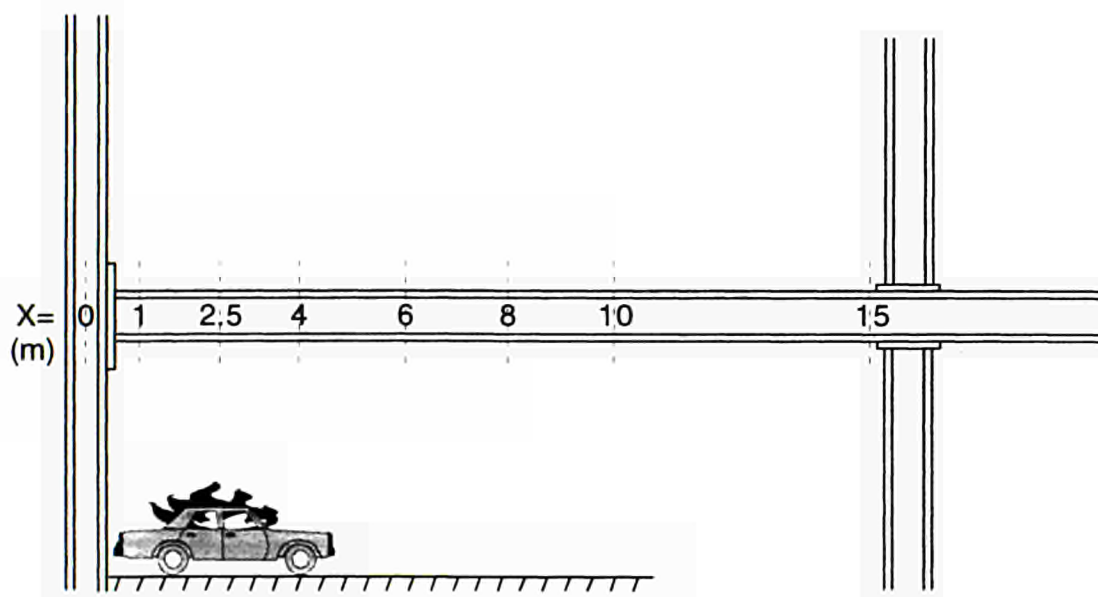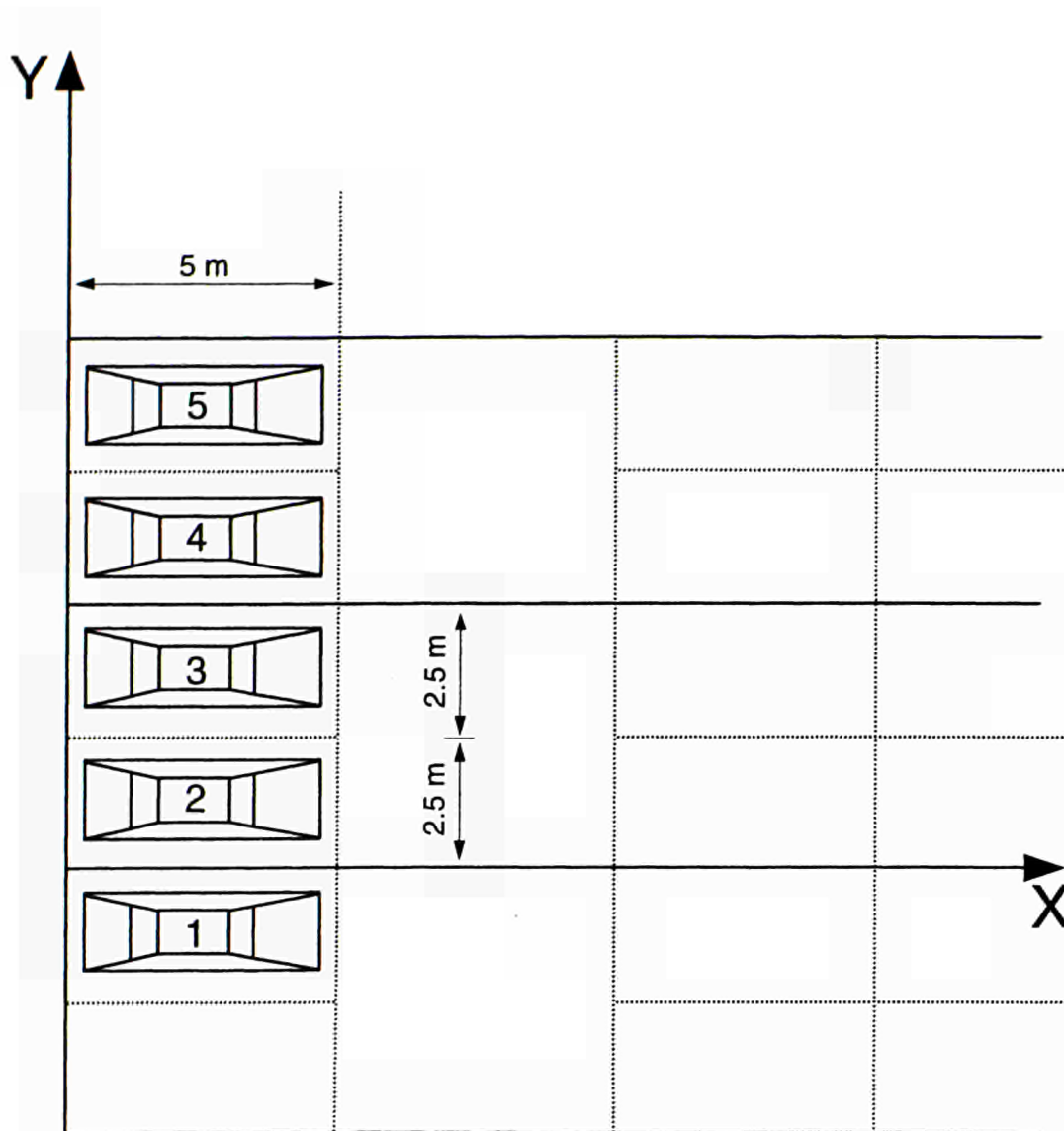
Figure 5.26

6. *TEMPERATURE IN THE STRUCTURE*

6.1. Fire scenario 1 : One burning car

6.1.1. CFD calculation - RHR curve based on VTT tests

In figure 6.1 -with the same 2-D viewpoint as in figure 5.7- the maximum steel temperatures along the most heated beam (above the fire) is given at t=2040 s. Because the steel temperature lags behind the air temperature (because of the thermal inertia of the beam) the peak steel temperature is much lower than the surrounding air/smoke temperature. The calculated steel temperature is well below 400°C. If the RHR in a real carfire is equal to the experimental values used for the modelling (peak RHR of 2 MW, see figure 5.3), the conclusion can be drawn that unprotected steel can be used in carpark construction.

The maximum steel temperatures given in figure 5.7 are a safe approximation, since the transport of heat in the steelbeam parallel to the beam is not taken into account. Peak values of the temperatures in the steel will be exaggerated. (The number of cells in the steel beam is 200 (5 in height and 41 for the length of the beam).

6.1.2. Simplified method

6.1.2.1. With the RHR curve based on the VTT tests

The method to calculate the steel temperature has been described in chapter 3.5 and is used here with the heat flux distribution q'' given in chapter 5.1.2.1.
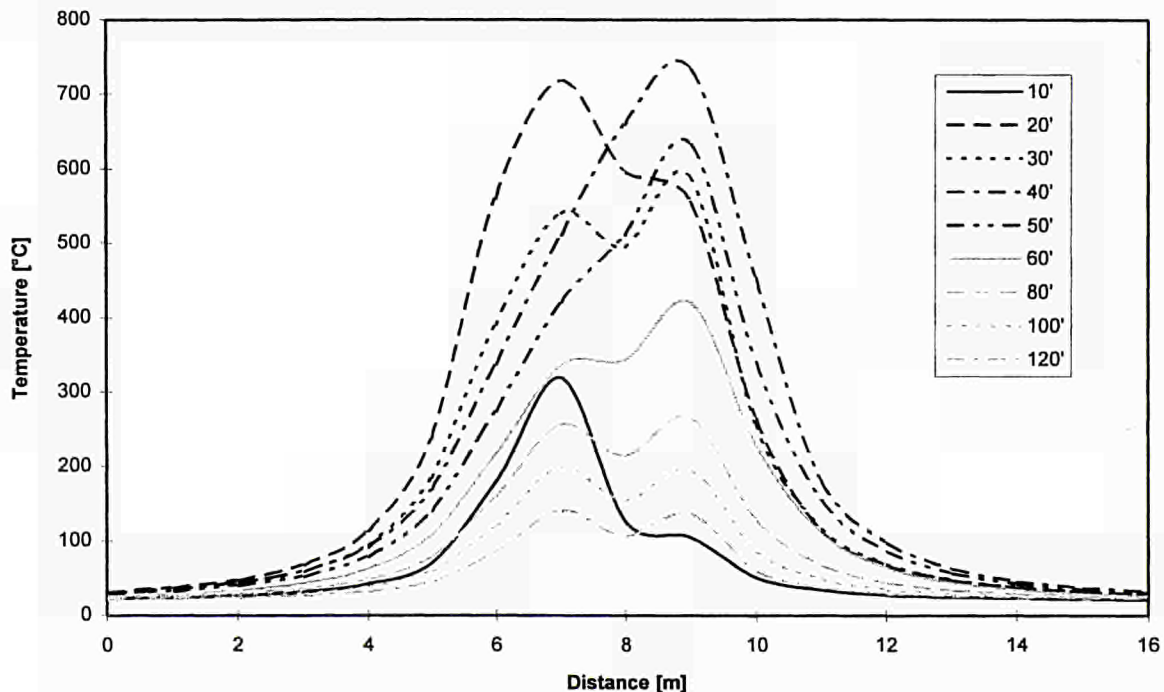
Figure 6.2 : Temperature in function of the distance for different times

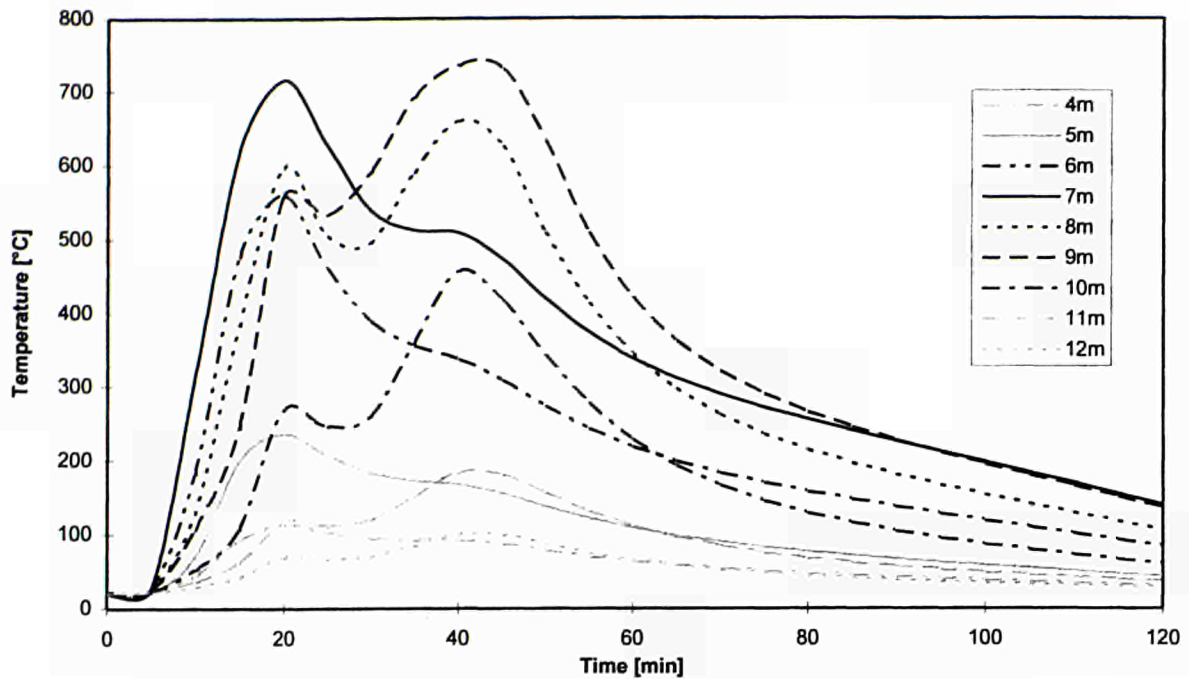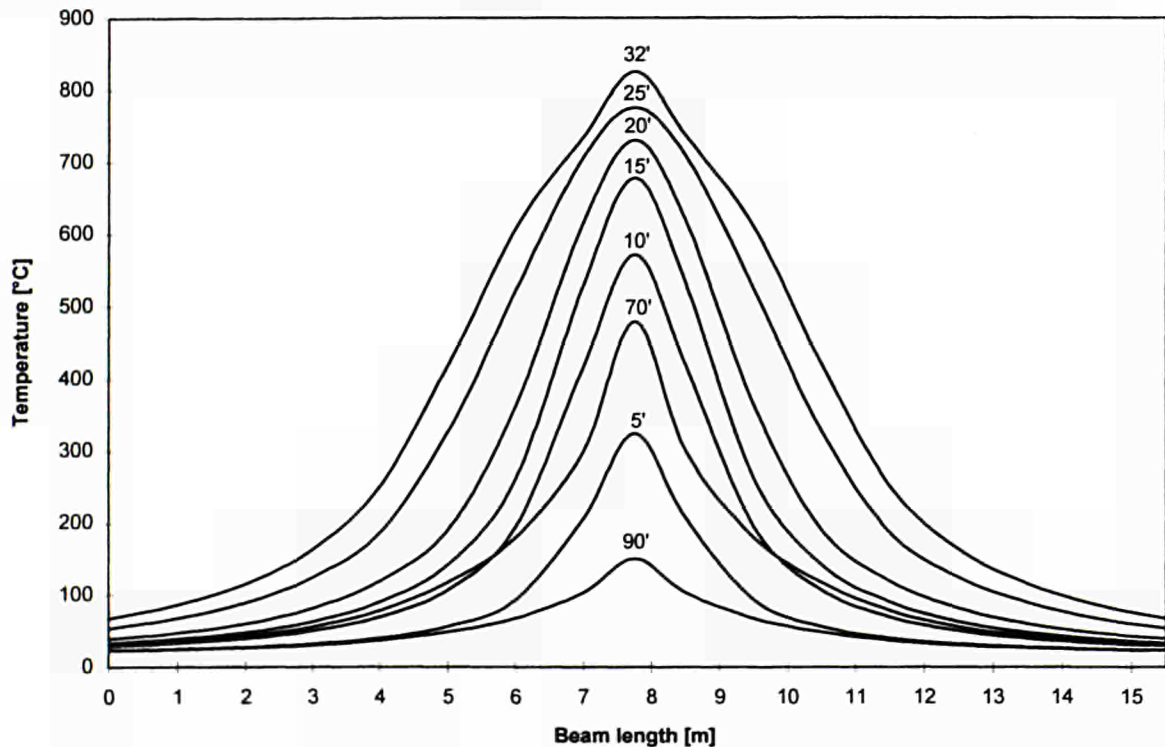This steel temperature field is very conservative compared to the CFD results of figure 6.1.

Figure 6.3 : Temperature in function of the time for different distances

6.1.2.2. With the reference RHR curve given in chapter 3.4.1.

The heat flux distribution q'' is given in chapter 5.1.2.2.

Figure 6.4 : Temperature in function of the distance for different times

This steel temperature field is very conservative compared to the CFD results of annex 3.
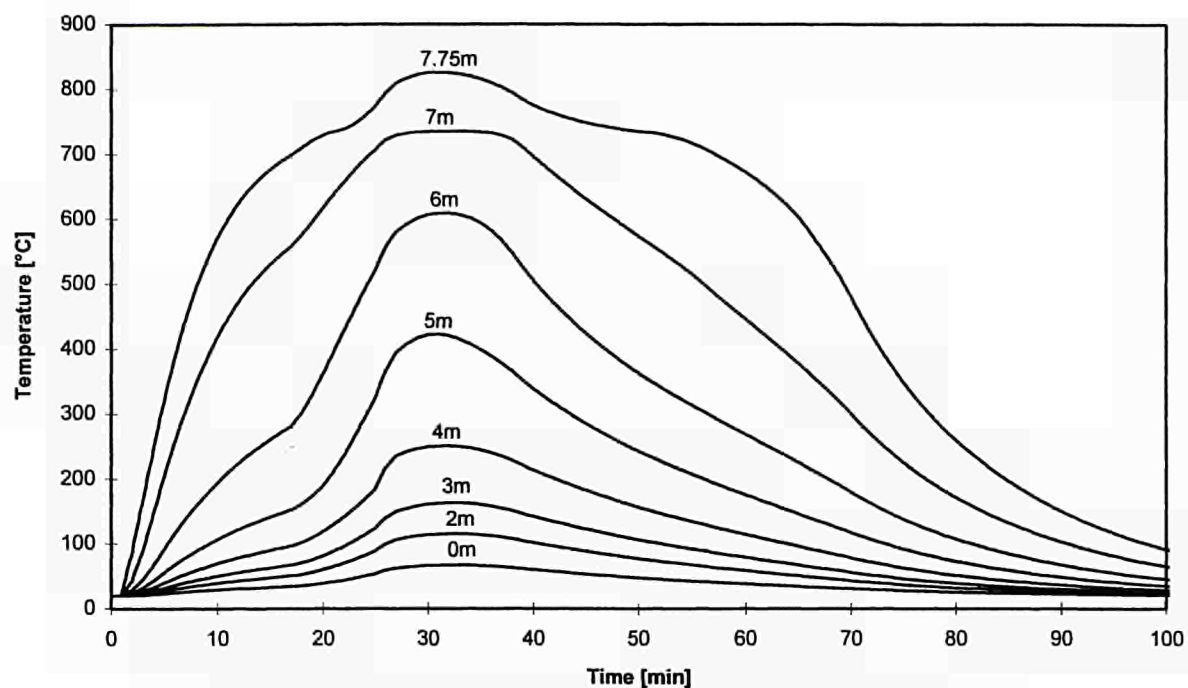
Figure 6.5 : Temperature in function of the time for different distances

6.2. Scenario 2 : wave of several burning cars

The heat flux q'' is given in chapter 5.2 and leads to the following steel temperature of the beam.
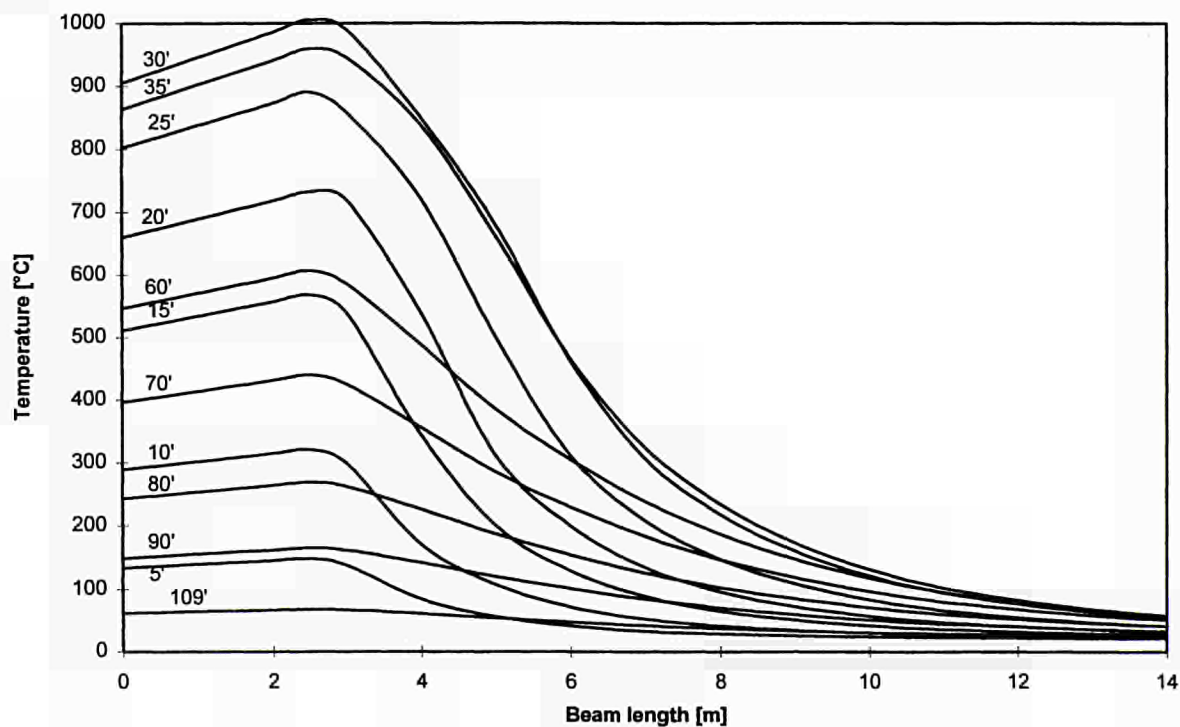
Figure 6.6 : Temperature in function of the distance for different times

100
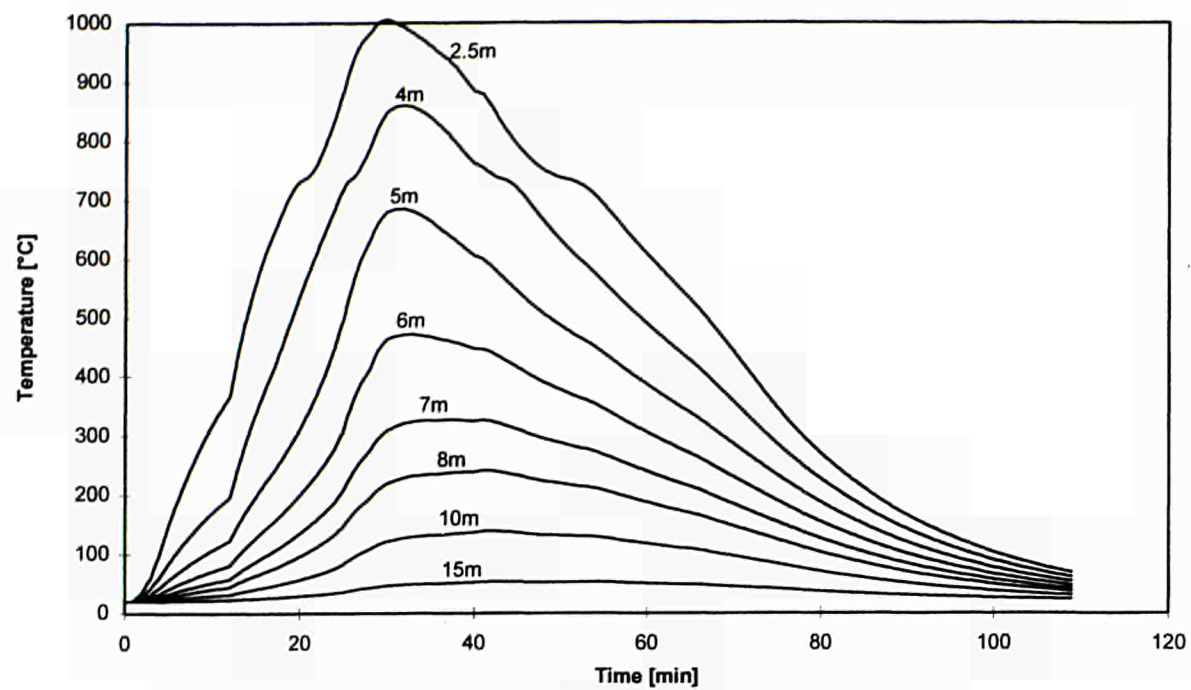
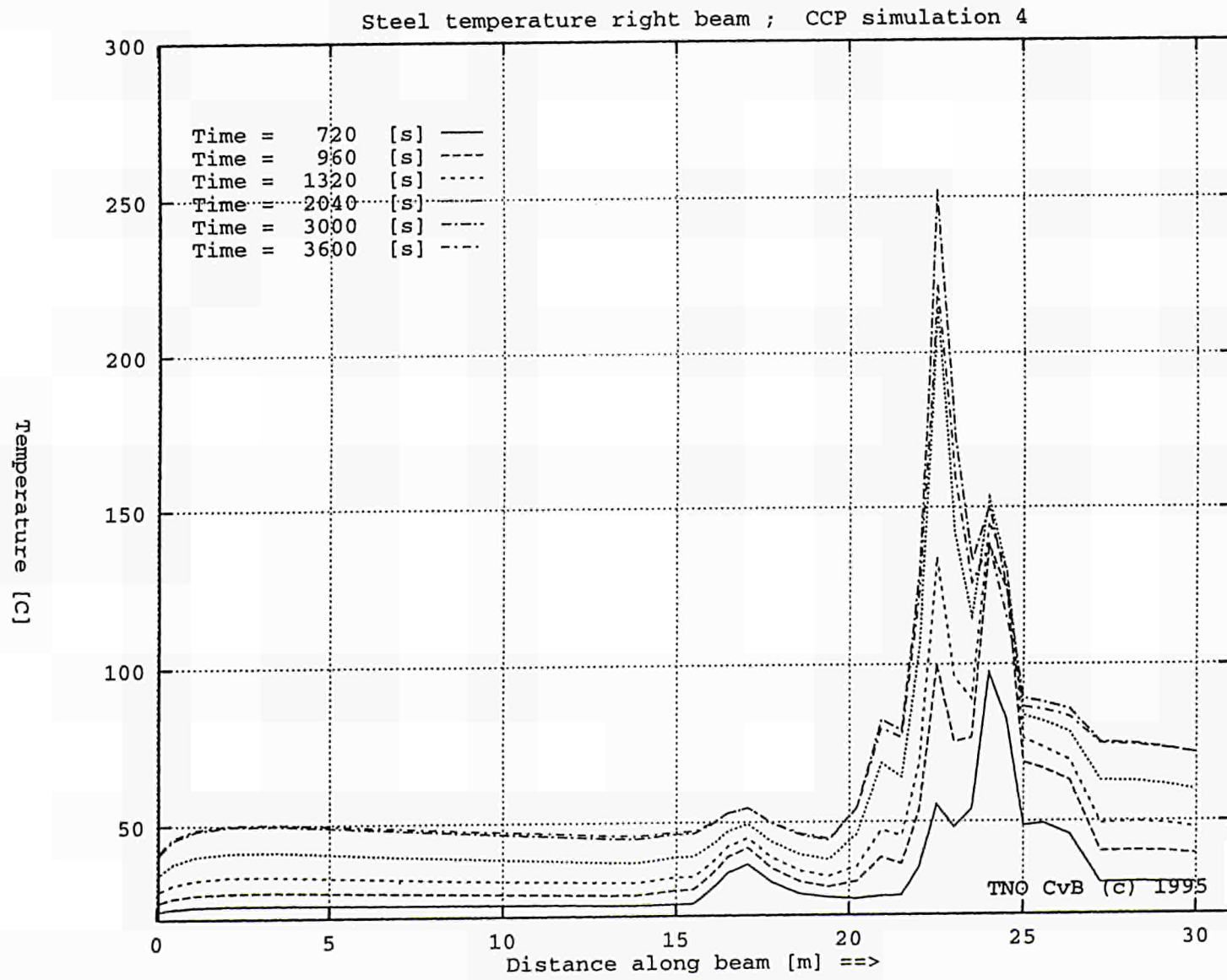*Figure 6.7 : Temperature in function of the time for different distances*

Figure 6.1 : Steel temperature along the most-heated beam at time T=2040s

7. *STRUCTURE BEHAVIOUR*

7.1. Introduction

The structure and the different fire scenarii have been described in the chapter 3.6. Two basically different types of structural systems will be scrutinized :

- Structural system 1 : Support beam as a single span girder with linked connections to the column (Joint type 1).
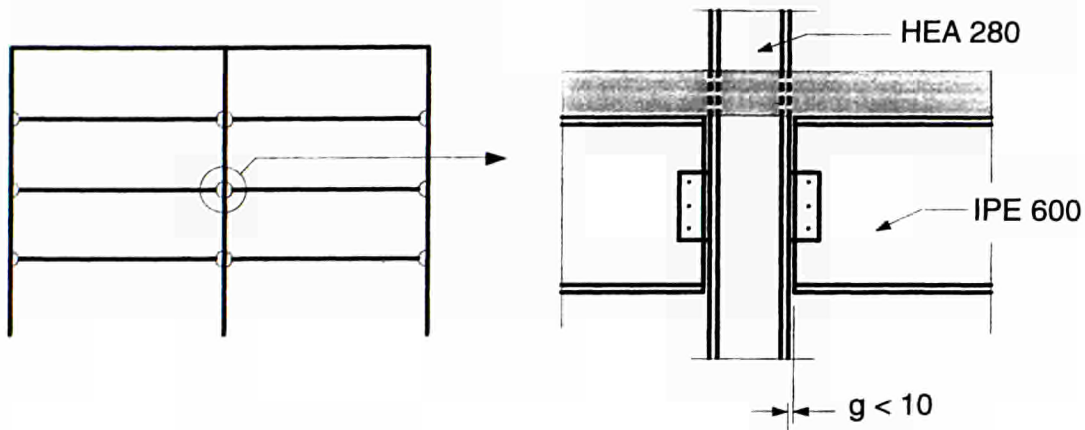
- Structural system 2 : Support beam as a continuous beam with rigid connections to the column (Joint type 2).
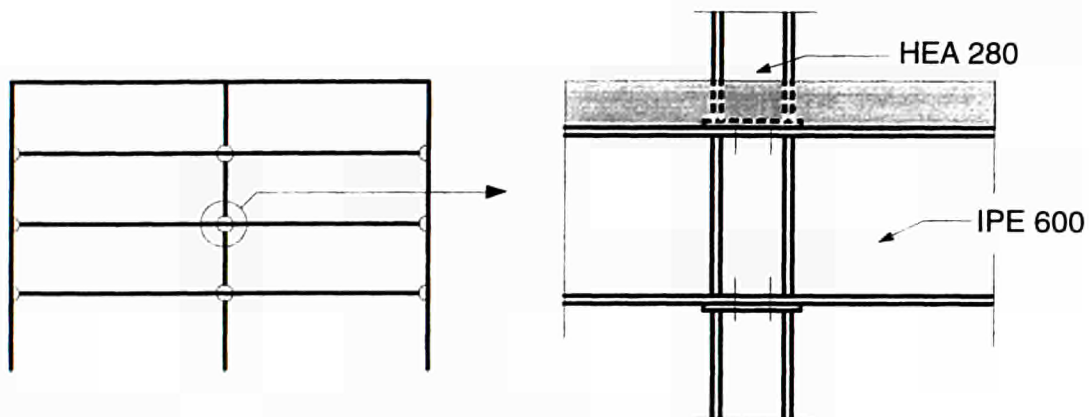
The applied loads are split up in the following way:

distributed load :
- dead load deck = 3,6 kN/m²
- dead load beam = 1,2 kN/m
concentrated load :
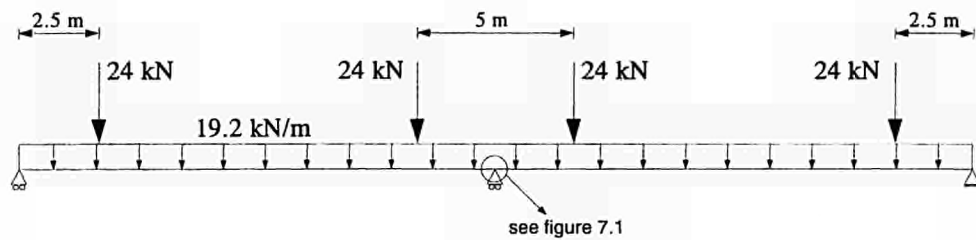A concentrated load equal to 12 kN is considered. This load corresponds to a medium size car (e.g. Opel Vectra).

With the distance between beams being equal to 5 meters, the total load on the beams becomes :

distributed load   q = 1,2 + (3,6 * 5) = 19,2 kN/m
concentrated load   Q = 2 * 12 = 24 kN

7.2. Fire scenario 1 : one burning car

The structural system 1 is considered

The heating of the beam is given by the figures 6.4 and 6.5. The figure 6.4 can be presented in the following way where, for each time step, the temperatures along the beam have been divided by the maximum temperature corresponding to the ceiling point just above the fire (see figure 7.2).
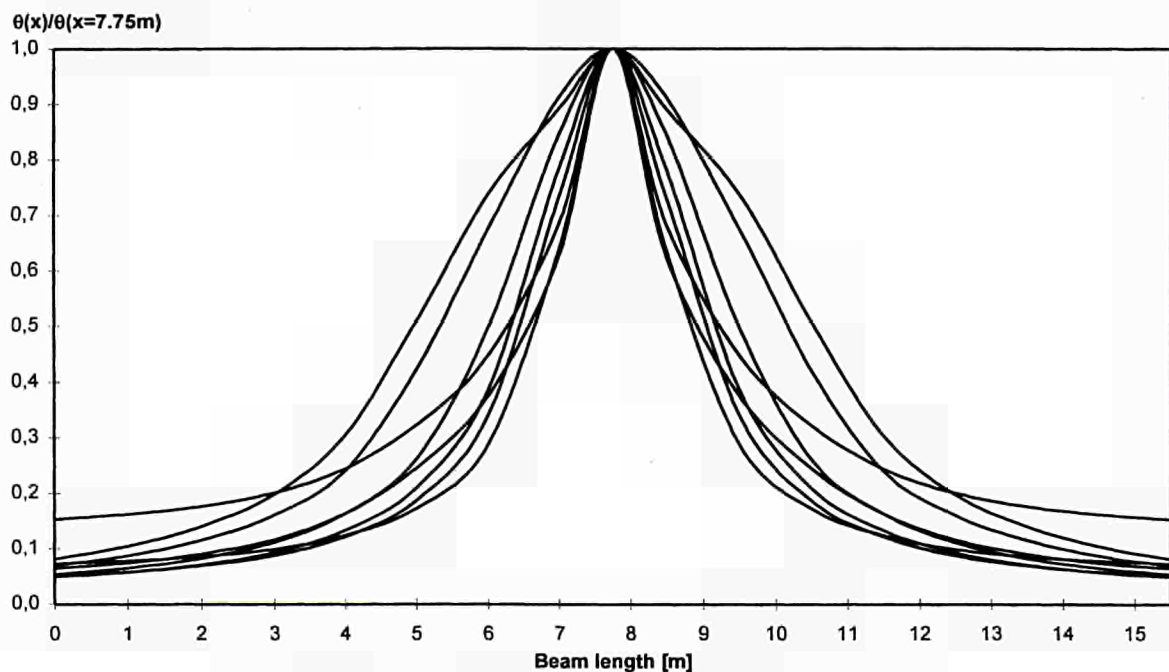

Figure 7.2 : Steel temperature reduction along the beam

In the program CEFICOSS [33] the temperature of the beam is the temperature just above the fire multiplied by the function of figure 7.3 which is the envelope curve of figure 7.2.
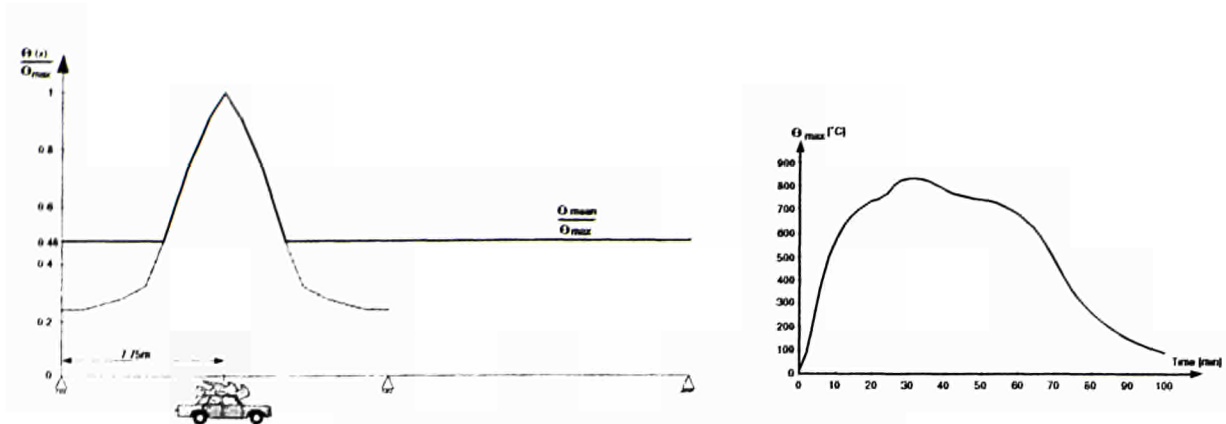
104

Figure 7.3 : Envelope curve of figure 7.2

In order to take into account the ventilation conditions, the maximum temperature between the temperature field given by Hasemi´s model and the mean temperature given by a two-zone model has to be adopted. In chapters 3.6 and 5.1, the ARGOS and CFD simulations have shown a mean air temperature of about 150°C in the case of the choosen example of car park with a ventilation for CO evacuation. In order to be on the safe side and to cover other conditions (smaller size, less efficient ventilation), a mean temperature in the air producing a steel temperature of 400°C has been assumed.

The figures 7.4 and 7.5 shows the evolution as a function of time of the vertical displacement at mid-span and the horizontal displacement at the end of the beam. The figure 7.6 enables to see the deformed beam when the deflection is maximum.

These results attest that the fire of one car at mid-span doesn´t endanger the structure.

Concerning the columns, their temperatures are equal to the mean temperature of 400°C. However, the scenario 1' consisting of a car burning in a parking bay is more dangerous for the columns above all if the column is nearby a wall. In that case, according to the chapter 3.5, the thermal action becomes (see figure 7.7) :
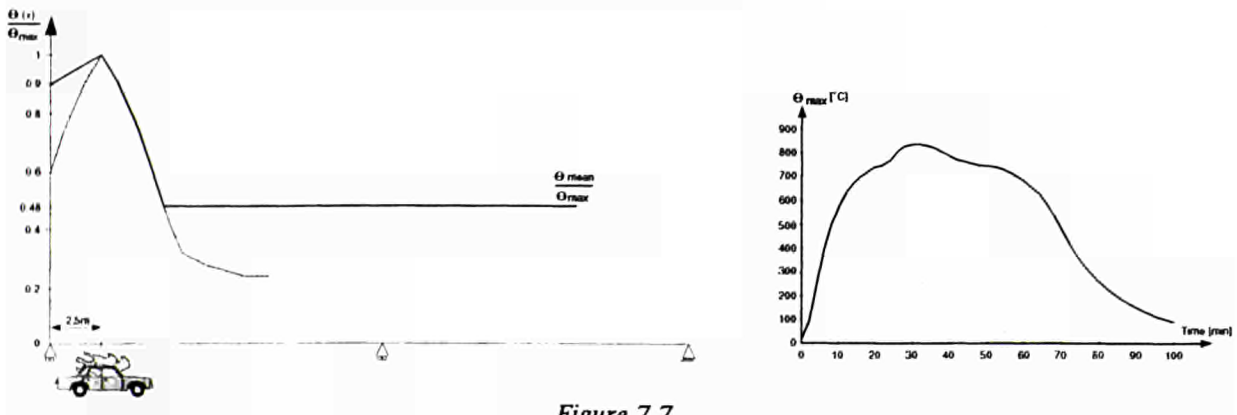

Figure 7.7

and the column is assumed to be heated on its whole length to $\approx 825°C * 0.9 = 742°C$ and to $825°C * 0.6 = 495°C$ if the column is not nearby the wall.

It can be concluded that the columns nearby a wall should be protected. In order to quantify the level of this fire resistance, the ISO equivalence based on the same temperature may be used. The maximum temperature of the column HEA 280 subjected to a car fire is equal to 742°C. The temperature of the same profile under an ISO heating is as follows (see figure 7.8) :
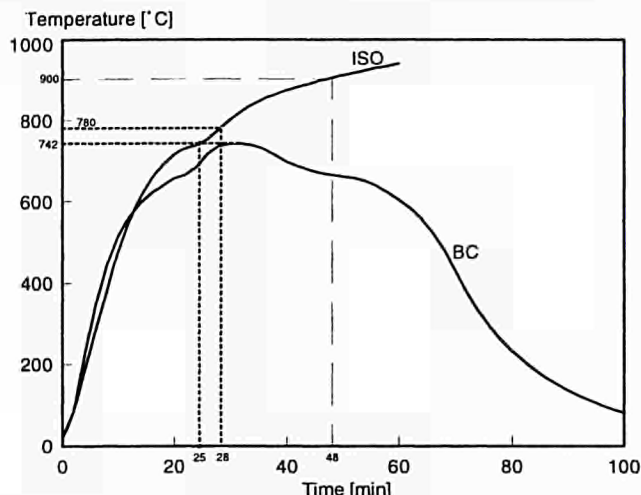

Figure 7.8 : Steel temperature in a HEA 280 under ISO heating and due to a burning car (BC)

It can be deduced that a car fire near a column nearby a wall is equivalent for this column to an ISO fire of 25 minutes. An ISO requirement R30 is thus sufficient for the column nearby a wall.
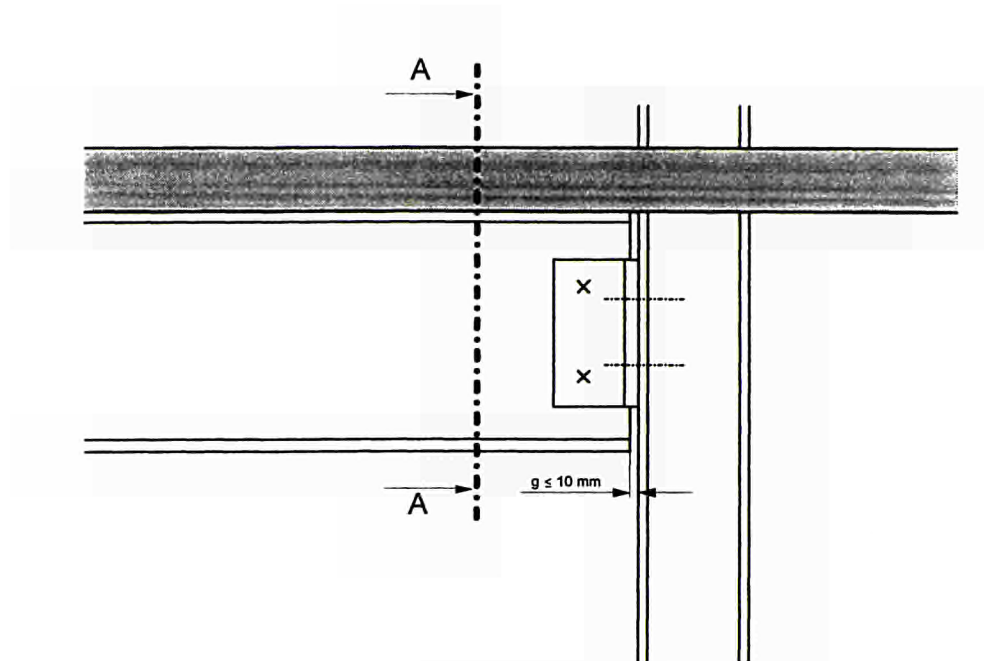
Conclusion

- If the ventilation has been designed to evacuate the CO at room temperature and if this ventilation is also effective in fire conditions (the fans and the ducts must have been designed for fire conditions, the inlets must be in the bottom part and the outlet near the ceiling in the smoke zone, the outlets and inlets have to be uniformly distributed in the car park), **the calculations of the example of a 31*50m car park have pointed out that the columns have to be protected R30 and that the steel beams can be unprotected provided that they have a composite behaviour** (steel profile connected to the concrete slab) **and provided that the concrete slab is continuous.**

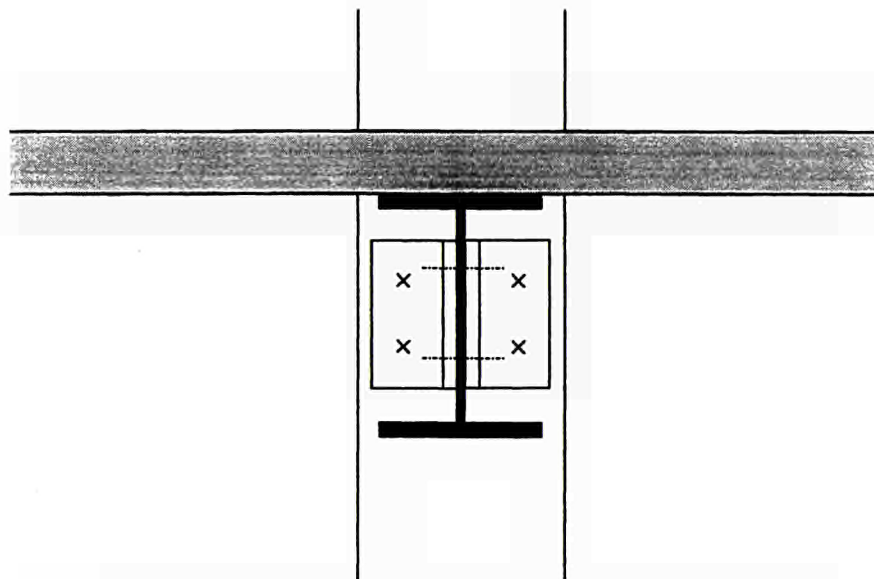End column   Central column

106
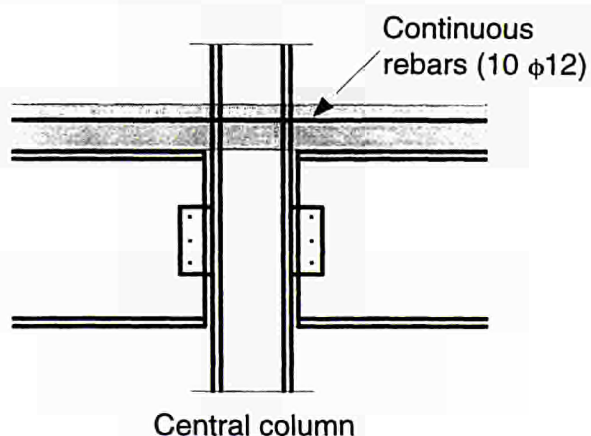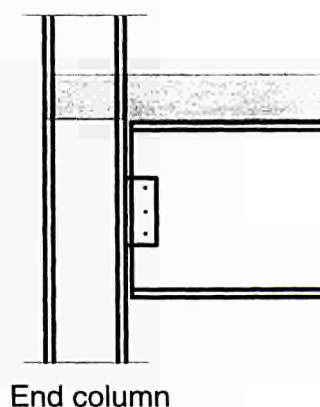
- If the ventilation has been designed for fire conditions (this means that the ventilation system is able to guarantee a free zone during the whole fire, that the outlets and inlets are numerous and very well distributed, that may be a valve system connected to smoke detector activates the extraction only where there is smoke in order to have the maximum extraction where needed), the conclusions are similar to the previous point except that the column may be also unprotected. This is justified by the fact that a powerful and efficient ventilation can avoid the smoke accumulation nearby the wall so that a column nearby a wall can be handled like a column inside the car park (see dotted line of figure 7.7).

A

×

×

g ≤ 10 mm

A

Section A - A

×   ×

×   ×

Simulated section for Beam / Central column

with upper and
lower meshes K7

rebars in tension (10 φ12)   material without mechanical characteristics (fy = 0)
and with thermal properties of the steel
fy = 500 N/mm²

steel material in compression
fy = 355 N/mm²
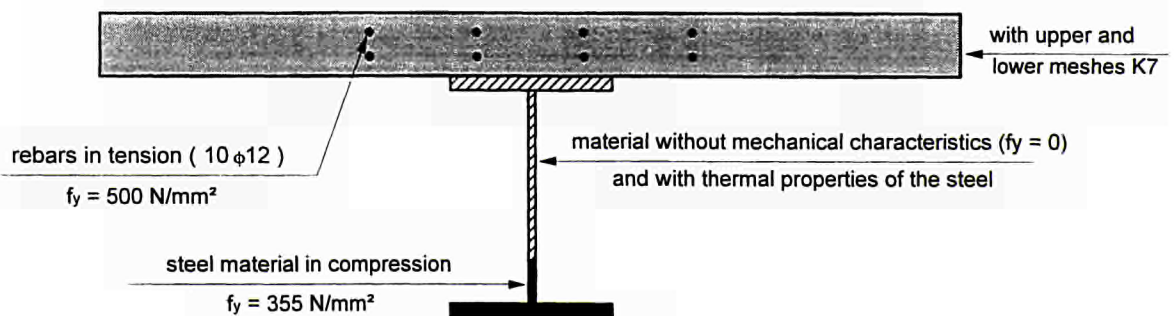
Figure 7.1 : Beam/Central column connection adopted in the simulation
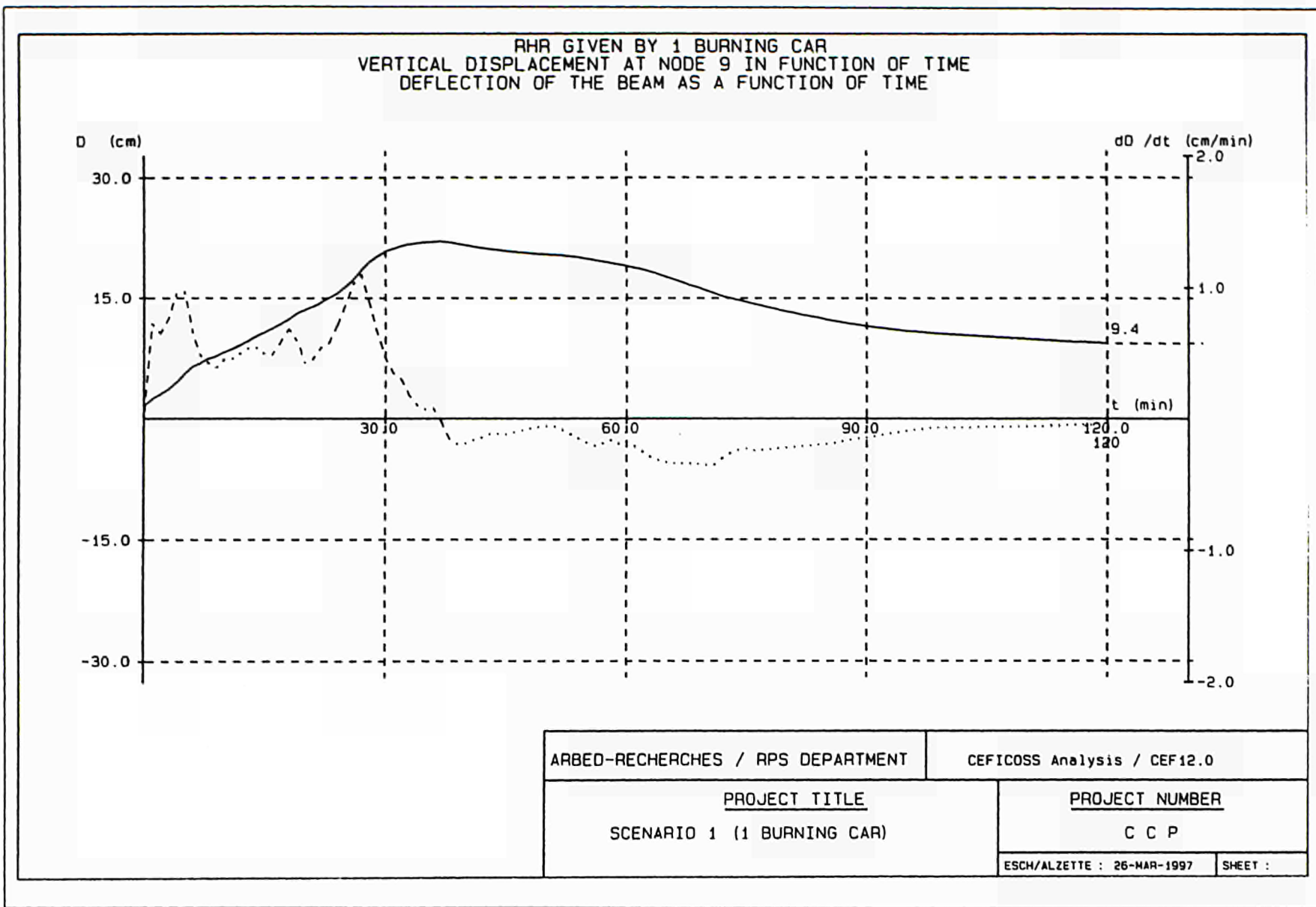
RHR GIVEN BY 1 BURNING CAR
VERTICAL DISPLACEMENT AT NODE 9 IN FUNCTION OF TIME
DEFLECTION OF THE BEAM AS A FUNCTION OF TIME

Figure 7.4

109

ARBED-RECHERCHES / RPS DEPARTMENT | CEFICOSS Analysis / CEF12.0

PROJECT TITLE
SCENARIO 1 (1 BURNING CAR)

PROJECT NUMBER
C C P

ESCH/ALZETTE : 26-MAR-1997 | SHEET :

RHR GIVEN BY 1 BURNING CAR
HORIZONTAL DISPLACEMENT AT NODE 1 IN FUNCTION OF TIME
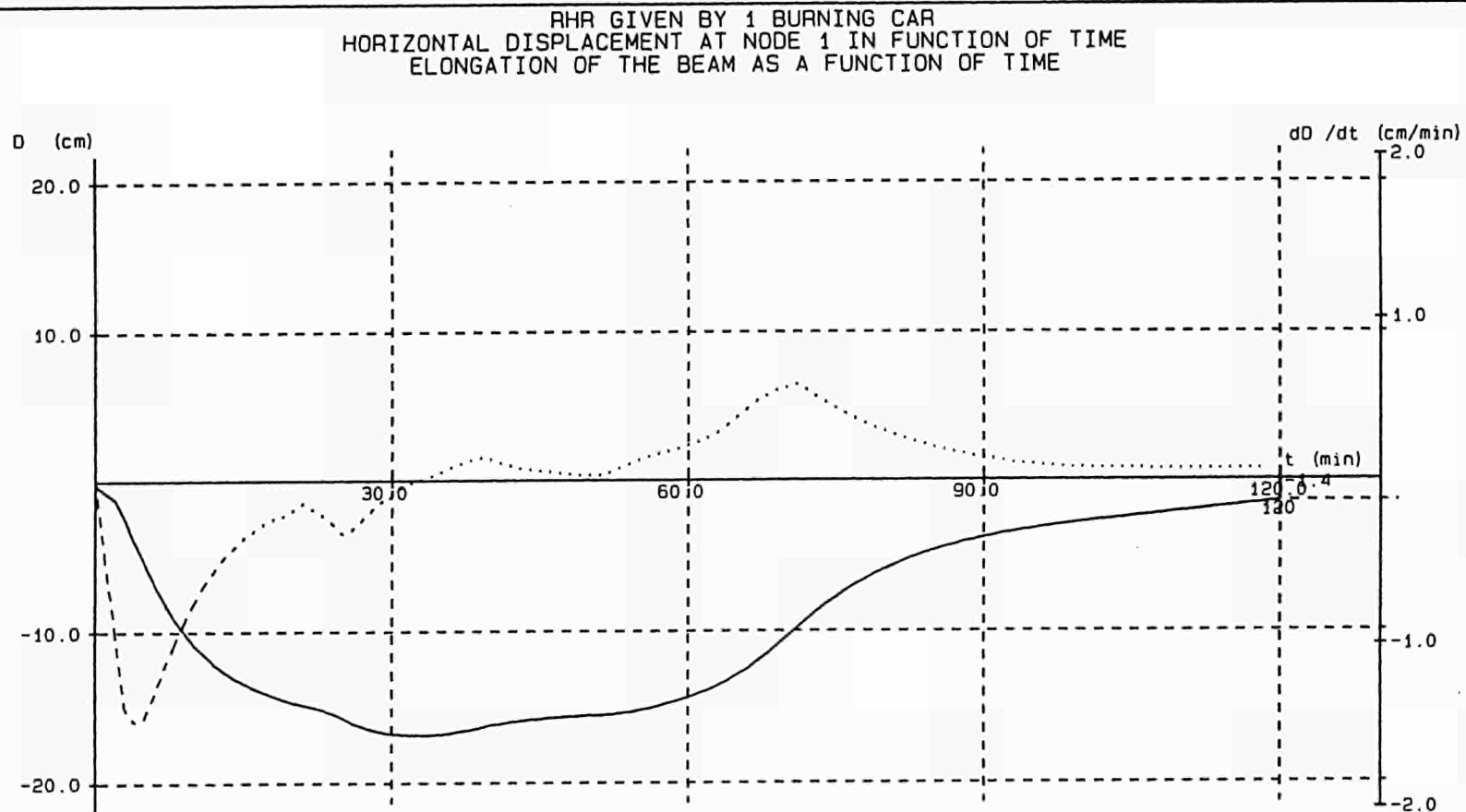ELONGATION OF THE BEAM AS A FUNCTION OF TIME

ARBED-RECHERCHES / RPS DEPARTMENT | CEFICOSS Analysis / CEF 12.0

PROJECT TITLE

SCENARIO 1 (1 BURNING CAR)

PROJECT NUMBER

C C P

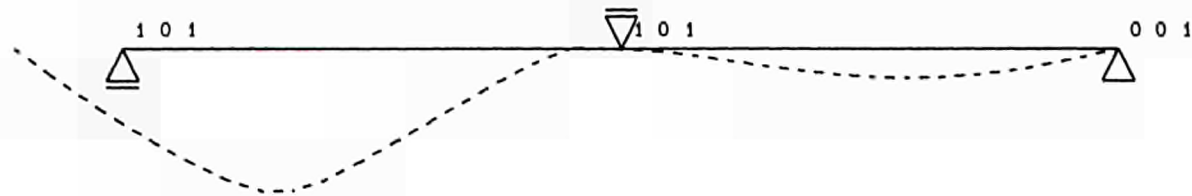ESCH/ALZETTE : 26-MAR-1997 | SHEET :

Figure 7.5

110

RHR GIVEN BY 1 BURNING CAR
DISPLACEMENT OF THE STRUCTURE AFTER   36.00 MINUTES

Maximum displacement

| Horizontal : | -16.696 cm |
| Vertical   : | 22.105 cm |

Δ H   +

Δ V

+

1 0 1   1 0 1   0 0 1
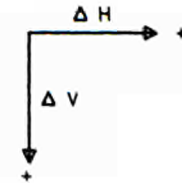
Scale of vertical displacements : 1 /10
Scale of horizontal displacements : 1 /10
Scale of the structure : 1 / 200

ARBED-RECHERCHES / RPS DEPARTMENT	CEFICOSS Analysis / CEF12.0
PROJECT TITLE	PROJECT NUMBER
SCENARIO 1 (1 BURNING CAR)	C C P
	ESCH/ALZETTE : 26-MAR-1997 SHEET :

Figure 7.6

111

7.3. Fire scenario 2 : wave of burning cars

The chosen structure is composed of several rows of three columns joined by a continuous beam with rigid connections to the external columns. The cross section of the columns is an HEA 280 section. An IPE 600 connected to a 15cm thick concrete slab forms the **composite beams**. The cross sections are given in figure 7.9. They show that the beams are composed of two different but similar sections : a 5m part on each side of the central column is reinforced by 10 ϕ 12 in addition to the mesh in the concrete slab; for the other part of the beam, only the mesh is taken into account. This K77 mesh provides 1,54 cm²/m ($\Rightarrow$ 1 ϕ 7 all the 25cm) of bars parallel to the beam axis. The distance between beams is 5,0m and the effective width considered in the calculations is 2,4m. The stability is ensured by a rigid core.
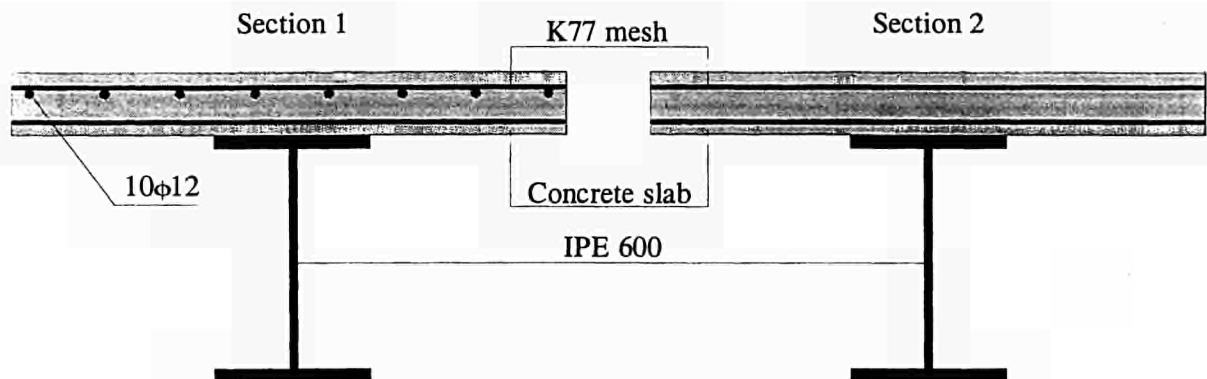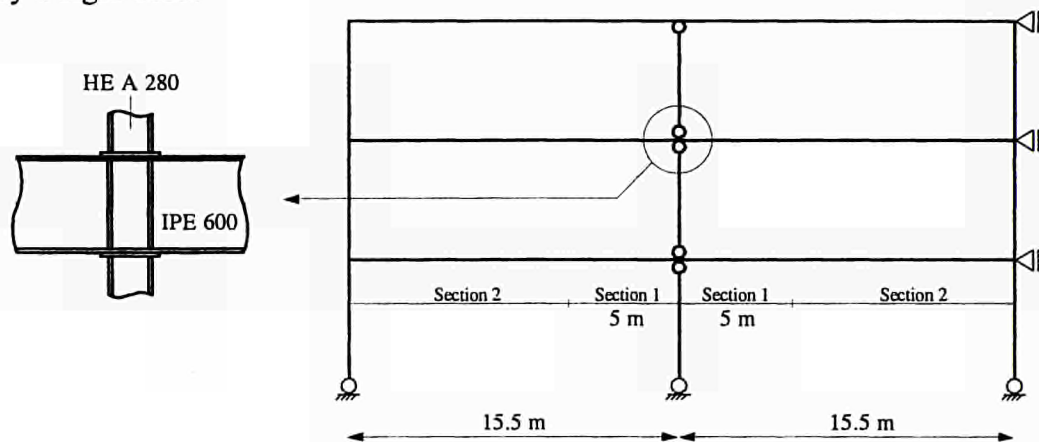
Figure 7.9 : Cross sections

Materials qualities

Steel profile :	S355 (f_y = 355 N/mm²)
Reinforcing meshes in the concrete slab :	S500 (f_y = 500 N/mm²)
Concrete slab :	C35 (β_{cyl} = 35 N/mm²)

The thermo-mechanical laws of both materials are simulated according to Eurocode 4/Part 1.2 [35], the strain hardening of the steel being taken into account.

The following figure 7.10 presents the loading of the structure considered in the CEFICOSS simulation (see also the introduction of the chapter 7.1).

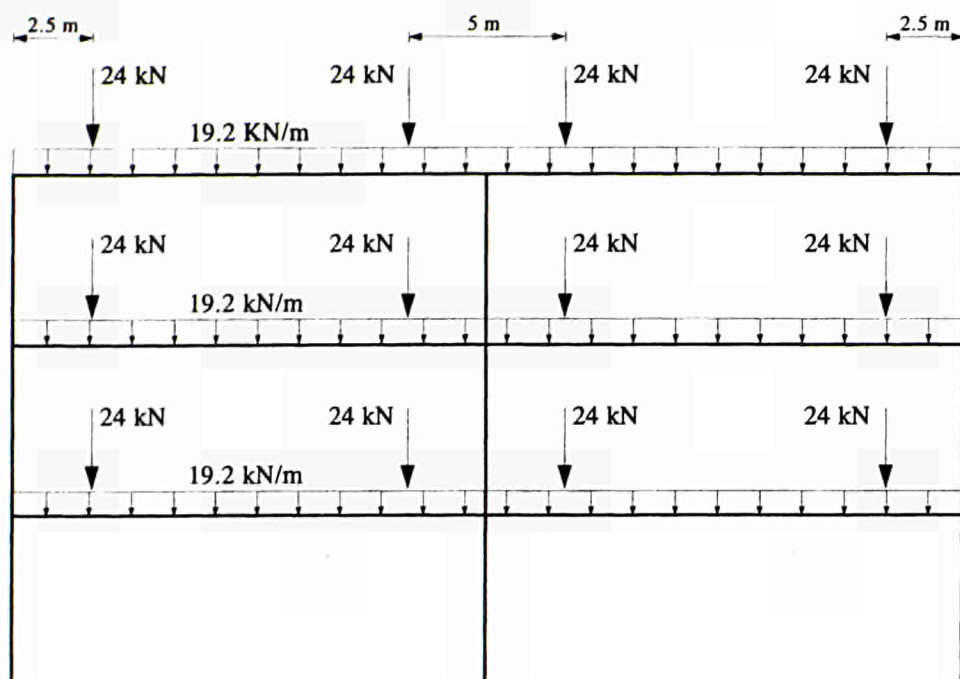Figure 7.10 : Loading of the structure

The heating of the beam is given by the figures 6.6 and 6.7. The figure 6.6 can be presented in the following way where, for each time step, the temperatures along the beam have been divided by the maximum temperature corresponding to the ceiling point just above the fire (see figure 7.11).
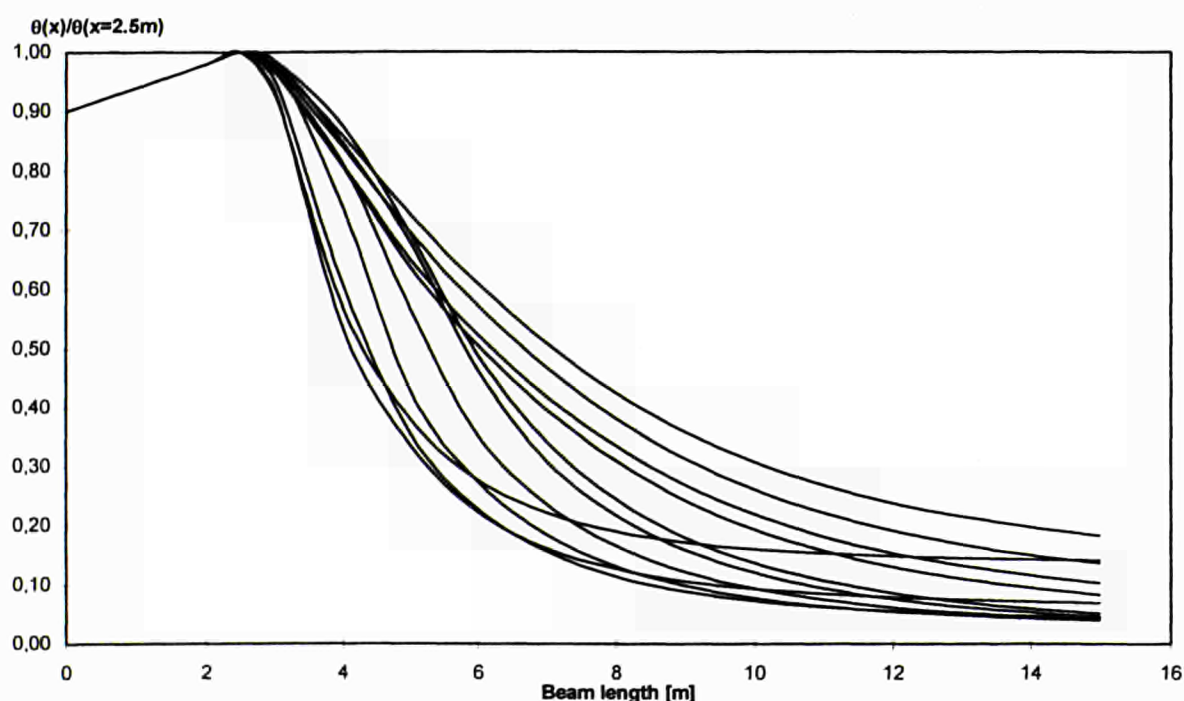

Figure 7.11 : Reduced function adopted to the temperatures

113

In the program CEFICOSS [33] the temperature of the beam is the temperature just above the fire multiplied by the function of figure 7.12 which is the enveloppe curve of figure 7.11.
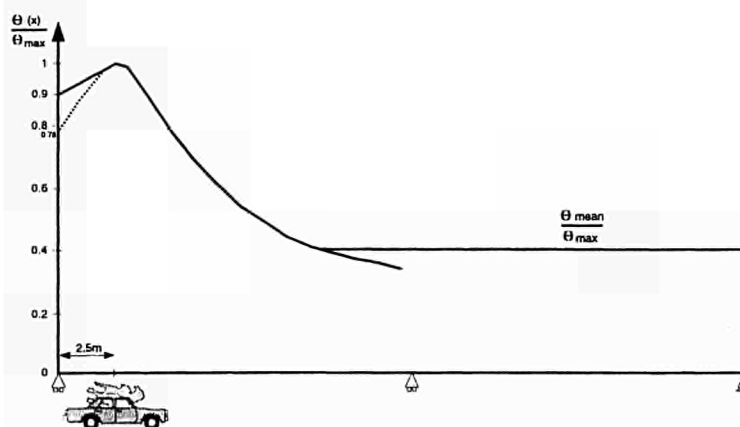

Figure 7.12 : Enveloppe curve of figure 7.11

In order to take into account the ventilation conditions, the maximum temperature between the temperature field given by Hasemi´s model and the mean temperature given by a two-zone model has to be adopted. In chapter 3.6, the ARGOS calculation has provided 200°C and 188°C respectively for room temperature and smoke evacuation ventilation. We have CFD results only for room temperature ventilation and one burning car. If we analyse the case of a smoke evacuation ventilation (=5 * room temperature ventilation) and five burning cars, the results should be similar because the smoke production is multiplied by 5 (5 burning cars) but also the smoke exhaust. The CFD calculation had provided a room temperature of 150°C (see chapter 5.1). In order to be on the safe side and to cover other conditions (smaller size, less efficient ventilation), a mean temperature in the air of 400°C has been assumed.

The figure 7.12 defines two situations for the column nearby the wall :

1. The maximum temperature of an unprotected column nearby the walls would be 900°C (see also figure 6.6), this corresponds to a ventilation which is not able to avoid the hot gas accumulation near the walls. According to the figure 7.8, a column with a fire insulation R60 is sufficient.
2. The maximum temperature of an unprotected column nearby the walls would be equal to 780°C (dotted line in figure 7.12), this corresponds to a powerful, efficient and well distributed ventilation which enables to avoid the hot gas accumulation near the walls. According to the figure 7.8, a column with a fire insulation R30 is sufficient.

If the columns are protected by an insulation material (f.i. sprayed mineral fiber) with the following thermal characteristics

$$\lambda = 0.1 \text{ W/m°C}$$
$$\rho = 300 \text{ kg/m}^3$$
$$C = 1100 \text{ J/kg°C}$$
$$\text{moisture} = 1\% \text{ per weight,}$$

the steel temperature reached in the profile is about 400°C after 30 minutes of ISO heating with 1cm of insulation material and after 60 minutes of ISO heating with 2cm of insulation material.

A CEFICOSS simulation corresponding to the situation 1 (full line of figure 7.12) has been performed with an heating as follows (see figure 7.13)
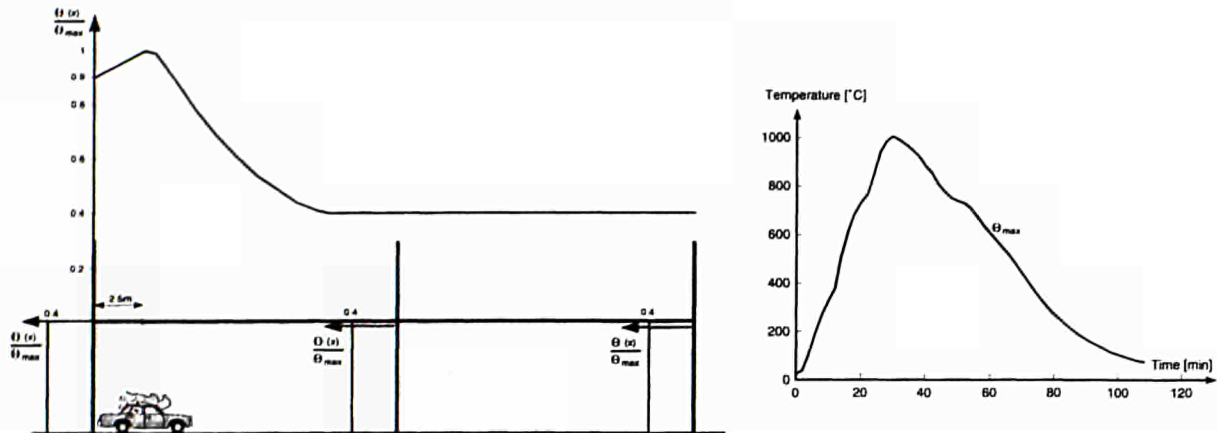
Figure 7.13

The figures 7.14 and 7.15 shows the evolution as a function of time of the vertical displacement above the fire (maximum deflection) and of the horizontal displacement of the end of the beam. The figure 7.16 represents the deformed structure corresponding to the maximum displacements.

The results attest that the fire of the wave of burning cars defined in scenario 2 doesn´t endanger the structure. It is also true for the situation 2 corresponding to a better ventilation and R30 columns as the maximum temperature of the column are the same and the temperature field around the beams is less important (see figure 7.12).
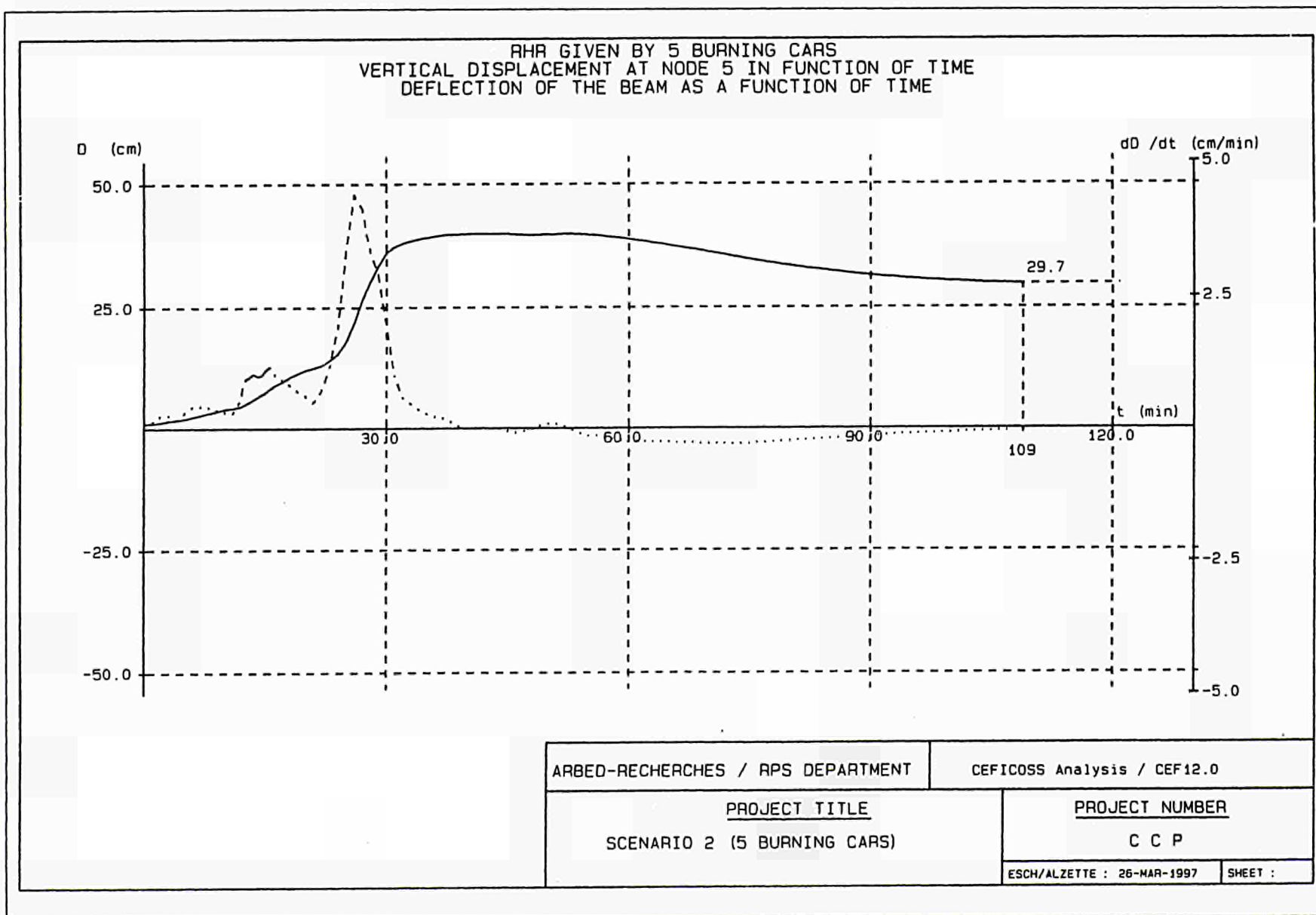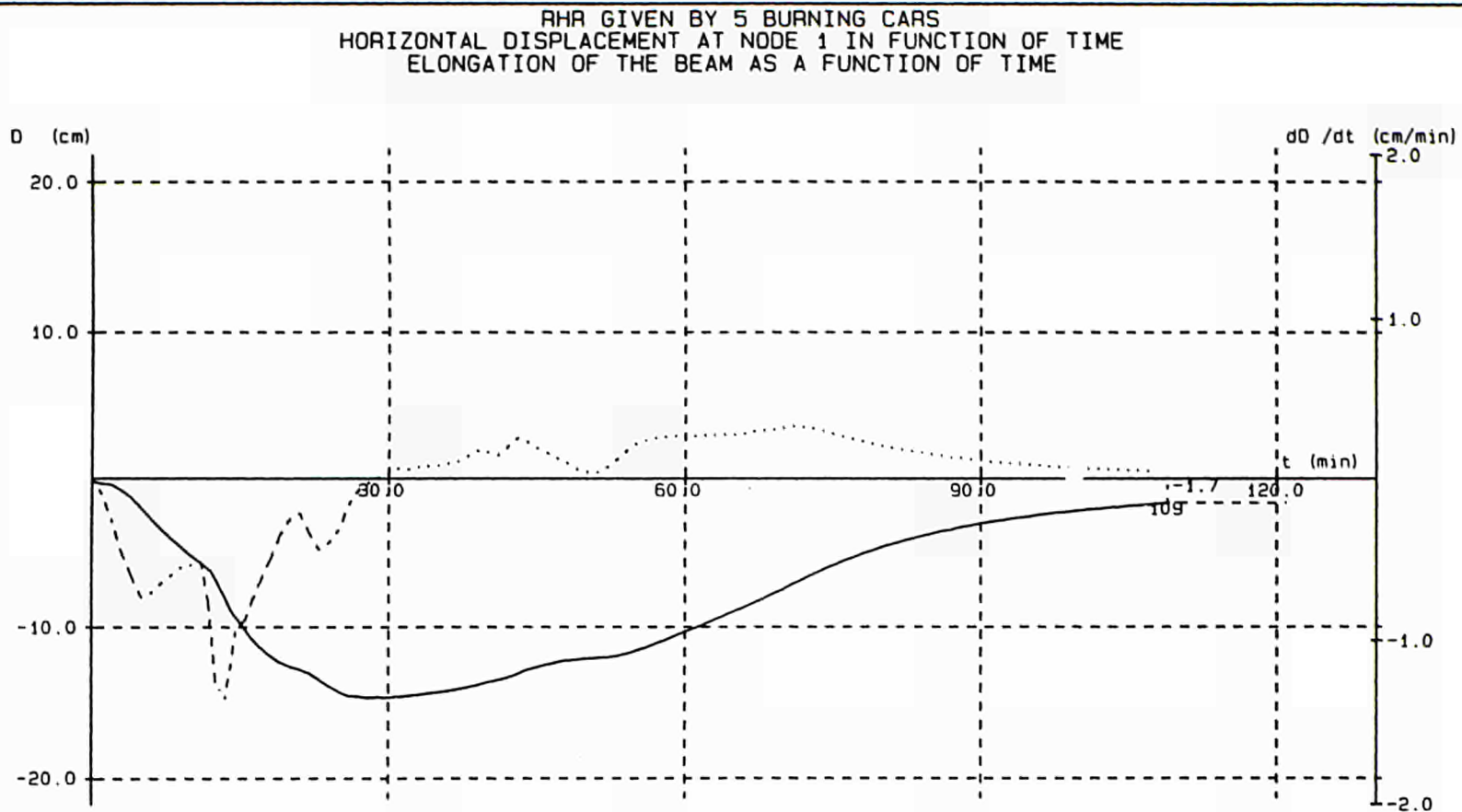
115

RHR GIVEN BY 5 BURNING CARS
VERTICAL DISPLACEMENT AT NODE 5 IN FUNCTION OF TIME
DEFLECTION OF THE BEAM AS A FUNCTION OF TIME

Figure 7.14

116

ARBED-RECHERCHES / RPS DEPARTMENT | CEFICOSS Analysis / CEF12.0

PROJECT TITLE

SCENARIO 2 (5 BURNING CARS)

PROJECT NUMBER

C C P

ESCH/ALZETTE : 26-MAR-1997 | SHEET :

RHR GIVEN BY 5 BURNING CARS
HORIZONTAL DISPLACEMENT AT NODE 1 IN FUNCTION OF TIME
ELONGATION OF THE BEAM AS A FUNCTION OF TIME

Figure 7.15

117

ARBED-RECHERCHES / RPS DEPARTMENT	CEFICOSS Analysis / CEF12.0
PROJECT TITLE	PROJECT NUMBER
SCENARIO 2 (5 BURNING CARS)	C C P
ESCH/ALZETTE : 26-MAR-1997	SHEET :

RHR GIVEN BY 5 BURNING CARS
DISPLACEMENT OF THE STRUCTURE AFTER 43.00 MINUTES

Maximum displacement

Horizontal :	−15.339 cm
Vertical :	40.034 cm

Δ H → +

Δ V
+

Scale of vertical displacements : 1 /20
Scale of horizontal displacements : 1 /20
Scale of the structure : 1 / 200

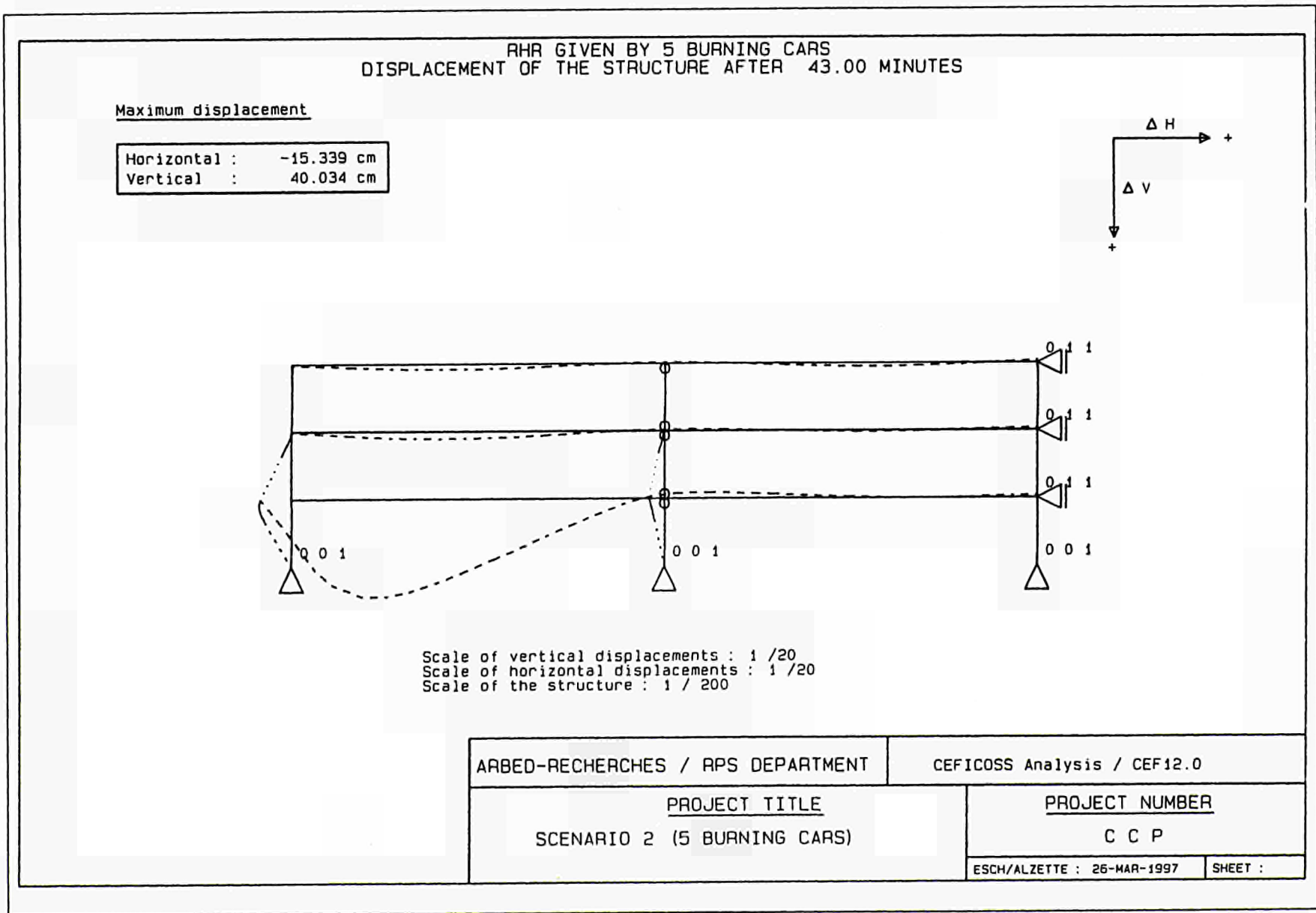| ARBED-RECHERCHES / RPS DEPARTMENT	CEFICOSS Analysis / CEF 12.0
PROJECT TITLE	PROJECT NUMBER
SCENARIO 2 (5 BURNING CARS)	C C P
	ESCH/ALZETTE : 26-MAR-1997 · SHEET :

Figure 7.16

118

8. CONCLUSIONS + DESIGN RULES

Owing to the fact that **the fire is localised**, the ISO requirements which assume a **uniform** temperature in the compartment are not suited to describe the severity of a fire in a closed car park. Indeed on one hand, the gas temperature curve near a car fire rises quicklier than the standard curve ISO and is thus more severe. On the other hand, the ISO curve gives much too high temperatures farther away from the fire. **The ISO curve is thus unsafe near the fire and too safe far away from the fire.**

The structure requirement should be in fact : **TO SURVIVE the fire.**

Only for columns nearby burning cars in which the temperature may be assumed uniform, it may be referred to ISO requirements. This is not valid for the beams.

As the fire is localised, it is possible to design a structure in such a way that the structure parts heated and weakened by the localised fire are sustained by the remaining parts of the structure which are farther away from the fire and therefore not so much affected by the high temperature. In the previous chapters it has been shown on the example of a representative car park that

- in case of only **one burning car** (fire scenario 1), an unprotected steel structure can possibly withstand the fire, but it is necessary that the sections of the beams have a composite behaviour and that the concrete slab is continuous according to the beam axis;
- in case of **several burning cars** (fire scenario 2), continuous beams and protected or composite columns should be foreseen.

The details like the level of protection, the rebars in the slab at the support of the continuous beam, the ventilation conditions must be calculated for each case depending on the parking geometry, the ceiling height, the beam size and the parking bays dimensions.

In case of sprinkler system or a reliable detection automatically connected to the fire brigade combined with sufficient fire fighting devices, the assumption of only one burning car could be adopted. Otherwise the hypothesis of a fire spread may not be excluded even if this is a very rare event according to the available surveys.

The calculations have been based on the following assumptions :

- Static loading : One car (12 kN) in each parking bay
- Floor to ceiling distance : $H_f = 2,6m$
- Design fire : Rate of Heat Release curve (see chapter 3.4)
  Fire diameter $= 3,91m$
  Vertical position of the fire $= 0,6m$
- Heat flux received by the beam : according to Hasemi´s model combined with a two-zone calculation (see chapter 3.5 and [1]).
- Steel temperature : according to fire part of Eurocode 3
  $\alpha = 25 \text{ W/m°C}$
  $\varepsilon = 0,5$

On the basis of the example analysed in the previous chapters, the conclusions can be summarized in the following table which gives the structural requirements for different fire scenarii and different ventilation design.

DATA	Fire scenario	One burning car (f.i. in case of sprinkler)			Wave of burning cars	
	Ventilation Design	for CO evacuation at room temperature		for smoke evacuation (see 3.6.4)	for CO evacuation at room temperature	for smoke evacuation (see 3.6.4)
Structural requirement	Steel Column	Column nearby a wall	Other Column	unprotected	R60	R30
		R30	unprotected			
	Composite beam and continuous concrete slab	unprotected		unprotected	unprotected and continuous beam	unprotected and continuous beam

This table may be used to proceed to a predesign, of course a final design requires a detailed static analysis.

9. NOTATIONS

A	$[m^2]$	Surface of the opening
A_m/V	$[m^{-1}]$	Section factor
b	$[m]$	Parking bay width
C	$[J/kg°C]$	Specific heat
Ca	$[\%]$	CO content in the fresh air
CO	$[-]$	Maximum allowed CO content
CO_A	$[\%]$	CO content in the fresh air
d	$[m]$	Mean distance between cars
dP	$[Pa]$	Pressure difference over the opening
D	$[m]$	Characteristic length of the fire source ($\equiv$Fire diameter)
f_y	$[N/mm^2]$	Characteristic value of the yield point of structural steel and reinforcing meshes
G_b	$[J]$	Turbulent kinetic energy source due to buoyancy
G_k	$[J]$	Turbulent kinetic energy shear production source
H_f	$[m]$	Height of the compartment
H_s	$[m]$	Vertical position of the fire source
L_{VIS}	$[m]$	Visibility through smoke for well lit objects
M	$[-]$	Maximum allowed CO content
P_{CO}	$[m^3/h]$	CO production of a car (=0,5 to 0,7)
q	$[kN/m]$	Distributed load
q_{CO}	$[m^3/h]$	CO production of a car (=0,5 to 0,7)
$\dot{q}_i$	$[kW/m^2]$	Heat flux produced by a car i
$\dot{q}_{net}$	$[kW/m^2]$	Net heat flux entering the profile
Q	$[kN]$	Concentrated load

r	[m]	Radial distance between the fire and the considered point at the ceiling level
R_f	[-]	Richardson number
SMF	[-]	Scaled mass fraction of smoke
t_1, t_2, t_3, t_4	[min]	Propagation time
T	[-]	$\sum_{i=1}^{n} \tau_i$ where τ_i is the running time of the car i and n is the number of cars which run per hour
T_s	[K]	Steel temperature
V	[m³/s]	Flow through the opening
Vol_{CCP}	[m³]	Total volume of the car park
V_{Total}	[m³/h]	Total flow into the CCP
W_{fi}	[m]	Fire perimeter
X_{vent}	[-]	Ventilation factor
y	[m]	Free zone layer height
α	[W/m²K]	Convection coefficient
β_{cyl}	[N/mm²]	Characteristic value for the compressive cylinder strength of concrete
$\Delta\theta_{a,t}$	[°C]	Increase of steel temperature at the time t
Δt	[s]	Time interval
ε	[-]	Emissivity
λ	[W/mK]	Thermal conductivity
ρ	[kg/m³]	Unit mass
σ	[-]	Stefan-Boltzmann constant

10. *REFERENCES*

[1] CEC Agreement 7210-SA/210/317/517/619/932 "Development of design rules for steel structures subjected to natural fires in LARGE COMPARTMENT" - Final Report - February 1997.

[2] Norme NBN S 21-208 "Protection Incendie dans les Bâtiments - Conception et calcul des installations d'évacuation de fumées et de chaleur - Partie 1: grands espaces intérieurs non-cloisonnés s'étendant sur un niveau", Mai 1995.

[3] Service d'Incendie et d'Aide Médicale Urgente de la Région de Bruxelles-Capitale "Conception et calcul des installations d'évacuation de fumées et de chaleur (EFC) - Partie 2 : Parkings couverts." Projet de Norme - 1996.

[4] "Flame Geometry Effects on the Buoyant Plumes from Turbulent Diffusion Flames", Y. Hasemi and Tazo Tokunaga. Fire Science and Technology, Vol.4, N°1, 1984.
"Numerical Analysis of Structures exposed to localized Fire", A. Ptchelintsev, Y Hasemi,   M. Nikolaenko, ASIAFLAM's 95, Hong Kong, 1995.
"Experimental Study on the Heating Mechanism of a Steel Beam under Ceiling exposed to a localized Fire", T. Wakamatsu, Y. Hasemi, Y. Yokobayashi, A. Ptchelintsev.
"Fire Safety of Building Components Exposed to a Localized Fire - Scope and Experiments on Ceiling/Beam System Exposed to a Localized Fire-", Y. Hasemi, Y. Yokobayashi, T. Wakamatsu, A. Ptchelintsev, ASIAFLAM's 95, Hong Kong, 1995.

[5] "Fire Safety in Open Car Parks" - Modern Fire Engineering: ECCS- Technical Committee 3 -Fire Safety of Steel Structures. Technical note, First Edition 1993 N°75.

[6] "Fire and Unprotected Steel in Closed Car Parks" -BHP Steel International group; Melbourne Research Laboratories Report, Number: MRL/PS98/87/001, ISBN0731622251.

[7] "Fire Safety in Car Parks" -BHP Steel: Structural Steel Development Group -June 1990, Report N°MRL/PS69/89/006 August 1989.

[8] "Fire Test with Steel Framed Parking Building", 16mm film, Nippon Steel, 1970.

[9] "Report on Fire Tests in the Seinenschanze Car Park, Basle, Switzerland, April 24, 1969".

[10] H. Burgi, "Fire Tests with Cars Parked in an Enclosed Car Park Building", Reprinted from "Schweizerische Feuerwehr-Zeitung" N°12/1970.

[11] MANGS J. and LOIKKANEN P. : 'Fire tests in passengers cars', VTT research report N°TSPAL00455/90, Espoo, Finland, 1991.

[12] MANGS J. and LOIKKANEN P. ' Average rate of heat release curve deduced from car fire tests' VTT research report N° PAL00455A/90, Espoo, Finland, 1992.

[13] SHIPP M. and SPEARPOINT M. :' Measurements of the severity of fires involving private motor vehicles', Fire Research Station, Building Research Establishment, Bucknalls Lane, Garston, Watford WD2 7JR, UK -27 March 1995.

[14] JOYEUX Daniel : ' Car fire test : study of car fire impact and car fire propagation ', INC-95/133-DJ, May 1995.

[15] JOYEUX Daniel : ' Car fire tests : study of car fire impact and rate of heat release of a car fire', INC-95/132-DJ, May 1995.

[16] JOYEUX Daniel : ' Car fire tests : 'Car fire impact and rate of heat release : A small car', INC-95/310-DJ, September 1995.

[17] JOYEUX Daniel : ' Car fire tests : effect of smoke extraction on fire impact and rate of heat release : A medium car', INC-95/311-DJ, September 1995.

[18] JOYEUX Daniel : ' Car fire tests : study of car fire impact and car fire propagation 2', INC-95/312-DJ, September 1995.

[19] JOYEUX Daniel : ' Car fire tests n°7 : rate of heat release of a large car made in 1995, test 96-S-251', INC-96/300-DJ/VG , September 1996.

[20] JOYEUX Daniel : ' Car fire tests n°8 : rate of heat release of a small car made in 1995, test 96-S-295', INC-96/299-DJ/VG , September 1996.

[21] JOYEUX Daniel : ' Car fire tests n°9 : rate of heat release of two cars made in 1995, test 96-S-400', INC-96/378-DJ/VG, November 1996.

[22] JANSSENS M. and PARKER W.J. : ' Oxygen consumption calorimetry' - chapter 3 Heat release in fires - Babrauskas V. and Grayson S.J. - Elsevier Applied Science.

[23] PARKER W.J. : ' Calculations of the heat release rate by oxygen consumption for various applications' - Journal of fire sciences - vol 2, pp380-395, September-October 1984.

[24] JOYEUX Daniel : ' Study of theoretical calorific potential of cars : comparison between cars of the 80s and cars of the 90s', INC-95/131-DJ, May 1995.

[25] Parking Garage Fires (A Statistical Analysis of Parking Garage Fires in the United States: 1986-1988) - Dale F. Denda, Director of Research Parking Market Research Company McLean, Virginia. April 1992.

[26] Dr. L.M. Harris: Survey of Fire Experience in Automobile Parking Structures in the United States and Canada. Marketing Research Associates, January 1972 (Published by the American Iron and Steel Institute, Washington, D.C.).

[27] I.D. Bennets, D.J. Proe, R.R. Lewins and I.R. Thomas: Fire Safety in Car Parks. BHP Melbourne Research Laboratories Report Number MRL/PS69/89/006, June 1990.

[28] R.G. Gewain: Fire Experience and Fire Tests in Automobile Parking Structures. Fire Journal, July 1973, pp 50-54.

[29] "Fournaise dans un parc de stationnement à Reuil (France)", FAX sent by Mr. Joyeux D. (CTICM) the 29th of September 1995.

[30] E. PEDERSEN, Danish Fire Protection Association; J-B. SCHLEICH, L-G. CAJOT, PROFILARBED Research Esch/Alzette - Luxemburg; H. EXNER, C. ANDRESEN, Rambøll & Hannemann A7S : Technical Note - Structural Fire Protection in multi-storey Open Car Park Buildings. Dansk Brandteknisk Institut, November 1989.

[31] ECCS - AC1 : Multi-storey car parks. Brussels, to be published in 1994.

[32] Danish Institut of Fire Technology; ARGOS - Computer Programme for Fire Risk Evaluation - 1991.

[33] REFAO I - CAFIR, Computer assisted analysis of the fire resistance of steel and composite concrete-steel structures, Report EUR 10828 EN, PA-RE, J.B. SCHLEICH, 1987.

[34] CEN; ENV 1993-1-2, Eurocode 3 - Design of steel structures, Part 1.2 - Structural Fire Design. CEN Central Secretariat, Brussels, Final Draft July 1995.

[35] CEN; ENV 1994-1-2, Eurocode 4 - Design of composite steel and concrete structures, Part 1.2 - Structural Fire Design. CEN Central Secretariat, Brussels, DAV 30.10.94.

[36] Règlement : Prévention Générale des Risques. « Sécurité contre l'Incendie; Etablissements recevant du public », Journal Officiel de la république française n°1540.
- Circulaire du 3 Mars 1975 relative aux parcs de stationnement couverts (Journal du 6 Mai 1975)

[37] Ministère de l'environnement : n°331bis - Parcs de stationnement couverts et garages-hôtels de véhicules à moteur. La surface étant supérieure à 6000m^2 mais inférieure ou égale à 20000m^2. Installations soumises à déclaration.

[38] Private communication between Dr. J.-M. Franssen, Mr. P. Hourlay and Commandant Rahier (Fireman of Liège).

[39] Reglementation of Switzerland concerning the car parks.

[40] Fire Safety Requirements for Car Parks in Spain (New 1996 Regulations). Ministery of Public Works, Transports and Environment - Posada Escobar.

CALCULATION OF RATE OF HEAT RELEASE OF BURNING CARS
IN FUNCTION OF TIME

INTRODUCTION

The theory of the O_2 consumption principle is now well-developed. This principle is based on the fact that for a large number of organic liquids and gases, a reasonably constant net amount of heat is released per unit mass of oxygen consumed for complete combustion. This has also been found true for organic solid, and an average value has been obtained. This value is 13.1 MJ/kg of O_2. its accuracy is within 5%. This technique is now being employed to determine the heat release rate of materials in various heat release rate calorimeters.

The obtained relations are based on the knowledge of the quantity of oxygen enters the local and the quantity of oxygen goes out by the extraction system. So the heat release rate can be calculated if mass flow rates are measured and if the mass fraction of oxygen in these mass flows is also recorded.

Unfortunately, in an open system as the test configuration, the mass flow rate in the exhaust duct is measurable but not the incoming air flow rate. So, the balance of oxygen quantity is not possible. To find a relation between the incoming mass flow and the mass flow rate in the exhaust duct, it has been defined two factors. The first is the oxygen depletion factor F that is defined as the fraction of the incoming air which is fully depleted of its oxygen. Calculations of the factor are function of the measurements of concentrations. In the simulated closed car park, only the concentrations of O_2, CO and CO_2 are recorded. In this case, the relation governing the depletion factor is shown herein below. Nevertheless, the relation between incoming and exhausting mass flow rates obtained with the depletion factor depends on composition of the material. This dependence is raised with the introduction of the expansion factor. This factor a is 1 for a complete combustion of pure carbon, 1.21 for a pure hydrogen flame and 1.105 for a methane pool fire. This last value is recommended for material for which the composition is not well defined.

Nevertheless, in an open or closed system, all the combustion products have to be collected by the exhausting system. If this point is not applied, it is impossible to know the real quantity of oxygen depletion and the resulting rate of heat release is improbable.

According to these statements and assumptions, M. JANSSENS and W. PARKER ([22],[23]) have developed series of equations - according to the quantity of measurements - to calculate the rate of heat release of furniture's by a calorimetry system. They assume that concentrations of all others' components that are not measured in the system are neglected. For example in the present test, CO, CO_2 and O_2 concentrations are measured. So it is assumed that soot, NO_x, hydrocarbon (etc.) concentrations are weak. But N_2 and H_2O are

major species. However, when they are not measured, one assumes the conservation of nitrogen and the trapping of water vapour before the sample reaches the gas analysers.

EQUATIONS

The equations governing the calculation of rate of heat release of burning cars in the configuration of the simulated closed car park are the following :

$$Q = E \frac{\phi}{1 + \phi(\alpha - 1)} \, m \frac{M_{O_2}}{M_{air}} \left(1 - X_{H_2O}^0 - X_{CO_2}^0\right) X_{O_2}^0$$

$$\phi = \frac{X_{O_2}^0 \left(1 - X_{CO_2} - X_{CO}\right) - X_{O_2} \left(1 - X_{CO_2}^0\right)}{\left(1 - X_{O_2} - X_{CO_2} - X_{CO}\right) X_{O_2}^0}$$

where ϕ is the oxygen depletion factor
X_i is the mole fraction of the species i
M_i is the molecular weight of the species i
α is the expansion factor due to uncompleted combustion
m is the mass flow rate of burned gases
E is the heat release per oxygen mass
the subscript ^{0} refers to the external conditions

The mole fractions X_i are defined as the mole number of the species i over the total mole number.

The different physical and chemical values used are:

E = 13.1 MJ/kg of O_2
M_{O_2} = 32 g/mol
M_{CO_2} = 44 g/mol
M_{CO} = 28 g/mol
M_{air} = 29 g/mol

and the empirical value α is 1.105.

The mass flow rate m is calculated with the measurements of volume flow rate and temperature of gases given the gas density. A density value of 1.19 kg/m^3 is assumed at T=300K.

CEFICOSS SIMULATION BASED ON THE CTICM TEST N°5
## WITH TWO BURNING CARS

A corner of a closed car park was simulated. This part, 5m x 5m, is shown in figure A.2.1. Both walls have been kept and the two other faces are completely open. Two places are simulated. The distance between the platform where the car is parked and the walls is about 0,9 meters. The ceiling is located at 2,60m. Some steel structure proofs (a one meter length IPE 240 and HEB 300) were placed under the ceiling just above the car.

A BMW 1980 (the ignition car) and a small french car were placed 70cm apart in order to check the fire spread. The gas temperatures above the car were measured with thermocouples. The location of thermocouples are presented in figures A.2.2 and A.2.3. A summary of the location of thermocouples is presented in the table A.2.4. Characters 'ni' and 'i' significate 'Non Initial fire place' and 'Initial fire place' respectively. The axis X and Y form the horizontal plane and the axis Z is the vertical direction. The following figure presents the location of thermocouples on the four beam proofs (IPE 240 and HEB 300 on both places).

where
h = 65.5 mm for the beam HEB 300
h = 55 mm for the beam IPE 240
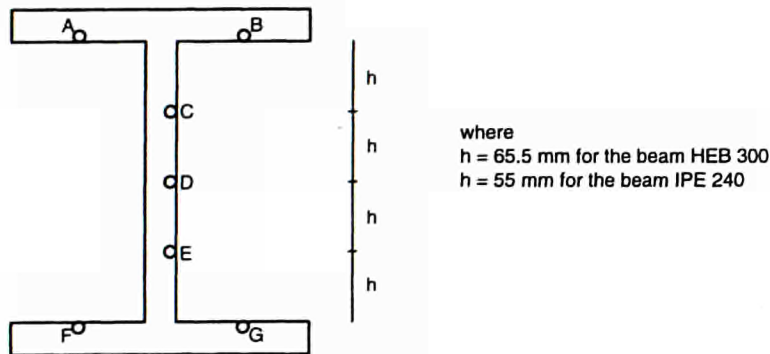
CEFICOSS simulation

The following description present a general view of the simulated closed car park.

θ measured during the tests   Wall
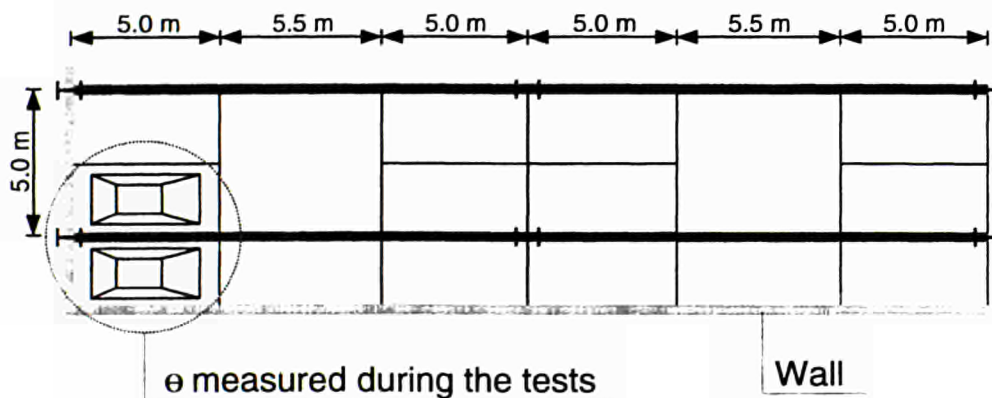
Two cars were placed to the left extremity of the closed car park. The structure consists of columns HEA 280 and beams IPE 600 with 150mm of concrete slab. The air temperature

field around the beam considered in the CEFICOSS simulation is presented on figure A.2.5; these temperatures have been deduced from the CTICM test for the first five meters of the beam. For the remaining part a linear decrease deduced from CFD simulations (see semestrial report 4 [26] and figure A.2.6) has been considered. The columns have been assumed **protected**.

CEFICOSS calculation

Comparison of the temperatures

A comparison between the temperatures provided by CEFICOSS (Tcef) and the temperatures measures during the test (Tci) is shown on figures A.2.7 to A.2.9.

The results show that for the bottom flange (figure A.2.7) and the web (figure A.2.8) of the profile, the path of the temperature curves are very similar.

But for the upper flange (figure A.2.9), the differences in temperature are more noticeable. This is due to the fact that, for the CTICM test, a different material was placed on the upper flange than in the CEFICOSS simulation. In the CTICM test, the ceiling was composed of a steel plate 5mm thick protected by 20mm of an insulating material while the ceiling is a concrete slab 150mm thick in the real car park and in the CEFICOSS simulation.

Displacements

Figure A.2.10 shows the dispalcement of the structure after 26 minutes of fire; this time corresponds to the maximum temperature recorded in the steel profile. Figure A.2.11 shows, in function of the time, the maximum deflection of the beam given by the displacement of the node 6. A maximum vertical displacement of 39cm can be seen.

This simulation points out that there is no danger to the stability of the structure. How can we explain that a steel structure with a temperature of about 1000°C is still able to bear the loads? The answer is that the fire is **LOCALISED** and that the beams are **continuous** and **composite**.

Indeed, as shown by the figure A.2.13, the very high temperatures affect only the first five meters of the continuous beam of which the remaining part (and for instance the central support which can activate a rather high negative bending moment) is not very hot. During the fire there is a load redistribution as shown by figure A.2.14 and a new static system appears (see figure A.2.13).

If we simplify, we can say that we can forget completely the steel beam for the first five meters where the 150mm thick concrete slab is sufficient to bear the loads; this concrete slab is supported at the left end by the protected column and at the right end by the cantilever part of the continuous composite beam.

The concrete slab is also sufficient enough to support the shear force in the first five meters because the load redistribution has strongly reduced the applied shear force at this position (see figure A.2.15).
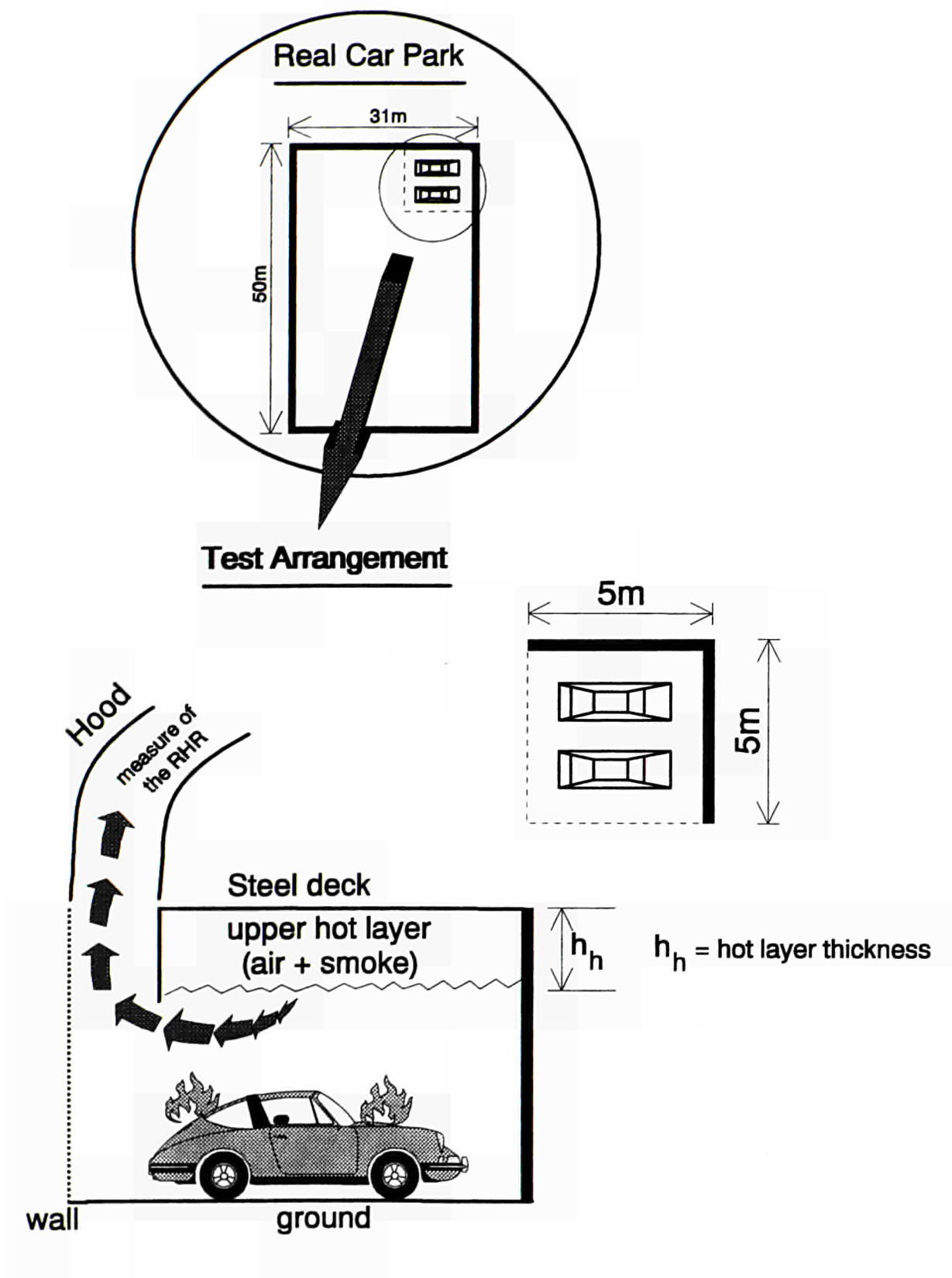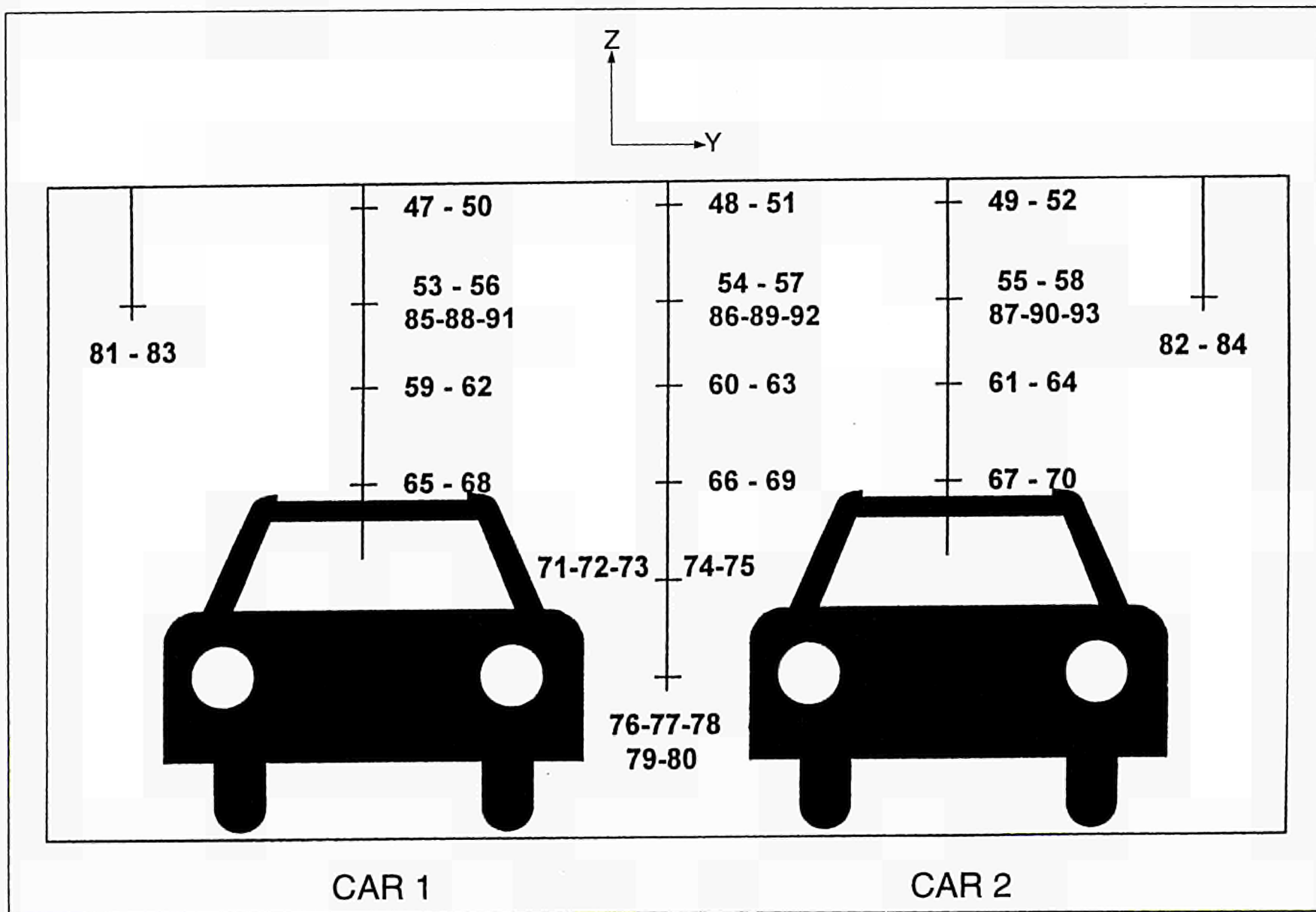
Real Car Park

31m

50m

Test Arrangement

5m

5m

Hood

measure of
the RHR

Steel deck

upper hot layer
(air + smoke)

h_h

h_h = hot layer thickness

wall   ground

Figure A.2.1 : CTICM test arrangement

Figure A.2.2 : Location of ambient thermocouples - Vertical plan
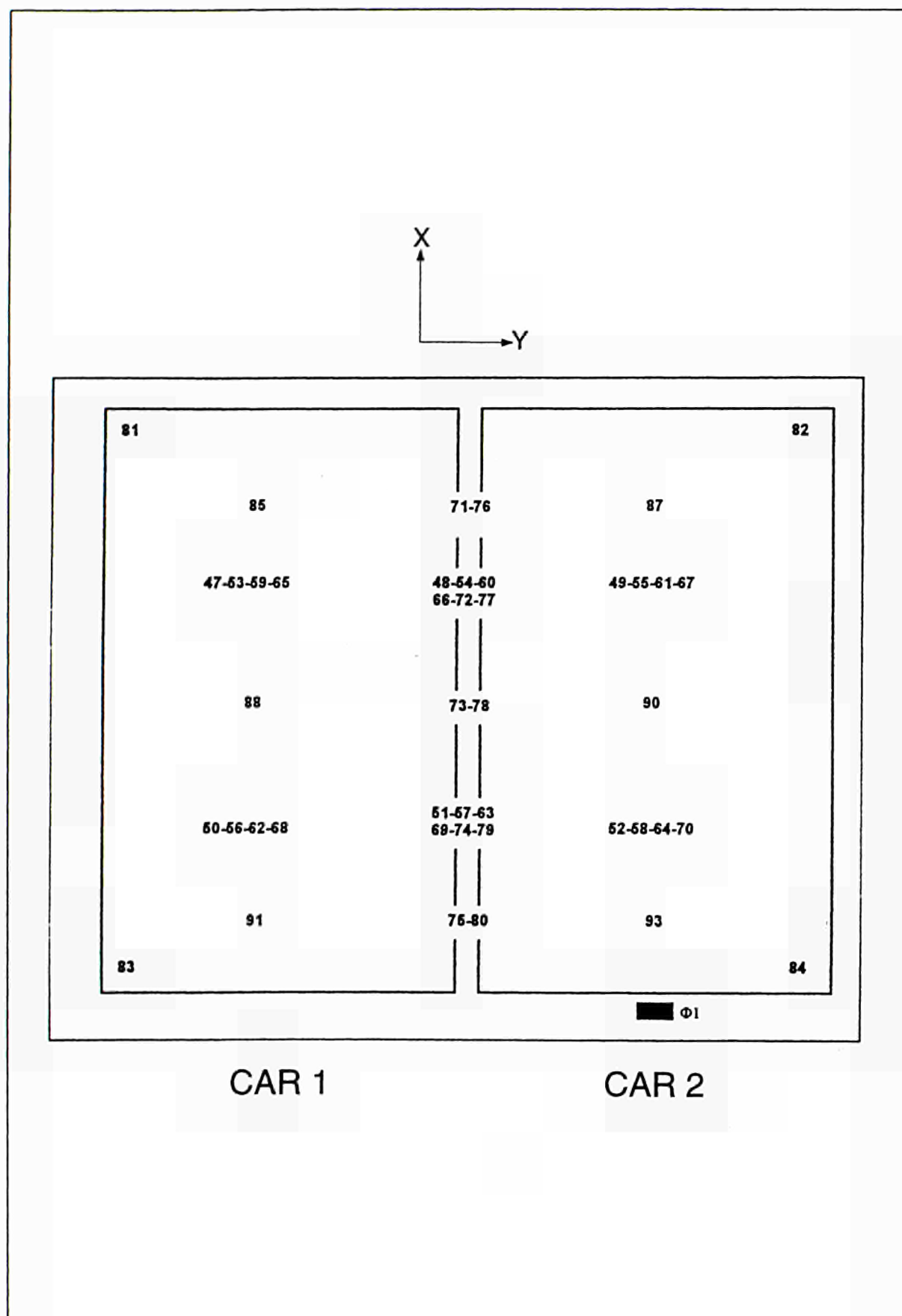
Figure A.2.3 : Ambient thermocouples and fluxmetre φ1 locations

n° TC	emplacement	n° TC	emplacement	X	Y	Z
1	HEB 300 ni A	47	windscreen n°2	1300	1300	2500
2	HEB 300 ni B	48	front door level between	1300	2600	2500
3	HEB 300 ni C	49	windscreen n°1	1300	3900	2500
4	HEB 300 ni D	50	rear window n°2	3300	1300	2500
5	HEB 300 ni E	51	rear wing level between	3300	2600	2500
6	HEB 300 ni F	52	rear window n°1	3300	3900	2500
7	HEB 300 ni G	53	windscreen n°2	1300	1300	2100
8	IPE 240 ni A	54	front door level between	1300	2600	2100
9	IPE 240 ni B	55	windscreen n°1	1300	3900	2100
10	IPE 240 ni C	56	rear window n°2	3300	1300	2100
11	IPE 240 ni D	57	rear wing level between	3300	2600	2100
12	IPE 240 ni E	58	rear window n°1	3300	3900	2100
13	IPE 240 ni F	59	windscreen n°2	1300	1300	1850
14	IPE 240 ni G	60	front door level between	1300	2600	1850
15	HEB 300 i A	61	windscreen n°1	1300	3900	1850
16	HEB 300 i B	62	rear window n°2	3300	1300	1850
17	HEB 300 i C	63	rear wing level between	3300	2600	1850
18	HEB 300 i D	64	rear window n°1	3300	3900	1850
19	HEB 300 i E	65	windscreen n°2	1300	1300	1500
20	HEB 300 i F	66	front door level between	1300	2600	1500
21	HEB 300 i G	67	windscreen n°1	1300	3900	1500
22	IPE 240 i A	68	rear window n°2	3300	1300	1500
23	IPE 240 i B	69	rear wing level between	3300	2600	1500
24	IPE 240 i C	70	rear window n°1	3300	3900	1500
25	IPE 240 i D	71	front wing level between	800	2600	850
26	IPE 240 i E	72	front door level between	1300	2600	850
27	IPE 240 i F	73	rear door level between	2300	2600	850
28	IPE 240 i G	74	rear wing level between	3300	2600	850
29	IPE 500 A S1	75	tank level between	3900	2600	850
30	IPE 500 B S1	76	front wing level between	800	2600	400
31	IPE 500 C S1	77	front door level between	1300	2600	400
32	IPE 500 D S1	78	rear door level between	2300	2600	400
33	IPE 500 E S1	79	rear wing level between	3300	2600	400
34	IPE 500 F S1	80	tank level between	3900	2600	400
35	IPE 500 G S1	81	corner	500	500	2100
36	IPE 500 H S1	82	corner	500	4400	2100
37	IPE 500 I S1	83	corner	4400	500	2100
38	IPE 500 A S2	84	corner	4400	4400	2100
39	IPE 500 B S2	85	bonnet n°2	800	1300	2100
40	IPE 500 C S2	86	front wing level between	800	2600	2100
41	IPE 500 D S2	87	bonnet n°1	800	3900	2100
42	IPE 500 E S2	88	roof n°2	2300	1300	2100
43	IPE 500 F S2	89	rear door level between	2300	2600	2100
44	IPE 500 G S2	90	roof n°1	2300	3900	2100
45	IPE 500 H S2	91	luggage boot n°2	3900	1300	2100
46	IPE 500 I S2	92	tank level between	3900	2600	2100
		93	luggage boot n°1	3900	3900	2100

CTICM STATION d'ESSAIS CTICM		Title	location of thermocouples		TEST	**95-E-344**
		Demander	CTICM		Figure	26

Figure A.2.4 : Location of thermocouples

134

Figure A.2.5

Temperature [°C]

Distance from fire [m]

Argos=2400
Labein=2400
TNO=2400
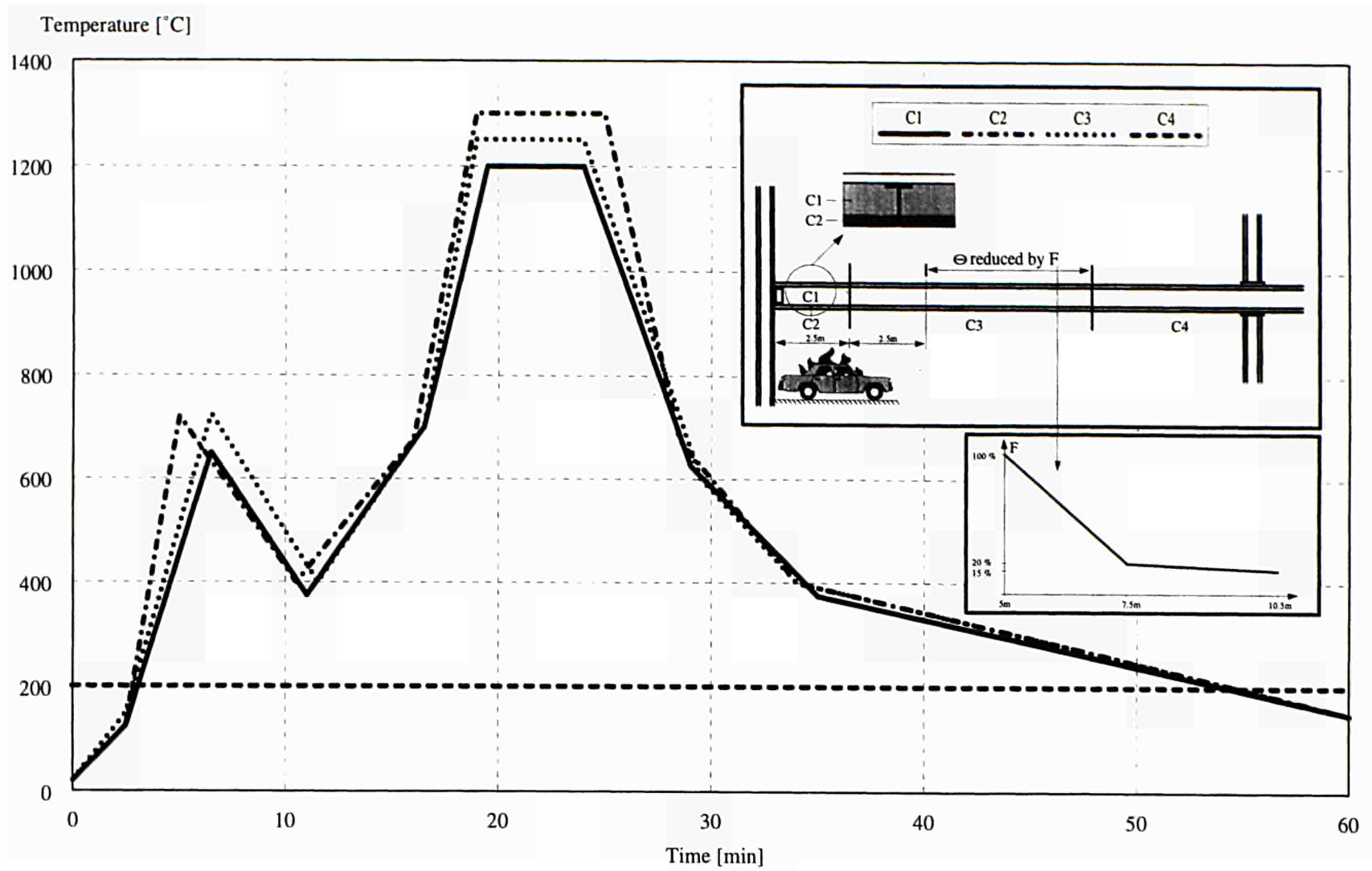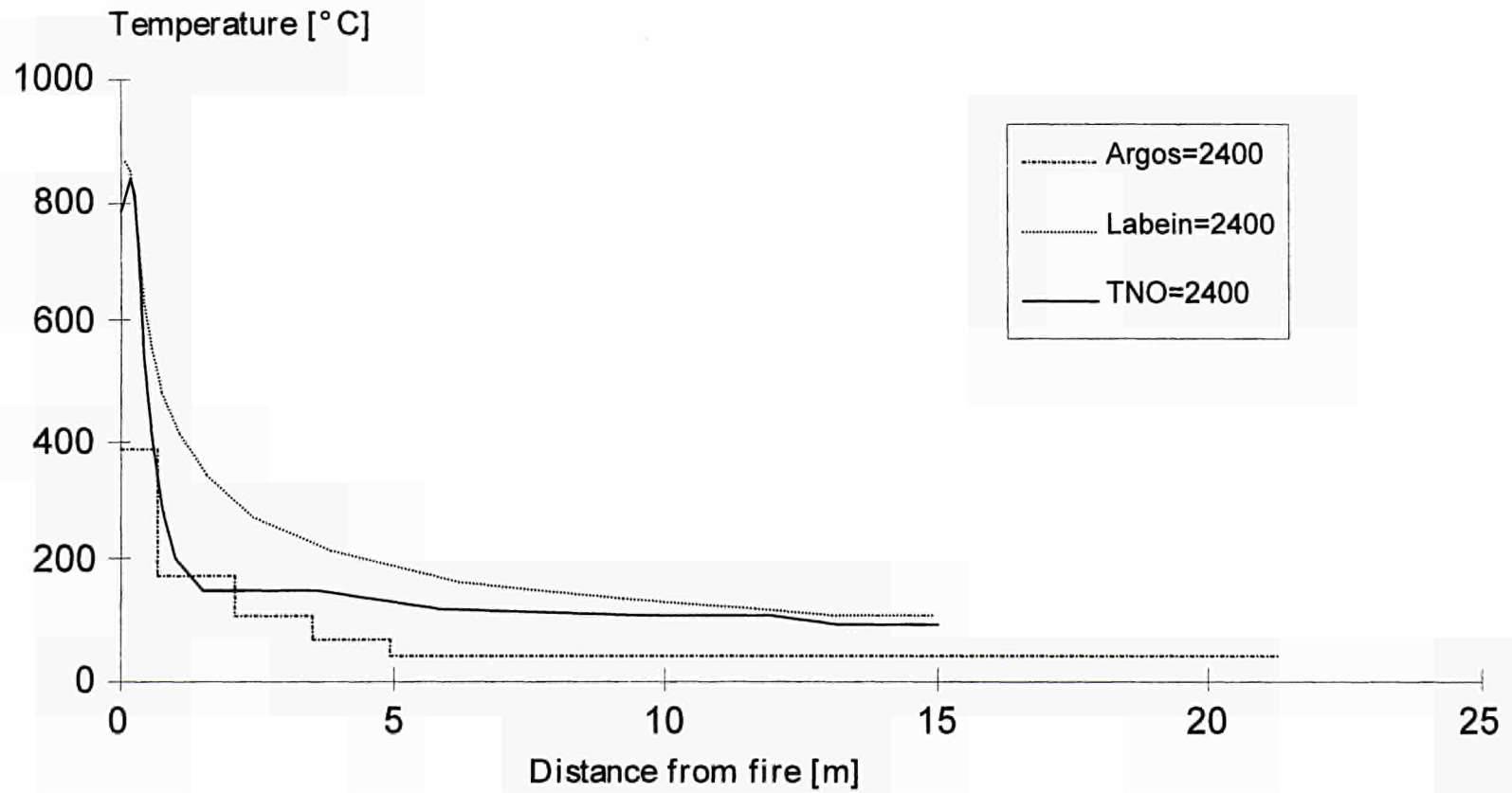
Figure A.2.6 : Simulation 3x - Temperature near the ceiling level.
Comparison ARGOS - FLUENT - VESTA 2400"

Temperature [˚C]

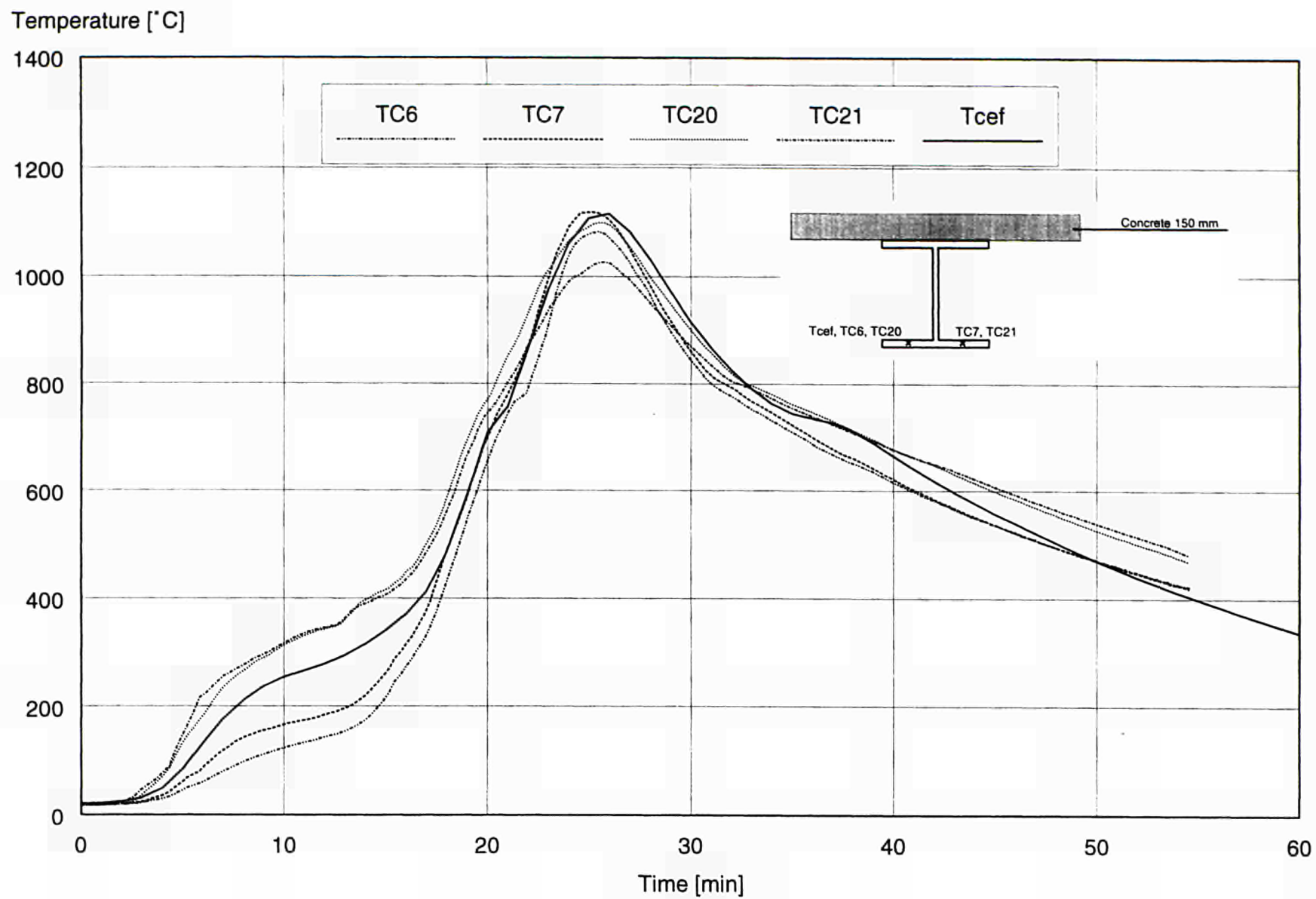| | TC6 | TC7 | TC20 | TC21 | Tcef |

Concrete 150 mm

Tcef, TC6, TC20   TC7, TC21

Time [min]

Figure A.2.7 : Comparison of the temperatures in the bottom flange
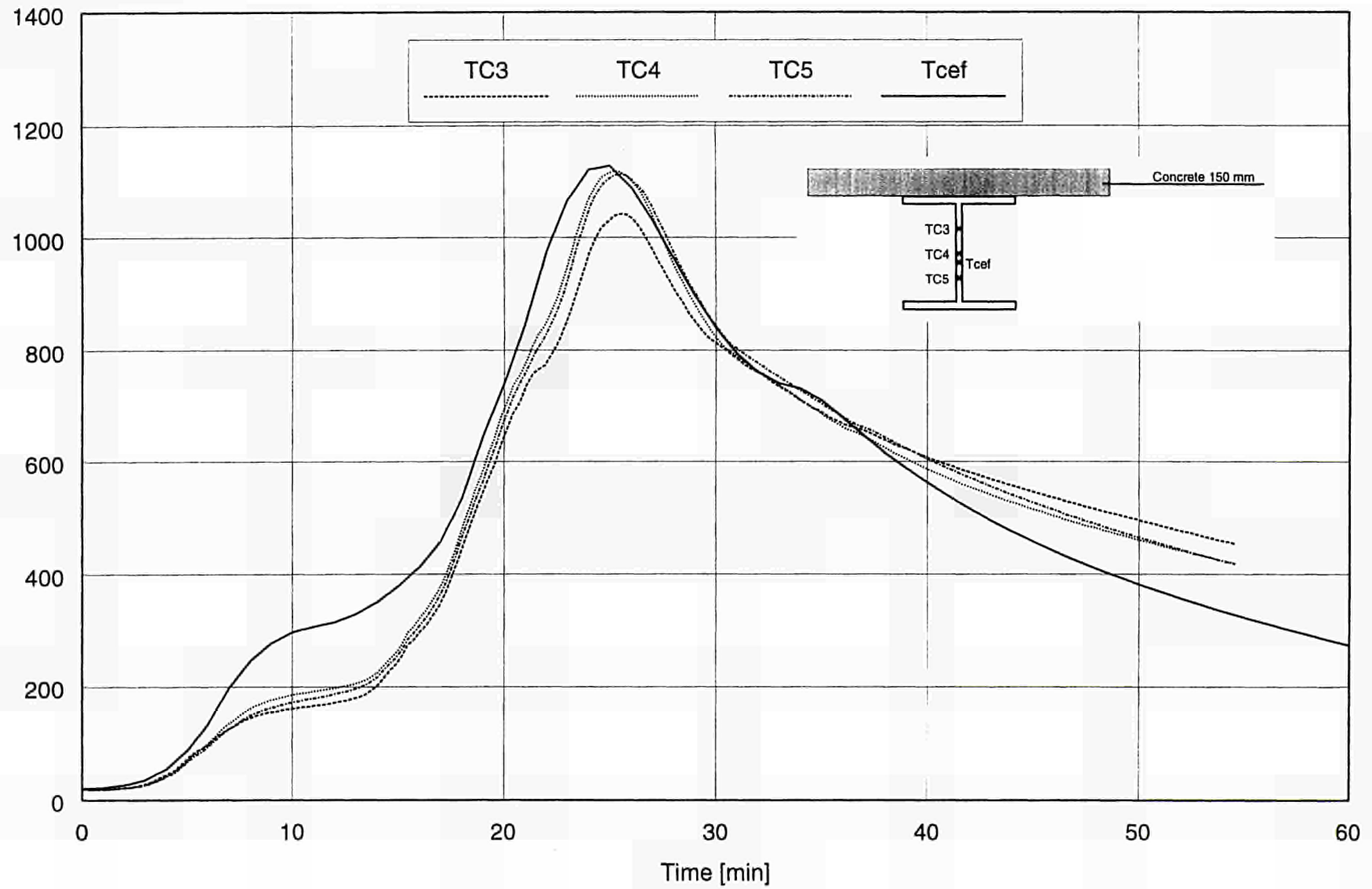
Figure A.2.8 : Comparison of the temperatures in the web
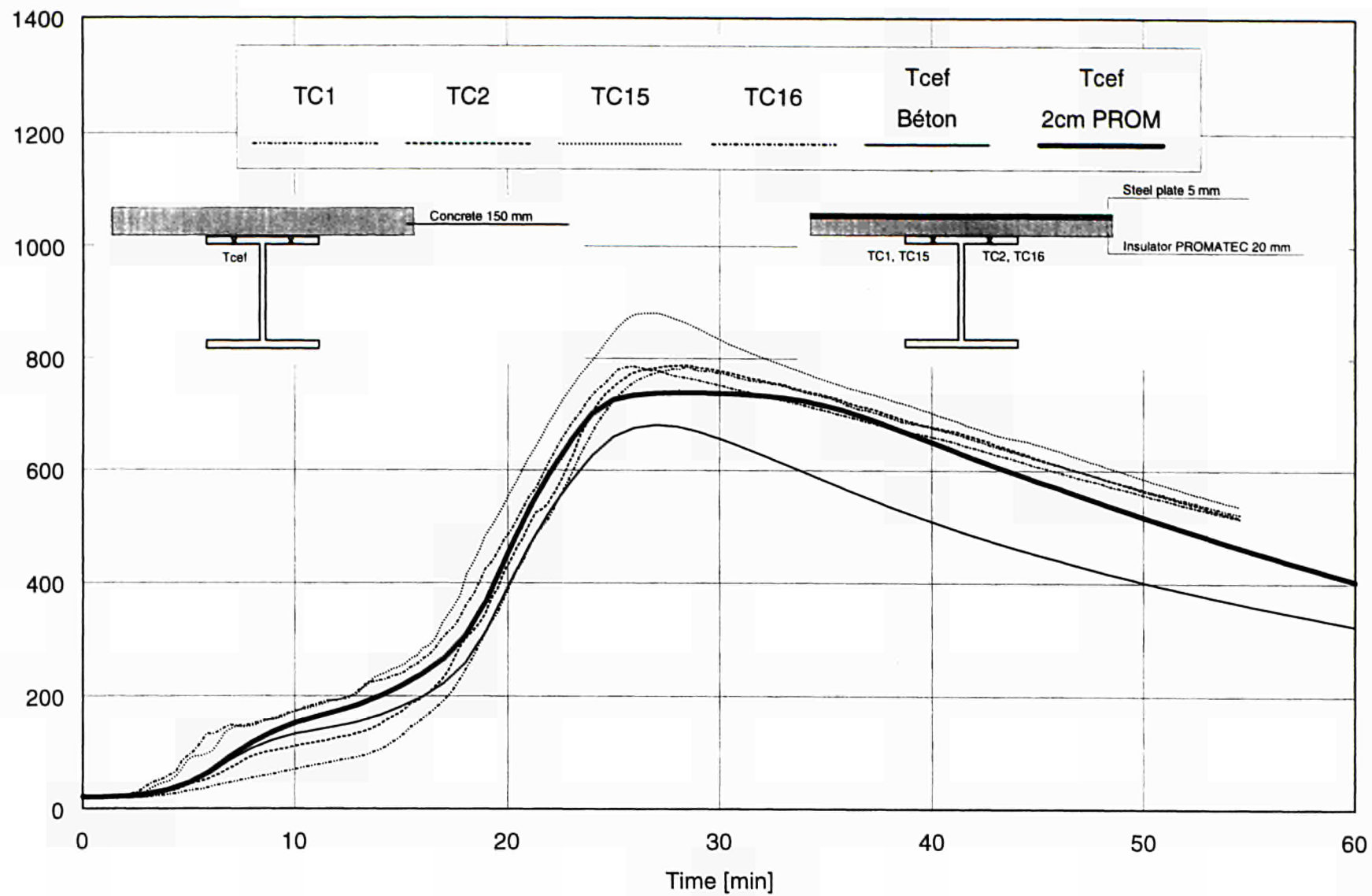
Figure A.2.9 : Comparison of the temperatures in the upper flange

139

CEFICOSS SIMULATION (FIXED-FIXED ; EPS = 0.4 ; REDUCED LOADS)
VERTICAL DISPLACEMENT AT NODE   6 IN FUNCTION OF TIME

Figure A.2.10

140
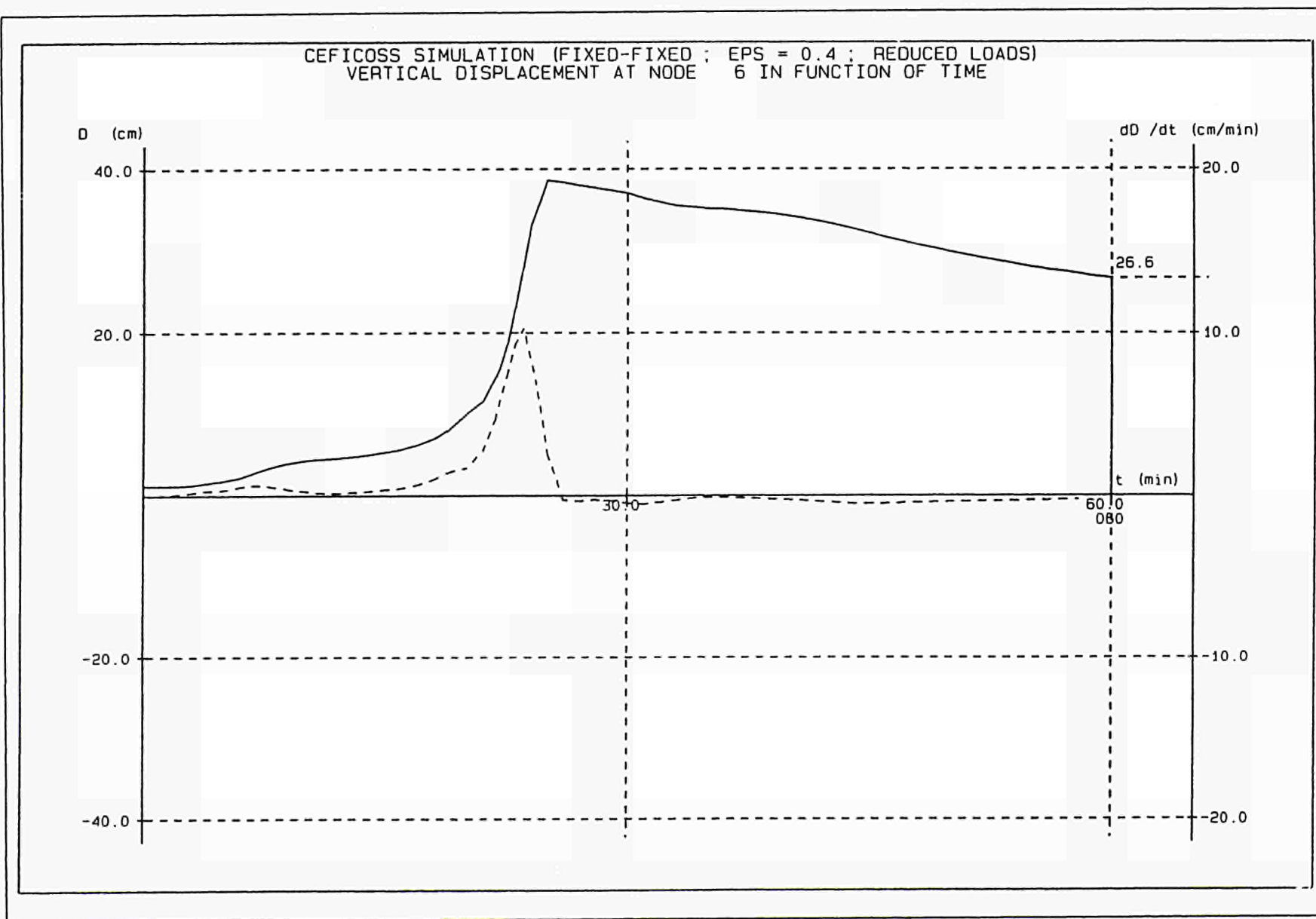
CEFICOSS SIMULATION (FIXED-FIXED : EPS = 0.4 ; REDUCED LOADS)
DISPLACEMENT OF THE STRUCTURE AFTER 26.00 MINUTES

Maximum displacement

Horizontal :	-8.903 cm
Vertical :	38.865 cm

Δ H → +

Δ V
↓
+

0 0 1

0 0 1

0 0 1
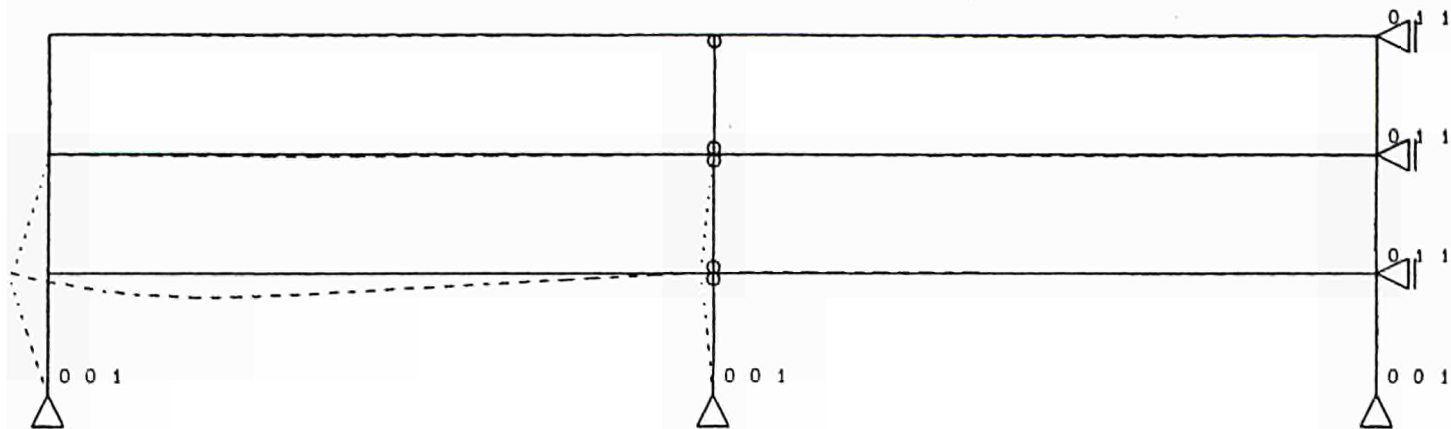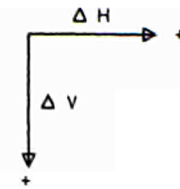
Scale of vertical displacements : 1 /100
Scale of horizontal displacements : 1 /10
Scale of the structure : 1 / 150

Figure A.2.11

141

CEFICOSS SIMULATION (FIXED-FIXED : EPS = 0.4 : REDUCED LOADS)
HORIZONTAL DISPLACEMENT AT NODE   1 IN FUNCTION OF TIME
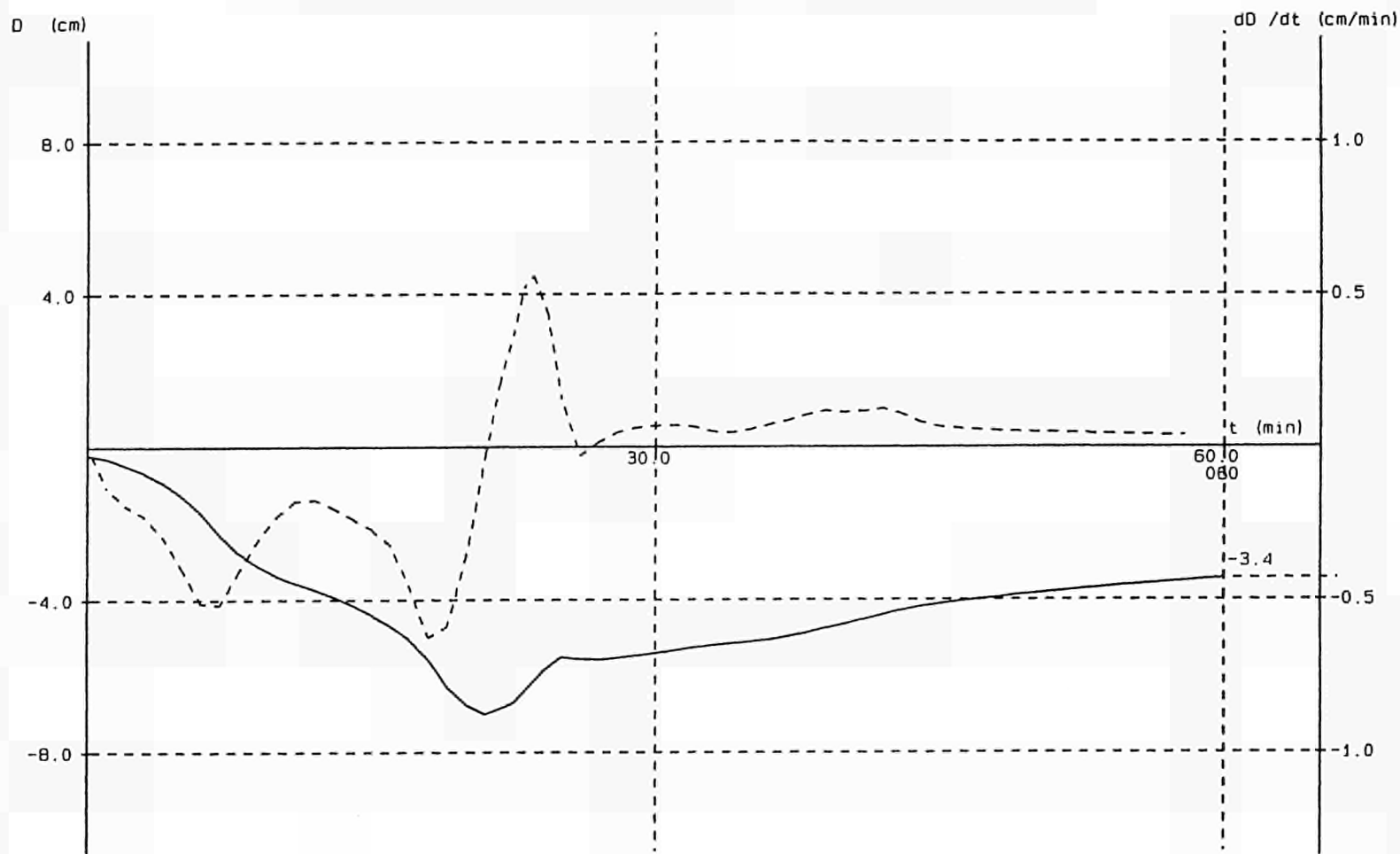
Figure A.2.12
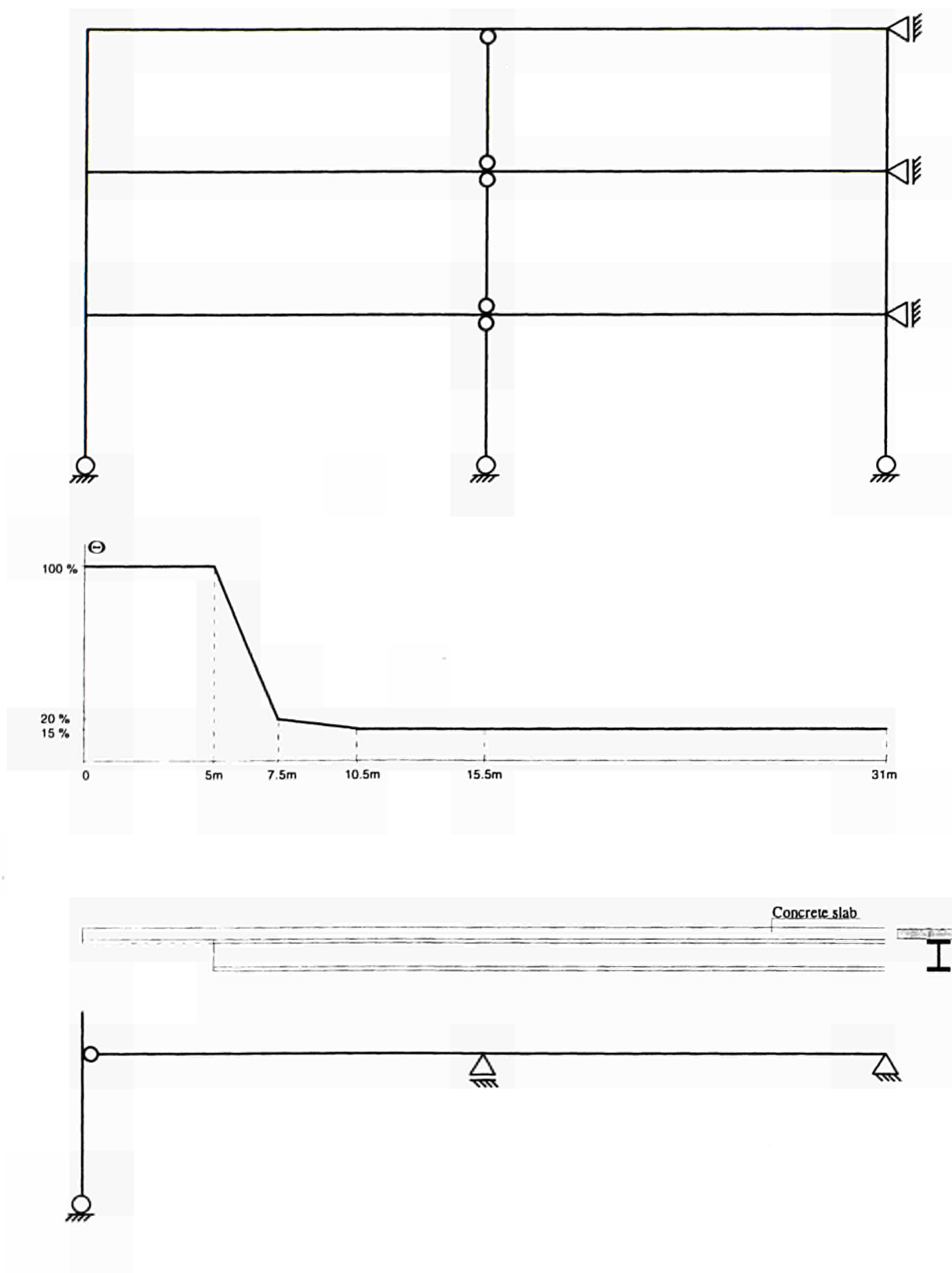
Figure A.2.13 : Temperature evolution along the beam and effect on the structure

CEFICOSS SIMULATION (FIXED-FIXED ; EPS = 0.4 ; REDUCED LOADS)
BENDING MOMENTS AFTER 26.00 MINUTES

Maximum bending moment : −1619.816 kNm
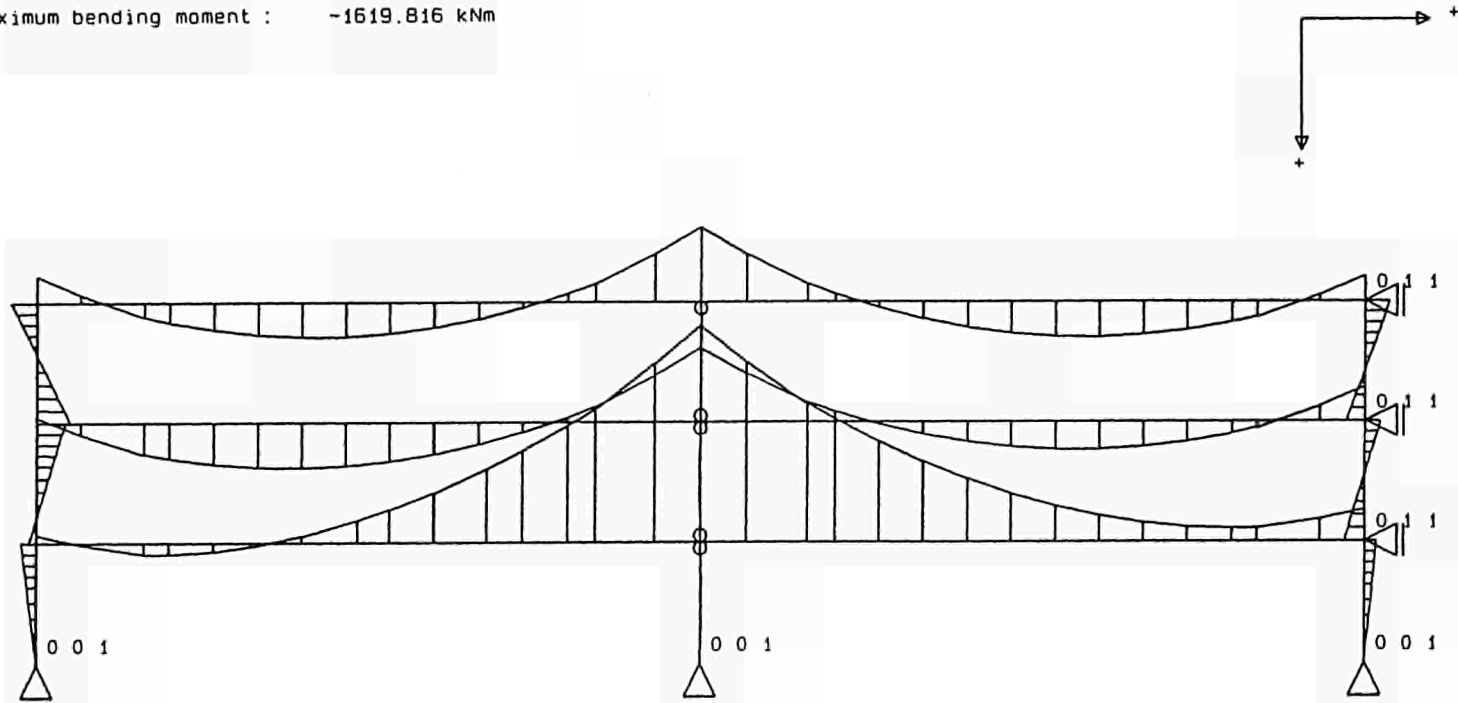
Scale of bending moments : 1 / 500
Scale of the structure : 1 / 150

Figure A.2.14

144

CEFICOSS SIMULATION (FIXED-FIXED ; EPS = 0.4 ; REDUCED LOADS)
SHEAR FORCE AT ELEMENT   1 IN FUNCTION OF TIME
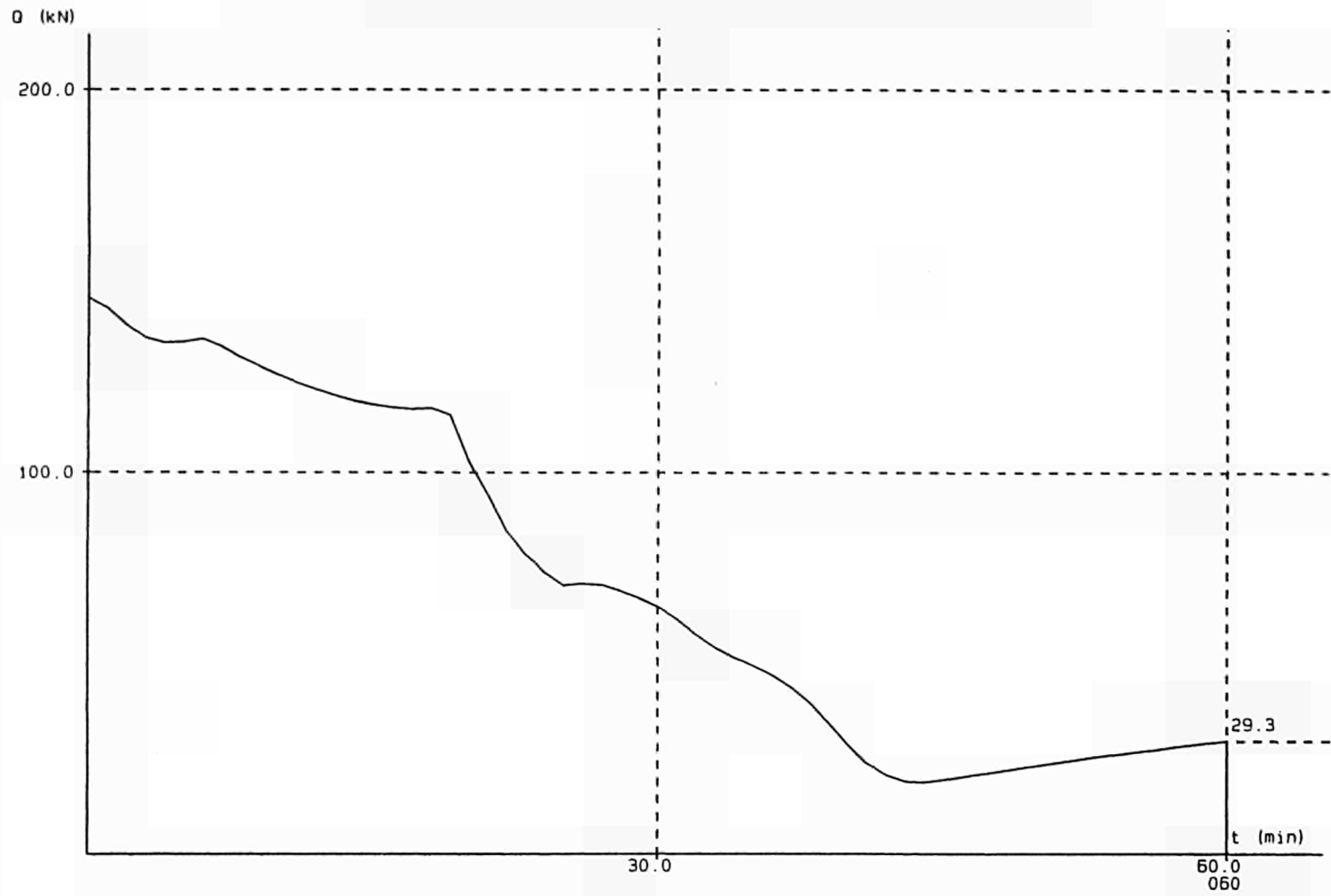
Figure A.2.15

ANNEX 3

CFD calculation of scenario 1 considering the RHR curve of chapter 3.4.2.

A.3.1. LABEIN simulation using the CFD FLUENT

Model

Fire scenario known as simulation 4 (see chapter 5.1.1) has been updated with a new RHR curve based on the measured data from recent car test (see chapter 3.4.2). This updated simulation 4 has been called simulation 4X. This curve provides data up to 70 minutes with a maximum of 5530 kW between 23th and 26th minute. The total heat released is 6.9375 GJ and its distribution along time can be seen in figure A.3.1.
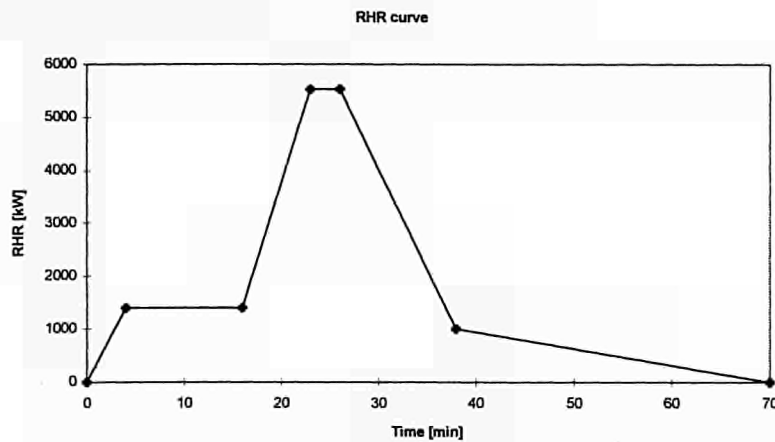
Figure A.3.1

The heat source is located under beam 1, its size being : 3m length, 1.71m width and 0.55m height.
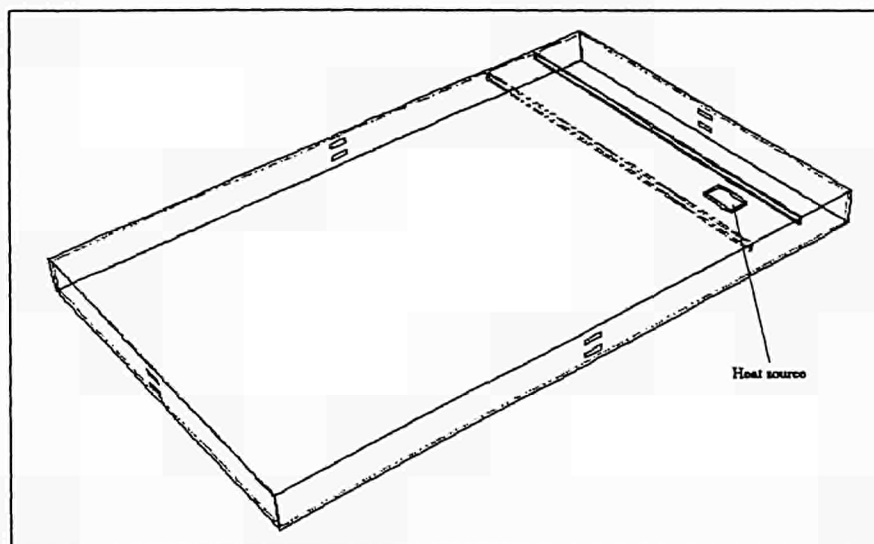

Figure A.3.2

146

Simulation 4X consists of the same geometry as for simulation 4. In order to achieve a precise temperature description in the steel beams, these were modeled as a 220 mm x 600 mm box composed of a surrounding steel sheet 11mm thick and a concrete core. A zero heat flux boundary condition at the interface between steel and concrete has been assumed.

Other general boundary conditions that remain as designed for simulation 4 are :

- Buoyant effect on turbulence (BEOT).
- All windows of the garage have a fixed plenum pressure and a temperature of 293 K.
- The external wall has a defined convection coefficient of 10 W/m^{2}K.
- The physical properties used for the concrete and steel are :

Concrete :   Conductivity = 1.6 W/mk
              Cp = 1000 J/kgK
              ρ = 2500 kg/m^3
              Emissivity = 0.94

Steel :   Conductivity 45 W/mK
              Cp = 520 J/kgK
              ρ = 7850 kg/m^3
              Emissivity = 0.6

The resulting model has a grid of 43 * 19 * 27 = 22059 cells.

Flow through windows

New numerical restriction has been used in this model. In order to make results comparable with TNO simulation results, cells that represent windows have been modeled as porous cells. These porous cells provide a negative source term in the momentum equation that has been adjusted to produce a coefficient of 0.57 in the Bernoulli equation at the windows.

$$v = 0.57\sqrt{\frac{2 \cdot \Delta P}{\rho}}$$

Results

Results of simulation 4X show that the new RHR curve gives, in general, a higher temperature distribution than previous simulations (Simu4 and Forced-Ventilation). Temperatures in the near by of the heat source (see figure A.3.3) increase to 6th minutes, in a first step, and, after a horizontal plateau, increase again between 16th and 23th minutes. The maximum values of temperature are reached after 23th minute where values are slightly below 900°C (see figure A.3.4). After the 39th minutes, the air temperature is less than 200°C.
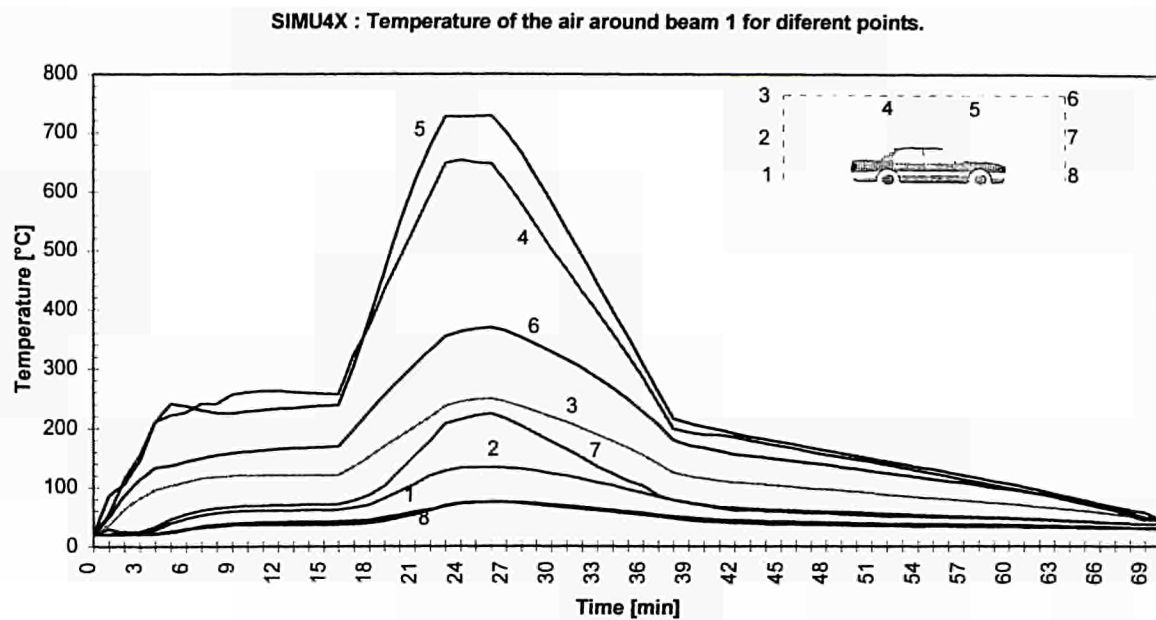
Figure A.3.3

As expected, the maximum values of temperature are located over the source and just below the beam. Figure A.3.4 shows the distribution of temperature below along the beam.
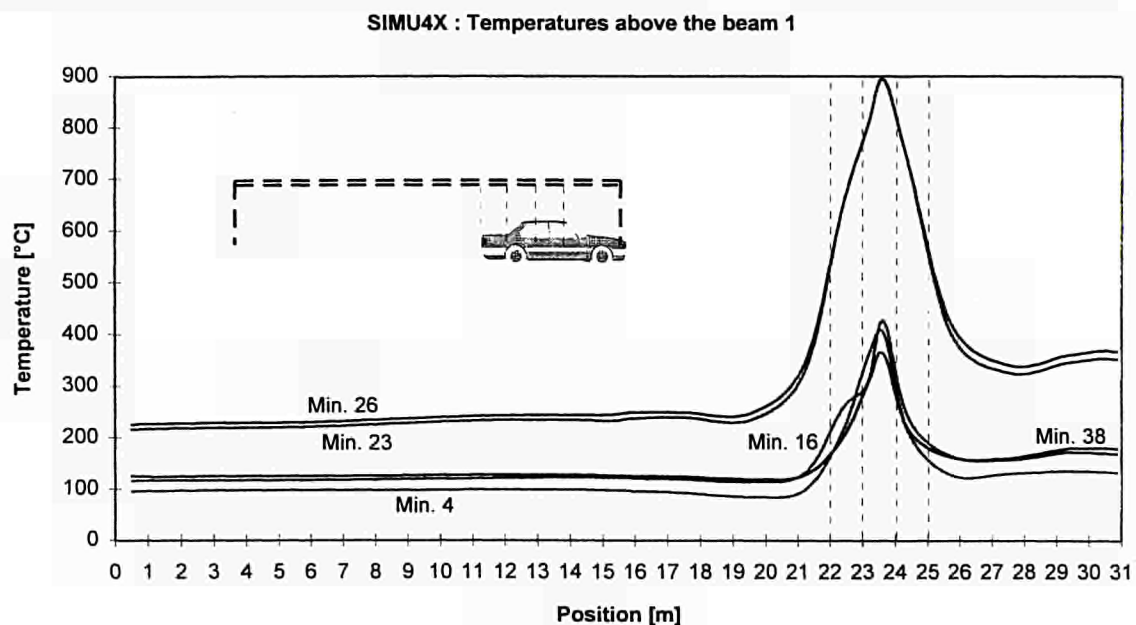
Figure A.3.4

Figure A.3.5 compares the temperatures of the air around beam 1 (in the central section of the heat source). As occurred in previous simulations (Simu4 and Forced-Ventilation), the highest temperatures are reached around the lower-right (shortest side of the room) corner of the beam (point 'c' in figures). For this point, temperature remains near 890°C between 23th and 26th minute.
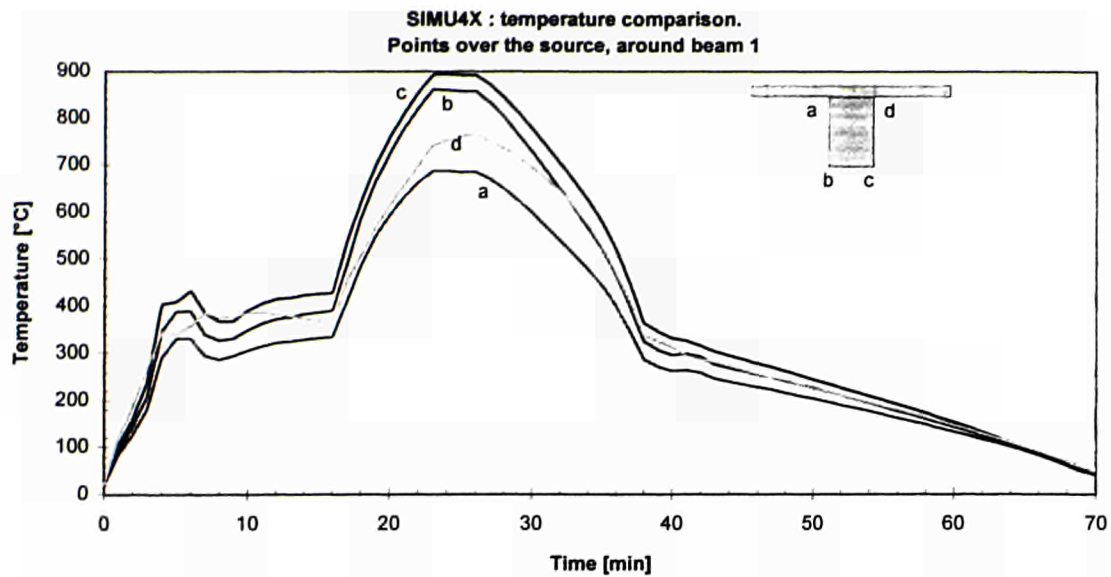
Figure A.3.5

Comparing temperatures in point 'c' with the temperatures found out in Simu4 and Forced-Ventilation, it is seen that they are very much higher (see figure A.3.6). Mainly, it can be attributed to two reasons :

- The first one, and **the most important**, the values of the RHR curve are higher than the previous RHR curves.
- The second one deals with the modification of the Bernoulli coefficient in the windows, which has the effect of diminishing the effective ventilation.
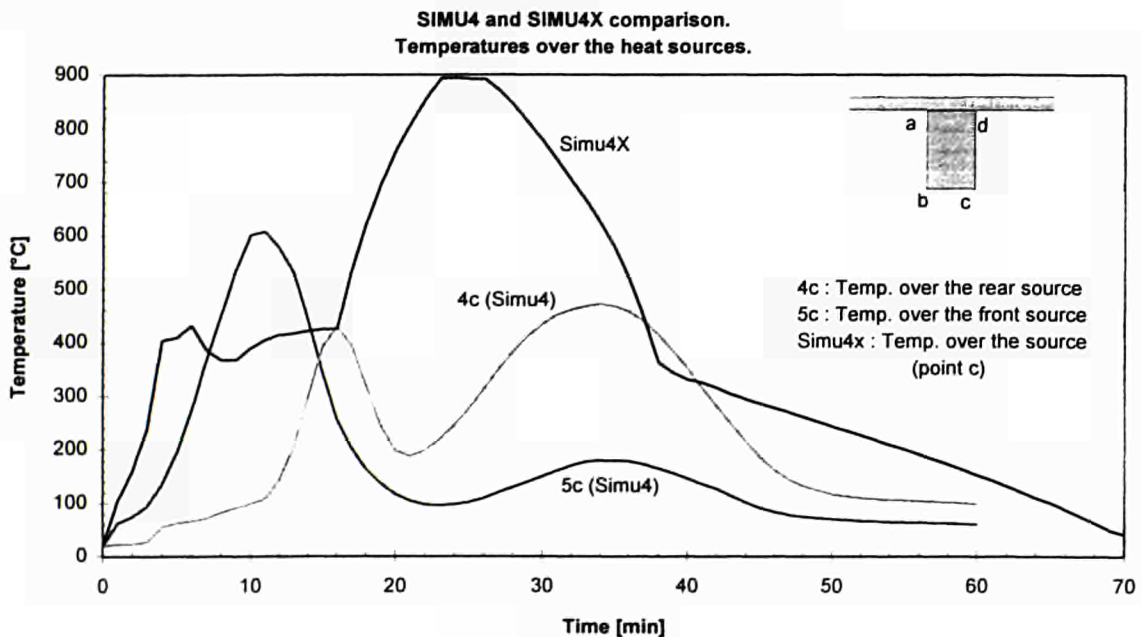

Figure A.3.6

Figure A.3.7 shows outlet velocities through four windows and compares them with the values obtained for the previous simulations. Once again, it is important to note that

149

Simu4X presents the lowest values of flow through windows in spite of its high RHR curve due to the use of the coefficient 0.57 in the Bernoulli equation.

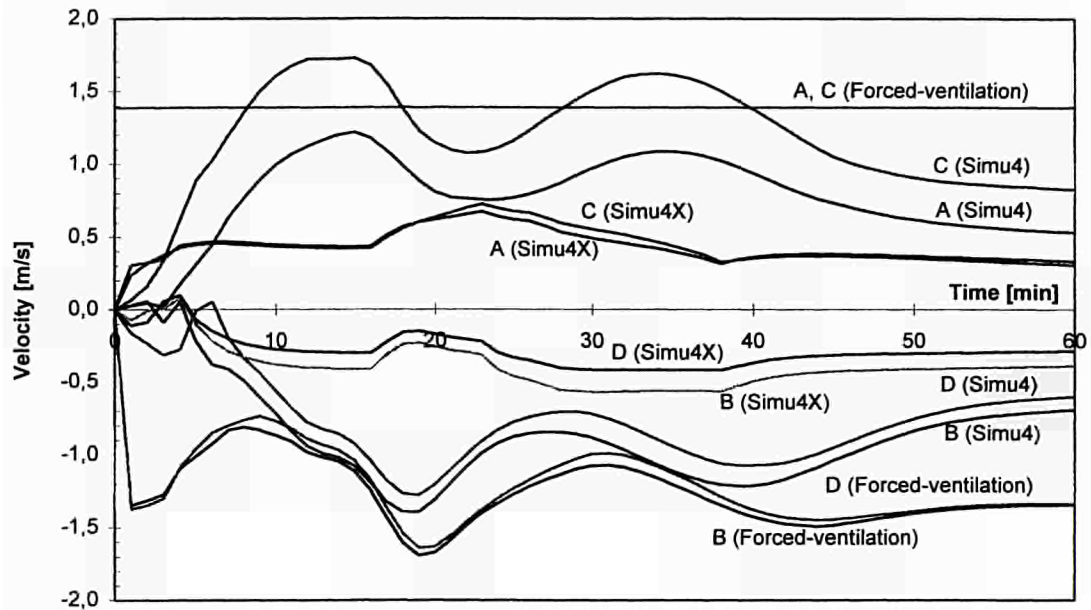**SIMU4X, SIMU4 and Forced Ventilation : Outlet velocities comparison.**
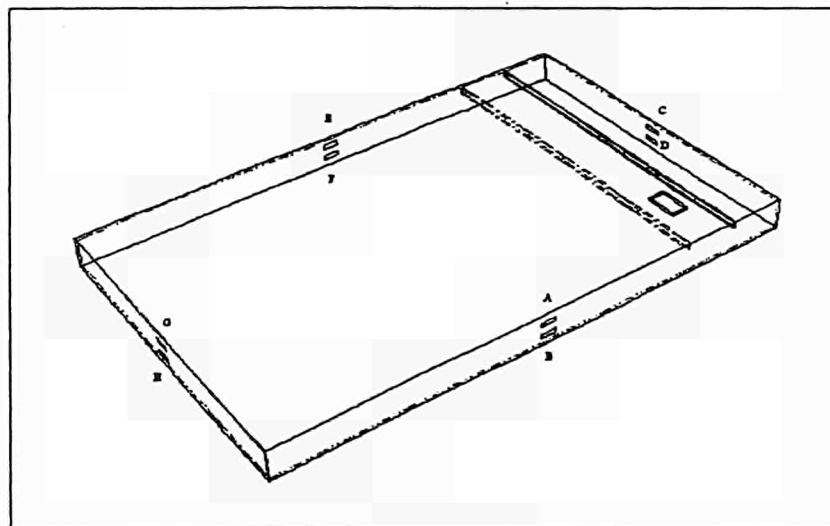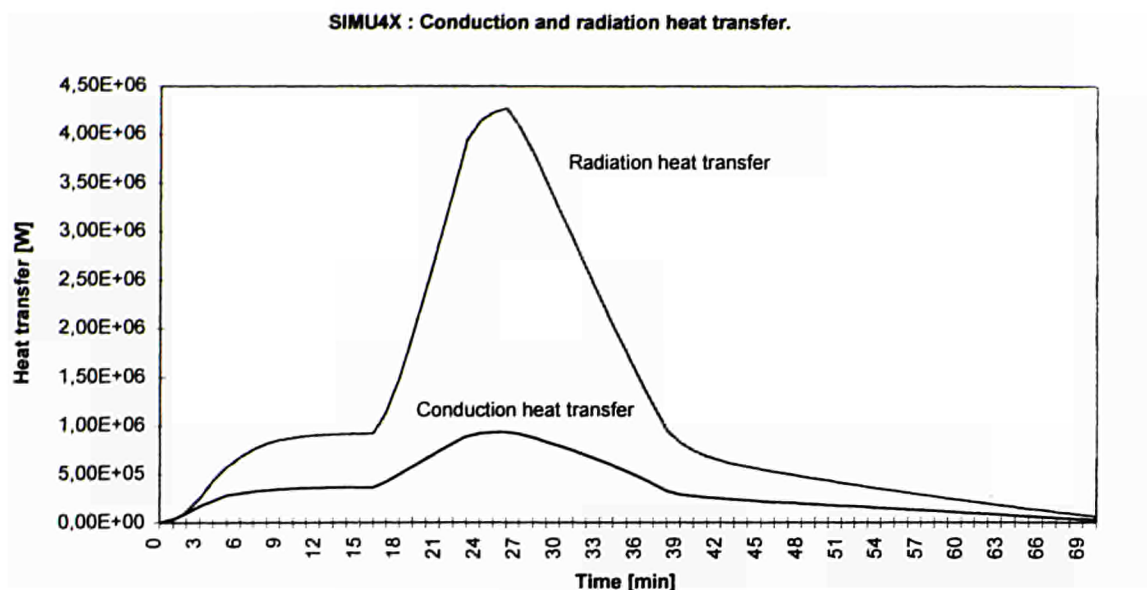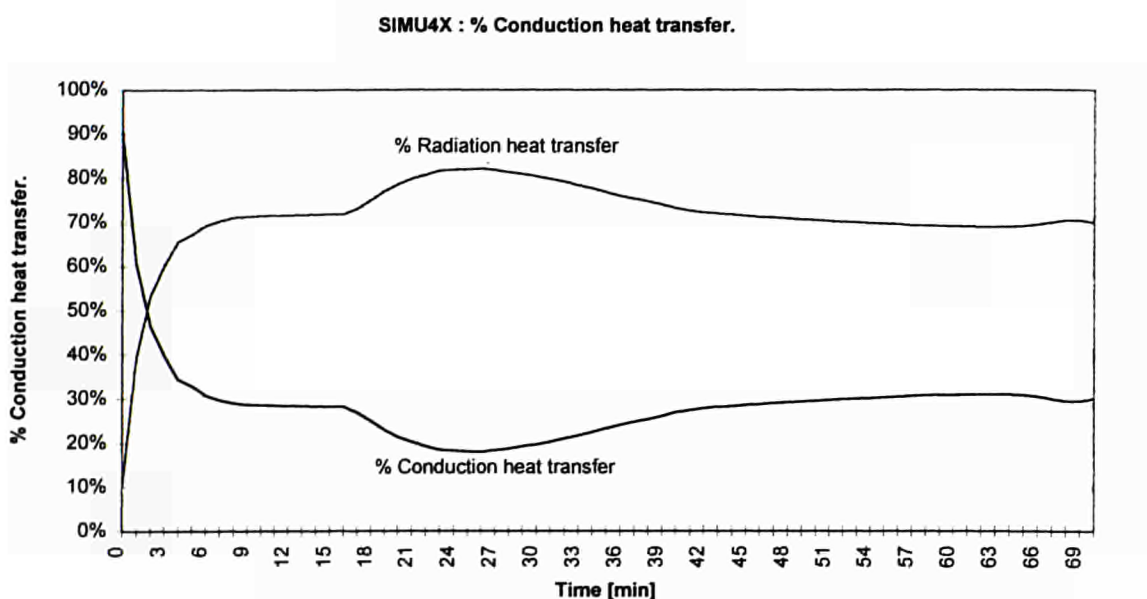

Figure A.3.7

Figure A.3.8

The figures A.3.9 and A.3.10 show the conduction and radiation heat transfer throughout the external walls and the distribution (percent) of the heat losses between conduction and radiation.

The steel temperatures are shown on the figure A.3.11. This figure can be compared to the figure A.3.5 giving the corresponding air temperature in the air.

SIMU4X : Conduction and radiation heat transfer.

Figure A.3.9

SIMU4X : % Conduction heat transfer.

Figure A.3.10

A.3.2. TNO calculation

The same simulation has been performed by TNO using the CFD VESTA.

The figures A.3.12 and A.3.13 are similar to the figure A.3.4 and A.3.11 provided by LABEIN. They point out the good accordance between the results provided by both CFD. The maximum air temperature is about 900°C (see figures A.3.12 and A.3.4) and the maximum steel temperature according to LABEIN is 620°C (see figure A.3.11) and 555°C according to TNO (see figure A.3.13).
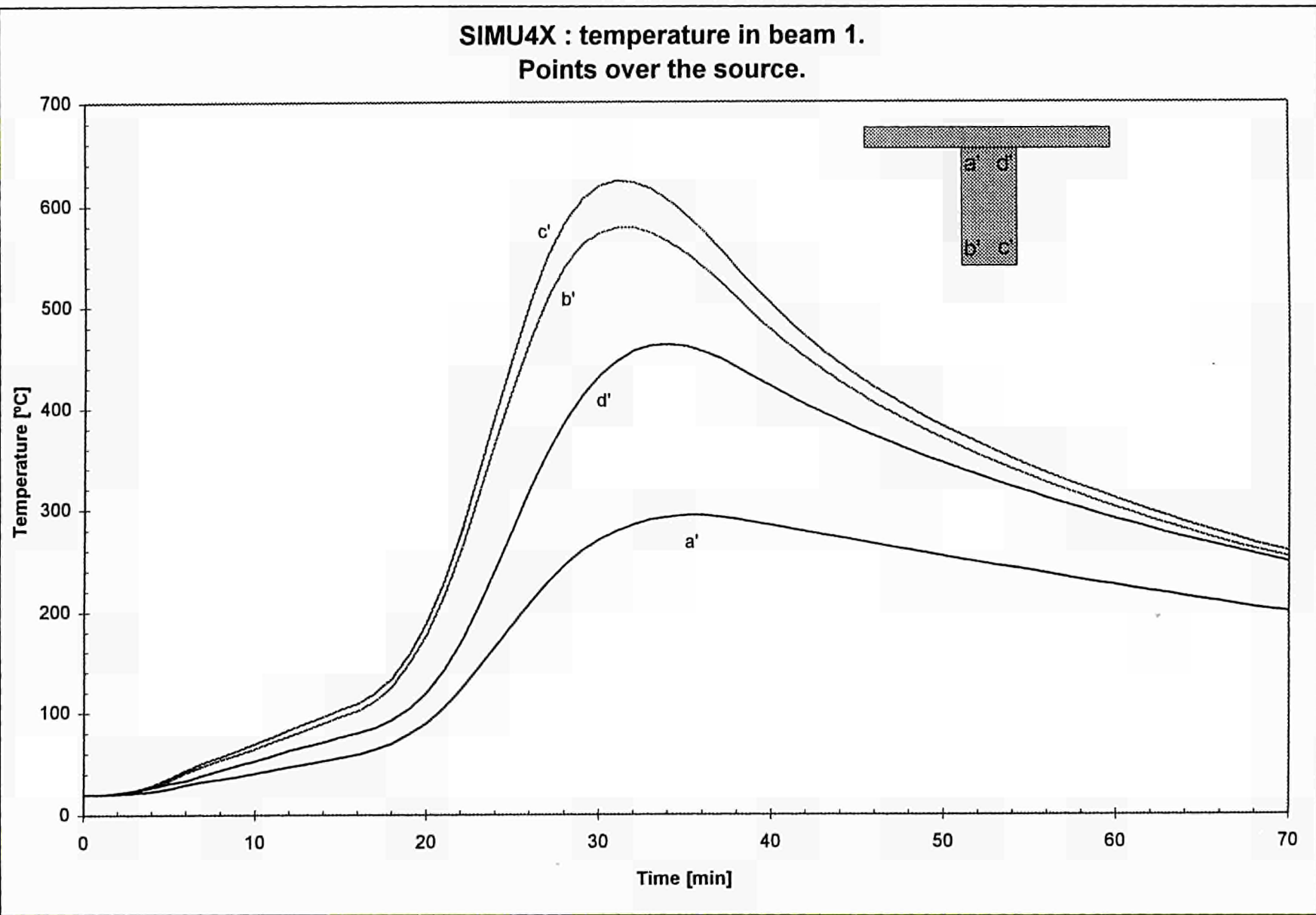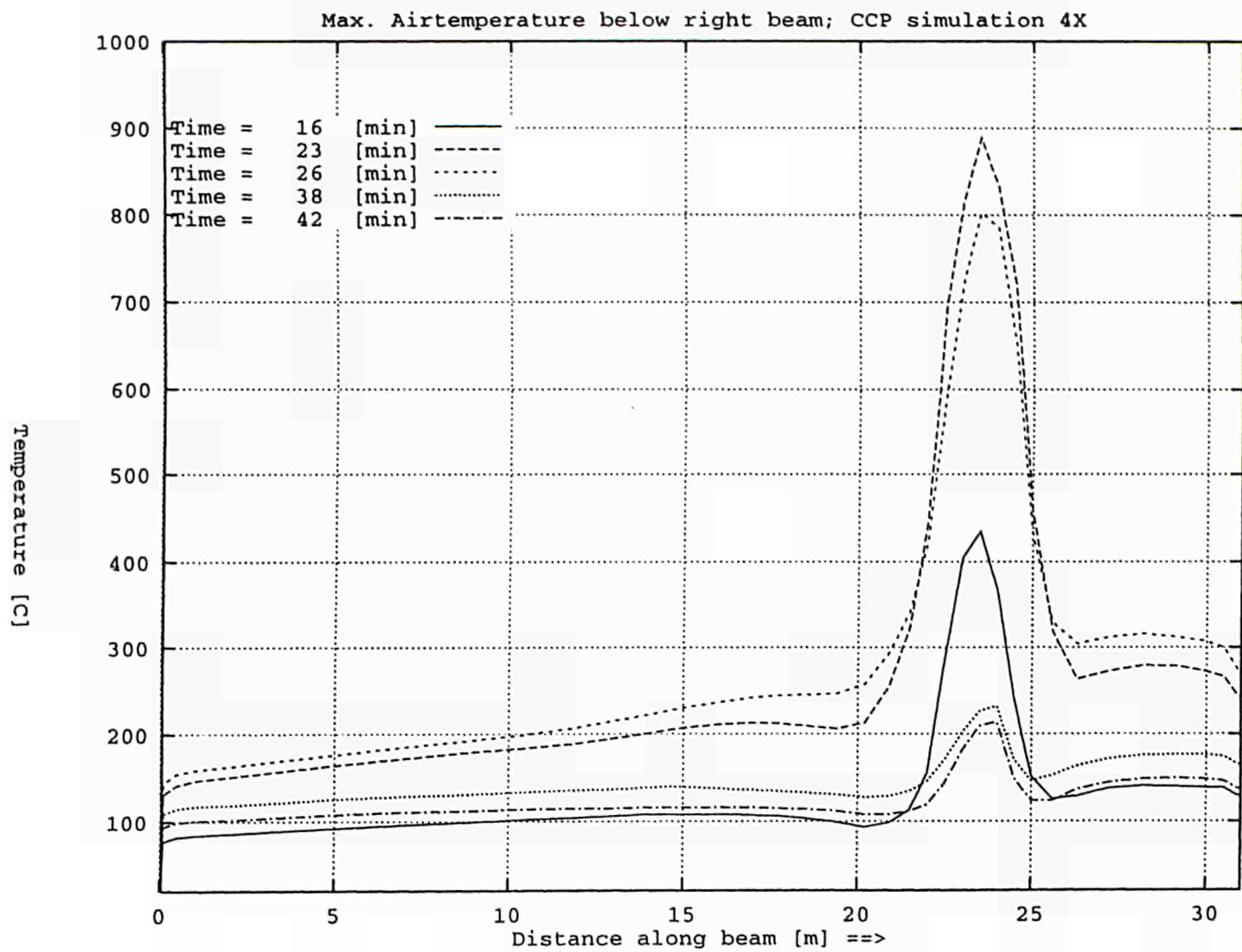
SIMU4X : temperature in beam 1.
Points over the source.

Figure A.3.11

Max. Airtemperature below right beam; CCP simulation 4X

Figure A.3.12

Steel temperature right beam ; TNO CCP simulation 4X

Figure A.3.13

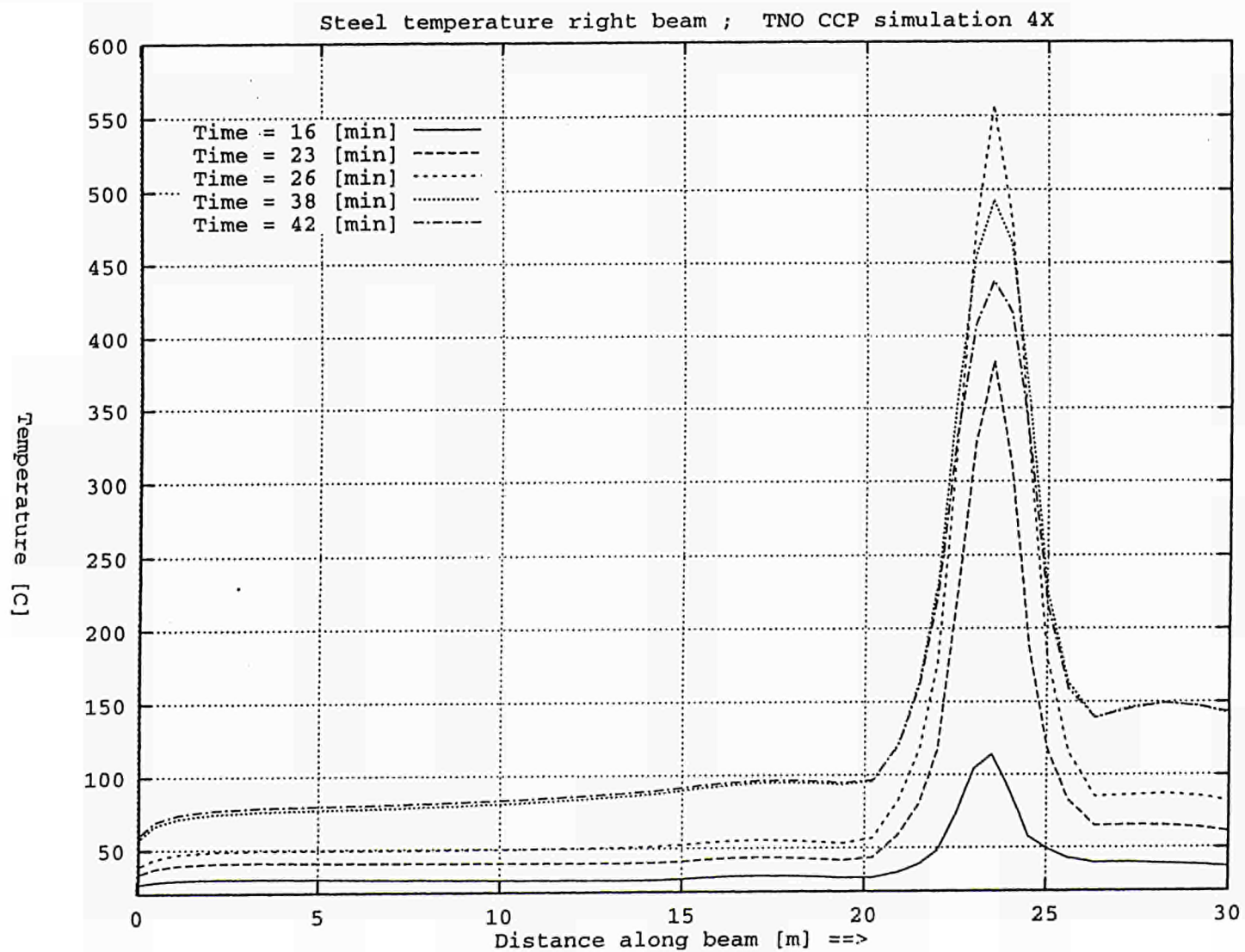# Venta • Salg • Verkauf • Πωλήσεις • Sales • Vente • Vendita • Verkoop • Venda • Myynti • Försäljning

BELGIQUE/BELGIË

Jean De Lannoy
Avenue du Roi 202/Koningslaan 202
B-1190 Bruxelles/Brussel
Tél. (32-2) 538 43 08
Fax (32-2) 538 08 41
E-mail: jean.de.lannoy@infoboard.be
URL: http://www.jean-de-lannoy.be

**La librairie européenne/
De Europese Boekhandel**
Rue de la Loi 244/Wetstraat 244
B-1040 Bruxelles/Brussel
Tél. (32-2) 295 26 39
Fax (32-2) 735 08 60
E-mail: mail@libeurop.be
URL: http://www.libeurop.be

Moniteur belge/Belgisch Staatsblad
Rue de Louvain 40-42/Leuvenseweg 40-42
B-1000 Bruxelles/Brussel
Tél. (32-2) 552 22 11
Fax (32-2) 511 01 84

DANMARK

J. H. Schultz Information A/S
Herstedvang 10-12
DK-2620 Albertslund
Tlf. (45) 43 63 23 00
Fax (45) 43 63 19 69
E-mail: schultz@schultz.dk
URL: http://www.schultz.dk

DEUTSCHLAND

Bundesanzeiger Verlag GmbH
Vertriebsabteilung
Amsterdamer Straße 192
D-50735 Köln
Tel. (49-221) 97 66 80
Fax (49-221) 97 66 82 78
E-Mail: vertrieb@bundesanzeiger.de
URL: http://www.bundesanzeiger.de

ΕΛΛΑΔΑ/GREECE

G. C. Eleftheroudakis SA
International Bookstore
Panepistimiou 17
GR-10564 Athina
Tel. (30-1) 331 41 80/1/2/3/4/5
Fax (30-1) 323 98 21
E-mail: elebooks@netor.gr

ESPAÑA

Boletín Oficial del Estado
Trafalgar, 27
E-28071 Madrid
Tel. (34) 915 38 21 11 (Libros),
    913 84 17 15 (Suscrip.)
Fax (34) 915 38 21 21 (Libros),
    913 84 17 14 (Suscrip.)
E-mail: clientes@com.boe.es
URL: http://www.boe.es

Mundi Prensa Libros, SA
Castelló, 37
E-28001 Madrid
Tel. (34) 914 36 37 00
Fax (34) 915 75 39 98
E-mail: libreria@mundiprensa.es
URL: http://www.mundiprensa.com

FRANCE

Journal officiel
Service des publications des CE
26, rue Desaix
F-75727 Paris Cedex 15
Tél. (33) 140 58 77 31
Fax (33) 140 58 77 00
URL: http://www.journal-officiel.gouv.fr

IRELAND

Government Supplies Agency
Publications Section
4-5 Harcourt Road
Dublin 2
Tel. (353-1) 661 31 11
Fax (353-1) 475 27 60

ITALIA

Licosa SpA
Via Duca di Calabria, 1/1
Casella postale 552
I-50125 Firenze
Tel. (39) 055 64 83 1
Fax (39) 055 64 12 57
E-mail: licosa@ftbcc.it
URL: http://www.ftbcc.it/licosa

LUXEMBOURG

Messageries du livre SARL
5, rue Raiffeisen
L-2411 Luxembourg
Tél. (352) 40 10 20
Fax (352) 49 06 61
E-mail: mail@mdl.lu
URL: http://www.mdl.lu

NEDERLAND

SDU Servicecentrum Uitgevers
Christoffel Plantijnstraat 2
Postbus 20014
2500 EA Den Haag
Tel. (31-70) 378 98 80
Fax (31-70) 378 97 83
E-mail: sdu@sdu.nl
URL: http://www.sdu.nl

ÖSTERREICH

**Manz'sche Verlags- und
Universitätsbuchhandlung GmbH**
Kohlmarkt 16
A-1014 Wien
Tel. (43-1) 53 16 11 00
Fax (43-1) 53 16 11 67
E-Mail: bestellen@manz.co.at
URL: http://www.manz.at/index.htm

PORTUGAL

Distribuidora de Livros Bertrand Ld.ª
Grupo Bertrand, SA
Rua das Terras dos Vales, 4-A
Apartado 60037
P-2700 Amadora
Tel. (351-1) 495 90 50
Fax (351-1) 496 02 55

Imprensa Nacional-Casa da Moeda, EP
Rua Marquês Sá da Bandeira, 16-A
P-1050 Lisboa Codex
Tel. (351-1) 353 03 99
Fax (351-1) 353 02 94
E-mail: del.incm@mail.telepac.pt
URL: http://www.incm.pt

SUOMI/FINLAND

**Akateeminen Kirjakauppa/
Akademiska Bokhandeln**
Keskuskatu 1/Centralgatan 1
PL/PB 128
FIN-00101 Helsinki/Helsingfors
P./tfn (358-9) 121 44 18
F./fax (358-9) 121 44 35
Sähköposti: akatilaus@akateeminen.com
URL: http://www.akateeminen.com

SVERIGE

BTJ AB
Traktorvägen 11
S-221 82 Lund
Tfn (46-46) 18 00 00
Fax (46-46) 30 79 47
E-post: btjeu-pub@btj.se
URL: http://www.btj.se

UNITED KINGDOM

The Stationery Office Ltd
International Sales Agency
51 Nine Elms Lane
London SW8 5DR
Tel. (44-171) 873 90 90
Fax (44-171) 873 84 63
E-mail: ipa.enquiries@theso.co.uk
URL: http://www.the-stationery-office.co.uk

ÍSLAND

Bokabud Larusar Blöndal
Skólavördustig, 2
IS-101 Reykjavik
Tel. (354) 551 56 50
Fax (354) 552 55 60

NORGE

Swets Norge AS
Østenjoveien 18
Boks 6512 Etterstad
N-0606 Oslo
Tel. (47-22) 97 45 00
Fax (47-22) 97 45 45

SCHWEIZ/SUISSE/SVIZZERA

Euro Info Center Schweiz
c/o OSEC
Stampfenbachstraße 85
PF 492
CH-8035 Zürich
Tel. (41-1) 365 53 15
Fax (41-1) 365 54 11
E-mail: eics@osec.ch
URL: http://www.osec.ch/eics

BĂLGARIJA

Europress Euromedia Ltd
59, blvd Vitosha
BG-1000 Sofia
Tel. (359-2) 980 37 66
Fax (359-2) 980 42 30
E-mail: Milena@mbox.cit.bg

ČESKÁ REPUBLIKA

ÚSIS
NIS-prodejna
Havelkova 22
CZ-130 00 Praha 3
Tel. (420-2) 24 23 14 86
Fax (420-2) 24 23 11 14
E-mail: nkposp@dec.nis.cz
URL: http://usiscr.cz

CYPRUS

Cyprus Chamber of Commerce and Industry
PO Box 1455
CY-1509 Nicosia
Tel. (357-2) 66 95 00
Fax (357-2) 66 10 44
E-mail: demetrap@ccci.org.cy

EESTI

**Eesti Kaubandus-Tööstuskoda (Estonian
Chamber of Commerce and Industry)**
Toom-Kooli 17
EE-0001 Tallinn
Tel. (372) 646 02 44
Fax (372) 646 02 45
E-mail: einfo@koda.ee
URL: http://www.koda.ee

HRVATSKA

Mediatrade Ltd
Pavla Hatza 1
HR-10000 Zagreb
Tel. (385-1) 481 94 11
Fax (385-1) 481 94 11

MAGYARORSZÁG

Euro Info Service
Európa Ház
Margitsziget
PO Box 475
H-1396 Budapest 62
Tel. (36-1) 350 80 25
Fax (36-1) 350 90 32
E-mail: euroinfo@mail.matav.hu
URL: http://www.euroinfo.hu/index.htm

MALTA

Miller Distributors Ltd
Malta International Airport
PO Box 25
Luqa LQA 05
Tel. (356) 66 44 88
Fax (356) 67 67 99
E-mail: gwirth@usa.net

POLSKA

Ars Polona
Krakowskie Przedmiescie 7
Skr. pocztowa 1001
PL-00-950 Warszawa
Tel. (48-22) 826 12 01
Fax (48-22) 826 62 40
E-mail: ars_pol@bevy.hsn.com.pl

ROMÂNIA

Euromedia
Str. G-ral Berthelot Nr 41
RO-70749 Bucuresti
Tel. (40-1) 315 44 03
Fax (40-1) 314 22 86

ROSSIYA

CCEC
60-letiya Oktyabrya Av. 9
117312 Moscow
Tel. (7-095) 135 52 27
Fax (7-095) 135 52 27

SLOVAKIA

Centrum VTI SR
Nám. Slobody, 19
SK-81223 Bratislava
Tel. (421-7) 54 41 83 64
Fax (421-7) 54 41 83 64
E-mail: europ@tbb1.sltk.stuba.sk
URL: http://www.sltk.stuba.sk

SLOVENIJA

Gospodarski Vestnik
Dunajska cesta 5
SLO-1000 Ljubljana
Tel. (386) 613 09 16 40
Fax (386) 613 09 16 45
E-mail: europ@gvestnik.si
URL: http://www.gvestnik.si

TÜRKIYE

Dünya Infotel AS
100, Yil Mahallessi 34440
TR-80050 Bagcilar-Istanbul
Tel. (90-212) 629 46 89
Fax (90-212) 629 46 27
E-mail: infotel@dunya-gazete.com.tr

AUSTRALIA

Hunter Publications
PO Box 404
3067 Abbotsford, Victoria
Tel. (61-3) 94 17 53 61
Fax (61-3) 94 19 71 54
E-mail: jpdavies@ozemail.com.au

CANADA

Les éditions La Liberté Inc.
3020, chemin Sainte-Foy
G1X 3V Sainte-Foy, Québec
Tel. (1-418) 658 37 63
Fax (1-800) 567 54 49
E-mail: liberte@mediom.qc.ca

Renouf Publishing Co. Ltd
5369 Chemin Canotek Road Unit 1
K1J 9J3 Ottawa, Ontario
Tel. (1-613) 745 26 65
Fax (1-613) 745 76 60
E-mail: order.dept@renoufbooks.com
URL: http://www.renoufbooks.com

EGYPT

The Middle East Observer
41 Sherif Street
Cairo
Tel. (20-2) 392 69 19
Fax (20-2) 393 97 32
E-mail: mafouda@meobserver.com.eg
URL: http://www.meobserver.com.eg

INDIA

EBIC India
3rd Floor, Y. B. Chavan Centre
Gen. J. Bhosale Marg.
400 021 Mumbai
Tel. (91-22) 282 60 64
Fax (91-22) 285 45 64
E-mail: ebic@giasbm01.vsnl.net.in
URL: http://www.ebicindia.com

ISRAËL

ROY International
41, Mishmar Hayarden Street
PO Box 13056
61130 Tel Aviv
Tel. (972-3) 649 94 69
Fax (972-3) 648 60 39
E-mail: royil@netvision.net.il
URL: http://www.royint.co.il

Sub-agent for the Palestinian Authority:

Index Information Services
PO Box 19502
Jerusalem
Tel. (972-2) 627 16 34
Fax (972-2) 627 12 19

JAPAN

PSI-Japan
Asahi Sanbancho Plaza #206
7-1 Sanbancho, Chiyoda-ku
Tokyo 102
Tel. (81-3) 32 34 69 21
Fax (81-3) 32 34 69 15
E-mail: books@psi-japan.co.jp
URL: http://www.psi-japan.com

MALAYSIA

EBIC Malaysia
Level 7, Wisma Hong Leong
18 Jalan Perak
50450 Kuala Lumpur
Tel. (60-3) 262 62 98
Fax (60-3) 262 61 98
E-mail: ebic-kl@mol.net.my

MÉXICO

Mundi Prensa Mexico, SA de CV
Río Pánuco No 141
Colonia Cuauhtémoc
MX-06500 Mexico, DF
Tel. (52-5) 533 56 58
Fax (52-5) 514 67 99
E-mail: 101545.2361@compuserve.com

PHILIPPINES

EBIC Philippines
19th Floor, PS Bank Tower
Sen. Gil J. Puyat Ave. cor. Tindalo St.
Makati City
Metro Manilla
Tel. (63-2) 759 66 80
Fax (63-2) 759 66 90
E-mail: eccpcom@globe.com.ph
URL: http://www.eccp.com

SRI LANKA

EBIC Sri Lanka
Trans Asia Hotel
115 Sir chittampalam
A. Gardiner Mawatha
Colombo 2
Tel. (94-1) 074 71 50 78
Fax (94-1) 44 87 79
E-mail: ebicsl@itmin.com

THAILAND

EBIC Thailand
29 Vanissa Building, 8th Floor
Soi Chidlom
Ploenchit
10330 Bangkok
Tel. (66-2) 655 06 27
Fax (66-2) 655 06 28
E-mail: ebicbkk@ksc15.th.com
URL: http://www.ebicbkk.org

UNITED STATES OF AMERICA

Bernan Associates
4611-F Assembly Drive
Lanham MD20706
Tel. (1-800) 274 44 47 (toll free telephone)
Fax (1-800) 865 34 50 (toll free fax)
E-mail: query@beman.com
URL: http://www.beman.com

**ANDERE LÄNDER/OTHER COUNTRIES/
AUTRES PAYS**

**Bitte wenden Sie sich an ein Büro Ihrer
Wahl/ Please contact the sales office
of your choice/ Veuillez vous adresser
au bureau de vente de votre choix**

**Office for Official Publications
of the European Communities**

2, rue Mercier
L-2985 Luxembourg
Tel. (352) 29 29-42455
Fax (352) 29 29-42758
E-mail: info.info@opoce.cec.be
URL: http://eur-op.eu.int

NOTICE TO THE READER

Information on European Commission publications in the areas of research and innovation can be obtained from:

♦ RTD info

The European Commission's free magazine on European research, focusing on project results and policy issues, published every three months in English, French and German.
For more information and subscriptions, contact:
DG XII — Communication Unit, rue de la Loi/Wetstraat 200, B-1049 Brussels
Fax (32-2) 29-58220; e-mail: info@dg12.cec.be